HYDROGEOLOGICAL AND HYDROGEOPHYSICAL INVESTIGATIONS OF OTUKPO AND ITS ENVIRONS, NORTH-CENTRAL NIGERIA

BY

AMEH, Igoche Mark
PhD/SPS/2016/854

DEPARTMENT OF GEOLOGY,
SCHOOL OF PHYSICAL SCIENCES,
FEDERAL UNIVERSITY OF TECHNOLOGY, MINNA

JULY, 2021

ABSTRACT

Hydrogeological and hydrogeophysical investigations of Otukpo and its environs, North-Central Nigeria has been carried out. Otukpo and its environs fall within the Cretaceous sedimentary formation of the Lower Benue Trough. This research is aimed at establishing and delineating the aquifer units within Otukpo and its environs using integrated geosciences techniques of hydrogeology and hydrogeophysics. The study is targeted at producing a geological map, subsurface geological model, groundwater potential map and to establish groundwater flow direction of Otukpo and its environs. Surface geological mapping employing the traverse mapping method was carried out to suit conditions in different part of the study area. Detail logging of exposures in hand dug wells and borehole cuttings were carried out. Hydrogeological mapping to establish water level map and ascertaining the direction of groundwater flow in the area was done. Hydrogeophysical investigations involving Induce Polarisation (IP), Vertical Electrical Sounding (VES) and geoelectric section development employing the Schlumberger configuration was done. 2-Dimensional subsurface electrical tomography survey and interpretation employing the Wenner-Alpha method to delineate lateral and horizontal lithological exaggeration of the shallow subsurface geology was carried out. A borehole was drilled at one of the investigated points to validate the integrated interpreted data using rotary drilling technique. Well inventory of about 200 hand dug wells was taken. The surface elevation above datum sea level ranged from 142 m to 208 m while the depth of hand dug wells ranged from 2.3m to 14.2m. Static water level in wells ranged from 1.4m to 14.0m and the hydraulic head of the well ranged from 113.0 to 201.9. Groundwater in the area flows in the northward direction. Vertical Electrical Sounding (VES) using the Schlumberger configuration and the Induced Polarization (IP) using the time-domain technique were adopted for the hydrogeophysical survey. The investigation of the deep subsurface was limited to a minimum AB/2 of 600m. The IP models showed considerably low (negative) chargeability at varying depth for the sounded points. The very low to negative chargeability is associated with clay/shale lithologies. An appreciable increase in positive chargeability value was observed at proximate sounded electrode separation of 500 m and 600 m in all the plots, indicating clay/shale free sediments composed of saturated sandstone. Qualitative and quantitative interpretation of the VES data was carried out employing the traditional curve matching and the digital computer iteration method using the Winresist command software. A total of 20 VES stations were established along five profiles. Five subsurface geoelectric units were delineated beneath the VES sections. Morphological analysis of the field curves indicated four geoelectric curve types with the QH having 65%, KH having 15% while the KQH and QHK having 10% each. The 2D Resistivity tomographic imaging employing the Wenner Alpha array was utilized in investigating the shallow subsurface system of the area. The inverse model sections show a decrease in resistivity with depth, going as low as 1 Ωm in less than 20 meters. Otukpo and its environs are stratigraphically underlain by shaley carbonaceous mudstones. The groundwater system of Otukpo and its environs is composed of two major types; the shallow unconfined layers and the deep confined aquifer, deeply seated at about 450 m to 600 m beneath the surface. The interpretation of the subsurface conditions of the study area, based on the integrated geoscientific methods, should be verified through deep well drilling

by relevant authorities in order to alleviate the need for potable water by the inhabitant of Otukpo and its environs.

TABLE OF CONTENTS

Title	**Page**
Cover Page	
Title Page	i
Declaration	ii
Certification	iii
Acknowledgements	iv
Abstract	vi
Table of Contents	vii
List of Tables	xiii
List of Figures	xiv
List of Plates	xvii
Abbreviations	xviii
CHAPTER ONE	
1.0 INTRODUCTION	**1**
1.1 Background to the Study	1
1.2 Statement of the Research Problem	7
1.3 Justification	8
1.4 Study Area Description	9

1.4.1 Physiography and drainage 11

1.4.2 Climate and vegetation 11

1.4.3 Soil and land use 11

1.5 Aim and Objectives 13

1.5.1 Aim 13

1.5.2 Objectives 13

1.6 Scope of the Present Study 13

1.7 Limitations of the Study 14

CHAPTER TWO

2.0 LITERATURE REVIEW 16

2.1 Review of the Geology, Hydrology and Hydrogeology of Africa 16

2.2 Geological Setting of Nigeria 23

2.3 Geological, Hydrogeological and Hydrological Synopsis 24

2.3.1 Regional stratigraphic setting of lower Benue valley 25

2.3.2 Local geology of the study area 28

2.3.3 Nigeria hydrological environments 30

2.3.4 Hydrogeological environment of Nigeria 32

2.3.5 Surface water 33

2.3.6 The river basin development authorities (RBDAs) in Nigeria 35

2.4 Review of Geophysical Related Literature 36

2.5 Origin of Water on Earth 41

2.5.1 The hydro-tectonic cycles 42

2.6.1 Hydrological cycles 43

2.6.2 Groundwater system in the hydrologic cycle 45

2.7 Lithology, Stratigraphy, and Structure of Geological Formations 48

2.8 Groundwater Occurrence and Distribution 49

2.8.1 Sedimentary formations 51

2.8.2 Groundwater flow system 53

2.8.2.1 Groundwater movement 53

2.8.2.2 Velocity of groundwater movement 55

2.8.2.3 Hydraulic head 55

2.9 The Relationship between Geology and Resistivity 57

CHAPTER THREE

3.0 **MATERIALS AND METHODS** **59**

3.1 Materials 59

3.2 Methods of Data Acquisition 63

3.2.1 Preliminary desk study and reconnaissance 63

3.2.2 Fieldwork 64

3.2.2.1 Geological mapping 64

3.2.2.2 Hydrogeophysical investigation 65

3.2.3 Geophysical data acquisition 65

3.2.4 Induced polarization (IP) 67

3.2.5 Resistivity 70

3.2.5.1 The four-electrode principle (Vertical Electrical Sounding VES) 72

3.2.5.2 Schlumberger array instrumentation and measurement 76

3.2.5.3 Two dimensional (2d) electrical subsurface imaging 77

3.3 Data Treatment 81

3.3.1 1-D VES preliminary data treatment 81

3.3.1.1 Types of curve 82

3.3.2 Two dimensional (2-D) data treatment 83

3.4 Data Presentation 84

3.5 Ambiguity in Electrical Resistivity 85

3.5.1 Near surface inhomogeneity 85

3.5.2 Topography 86

3.5.3 Equivalence 86

3.5.4 Conductive overburden 86

3.5.5 Anisotropy 87

3.5.6 Natural noise 87

3.6 Hydrogeological Mapping 87

3.6.1 Hydraulic head/Groundwater flow direction 89

3.6.2 Borehole drilling and logging 90

CHAPTER FOUR

4.0 RESULTS PRESENTATION AND DISCUSSION 92

4.1 Geology of the Area 92

4.2 Hydrogeology 94

4.2.1 Shallow groundwater abstraction 97

4.3 Hydrogeophysics 100

4.3.1 Induced polarization 101

4.3.1.1 Summary of IP Survey 106

4.3.2 1-D Vertical electrical sounding 107

4.3.2.1 Summary of VES investigation 112

4.3.3 Correlation of resistivity and IP sections 113

4.3.4 Isoresistivity Interpretations 114

4.3.5 2D Geoelectric subsurface tomography 120

4.3.5.1 Discussion of 2-D subsurface tomography 125

4.4 Direct Subsurface Exploitation (Drilling) 126

4.4.1 Lithologic logging 128

4.5 Groundwater Potential 131

CHAPTER FIVE

5.0 SUMMARY, CONCLUSION AND RECOMMENDATION 133

5.1 Conclusion 133

5.2 Recommendations 136

REFERENCES 137

APPENDICES 144

LIST OF TABLES

Table		Page
2.1	Regional Stratigraphy of the Lower Benue Trough	27
2.2	Expected Groundwater Recharge at a Regional Level	32
2.3.	Estimated World Water Balance	51
2.4	Resistivity of some Common Rocks, Minerals and Chemicals	58
4.1	IP Chargeability (msec) Data for Otukpo and Environs	102
4.2	Summary of the Geoelectric Parameters Including their respective Resistivity, Thickness, Depths and Curve Types 109	
4.3	Apparent Resistivity and Chargeability Data of Otukpo and its Environs	115
4.4	IP and VES Data for Drilled Borehole Point	128

LIST OF FIGURES

Figure		Page
1.1	Location of Otukpo and its Environs	10
2.1	Africa Groundwater Storage	18
2.2.	Aquifer Productivity	19
2.3	Estimated Depth to Groundwater in Africa	20
2.4	The Hydrogeological Environments of Africa	22
2.5	General Geology of Nigeria	23
2.6	Generalized Cretaceous Stratigraphy in the Southern, Central and Northern Benue Trough	28
2.7	Hydrological Areas of Nigeria	30
2.8	Hydrological Setting depicting Relative Permeability and Runoff Potential	31
2.9	Nigeria Aquifer Type and Productivity	34
2.10	Nigeria Drainage Systems	35
2.11	Schematic illustration of the Hydro-tectonic Cycle	43
2.12	The Hydrological Cycle	44
2.13	Schematic Illustration of hydraulic cycle	47
2.14	Subsurface Water	50
2.15	Darcy's Experiment	54
2.16	Schematic Illustration of Hydraulic Head	56
3.1	Time domain IP signal received showing measured parameters	68

3.2	Schematic Illustration of IP Method	69
3.3	Common configuration of four-electrode	73
3.4	Wenner Array of Electrical Resistivity Method	75
3.5	Schlumberger Array of Electrical Resistivity Method	75
3.6	Regular configurations used in resistivity surveys and their geometric factors	78
3.7	Wenner Alpha Configurations for 2-D Subsurface Electrical Imaging	79
3.8	Sequence of 2-D Wenner Alpha Resistivity Measurement	80
3.9	Types of Apparent Resistivity Curve	83
4.1	Geology of Otukpo and its Environs	94
4.2	Well Depths in Otukpo and its Environs	95
4.3	Groundwater Level in Hand-Dug Wells of Otukpo and its Environs	96
4.4	Groundwater Flow Direction of Otukpo and its Environs	98
4.5	Location of VES Points and Geoelectrical Survey Profile Lines	101
4.6	OTK 01 Chargeability Curves	103
4.7	OTK 02 Chargeability Curves	104
4.8	OTK 03 Chargeability Curves	104
4.9	OTK 04 Chargeability Curves	105
4.10	OTK 05 Chargeability Curves	106
4.11	OTK 06 Chargeability Curves	106
4.12	QH Curve Type	110
4.13	KH Curve Type	110
4.14	KQH Curve Type	111
4.15	QHK Curve Type	111

4.16	Isoresistivity at 25m Depth in Otukpo and its Environs	116
4.17	Isoresistivity at 100m Depth in Otukpo and its Environs	117
4.18	Isoresistivity at 200m depth in Otukpo and its Environs	118
4.19	Isoresistivity at 400m depth in Otukpo and its Environs	119
4.20	Isoresistivity at 500m depth in Otukpo and its Environs	120
4.21	Isoresistivity at 600m depth in Otukpo and its Environs	121
4.22	Measured Apparent Resistivity Pseudosection for Profile OTK 01	122
4.23	Measured Apparent Resistivity Pseudosection for Profile OTK 02	123
4.24	Measured Apparent Resistivity Pseudosection for Profile OTK 03	124
4.25	Measured Apparent Resistivity Pseudosection for Profile OTK 04	124
4.26	Measured Apparent Resistivity Pseudosection for Profile OTK 05	125
4.27	Measured Apparent Resistivity Pseudosection for Profile OTK 06	126
4.28	IP, VES Curves and Geoelectrical Log for Borehole Point	128
4.29	Simplified Borehole Lithologic log	131
4.30	Areas shallow groundwater potential in Otukpo and its environs	132
4.31	Deep groundwater potential zones (500 – 600 m) in Otukpo and Environs	133

LIST OF PLATES

Plate		Page
I.	Field Note Book and Pencil	59
II.	Garmin Etrex GPS	59
III.	Compass Clinometer	60
IV.	Hammer	60
V.	Measuring tape	60
VI.	Dip meter	61
VII.	Electrical Resistivity Meter	61
VIII.	Rotary Drilling Rig	62
IX.	Hydrogeophysical Exploration	66
X.	Measuring Water Level in Well	90
XI.	Drilling in progress	91
XII.	Section of Okokolo Spring at its source	98

XIII. The Downstream side of Okokolo Springs 99

XIV Sample Log Box 128

ABBREVIATIONS AND DEFINITIONS

1D	One Dimensional
2D	Two Dimensional
ACPC	African Climate Policy Centre
BSRWSSA	Benue State Rural Water Supply and Sanitation
FMWR	Federal Ministry of Water Resources
GPS	Global Positioning System
HEP	Horizontal Electrical Profiling
IP	Induce Polarization
LBRBDA	Lower Benue River Basin Development Authority
NGSA	Nigerian Geological Survey Agency
OTK	Otukpo

RBDA	River Basin Development Authorities
SPT	Standard Penetration Test
UNESCO	United Nations Educational, Scientific and Cultural Organization
VES	Vertical Electrical Sounding
WHO	World Health Organization
WRI	World Resources Institute
WWAP	World Water Assessment Program

CHAPTER ONE

1.0 INTRODUCTION

1.1 Background to the study

Water serves as an elixir of life, the quality of a human life is the functions of the quality of water he/she drinks (Amadi *et al.*, 2017). The World Health Organization (WHO, 2010), about one billion persons cannot access potable water supply and about two million persons die annually due to water-borne or water-related diseases. WHO, (2010) in economic terms has shown that there is an economic return of between $3 and $34 for every one American dollar ($1) invested in water and sanitation. Not more than 30% of Nigeria's population has access to the recommended potable water, WHO's standard of 120 litres per person per day for total domestic use and about 3 litres per day per person to maintain essential body metabolism (WHO, 2010). 40 billion man-hours are lost per annum in collecting water from sources other than groundwater in Sub-Saharan Africa according to the United Nations. This implies that the non-accessibility to potable water constitutes one of the reasons why poverty persists in most parts of Africa. The reasonable times lost to accessing and collecting water are often the variance between the period needed to be positively educated or carry out a trade and earn a livelihood. The World Resources Institute (WRI, 2018) reported that the water system of the world faces difficult and alarming threats. More than one billion persons are currently living in water-scarce areas in the world; also up to 3.5 billion people could witness serious water scarcity/shortage by the year 2025 (WRI, 2018).

Water is found in lakes, springs, lagoons, rivers and streams as surface water. As rain it, falls to the ground, infiltrate through porous and permeable rock formations into the

saturated subsurface as groundwater. The overlapping and interacting natural surroundings that exist between groundwater and the rock that hosts it have made hydrogeology an indispensable tool in groundwater science and management (Fetter, 2007). The mystery of groundwater occurrence and distribution can be untangled by the science and art of hydrogeology. The use of geological, hydrogeological and hydrogeophysical methods for groundwater investigation has been motivated in part by a desire to reduce the risk associated with the drilling of abortive boreholes. The data supplied by geoscientific techniques are partly reliable and less expensive. These geoscientific techniques give only indirect indication of groundwater so that the subsurface hydrogeological records can be inferred from the geoscientific investigations.

The study of groundwater is interdisciplinary as it involves the theories and principles of chemistry, physics, mathematics and biology (Olasehinde, 1999). Comprehensive knowledge regarding the availability, amount and hydraulic characteristics of natural groundwater resource in an area is fundamental to sustainable improvement of water resources (Amadi and Olasehinde, 2009).

Hydrogeology has to do with the study of groundwater in relation to its occurrence, movement, exploration, exploitation, quality, utilization and management, thereby making it a descriptive and analytical science (Todds, 1980; Offodile, 2002; Kelvin, 2005; Fetter, 2007).

Groundwater is that water that fills up all the subsurface pore spaces of soil/rock particles (in sedimentary formations) and fractures/fault (in crystalline basement) that is found within the zone of subsurface saturation below the natural water table (Olasehinde, 1999; Offodile, 2002; Fetter, 2007). Groundwater as a precious natural resource is sometime

scarce and unevenly distributed, both in space and time within geological formations (Amadi and Olasehinde, 2009). The lithology of sedimentary frame work is the principal factor controlling the distribution of aquifer permeability and porosity in any given sedimentary setting, and it serves as the dominant control over groundwater accumulation, movement and exploitation. Groundwater is one of the safest forms of water for domestic use due to the fact that it is not prone to pollution like surface water (Amadi, 2007). Occurrence and distribution of groundwater is mainly dependent on local and regional geology of an area, geomorphology/weathering and precipitation. These factors determine the occurrence of groundwater and give rise to composite hydrogeological environment with variation in accessibility, quality and quantity (Nwankwoala, 2015; Adelana *et al.*, 2008). The development of groundwater as a resource depends on the detail understanding and comprehension of the geology and hydrogeological setting of an area. This is imperative because, lack of sufficient and accurate information makes it difficult to successfully access groundwater resource for domestic, irrigational and industrial use. Groundwater management is therefore directly dependent on hydrogeological conditions and the characteristics of the aquifer's system (Zektser and Everett, 2004; Amadi *et al.*, 2017).

Comprehensive strategy geared toward detail subsurface investigation is needed to improve potable water accessibility and security. Development of groundwater resources is a major factor for economic growth and poverty alleviation. Sustainability of agriculture, industrialization and human civilization hinges on availability of groundwater supply.

Poverty in Africa stands as an epidemic for some causes; political insecurity, ethnic and religious encounters, climate alteration and additional man-made reasons (WaterAid, 2016).

One of the utmost causes of poverty in Africa which has been undermined in recent times is lack of access to potable water (WaterAid, 2016).

Access to potable water through groundwater resource would spare abled men, women and children long and difficult times they undertake to source for potable water. Children are more likely to attend school and families are more able to support themselves when groundwater sources are available and accessible (WaterAid, 2016). According to WaterAid Nigeria (2016), communities without safe potable water have higher rate of illness and are held back from economic progress. The new United Nations Sustainable Development Goal has access to potable water as one of the key factors in helping to achieve the new set goals. Groundwater is naturally protected from contamination by the overlying geological formations with little or no treatment required (Amadi, 2007). Potable groundwater is a vital resource that improves several health conditions such as dehydration, toxin removal and good kidney function among others (Nwankwoala, 2015).There has been increasing recognition amongst geoscientist and stakeholders in the water sector in developed and developing countries of the rising importance of hydrogeological exploration. Particularly in those parts of the world that have been characterized by abject potable water scarcity (Offodile, 2002).

A requisite requirement for locating, assessing, developing and utilizing groundwater resource is to be equipped with a detailed hydrogeological knowledge of the subsurface to guide placement of boreholes or water wells (Dwain, 2015). The search for the unevenly distributed groundwater resources by geophysical technique is known as hydrogeophysics.

Hydrogeophysical investigation is an indirect technique of acquiring generalized sub-surface geological data by using special instruments to make definite physical

measurements (Reinhard, 2006). Groundwater investigation generally occurs within the upper few hundred meters of the earth's subsurface. The use of geophysical exploration methods especially the electrical resistivity method has become increasingly acceptable and popular due to its efficiency and economy.

It has been employed not merely in the indirect finding of the presence of water, but also in the assessment of aquifer properties and the quality of groundwater (Reinhard, 2006; Fetter, 2007). Hydrogeophysics provides detail subsurface information that will serve as a guide when taking hydrogeological decisions (Sandberg *et al.*, 2002).

Hydrogeophysical explorations using electrical resistivity methods have confirmed to be an effective and efficient tool in groundwater exploration (Offodile, 2002; Reinhard, 2006 and Selemo, 2011). Indirect method of sub-surface exploration like the resistivity technique is an excellent geophysical method for the detection of very shallow as well as deep layer geological interfaces. Electrical resistivity method can delineate and infer aquiferious zones within any geological formation (Olasehinde, 1999; Adelana *et al.*, 2008). The natural resistivity of subsurface geological materials is intensely swayed by the occurrence of groundwater that serves as a good conductor of electricity (electrolyte). The minerals which form the background of rocks are commonly lesser electrical electrodes compared to groundwater. Therefore the electrical conductivity of geological materials is related to the amount and quality of groundwater it holds (Lowrie and Fichter, 2019). The diverse and complex nature of groundwater occurrence in most geological settings is the major reason why any development of the resource in an area requires a comprehensive hydrogeological and geophysical investigation (Reinhard, 2006 and Olasehinde, 1999). Employing the most suitable geophysical method based on the geology and hydrogeological conditions in

groundwater exploration would minimize the risk of groundwater exploitation failures (Mbiimbe, *et al.,* 2016). The Vertical Electrical Sounding (VES) method has proved very successful in searching for groundwater on an account that it is effective and the technique is simple to run (Reinhard, 2006; Mijinyawa *et al.,* 2013).

Benue State of Nigeria, popularly referred to as the Nation Food Basket for the reason that it is involved in massive agricultural activities, has in recent time experienced spiral increase in population which has in return placed greater demand on potable water resource. Otukpo is the commercial hub of the southern Benue State and the traditional nerve centre of Idoma people where its supreme ruler the Och'Idoma palace is situated. Otukpo is known for its agricultural activities as it contributes to the nation's food security and accommodates one of the largest rice mill factories in the country. In addition to Otukpo municipality, other notable places around Otukpo metropolis include Adoka, Ogobia, Upu, Akpa-Igede, Otobi, Oyagede and Otukpoicho. When the inhabitants of Otukpo and environs speak of their own development, the highest priority is accrued to the collective economic effect triggered by lack of potable water resources. Otukpo and its environs are saddled with water supply issues, despite frantic efforts have been made by government and some individuals to sink water boreholes but these boreholes turn to be abortive. Water boreholes drilled in the area are often outright abortive and it has been a burning issue in the minds of Otukpo people. Often times, less emphasis have been placed on groundwater exploration through geophysical principles in the area.

Otukpo is a sedimentary environment and groundwater in such environment exists in porous and permeable formations (Offodile, 2002). A detailed understanding of the

sedimentary architecture through hydrogeological and hydrogeophysical investigation will aid the successful identification of groundwater prolific zones. The high failure rate in most groundwater projects recorded in Otukpo and its environs has informed the application of detailed and coherent hydrogeological and hydrogeophysical investigations. These investigations serve as a prerequisite to successful water well drilling project in the area. Mobilizing resources to prioritising exploration and exploitation of groundwater in Otukpo and its environs cannot therefore be overemphasized.

1.2 Statement of the Research Problem

About 1.1 billion people worldwide are unable to access potable water resulting in about two million deaths from water related diseases every year (World Health Organization, 2010). There is scarcity of surface and groundwater resources in Otukpo and its immediate environs. Upward increase in human population has made accessibility to potable water more difficult for the inhabitant of Otukpo and its environs. Hand-dug wells are seasonal, existing boreholes are unable to maintain stable water supply and pipe borne water is non-existent in Otukpo and its environs. The demand for water exceeds its availability as a consequence of population growth and lack of access to potable water which has resulted in the supply of water for domestic use from questionable sources. Offodile (1991) asserted that the Lower Benue Trough is hydrogeologically problematic.

The high failure rates of boreholes, low yields in wells and poor maintenance of water wells in Otukpo point to the fact that a good background comprehension of the surface hydrogeology and geology of the area is vital to unravel the possible causes of high failure

rates of borehole in the area. Detailed knowledge on aquifer systems, their spatial extent and hydraulic characteristics in Otukpo and its environs is very scanty. Geoscience work in Otukpo area has been confined to geomagnetic investigation for mineral exploration (Ogah and Jatau, 2014).

Integration of geology, hydrogeology, induced polarization, vertical electrical sounding and 2D subsurface tomography constitutes a sound technique to establish the required subsurface stratigraphy for prolific borehole drilling and hand-dug well siting

The determinations of sites for successive boreholes require research into available lithofacies and hydrodynamic parameters as well as their respective architecture in the sedimentary terrains. Such geoscience investigations skewed at groundwater development is yet to be embarked upon in the area on a detail and extensive scale.

1.3 Justification of the study

The upsurge in groundwater request for various human undertakings in Otukpo and environs as a result of scarcity of surface water has made groundwater exploration and exploitation a necessity. Detailed knowledge on aquifer systems, their spatial extent and hydraulic characteristics in Otukpo and its environs is very scanty. Previous workers in the area concentrated their works on surface geology and geomagnetic investigation for mineral exploration (Ogah and Jatau, 2014). Due to poor understanding of the subsurface geology in the study area, majority of the boreholes drilled has been abortive, while the successful ones have low yield. Due to the upsurge in population coupled with the increase

in the number of agro-based cottage industries, the need to understand the subsurface configuration of the aquiferous unit in Otukpo and environs cannot be overemphasized.

Understanding the local geology will lead to delineation of the aquifers in the area, and it will greatly reduce the great rate of borehole failure in Otukpo and environs. This makes the crux of the existing research.

1.4 The Study Area Description

Otukpo and its environs fall within the southern portion of Benue State, Nigeria and it geologically falls inside the Southern Benue Trough. It lies between longitudes $8^{0}00'$E to $8^{0}30'$E and latitudes $7^{0}00'$N to $7^{0}30'$N on an average altitude of 270m above the sea level (Figure 1.1). The area is generally low lying with few gently undulating ridges. The area is part of Otukpo Sheet 270 SW and classified under the Lower Benue River Basin hydrological area of Nigeria.

Otukpo has a probable landmass of about 390 sq. km, with a likely population of 266,411 (National Population Commission, 2006). It serves as the headquarters of the Idoma ethnic group where the palace of the paramount ruler, the Och'Idoma is located. Some prominent locations proximate to Otukpo metropolis includes but not limited to Otukpoicho, Otobi, Akpa-Igede, Adoka, Ogobia, Upu and Oyagede. Otukpo is constrained northwardly by Apa Local Council Area, in the southeast by Ohimini, in the south by Ado and in the west by Olamaboro Local Government Areas respectively. The area is accessible through Makurdi/Enugu express way as well as Naka/Ankpa road.

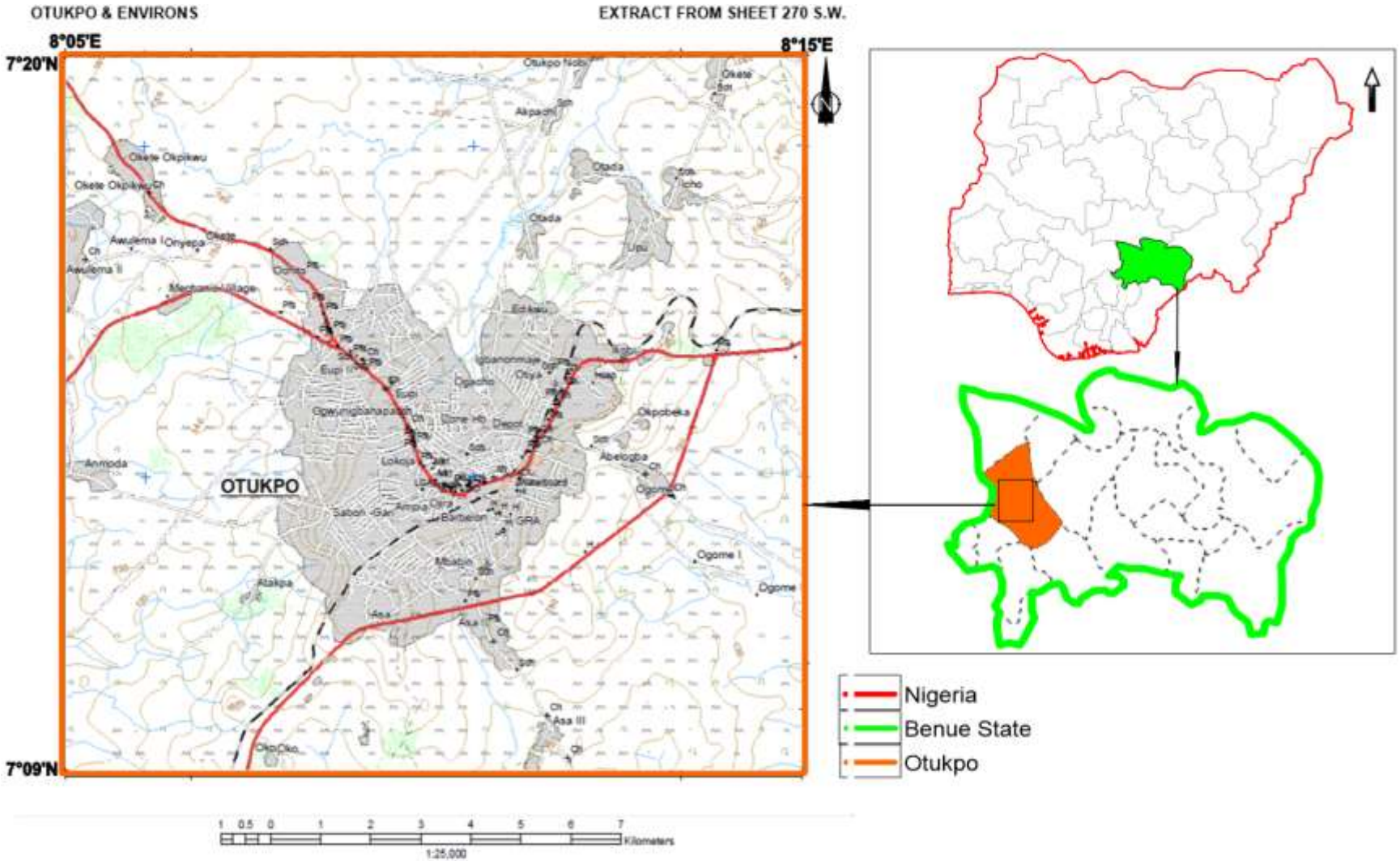

Figure 1.1: Location of Otukpo and Environs (Modified After Office of the Surveyor General of the Federation (OSGF), 2018)

1.4.1 Physiography and drainage

Otukpo is morphologically characterized by valleys, gently undulating plains and few hills with an average elevation of 160 m to 250 m above sea level. The area is majorly drained by Okpokwu tributary. All active streams around Otukpo and its environs drain into the River Okpokwu catchment basin. Furthermost tributaries of the River Okpokwu are transitory and dry up all through the peak of the dry period (Lower Benue River Basin Development Authority, 2014).

1.4.2 Climate and vegetation

The area is characterised by annual mean rainfall of between1500 mm and 1800 mm and a monthly temperature range of 25°C to 33°C. The predominant climatic situation in Otukpo area comprises the rainy season (March to October) and dry season (November to February) time of year accompanied by high temperatures, low pressure and great relative humidity throughout the year (Lower Benue River Basin Development Authority, 2014).

1.4.3 Soil and land use

The soil in the area is characterized by sandy and loamy soil while the topsoil is dominated by lateritic soil. The lateritic soils are light brown to reddish brown while the loamy soils are dark brown.

Four types of land use and land cover forms are identified within the area of study. These include agricultural land, forest, settlements and lateritic mudstone quarry for bricks

making. Agriculture is the major source of economy and livelihood of Otukpo people providing employment for about 70% of the population.

Farming is practiced at both local and mechanized levels in the area. The seasonal climate variation allows the farmers to produce a diversity of food and economic/cash crops.

Farmers in the area based on the soil types available, cultivate agricultural products. Elements in the earth beneath shallow sub-surface influence the growth of plants (John and Richard, 2004). The food crops produced include cassava, yam, corn, beans, rice, sweet potato, millet, and a diversity of fruits and root vegetable. The foremost cash crops produced by the farmers in the area include groundnut (peanut), palm oil and palm kernel. The area is part of the main export destination of agricultural products in Nigeria, hence the name ‘Food Basket of the Nation’.

1.5 Aim and Objectives of the Study

1.5.1 Aim

This study is aimed at establishing and delineating the aquifer units within Otukpo and environs using integrated geosciences technique.

1.5.2 Objectives

The objective of this study is to:

i. produce a geological map of Otukpo and its environs

ii. produce subsurface geological model for Otukpo and its environs

iii. produce groundwater potential map and establish groundwater flow direction in Otukpo and its environs

iv. develop maps showing areas with potential prolific aquifer at various depth

1.6 Scope of the Present Study

The present research involved desk study relating to hydrogeological and geophysical investigations. The concise activities of the field study involved:

i. Surface geological mapping: traverse geological mapping method was employed to suit conditions in different part of the study area. The mapping involved detail logging of exposures in hand-dug wells and boreholes so as to record factual,

unswerving and comprehensive information based on objective examination of the lithologies underlying the area

ii. Hydrogeological mapping: this involves well inventory (well coordinates, elevation above sea level, depth of well and depth to static water level) to establish water table map and determine the direction of groundwater flow in the area.

iii. Hydrogeophysical investigations: Induce Polarisation (IP), Vertical Electrical Sounding (VES) and geoelectric section development employing the Schlumberger configuration

iv. 2-Dimensional subsurface electrical tomography acquisition and interpretation employing the Wenner-Alpha method to delineate lateral and horizontal lithological exaggeration of the shallow subsurface

v. Borehole drilling: Validating integrated interpretation data using rotary drilling technique

1.7 Limitations of the Study

Due to the high failure rate of boreholes in the study area, subsurface information is virtually absent in the study area. Benue State Water Board has scanty data on pre-drilling and post-drilling activities in Otukpo area. Lack of the accessibility of longer length of undeviating space and hindrance of existing tarred roads and built-up environment limited the electrical cable spread length during some of the VES survey. Due to the paucity of

funds, only one borehole was drilled in order to validate the result of the geoelectric sections from the geophysical survey carried out within study extent.

CHAPTER TWO

2.0 LITERATURE REVIEW

2.1 Review of the Geology, Hydrogeology and Hydrology of Africa

African Climate Policy Centre (ACPC) in the policy brief No.5 of 2013 anticipated that there will be a substantial impact of climate change on water properties. This will involve a collective number of the world, mostly African countries which will likely face bigger water stress by 2025. Groundwater resources represent 15% of African's renewable water resources. The total volume of water believed to be in storage when taken into account, comprising generic and fossilized water, groundwater is considered the most profuse water source in Africa (Tijani *et al.*, 2016).

The subsurface nature of groundwater has made it to be largely underutilised. As a result of climate change, the availability of surface water from lakes and streams will become more erratic, unevenly distributed and less reliable over space and time. Groundwater answers much more gradually to meteorological circumstances responsible for climate change compared to surface water and, as such, delivers a normal natural buffer in contrast to climate inconsistency. At regional and sub-regional scale, groundwater resource availability is relatively well known but at lesser scales where grass root development is concentrated, knowledge of groundwater resource is inadequately understood in Africa (ACPC, 2013). Characterising the accessibility and dissemination of groundwater resources is a critical and vital prerequisite in finding the most prospective sites for groundwater development and for determining the likely developmental potential of groundwater resource.

Scientific research is needed on how to overcome the challenge of high cost of water well erection and the incomplete understanding of groundwater resources, which is at present responsible for the restricted development of groundwater resource in most parts of Africa (ACPC, 2013).

MacDonald *et al*. (2012) reported that despite the fact that groundwater serves as the biggest and utmost extensively disseminated form of potable freshwater in the Africa region, there is a slight fact on groundwater resource in the African continent. They presented quantitative Africa continent maps of aquifer (groundwater) storage and potential water borehole yields created from widespread review of maps that are available in publications (Figure 2.1 to Figure 2.4). The African groundwater potential storage is estimated to be about 0.66 million km^3, but this groundwater resource has not been adequately accessed due to inadequate knowledge of the subsurface geology.

Across the African continent, groundwater reserve has stayed projected by merging the saturated aquifer thickness and effective aquifer porosity of diverse aquifers. Largest volumes of groundwater are located in huge sedimentary areas in the North African countries which include but not limited to Libya, Chad, Sudan, Algeria and Egypt. Nonetheless, for most African states, properly placed and constructed boreholes can care for groundwater abstraction through inter-annual variations in recharge. Quantitative, spatially unambiguous facts on groundwater resource in Africa cities is needed to depict groundwater resource in ways that could helpfully enhance approaches to solve the rising potable water request. This demand is allied not only with geometric inhabitants' growth but also with climate inconsistency and change. The African quantitative groundwater

related atlases are anticipated to point to more representative valuations of water related security, and to encourage a further quantitative methodology of representing groundwater resources on maps (Figure 2.1) at regional and national levels (MacDonald *et al.*, 2012; Tijani *et al.*, 2018).

The likelihood for water borehole yields greater than 5.0 l/s is not evenly distributed in the continent, though in area where detailed and effective hydrogeological and hydrogeophysical investigations are carried out, higher yield borehole may be successful. The potential for transitional boreholes yields of 0.5 to 5 ls^{-1} is much higher.

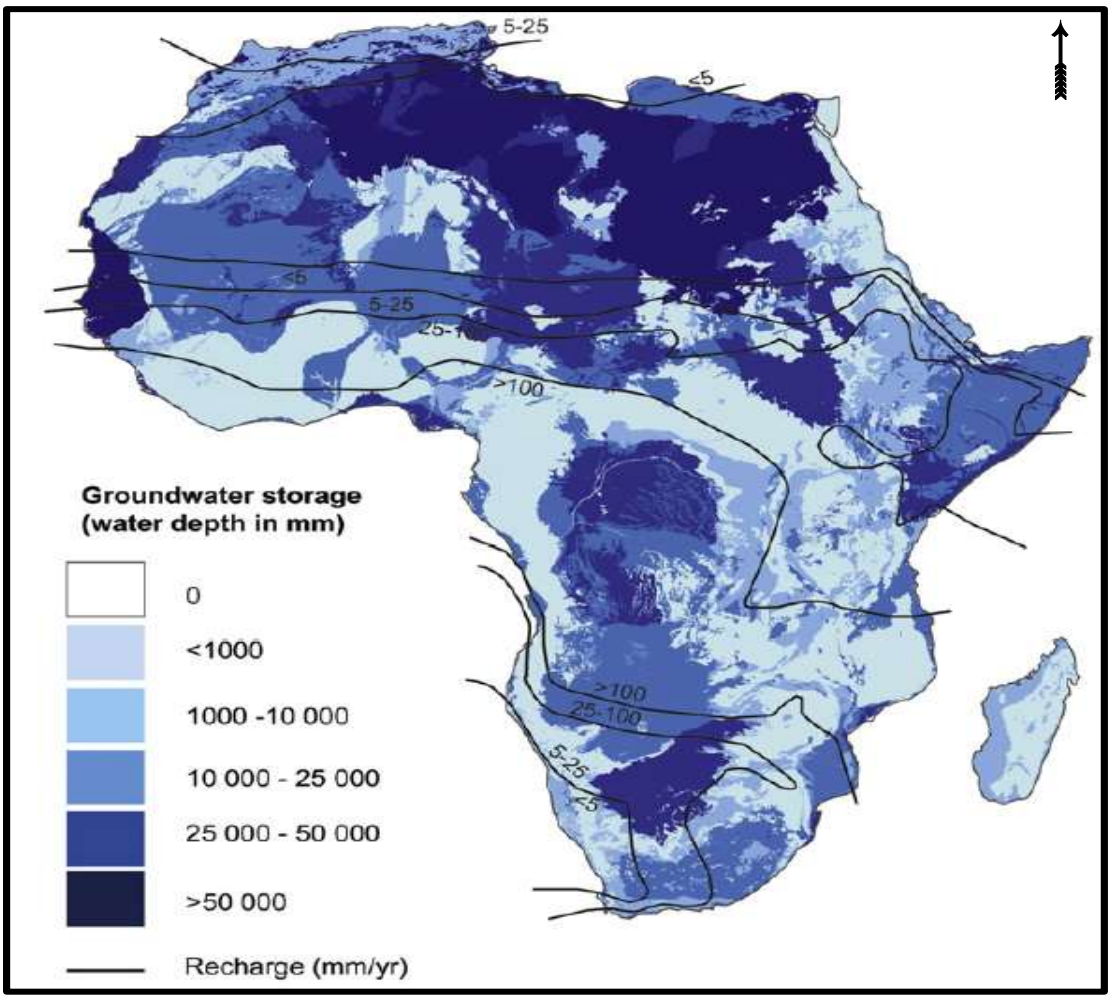

Figure 2.1: Africa Groundwater Storage (Tijani *et al.*, 2018)

The aquifer productivity map (Figure 2.2), is a representation of what borehole yields can rationally be anticipated in diverse hydrogeological entities within the continent. The varieties show the estimated interquartile array of the yield of drilled water boreholes using appropriate techniques.

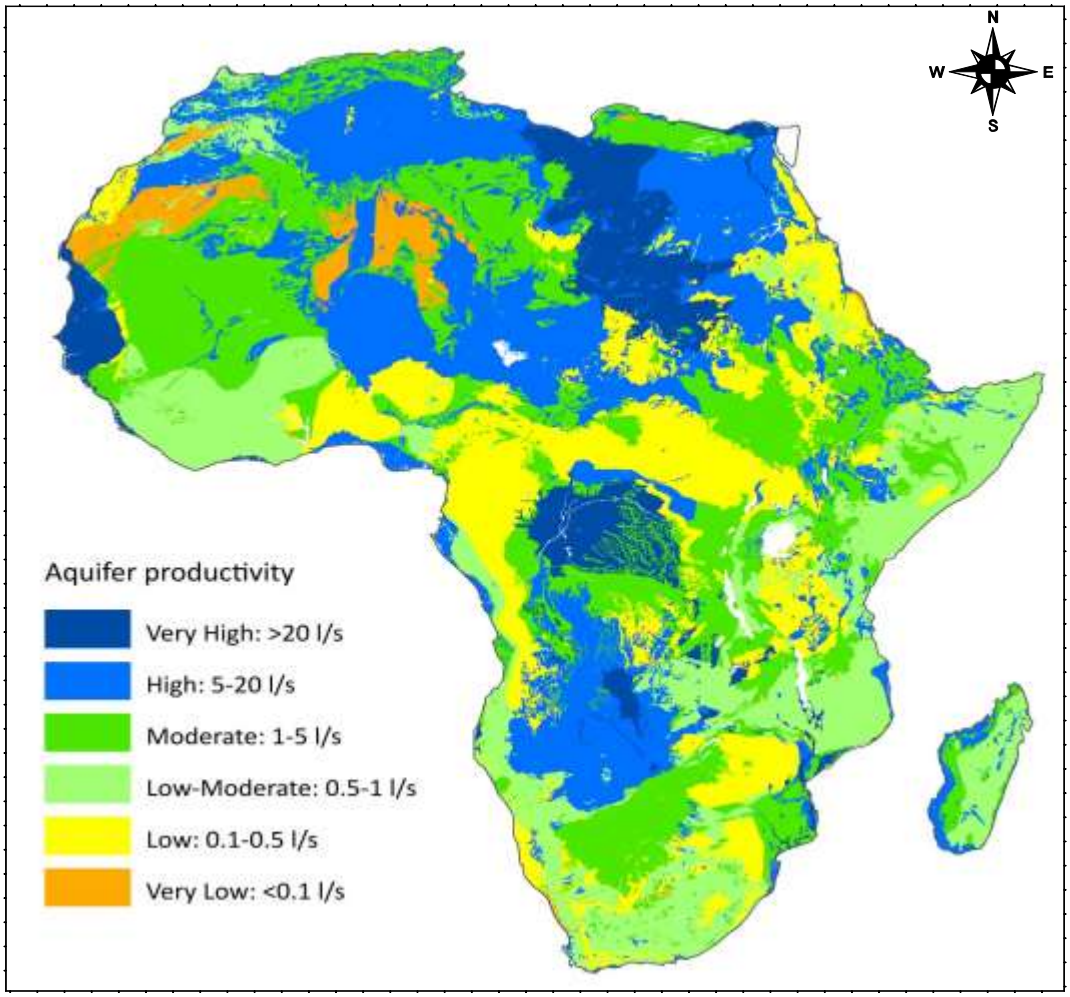

Figure 2.2: Aquifer productivity in Africa (Tijani *et al.*, 2018)

One of the factors that control the availability and economy of groundwater resource is depth to groundwater (Figure 2.3). The variation in lithogical depth to approximate groundwater depth in Africa is associated with variable lithological formations underlying

the continent. Greater depth to groundwater aquifers are encountered in the northerly sector of the African continent (MacDonald *et al.*, 2012).

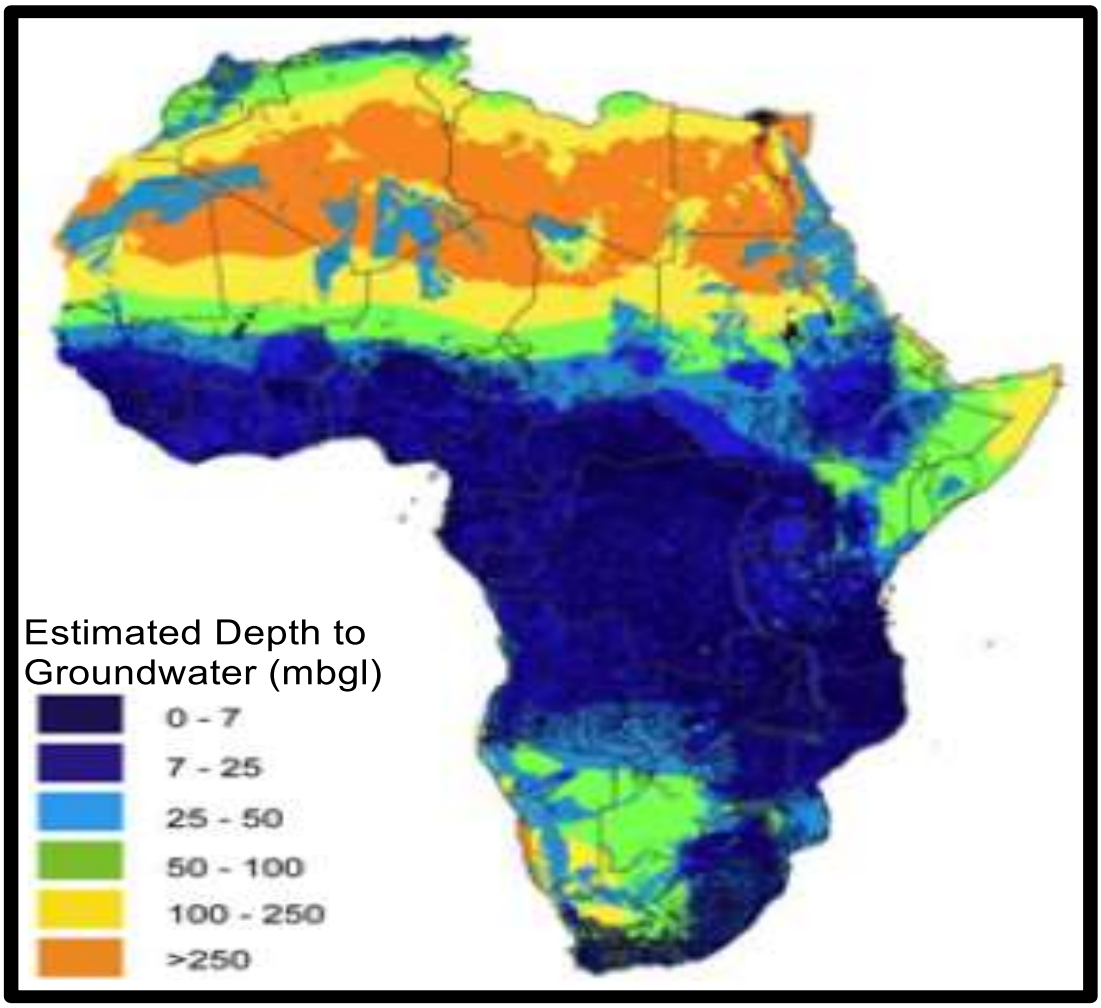

Figure 2.3: Estimated depth to groundwater in Africa (Tijani *et al.*, 2016)

MacDonald and Davies (1998) studied the hydrogeology of the Oju/Obi area at Ochingini in Benue State. The survey was carried out employing EM34-3 and magnetic profiles across an 8.2 km traverse along Ochingini axis. The Upper Eze-Aku and the Makurdi sandstone overlain the study area. The Upper Eze-Aku contains soft mudstones with quite a lot of important sandstone strata and thin bed of limestones. The Makurdi sandstone contains inter-bedded sandstone of fine-medium grained and thin mudstones, the

sandstones are generally cross-bedded; with observable load cast elements. The borderline between the Makurdi Sandstone and Eze-Aku is vague and is demarcated only by varying quantities of sandstone and mudstone. The sandstone within the area is understood to have abundant groundwater for hand-dug wells if sunk to below 15 m. Resistivity investigations (VES) were used to differentiate sandstone and mudstone by changes in the weathered zone of the Ochingini area.

The British geological survey (2011) concluded that groundwater occurrence is dependent primarily on the interaction between geology, geomorphology/weathering and precipitation (both present and ancient) which gives rise to environments of complex hydrogeology. The successful development of groundwater is dependent on a good understanding of the hydrogeological environment. There exist four aquifer types on a continental scale; the basement, volcanic, consolidated sedimentary and unconsolidated sedimentary aquifers.

The basement aquifers are Precambrian in age and underlie most part of Africa, volcanic aquifers underlie a small portion of the continent; consolidated sedimentary aquifers underlie about one third of African land mass and the unconsolidated sedimentary aquifers underlie the remaining portion of the continent (Figure 2.4).

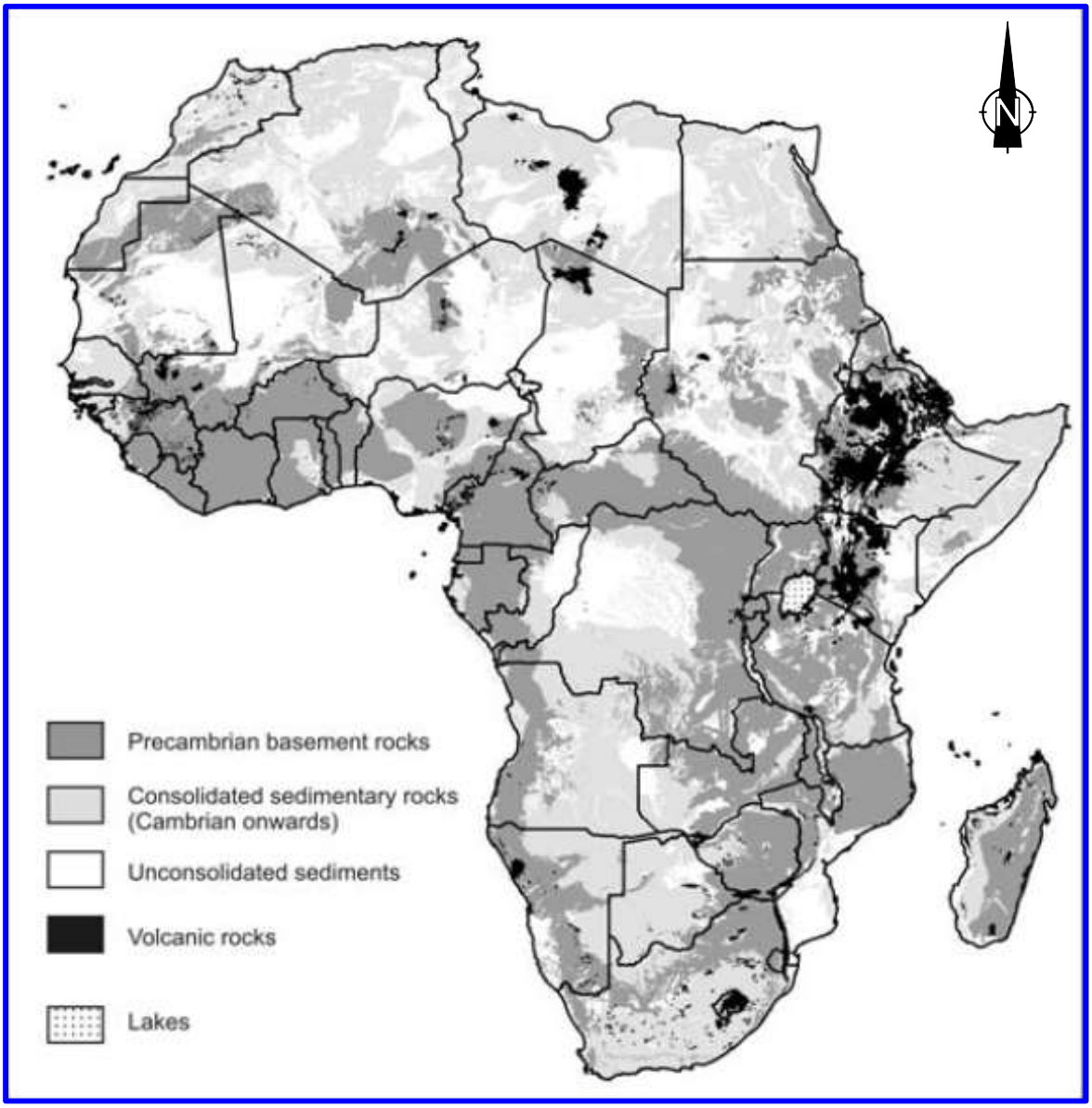

Figure 2.4: The hydrogeological environments of Africa (Mc Donald *et al.*, 2008)

2.2 Geological Setting of Nigeria

The geology of Nigeria is split into three broad litho-stratigraphical units (Figure 2.5):

1. The Precambrian Basement Complex.

2. The Cretaceous to Recent Sedimentary Basins.

3. Jurassic Younger Granites

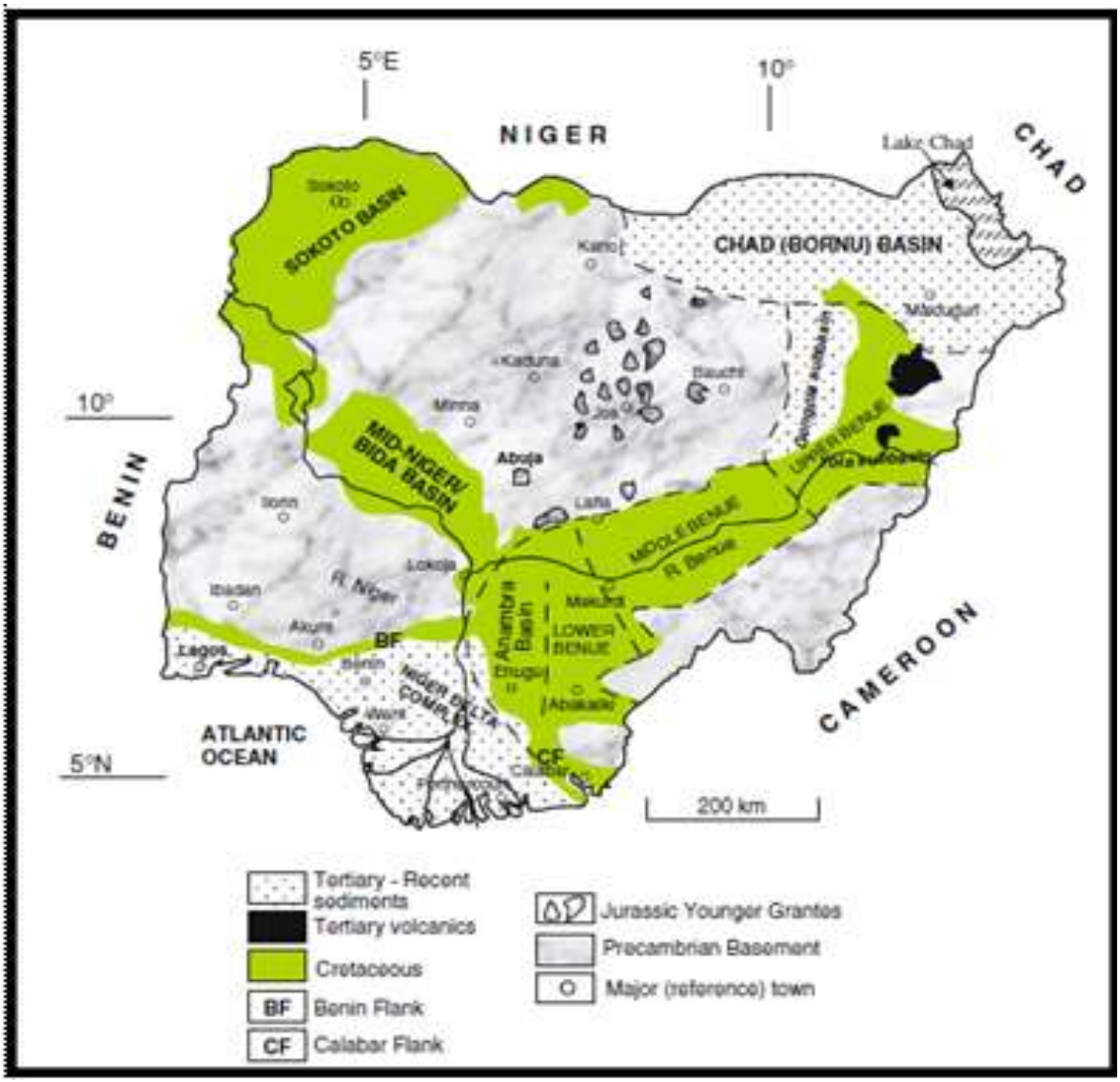

Figure 2.5: Generalize geology of Nigeria (After Obaje, 2009)

2.3 Geological, Hydrogeological and Hydrological Synopsis

Nwajide (2013), described the Benue Trough as an important tectonosedimentological quantity in the development of the Nigerian Cretaceous and Tertiary geology. The Benue valley contains a linear expanse of sedimentary basin extending from almost the current confluence of the rivers Niger and Benue. It is bounded by crystalline basement rocks of the Jos Plateau Younger Granites (Wase) to the north and the Cameroon Basement Massif to the south (Offodile, 2002). The Benue Trough is an elongated intracratonic structure more than 1000 km in length and about 250 km at its broadest sections (Nwajide, 2013). The sediment thickness from Albian to Maastrichtian in the lower Benue rift as projected from the singular parts based on stratigraphic evidence is given as 4km to 6km (Cratchley and Jones, 1965; Benkhelil, 1986). The formation and sequence evolution of the Benue Trough is consequently from trans-current movement and the lineament which is the structural direction that controls the Trough tends between 040° and 073° (Nwajide, 2013). According to tectonic, geographical and stratigraphical feature the Benue Trough was subdivided into northern, central and southern segment (Nwajide, 2013)while Offodile (2002) divided the Benue Trough into upper, middle and lower. Hydrologically the Trough is classified into Upper and Lower River Basins.

The lower Benue Trough comprises of two structural units, the N60°E trending Abakaliki Anticlinorium bordered by the Anambra syncline trending N30°E (Crachley and Jones, 1965 and Offodile, 1976). The Pre-Cambrian basement rock underlying the Benue valley is overlain unconformably by the lower Cretaceous sediments (Reyment, 1964).

The fossiliferous marine sequences outcropping all through the Benue Trough belongs to the Turonian age. In the Middle and Lower Benue, it is characterized by the Eze-Aku Formation, which contains hard black and grey calcareous shale, siltstone and limestone. The Eze-Aku Group is divided into two formations: the Eze-Aku shale Formation where mudstone dominates. Locally, the shale overlaps with the sandstone (Amaseri sandstone) near Afikpo. The second is the Makurdi Sandstone Formation which is composed of hard, well cemented medium to fine grained sandstones, interbedded with varying thicknesses of soft shale and occasional limestone (Nwajide, 1986). The Eze-Aku Formation varies in thickness up to 1200m (Reyment, 1965; Cratchly and Jones, 1965).

2.3.1 Regional stratigraphical setting of lower Benue valley

Stratigraphically three major depositional cycles are noted in the Benue Trough (Reyment, 1965; Wright, 1981). The lower Cretaceous sedimentary cycle is the first major cycle. It started during the middle Albian transgression. The Middle Albian transgression occasioned the deposition of very thick marine, dark, grey shale, siltstone and subordinate limestone of the Asu River Group. The group is said to be the oldest in the study area and it uncomformably overlies the crystalline basement rocks of Pre-Cambrian age (Nwachukwu, 1972). Except for fractured areas, the Asu River Group is poor in groundwater yield (Nwajide, 2013).

The upper-Cretaceous with a transgression at the termination of the Cenomanian and terminated in the early Turonian with a regression and began the second cycle. The

deposition of the Eze-Aku Group is the product of the second cycle. The Eze-Aku Group overlying the Asu River Group consists of compact flaggy calcareous and non-calcareous shales, sandy or shaly limestones, and calcareous sandstones. Aquifers in the Eze-Aku Group are found in sandstones and fractured limestones with solution cavities (Nwajide, 2013).

The third main cycle of sedimentation in the Lower Benue Valley happened between late Turonian to lower Santonian. The Awgu Formation was deposited in the Senonian stage. Reyment (1965) described a large number of lithostratigraphical and biostratigraphical divisions of the Awgu Formation. The stratigraphical and lithological relations of the sediments located in Southern Benue Trough consist of marine fossiliferous grey-blue shales associated with secondary limestone and calcareous sandstones (Kogbe, 1981). Apart from these major depositional cycles, geological studies have shown that there were other minor cycles during the Maastrichtian age. The Awgu Formation has thin lenses of sandstones which are laterally limited. The non-lateral extent (localization) of this sandstone unit within the Awgu Formation (Figure 2.6) accounts for the poor groundwater yield in the area (Nwajide, 2013).

The Enugu-Nkporo Shale, Ajali, Mamu and Nsukka Formations were deposited during the Maastrichtian cycle. The Awgu Formation is overlain by the Nkporo Shales which are found to constitute marine shale in the Nigerian sedimentary basin. Mamu Formation overlies Nkporo shale and consists mainly of sandstones, carbonaceous shale, sandy shale, and some coal seams (Table 2.1). This marks a phase of deltaic-lagoonal environment

(Offodile, 1976). Ajali Formation (false bedded sandstone) superimposes the Mamu Formation.

Table 2.1. Regional Stratigraphy of the Lower Benue Trough.

Age		Group	Formation	Description
Maastrichtian		Nsukka	Upper coal measures	Carbonaceous shales, sandstone and thin coal seams
		Ajali	False bedded sandstone	Coarse grained current bedded sandstone
		Mamu	Lower coal measures	Sandstone carbonaceous shales, sandy shales and coal seams
Senonian	Campanian	Agwu Group	Enugu-Nkporo Shale	Marine shales
	Santonian			NE-SW Trending elongate folds and faulting; igneous intrusions
	Coniacian		Agwu Shale FM	Shaley carbonaceous mudstones with thin shaley limestones and sandstones
			Agbani Sandstone FM	Fine to medium sandstones with siltstone and mudstones
Upper Turonian		Eze-Aku Group	Upper Eze-Aku FM	Shaley mudstones and siltstones with thin sandstones and limestones
			Makurdi/Otobi	Fine to coarse sandstones with siltstones and mudstone
Lower Turonian			Lower Eze-Aku FM	Shaley mudstones and siltstone with thin sandstones and limestones
Cenomanian			Makurdi	Hiatus/unconformity
Upper Albian		Asu River Group	Asu River FM	Carbonaceous Shaley mudstone, limestone, sandstone and siltstone
Lower Albian			Metamorphased Asu River FM	Pyroclastics and intrusives with contact metamorphosed mudstone, shale and sandston
Pre-Cambrian Basement			Crystalline Basement	N-S trending fault

Source: McDonald, (2012)

It contains about 330m of coarse-grained current-bedded sandstones (Cratchley and Jones, 1965). The Nsukka Formation is the last Cretaceous sediment deposited in the area. The Nsukka Formation is marked by the deposition of carbonaceous shale and sandstone and some thin coal seams (Nwajide, 2013).

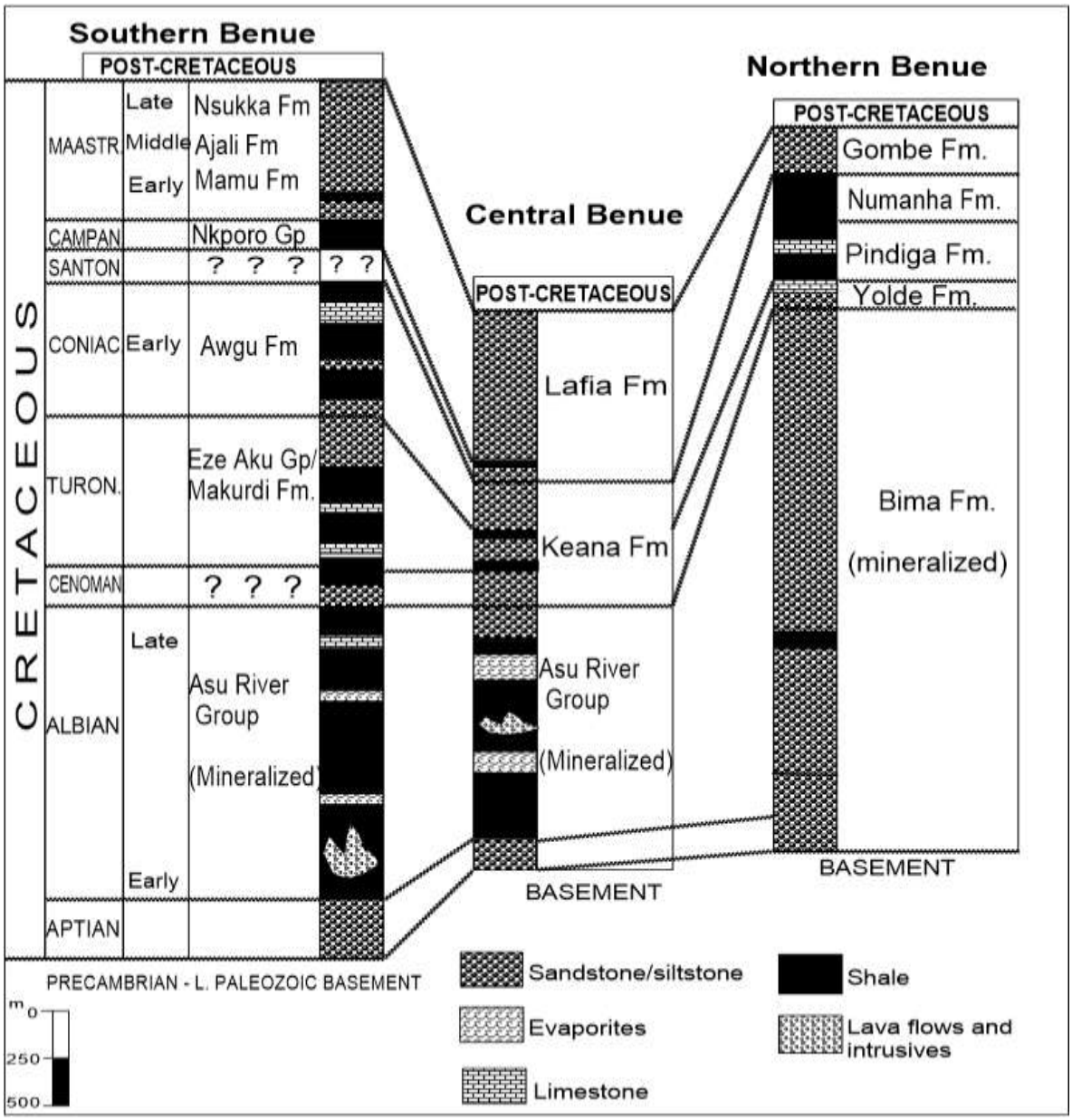

Figure 2.6: Generalized Cretaceous Stratigraphy in the southern, central and northern Benue Trough (Nwajide, 2013)

2.3.2 Local Geology of the Study Area

Otukpo is a major landscape feature that owes its origin to the Cretaceous sediments of the Benue Trough. It is classified geologically and hydrogeologically under the Southern

Benue Trough and Lower Benue River Basin (Nwajide, 2013; Offodile, 2002). The Otukpo unit of the trough consist of an intercalation of mudstone, shale, sandstone and limestone. The Benue Trough has been described as an intracontinental Cretaceous basin (Nwajide, 2013). The basin is said to be occupied by up to 6,000m of marine and fluvio-deltaic sediments that have been compressionally folded in a non-orogenic shield environment (Nwajide, 2013). The extended trough-like basin is unceasing with the coastline, and has been termed as the long arm of the coastal basin of Nigerian (Rayment, 1965).

The Cretaceous sediments of the Otukpo area are composed of the Asu River, the Eze-Aku and the Awgu Groups which are presumed to unconformably overlie the Precambrian basement rocks (Reyment, 1965). The lithological unit that characterises the area includes clay, shale, sandstone and limestone (Offodile, 2002). The folds, faults and fractures in the area are as a result of the major Santonian deformation in this area (Nwajide, 2013).

The overlapping of these different formations (Asu-River, Eze-Aku and Awgu) in Otukpo axis makes groundwater studies in the area very complex and difficult.

The stratigraphic architecture of the Otukpo axis of the Benue Trough makes it hydrogeologically complex for groundwater exploration and exploitation. Stratigraphically, the aquifer within the area is expected to be in the Agbani Sandstone formation underlying the Awgu shale within the Awgu Group (Table 2.1).

The numerous failures of boreholes in the area can be related to the complex geology and Cretaceous stratigraphy of the area (Figure 2.6). The current research will, through the

geological, hydrogeological and multi-geophysical techniques, unravel the mystery by correctly delineating the aquiferous zones within the study area.

2.3.3 Nigeria hydrological environments

Nigeria is split into eight hydrological catchments described as Hydrological zones (Figure 2.7). The hydrological catchment areas of Nigeria serve as units for surface water resources management by River Basin Development Authorities.

The complexity of the hydrologic setting of Nigeria is associated with the surface and subsurface lithologies that host the water resources in relation to climatic factors, since some surface water are recharged by groundwater and vice versa.

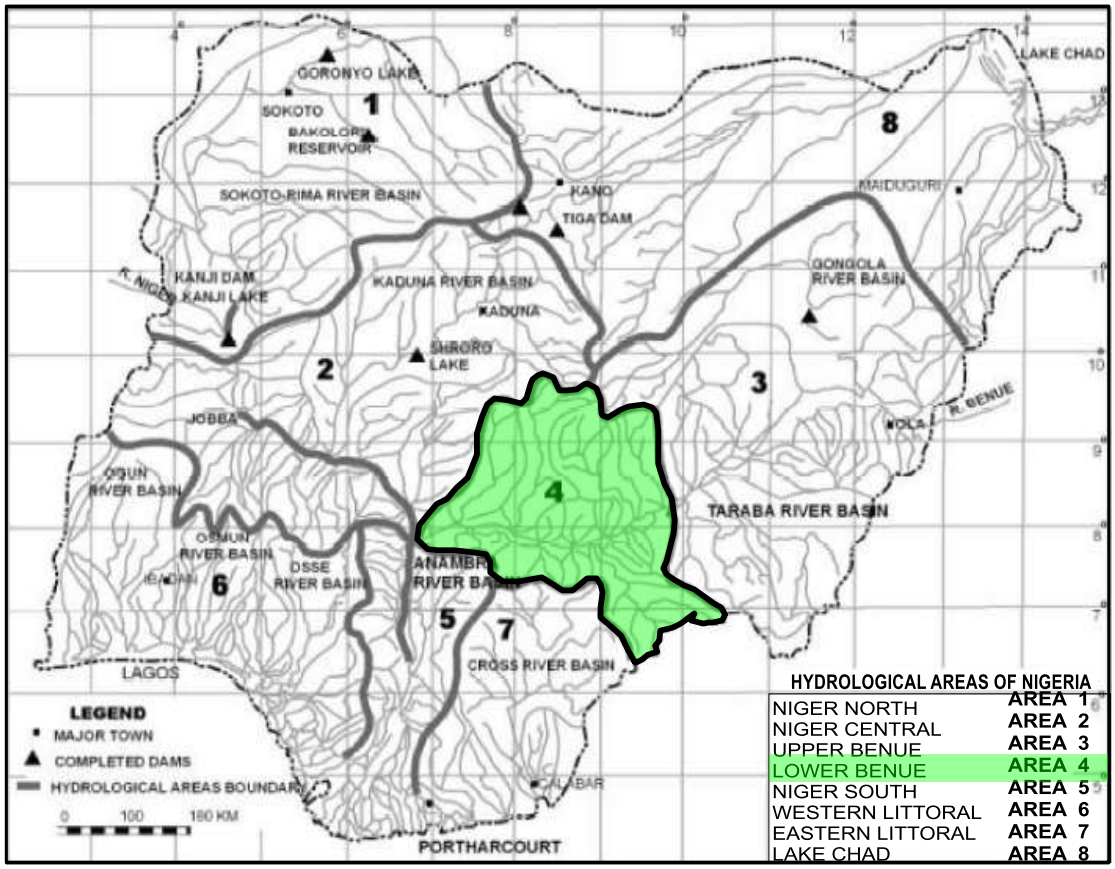

Figure 2.7: Hydrological areas of Nigeria (After FMWR, 1999)

The Nigeria's hydrological setting is characterised by areas of high permeability, moderate permeability, low permeability, high gradient, moderate gradient, high runoff, moderate runoff and low runoff, highly fractured basement and fresh basement rocks (Nwankwoala, 2015; Figure 2.8).

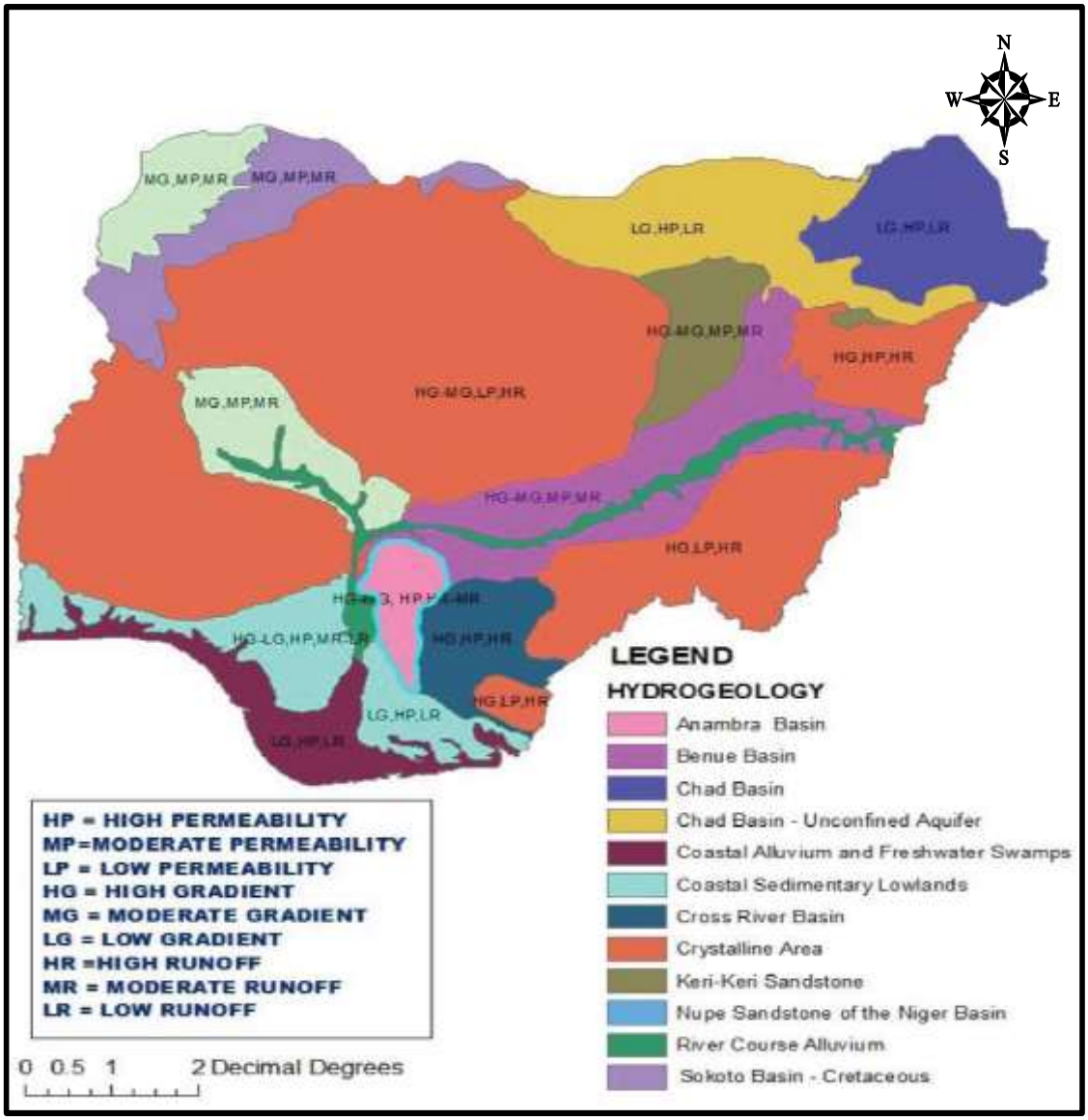

Figure 2.8: Hydrological setting depicting relative permeability and runoff potential (Nwankwoala, 2015)

2.3.4 Hydrogeological environment of Nigeria

A number of trans-boundary aquifers exist in Nigeria (Groundwater Atlas, 2019), these include:

i. The Benue Trough, shared by Nigeria and Cameroon
ii. The Chad Basin aquifer, shared by Chad, Niger, Cameroon, Nigeria and Central African Republic
iii. The Aquifer Systems of Iullemmeden, Taoudeni/Tanezrout (ITAS), shared by Nigeria, Benin Republic, Algeria, Mali, Burkina Faso, Mauritania and Niger.
iv. The Keta Basin Aquifer is shared by Nigeria, Benin, Ghana and Togo.
v. The aquifer of the Rio Del Rey Basin which is shared by Nigeria and Cameroon along the seashore

According to the groundwater report by Japan International Cooperation Agency (JICA, 2014), groundwater recharge is largely controlled by climatic factors which make recharge variable across the country. The total number of replenishable groundwater prospect across Nigeria is projected to be 155.8 billion cubic meter per year (bcm/yr). JICA (2014) gave an estimated groundwater recharge at regional level across Nigerian (Table 2.2)

Table 2.2 Expected groundwater recharge at regional level

Region	Estimated Groundwater Recharge (BCM/year)
Niger North (Northwest Nigeria)	5.0
Niger Central (West-central Nigeria)	20.5
Upper Benue (East-central Nigeria)	19.3
Lower Benue (East Nigeria)	18.6
Niger South (South-central Nigeria)	31.9
Western Littoral (Southwest Nigeria)	23.4
Eastern Littoral (Southeast Nigeria)	32.8
Chad Basin (North-east Nigeria)	4.3
Total	155.8

Source: JICA Report, (2014)

The aquifer systems are further grouped into compartmental aquifer type with potential groundwater yield (Tijani *et al.*, 2016; Figure 2.9), these include the following:

i. unconsolidated; high to very high,
ii. unconsolidated; high,
iii. volcanic igneous; low to moderate,
iv. sedimentary intergranular/fractured to moderate (locally high),
v. sedimentary intergranular; moderate to high,
vi. sedimentary intergranular; low to moderate and
vii. basement; low to moderate aquifers.

The complex hydrogeological setting of Nigeria is in control of the uneven distribution of groundwater across the country.

2.3.5 Surface water

Nigeria is rich in surface water resources even in the extreme NW for example, from the highlands to the lowlands. In Nigeria, there are two main rivers namely: Rivers Niger and Benue. Several rivers are a tributary of either River Niger or River Benue (Figure 2.10) while others discharge into the Atlantic Ocean directly. These tributaries of the major rivers include but not limited to Anambra River, Kaduna River, Taraba River and Cross River. Surface water is not totally unconnected with groundwater in most cases. The streams are either being fed by the groundwater system (gaining stream) or the groundwater is being recharged by the streams or rivers (losing stream). A stream can contain both losing and gaining reaches.

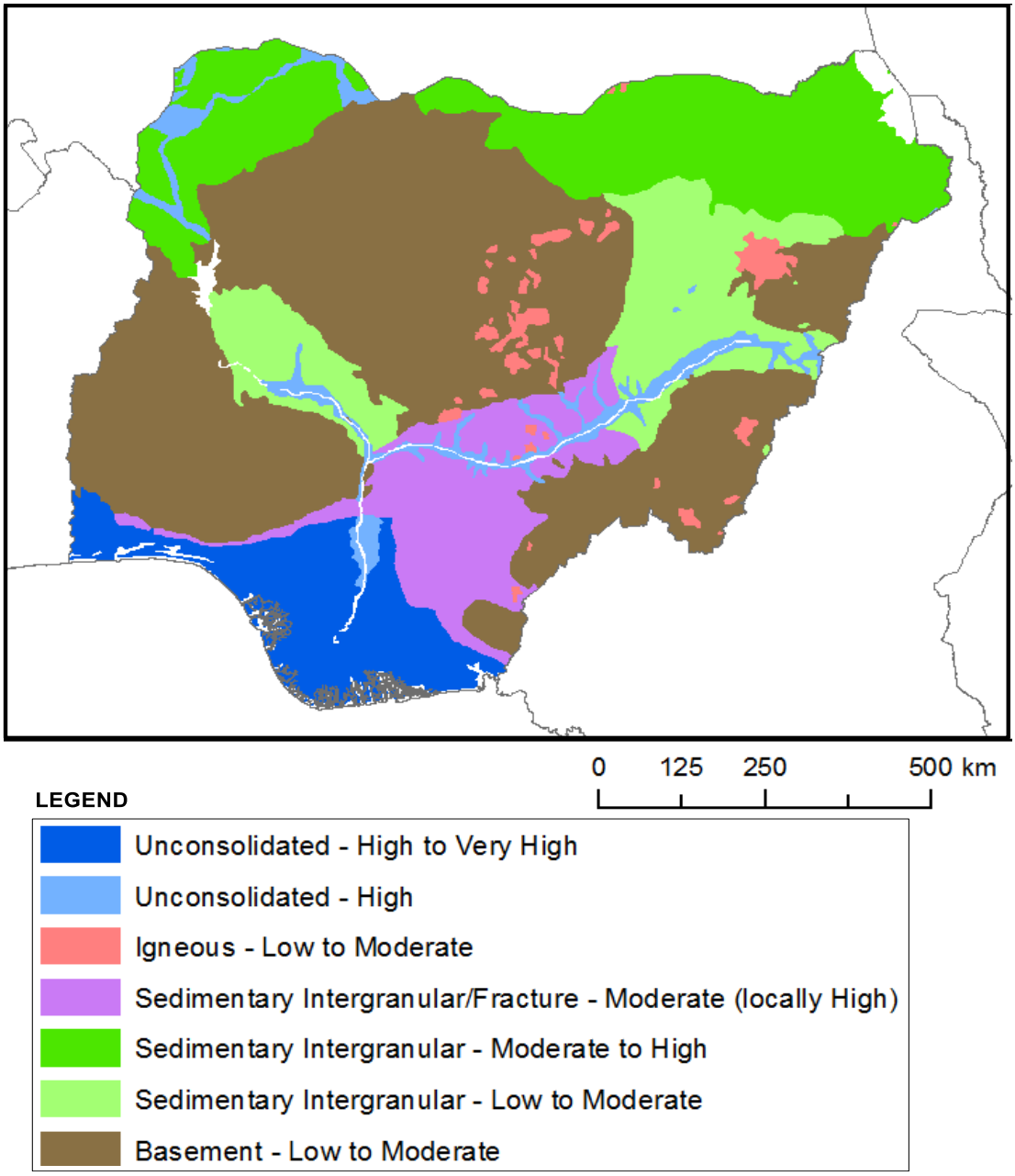

Figure 2.9: Nigeria Aquifer Type and Productivity (Tijani *et al.*, 2016)

A gaining stream is a stream that is being fed by an unconfined aquifer, which water-table is normally above the stream level. The downstream flow of a gaining stream is perennially sustained due to their recharge by groundwater.

A losing stream is a stream that literally recharges the groundwater system. The water table along losing stream is generally below the stream bed. Most losing streams will contain some water flow after an appreciable precipitation while other losing streams are essentially dry most of the time (seasonal).

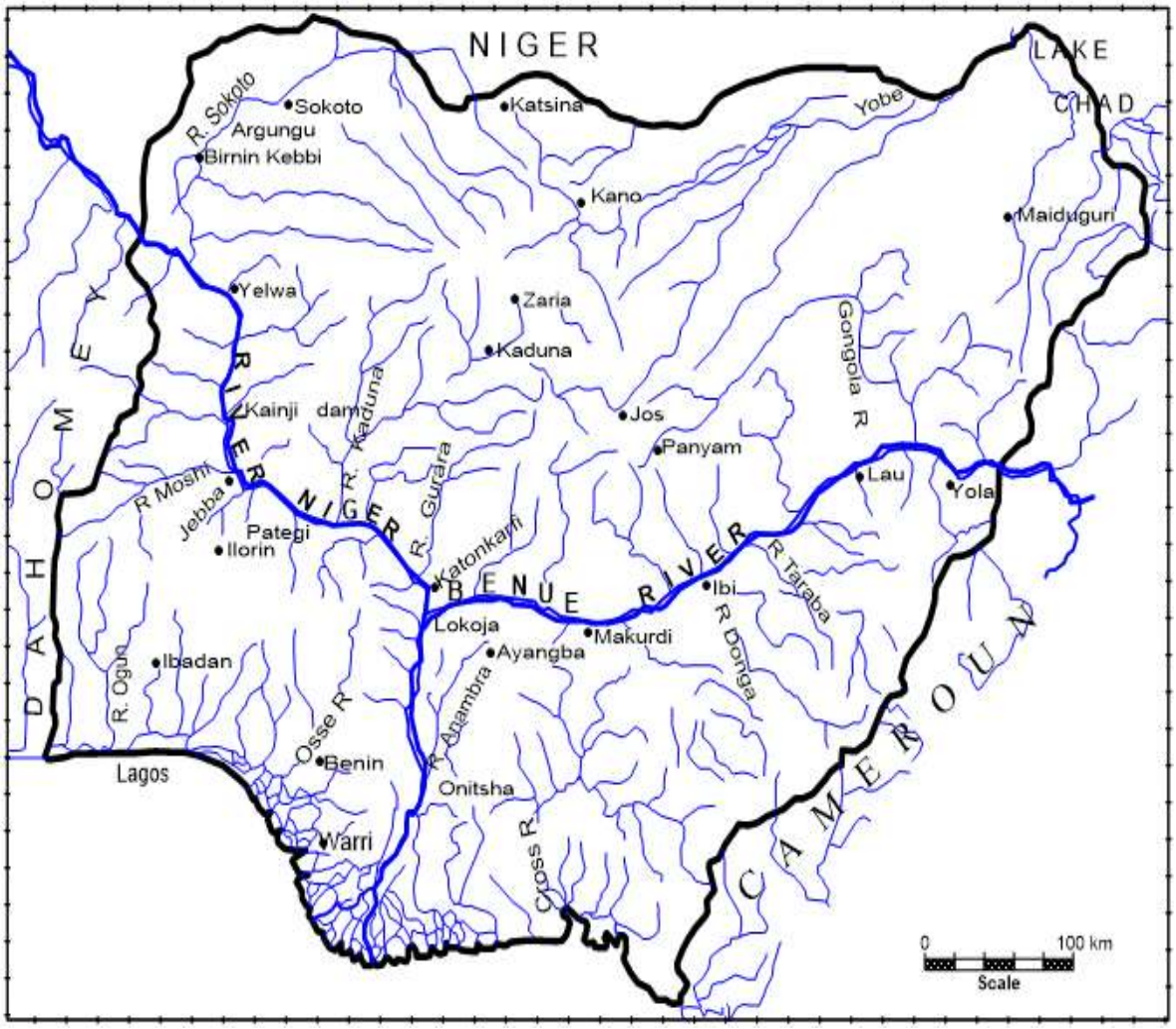

Figure 2.10: Nigeria Drainage Systems (Taiwo *et al.*, 2012)

2.3.6 The river basin development authorities (RBDA) in Nigeria

This body came into being in the wake of the proclamation of Decree 25 of 1976. The RBDA Act; cap 396 Laws of the Federal Government of Nigeria, 1990 established 12

RBDA in Nigeria. The river basin authorities include the Anambra-Imo Basin, Benin-Owena Basin, Chad Basin, Cross River Basin, Hadeja-Jamaare Basin, Lower Benue Basin, Niger Delta, Lower Niger Basin, Ogun-Oshun Basin, Sokoto-Rima Basin, Upper Benue Basin and the Upper Niger Basin. The authorities are liable for the development, procedure, management and maintenance of natural water resources in various catchment areas of Nigeria. The river basin authorities of Nigeria do not have adequate coverage and extent of hydro-geological units that can aid and enhance capable groundwater administration in the country (Nwankwoala, 2015).

The disconnection in the management of surface water reserves deprived of due consideration of groundwater resource has provided meaningfully to unmaintainable and insufficient supply of water in the country.

2.4 Review of Geophysical Related Literature

Nwabineli *et al.* (2012) used electrical resistivity method to define lithological units, geological formations and depth to water table in the Lafia sub-basin of the Lower Benue valley. It was revealed that the Lafia sandstone upper aquifer take in the Awgu Formation which consist of grey bedded shale with intermittent sandstone beds and limestone in the area of study. The sandstone was revealed to extend to the depth of 220 x 0.3048 m approximately 67.1 m (220 feet) within the studied area. Amadi *et al.* (2013) used geological and geophysical principles to investigate groundwater in and around Paiko area. The quantitative and qualitative interpretation of resistivity data using Schlumberger configuration of electrical resistivity approach was utilized to establish viable point for borehole siting.

A comprehensive geophysical and hydrogeological study aimed at locating optimal drilling points at Daura was carried out by Mijinyawa *et al.* (2013). Lithological logs from the adjourning towns of the study area were used to decipher the subsurface geology of the area. The Schlumberger configuration was utilized with the AB electrodes separation of up to 350 m. Quantitative treatment and analysis of data was used to delineate distinct geoelectric layer. It was noted that qualitative interpretation of subsurface information provides control and confirms the inference drawn from geophysical investigation. Three optimal drilling points for groundwater development were identified based on the study.

Ogah and Jatau (2014) observed two layers of sedimentary features in Otukpo area using airborne magnetic survey. They established that the average thickness for the first and second observed layers is 0.37 km and 1.8 km respectively. It was stated that the depth to basement within Otukpo area ranges from 3 to 8.2km. Omali (2014) worked on the geophysical investigation of groundwater in Lokoja. The research investigated the continuous borehole collapses attributed to poor groundwater exploration in the area. Types of aquifer, depth to aquiferous units and geoelectric layers were determined from geophysical investigation. Idri-Nda *et al*. (2015) stated that groundwater occurrence is the outcome of a limited pattern of climatic, hydrological, topographical, geological and soil producing elements which all together structure an incorporated active system. Identifying these procedures will go far in guaranteeing that groundwater is established maximally for use. In their study of the sedimentary deposit (sand, clay and shale) of the mixed geological terrain, it was discovered that groundwater occurs in the sandstone formation.

Nwankwoala (2015) worked on the hydrogeology and groundwater resource of Nigeria. It was noted that groundwater basins in Nigeria are difficult to manage as a result of insufficient information. Emphasis was made on the necessity for dependable figures and precise information and suitable know-how in furtherance of water resource development for any meaningful water resource strategy in Nigeria. Unuevho *et al*. (2016) integrated geophysical technique of low resistivity anomaly, electrical anisotropy, longitudinal unit conductance and traverse unit resistance to identify areas with deep water bearing fractures in north-eastern Bosso, Minna.

Wait (1982) defined the time domain induced polarisation attribute as the upsurge with time of the overvoltage initiated by an immeasurable unit current step.

Slater and Glaser (2003) provide an expression and suggest that opposing special effects of exterior density charge and surface ionic movement on exterior surface conductivity may give reasons for the dependency of IP measurements on fluid conductivity in the materials. They showed that IP factors are a major function of lithology saturation and display hysteretic behaviour over a cycle of drainage and imbibition. Their study recognised relations between induced polarization (IP) dimensions and lithological factors are noticeable even when lithologic inconsistency is limited to a slight range, as is typically come across in a sequence of sandy and clayey deposits. They suggest that competing special effects of near surface density charge and near surface ionic mobility on near surface conductivity (resistivity) may expound the reliance of IP measurements on the fluid conductivity in earth geomaterials. Their submission favours the utilization of IP for examining lithological inconsistency in near-subsurface. Slater and Lesmes (2002) in

applying field studies illustrated how areas of high and low clay matter may be defined regardless of pore fluid interaction.

Braga *et al.* (1999) correlated induced polarization and electrical resistivity data with geotechnical survey standard penetration test measurements. The work characterizes the geoelectric nature of clayey and sandy formations and targeted at obtaining a correlation of the geoelectrical parameters with the geotechnical Standard Penetration Test (SPT). The work shows geoelectrical identification of lithology and an approximation of the link between the geoelectrical parameters (resistivity and chargeability) and Dar Zarrouk parameters (transverse unit resistance *T* and longitudinal unit conductance *S*) with the geotechnical survey Standard Penetration Test (SPT). It was established that the studied clay presented resistivity and chargeability values decreasing in relation to increase in the clay degree, changing from 35 ohmm to 12 ohmm and 45.0 mV/V to 1.5 mV/V. Unpolluted clays are typified by low resistivities and low polarizabilities while strata of clay-siltstones are characterized with intermediate resistivities and high polarizabilities.

The IP survey information gives access to extra information around the spatial dissimilarity in fluid chemistry, pore-water content and grain-surface geometry determination. This is because both the capacitive and resistive properties of the soil are determined in IP survey method (Binley and Kemna, 2005).

Andy *et al*. (2012) reported that it is possible to resolve for geological structure using both electrical resistivity and induce polarization method. Gonzales *et al*. (2016) studied the geometry of the aquifer structure in the alluvial fan Punata using geoelectrical techniques of electrical resistivity tomography and IP. The study proved the applicability and

effectiveness in describing the layering and thicknesses of the diverse geological elements in the alluvial fan of Punata. They resolved that the geoelectrical procedures of electrical resistivity tomography and standardized chargeability are valuable and efficient methods for mapping the aquifer systems in the Punata alluvial fan, and in other geological terrains.

Brandes (2005) reported that clay chargeability not attributed to geometric effect can be negative. It was established that, contrary to previous views, negative chargeability effects can be an intrinsic property of clay-rich sediments. The obvious distinction made is that negative chargeability outcomes are noted down when the density of current is non-linear.

Brandes and Acworth (2003) demonstrated the fundamental negative chargeability of soft clays. Lithologies possessing high clay matters could have negative chargeability. This reaction is commonly credited to symmetrical outcomes in electromagnetic and induced polarization surveys. Negative chargeability is attributable to electrical storing practices that scatter to create potentials in the reverse view to the employed potential. It was suggested that cation exchange processes, oxidation reduction reactions, peripheral dispersions are not a basic cause of the negative chargeability. It was suggested that electrokinetic fluidities may give negative chargeability outcomes, but at possibly too low frequencies. Near-surface diffusion of OH^- and H^+ ions towards clay lattice yields electrical currents in the reverse direction to the current applied, and therefore produces negative chargeability. Chargeability can likewise give a signal of clay water content: as negative chargeability results are only probable in clays with contents of water exceeding roughly 45% of their liquid limit.

There is at the moment, no readily available source of data on the hydrogeology and hydrogeophysics of Otukpo and its environs; the gap which this research intends to fill.

The study will among other things provide qualitative, quantitative and scientific base models for aquiferous units in the study area.

2.5 Origin of Water on Earth

The hydrosphere is the inter-relationship amongst the atmosphere, biosphere and lithosphere. There exist an assimilating in the fluxes of energy, water and geochemical compounds between the spheres. The hydrosphere is estimated to contain about 1.4×10^9 km^3 of water, which is about 17% of the earth's water quantity. Of the earth's water quantity, 96% is accumulated as saline water in oceans and seas.

It is largely recognized that the earth's mantle degassing by eruptions of volcanoes and sprouting lava (basalt) in the progression of the 4.5 billion years of the existence of the Earth is responsible for the hydrospheric water origin. An extra-terrestrial origin of the earth's water is believed to be from the earth's exposure to collisions with cosmic material, which included ice comets **(**David and Larry, 2005).

Almost all the groundwater on earth is considered to be a part of the hydrological cycle, to this fact, there is exception of some genetic groundwater which exists but have been in no interaction with the atmosphere for a considerable part of the geologic history. This genetic groundwater types include juvenile water, connate water, metamorphic water and magmatic water (plutonic and volcanic waters) (Figure 2.12).

Juvenile water consists of water of cosmic or magmatic origin that has not been a part of the hydrosphere for an appreciable geological time.

Connate water is water trapped in the interstices (pores) of sedimentary rock (subsequently buried by younger sediments) or igneous rock when it was deposited and has been in no interaction with the atmosphere for a considerable geological time.

Metamorphic water is the water associated with geological formations during early stage of metamorphism.

Meteoric water is the recent water that is contained in the atmospheric space and falls to the surface of the earth as dew or rain.

2.6 The Hydro-Tectonic Cycles

The Earth is characterised by an active system, by means of inner activities powered by interior production of heat and the exterior activities powered by solar energy. Both the internal and external processes, each with its own temporal and spatial scale work together in phases of nature's substance and flows of energy.

The hydro-tectonic activity is powered by currents of thermal convection (internal heat), which shift the inflexible lithosphere above the more flexible asthenosphere (Figure 2.13). Magma ascends upward into up-lying fractures (spreading centres) in the sea floor, where novel oceanic crust is produced. This makes the lithosphere to shift away from the centre of spreading from one end. At the further end of the convection cell, the lithosphere descends down in a zone of subduction. Where older lithosphere vanishes in the mantle, ocean water is pulled with the crust to depths of hundreds of kilometres beneath the earth and come to be included in the re-melting of sediments to form new magma. The associated volcanic and magmatic activity exhaled part of the water in the subsurface. This complete development is known as the hydro-tectonic cycle (Figure 2.11).

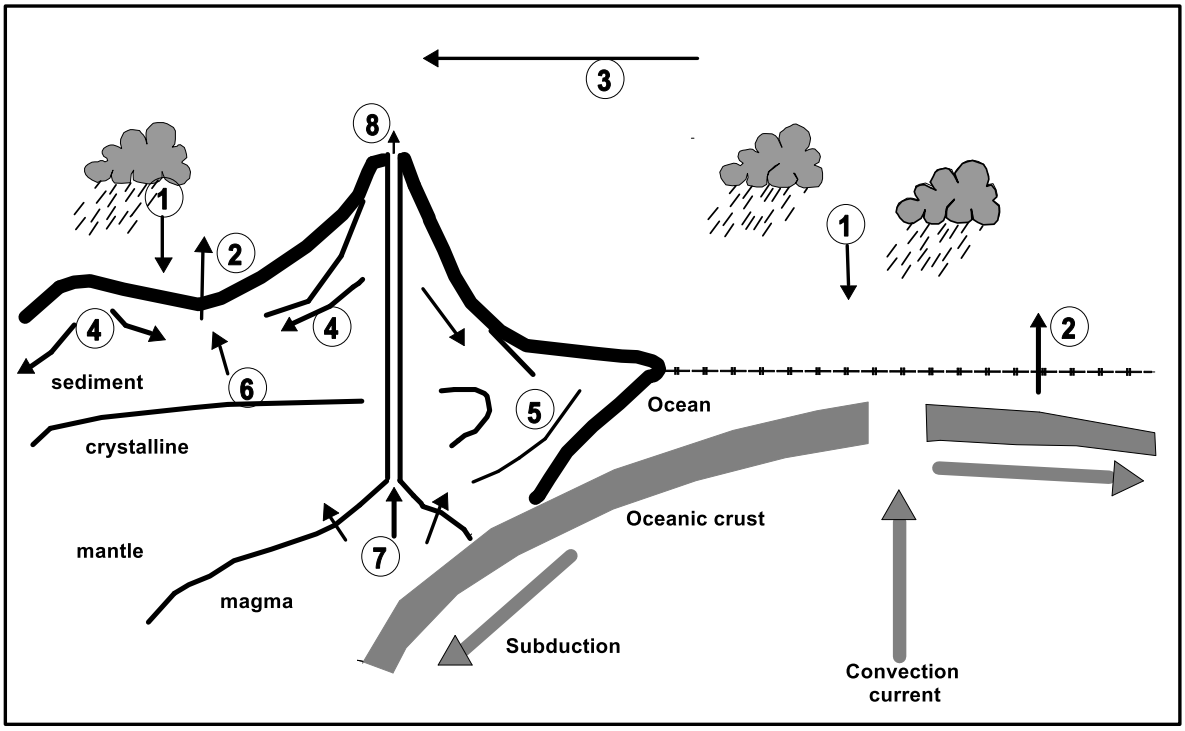

Figure 2.11: Schematic illustration of the hydro-tectonic cycle (IAEA-UNESCO, 2000)

1 Precipitation
2 Evapotranspiration
3 Vapour transport reactions
4 Topography driven flow
5 Sea(water) trapped in subducted sediments(connate water)
6 Fluid released by deformation
7 Fluid released from magma and metamorphic(meteoric water)
8 Volcanic emissions

2.6.1 Hydrological cycle

The hydrological cycle is characterised by the continuous recirculation and perpetual interchange of water between oceans, land and atmosphere (Figure 2.12). The water on earth now has been the same water on earth since the beginning of the earth according to the book of Ecclesiastes Chapter one, verse seven. In the hydrological cycle, water is believed to evaporate from the surface (Ocean) into the atmosphere; condenses to produce clouds, drops unto the land as rain, moves through wetlands, rivers, lakes and underground

then comes back to the ocean. The principal motivating force aiding the hydrological cycle is solar energy.

A shift in one of the components of the hydrologic system should result in a modification somewhere in the structure, which consequently can initiate alterations in other systems. Prevailing climatic conditions and vegetation cover are responsible for the seasonal variation in the hydrological cycle leading to change in the meteorological conditions. There are three key phases in the water cycle which includes evaporation, condensation and precipitation. Other components that constitute the hydraulic cycle include infiltration and surface runoff.

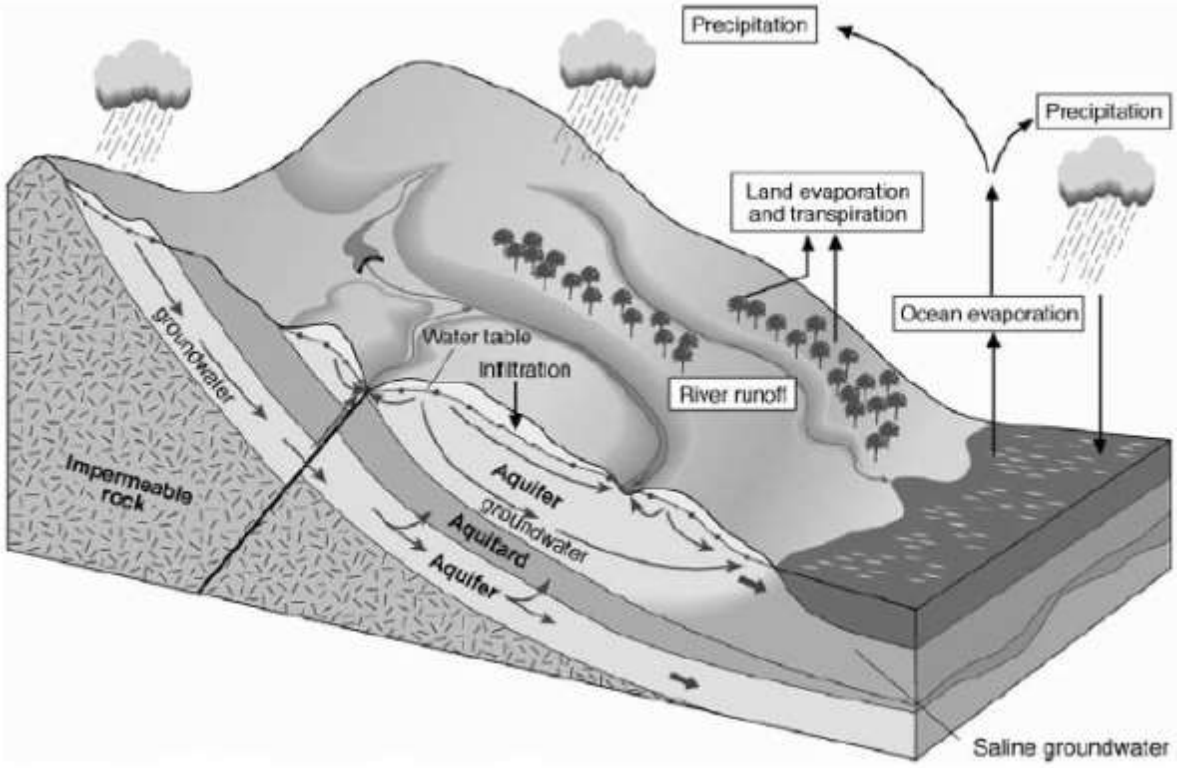

Figure 2.12: Hydrological Cycle (After Morris *et al*, 2003).

Precipitation in the mode of rainfall and melting from ice and snow are the major sources of recharge or inflow into the hydrologic system. Runoff and evapotranspiration (evaporation from water surface, soil and transpiration from plant) are the primary sources of outflow in the system. Precipitations reach the rivers and streams on the surface of land as overland current to tributary outlets, and infiltrate the subsurface as base flow or interflow (Figure 2.12). Section of the precipitation that permeates greatly into the subsurface might build up atop an impervious lithological layer and inundate the existing opening to create a groundwater body which leads to aquifer formation under favourable geological conditions. The water held in aquifers adds to the groundwater constituent of the hydrologic cycle from which natural seepage enter rivers, streams, wetlands and the oceans.

2.6.2 Groundwater system in the hydrologic cycle

Groundwater constitutes one of the earth's water circulatory systems. Porous and permeable geological formations of the earth serve as conduits for water transmission and as reservoirs for water storage in the subsurface. All groundwater practically originates as surface water (David and Larry, 2005). Water infiltrates the subsurface from the surface of the ground or from surface water bodies. The infiltrated water travels gradually for several expanses till it come back to the surface by the actions of humans, plants, evaporation and natural flow to the surface such as springs. Some of the infiltrated water reaches beyond the water-table where it becomes groundwater. Where hydraulic gradient drops down in an inland trend along the coast, sea water can move into groundwater. The natural discharge of groundwater may occur as flow into surface water reservoirs such as oceans, streams, lakes

and rivers. The artificial discharge of groundwater is through pumping from constructed water wells (Willem, 2000).

The descending passage of infiltrated water into the ground in unsaturated region is through the influence of gravity, while in the saturated zone water movement is determined by the surrounding hydraulic head situation (Allen and John, 1979). The groundwater system constitutes the flow and storage patterns of water. The groundwater flow system constitutes the lithologic porous and permeable media containing the water, surface water, flow boundaries, outcrop areas, springs, inter-aquifer flow and wells that penetrates the aquifer. The groundwater travel time under natural conditions can range from less than a few hours to more than a million years while the age of the water can range from recent precipitation to water trapped in formations in geological time.

The interactions between groundwater and surface water are dependent upon factors which include position of the groundwater system relative to the surface water system, climatic condition and characteristics of the groundwater and surface water systems and their underlying materials (David and Larry, 2005).

Typically, most infiltrated water from precipitation source does not recharge groundwater directly; instead it is intercepted and stored in soil and plant zones. Precipitation ultimately restored to the atmosphere via the means of vaporization and transpiration (Figure 2.13).

Groundwater flow system can be on a regional, intermediate or local basis. On a regional groundwater flow system, the groundwater revitalize zones are by groundwater divides while the discharge zones are located at the tail foot of drainage divides. In the intermediate

groundwater flow system, the groundwater discharge and recharge areas are divided by topographic high and low.

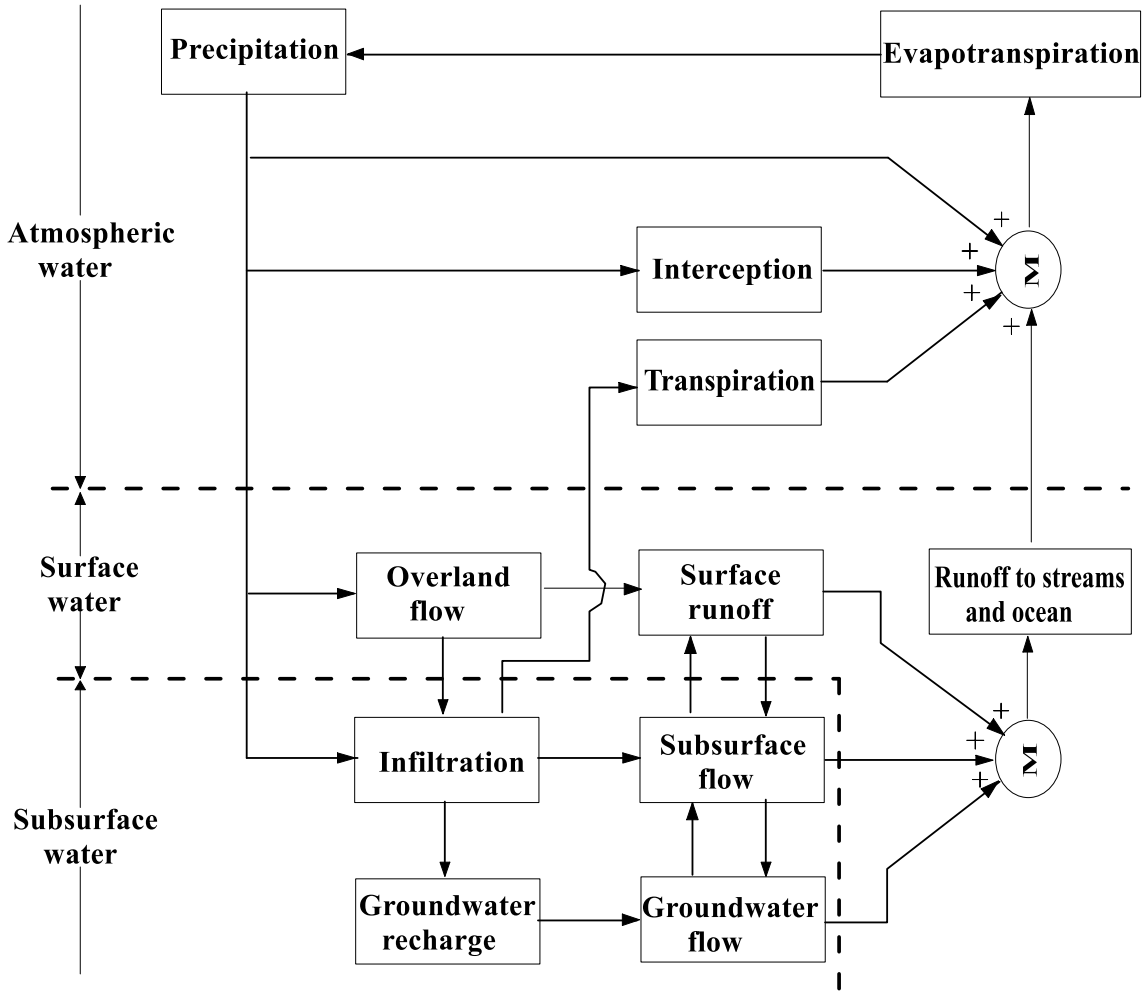

Figure 2.13: Schematic illustration of hydraulic cycle (Allen and John, 1979 & David and Larry, 2005)

In the confined groundwater flow system, discharge and recharge areas are bordering each other. The largest amount of groundwater movement occurs in the local system of flow. The regional groundwater flow system is less transient than the local and intermediate groundwater flow systems. All aquifers are not synonymous with each of this groundwater flow types (David and Larry, 2005).

A quantifiable method of estimating the hydrological cycle is through hydrological equation. It is expressed as Precipitation = Infiltration + Runoff + Evapotraspiration ± Soil Storage i.e. $P = I + R + E_T \pm S_S$. It can also be stated as: Inflow = Change in storage ± Outflow. The expression is time supported. The fundamentals of inflow ought to be determined over the same time episode as the discharges.

2.7 Lithology, Stratigraphy, and Structure of Geological Formations

Lithostratigraphical and structural signature of formations and deposits are the factors responsible for the control of the nature and distribution of aquifer systems (David and Larry, 2005). The physical and geometrical makeup of the geological system including the grain size, grain packing and mineral composition determine whether a formation is aquiferous or not. Stratigraphy as a geological term describes the geometrical and age between beds of sedimentary origin. Stratigraphic features such as unconformities are important in hydrogeology. Structural features are geometrical properties of a geological system produced by deformational processes after deposition, crystallization and or tectonism.

Understanding of the stratigraphy, lithology and structure of geological formations steers openly to a conception of the circulation of groundwater systems in any locality (Amadi *et al*., 2013). An unconformity is a surface in the geological process that signifies a period of time in which accumulation was insignificant or non-existent. It can also be associated with the outcome of the process through which the surface of the obtainable rocks were fractured, weathered or wear down. Before the accumulation of new geological matters on

the unconformity the underlying formations are distorted or tilted. Aquifers are associated with unconformities (Offodile, 2002).

Because of the geological complexity associated with geological unconformity due to faulting and folding, aquifers are difficult to detect. In a complex situation such as this the main form of groundwater investigation is often large-scale structural analysis of the geological feature.

2.8 Groundwater Occurrence and Distribution

The entire column of water below the surface of the earth is denoted subsurface water. Groundwater describes only the water in the zone of saturated below the water-table.

The occurrence of subsurface water could be split into two areas which include aeration zone and the saturation zone. Zone of aeration, is the sector partly filled by air and water while the saturation zone is the zone which the pores are filled with water in hydrostatic pressure. Vadoze zone which exist within the zone of aeration is characteristically divide up into the zone of soil water, middle zone and the capillary zone (Figure 2.14). The boundary of the saturated zone is marked from the greater surface of the saturated zone down to the impervious rock underlying the area. The water found within the zone of saturation is called groundwater (David and Larry, 2005).

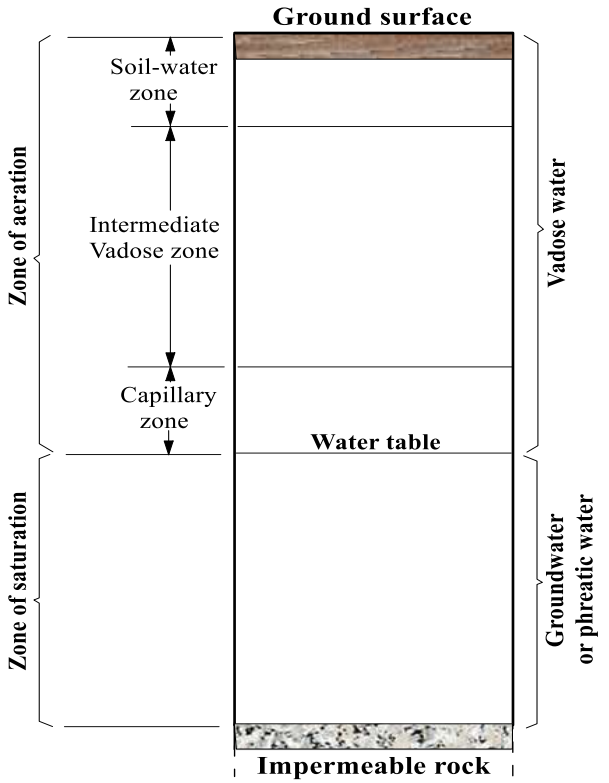

Figure 2.14: Subsurface Water (David and Larry, 2005)

The depth upon which groundwater is met is governed by topography, subsurface lithology and climatic conditions. The occurrence and distribution of groundwater in different geological formations (aquifers, aquitards, aquiclude and aquifuge) in a region are determined by the hydraulic properties of the formation in terms of the porosity and permeability.

In terms of volume, the most essential part of the effective earthly hydraulic cycle is groundwater (Table 2.3). The oceans and sea contains about 97.5% of water. Excluding the water in the polar ice caps and glacier, groundwater accounts for nearly all the useable fresh water resource on earth. Groundwater constitutes about 95% of the total fresh water on

earth while rivers, lakes, swamps and reservoirs contains 3.5% and soil moisture contains only about 1.5% (Freeze and Cherry, 1979).

Table 2.3. Estimated World Water Balance

Parameter	Surface area (10^6 km^2)	Volume (10^6 km^3)	Volume (%)	Residence time
Oceans and seas	361	1,370	97	~ 4000 years
Groundwater	130	8	0.5	Weeks – 100 000 years
Icecaps and glaciers	17.8	27	2	10-100 000 years
Lakes and reservoirs	1.55	0.13	< 0.01	~ 10 years
Soil moisture	130	0.07	< 0.01	2 weeks – several years
Atmospheric water	504	0.01	< 0.01	~ 10 days
Swamps	< 0.1	< 0.01	< 0.01	1 – 10 years
River channels	< 0.1	< 0.01	< 0.01	~ 2 weeks
Biospheric water	< 0.1	< 0.01	< 0.01	~ 1 week

Source: UNESCO, (1999)

2.8.1 Sedimentary formations

Sandstone: According to Freeze and Cherry (1979), sandstone represents roughly 25% of the Earth's sedimentary rock. Sandstone strata, form regional aquifers with high quantity of groundwater storage. Sandstone bodies own their origins to depositional environments such as marine shoreline, floodplain, aeolian and deltaic environments. Compacted standstone commonly have lower porosity because of the cementing materials between the grains compared to non-indurated sands which are free of any binding materials. The most common cementing materials binding sedimentary grains together include silica, calcite, and clay minerals. In severe situations, porosity of indurated sandstone is below one percent and their hydraulic conductivities come close to those of shale and unfractured siltstone.

Carbonate Rock: Calcite and dolomite are the minerals that constitute the major carbonate rocks which include limestone and dolomite. Dolomites are considered as secondary rock produced by the geochemical modification of calcite. The mineralogical conversion of calcite to dolomite causes an increase in porosity and permeability (Freeze and Cherry, 1979). Geologically the porosities of young carbonate rocks commonly range from 20% for limestone that are coarse and blocky to above 50% for poorly indurated chalk (Davis, 1969). Appreciable secondary permeability is associated with most carbonate strata due to fractures all along bedding planes. Stress conditions consequent of dissolution of calcite or dolomite by saturated groundwater can also cause changes that would enlarge secondary openings in carbonate rocks (Freeze and Cherry, 1979)**.** The pattern of flexible carbonate minerals is usually recrystallized and compressed into a less permeable, denser rock stack.

Intensive studies of lineaments in carbonate rock by Lattman and Parizek (1964) have revealed that the chance of obtaining productive wells in carbonated rock is critically improved if drilling locations are situated along lineaments or at lineament intersections.

Coal: Coal beds mostly occur within sequence of sedimentary rocks formed in deltaic environment of floodplains. Joints and fissures along bedding planes are responsible for the bulk hydraulic conductivity of coal seams. The bulk fracture porosity of coal seams is mostly a minor portion of 1%. In fewer cases, the coal seams occur below or above sandstone originating from floodplain but in cases where sandstone and coal occur jointly, they function as a sole aquifer unit (Freeze and Cherry, 1979).

Shale: Freeze and Cherry (1979) reported that the densest and most widespread aquitard in the sedimentary architecture is the shale bed. Shale is a product of clay as a result of

diagenetic processes that are associated with the compaction and tectonic activity that takes place in the ocean bottom or swamp environments of broad floodplains. The clay from which shale is formed prior to its burial can have porosity of up to 70% to 80% but after diagenesis the shale commonly has a main porosity of below 20% and in some instances below 5% (Freeze and Cherry, 1979). Most shale outcrops are generally brittle, fractured and permeable but at depths they are softer (plastic shale) with insignificant fractures and very low permeability. It is shown from the relation of Darcy (Darcy, 1856) that yet under resilient hydraulic gradient; groundwater in plastic shale cannot travel at levels exceeding a few centimetres per period. These rates of groundwater movement are barely important on a time scale of man, but then on the time scale of geology the groundwater flowing across complete shale can be an important part in the water finances of regional aquifers restrained by shale (Freeze and Cherry, 1979).

2.8.2 Groundwater flow system

Groundwater system of flow is a distinct, inaccessible three-dimensional system having water flow pathways from the spot at which revitalizing water go into an aquifer to the topographically lower spot at which the water exits the aquifer (Chilton and Seiler, 2006).

2.8.2.1 Groundwater movement

The factors that influence groundwater movement are on the bases of Darcy's law (Darcy, 1856; Ford and Williams, 1989). These features comprise hydraulic head, hydraulic

gradient, velocity, geology, topography, aquifer type, soil and aquifer property. Groundwater moves from higher potential energy to lower potential energy.

Darcy's Law was stated by Henry Darcy in 1856. The law states that the amount of water flowing past a conduit is proportional to the variance in the height of the water between two ends of the conduit (hydraulic head) and inversely proportionate to the flow length in the conduit. Flow is likewise proportional to a constant, K, which is known as hydraulic conductivity (Figure 2.15). Darcy's Law offers an effective depiction of the groundwater flow in most naturally arising lithological/hydrogeological states (Chilton and Seiler, 2006).

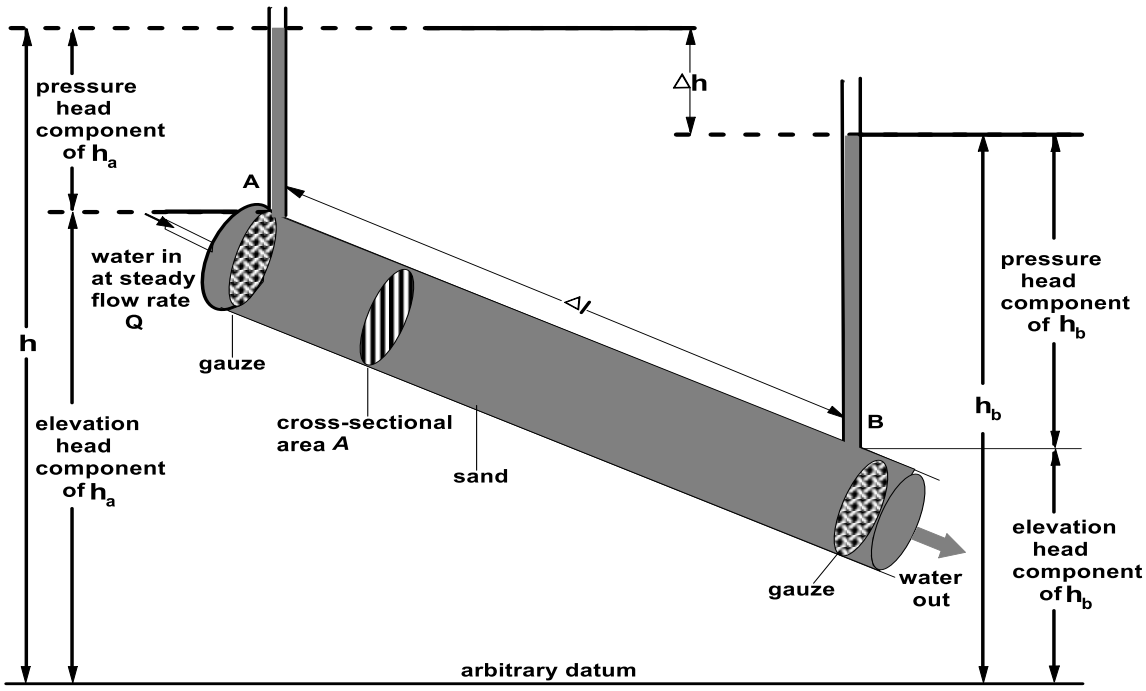

Figure 2.15: Darcy's experiment (After Fetter, 2007)

Q˜ h_A - h_B and Q˜ 1/L and Q˜K

Mathematically Darcy's law is expressed as

Q = KA [(h_A - h_B) / L] or Q = KA/ (dh/dl)

Where:

Q = water flow volume in m^3/day

K = hydraulic conductivity in m/day

A = cross sectional area in m^2

dh/dl = hydraulic gradient

Conventionally the Darcy's Law equation is written with a minus mark for flow in the trend of reducing hydraulic heads (Chilton and Seiler, 2006).

2.8.2.2 Velocity of groundwater movement

From Darcy's law how fast water can move from one point to the other or the velocity of water can be estimated. Porosity (n), hydraulic conductivity (K) and hydraulic gradient (dh/dl) are the major parameters used in computing the velocity of groundwater.

V = (K/n)/(dh/dl)

2.8.2.3 Hydraulic head

Head is the altitude of a column of water above a datum plane (Figure 2.16). Total Hydraulic head (H_T) is the determination of the energy (mechanical) that triggers the flow of groundwater. Groundwater flows in the direction of decreasing hydraulic head (from high to low head). Groundwater recharge zones are regions of high hydraulic head while regions of low hydraulic head are typical of groundwater discharge zones (Dawei, 2010; Kelvin, 2005)

Hydraulic head can be determined by two methods

(a) The addition of elevation heads (z) and pressure heads (h_p).

$h = (h_p+z)$

(b) The difference between the ground surface elevation and the depth to water level in well.

h = (land surface elevation – depth to water in a well)

The pressure head (h_p) is the altitude that water increases in a piezometer (well that is exposed simply at the bottom and top of its casing). Elevation head (z) is the bottom of the piezometer elevation or evaluating point in feet above mean sea level. The velocity head in groundwater flow is often negligible, and therefore neglected in the parameter computation.

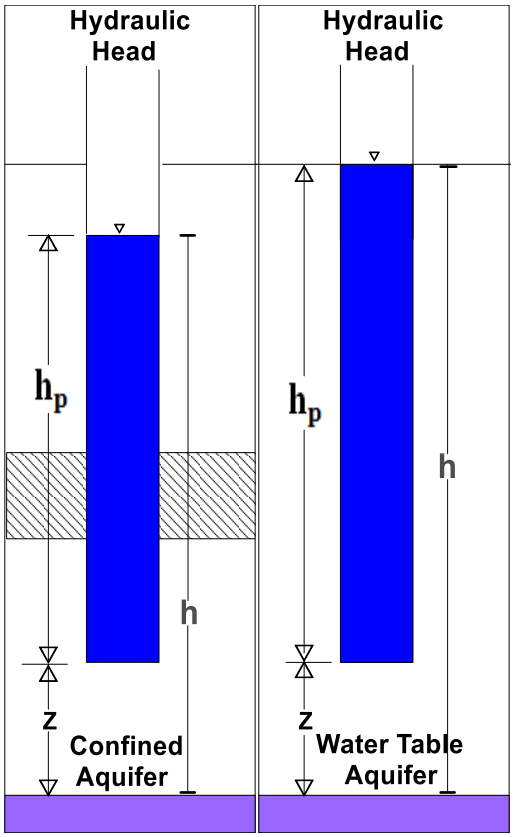

Figure 2.16: Schematic illustration of hydraulic head

2.9 The Relationship between Geology and Resistivity

Resistivity surveys provide a depiction of the distribution of the subsurface resistivity. Several information of the typical values of resistivity for diverse varieties of near subsurface materials and the lithology of the area investigated is useful in converting the resistivity values into a geoelectric value for corresponding subsurface formations (Loke, 1999).

Table 2.4 shows the values of resistivity of soil natural materials, ordinary rocks and chemicals (Loke, 1999; Daniels and Alberty, 1966; Keller and Frischknecht, 1966). Metamorphic and igneous rocks show high values of resistivity. The resistivity of the crystalline rocks is significantly reliant in the amount of rock fracturing, and the fraction of the fissures occupied by groundwater. Sedimentary lithologies are extra porous and have greater content of water. Compared to the fresh basement rocks, sedimentary rocks usually have lesser values of resistivity. Wet subsurface soils and fresh groundwater have even lesser values of resistivity. Clayey/shale soil also has lesser value of resistivity than sandy/silt soil. They normally occur as overlay in the values of resistivity of the diverse types of rocks and soils as they turn to exist without a definite boundary in the subsurface. This is as a result of the resistivity of a specific soil or rock sample that depends on a number of elements, for example the porosity, the amount of saturation of water and the concentration of liquefied salts (Loke, 1999). The groundwater apparent resistivity diverges from 10 Ωm to 100 Ωm dependent on the dissolved salts concentration. Geological formations which contain natural chemicals that are good electrolytes, for example potassium chloride and sodium chloride, can consequently decrease the resistivity of groundwater to a reduced amount of 1 Ωm even at a justly little concentrations. Resistivity

values of geological materials have a much greater variety in comparism to other physical measures mapped by other geophysical techniques. The soils and rocks resistivity in an investigated area can differ by numerous series of magnitude. Clay for instance has low resistivity than sand because of the occurrence of iron cluster on the surface of clay soil. This presents the resistivity and other electrical based methods of very resourceful geophysical methods.

Table 2.4 Resistivity of some common rocks, minerals and chemicals

Material	Resistivity (Ω•m)	Conductivity (Siemen/m)
Igneous and Metamorphic Rocks		
Granite	$5x10^{3}$ - 10^{6}	10^{-6} - $2x10^{-4}$
Basalt	10^{3} - 10^{6}	10^{-6} - 10^{-3}
Slate	$6x10^{2}$ - $4x10^{7}$	$2.5x10^{-8}$ - $1.7x10^{-3}$
Marble	10^{2} - $2.5x10^{8}$	$4x10^{-9}$ - 10^{-2}
Quartzite	10^{2} - $2x10^{8}$	$5x10^{-9}$ - 10^{-2}
Sedimentary Rocks		
Sandstone	8 - $4x10^{3}$	$2.5x10^{-4}$ - 0.125
Shale	20 - $2x10^{3}$	$5x10^{-4}$ - 0.05
Limestone	50 - $4x10^{2}$	$2.5x10^{-3}$ - 0.02
Soils and waters		
Clay	1 - 100	0.01 - 1
Alluvium	10 - 800	$1.25 x10^{-3}$ - 0.1
Groundwater (fresh)	10 - 100	0.01 - 0.1
Sea water	0.2	5
Chemicals		
Iron	$9.074x10^{-8}$	$1.102x10^{7}$
0.01 M Potassium chloride	0.708	1.413
0.01 M Sodium chloride	0.843	1.185
0.01 M acetic acid	6.13	0.163
Xylene	$6.998x10^{16}$	$1.429x10^{-17}$

Source: Loke (1999)

CHAPTER THREE

3.0 MATERIALS AND METHODS

3.1 Materials

The geomaterials used for this research work includes rocks and water.

To effectively carry out the study so as to accomplish the aim and set objectives, the following digital and analog software and hardware materials were employed:

i. Book for data recording and pencil (Plate I): used for documenting field data all through the time of the study.



Plate I: Field Note Book

ii. Global Positioning System (GPS): find application in field navigation and the recording of the geographic co-ordinates of the points of sampling in the field (Plate II).



Plate II: Garmin etrex GPS

iii. The area of study digital satellite: applied to appropriately recognize a particular site locality on the field of study.

iv. Compass with clinometer: find application in measuring azimuth bearings on site (Plate III).



Plate III: Compass-clinometer

v. Hammer and measuring tape: the hammer was employed to drive electrodes into the ground. The tape was used to take liner measurement on the field (Plate IV and V).



Plate IV: Hammer



Plate V: Measuring tape

vi. Dip meter: was used for water level measurement down hole (Plate VI)



Plate VI: Dip meter

vii. Electrical Resistivity (ER) meter with entire collection of electrodes and cable realms: used in taking resistivity values of the subsurface (Plate VII).



Plate VII: Electrical Resistivity Meter **(**ABEM *SAS 4000 (Sweden, 2010)***)**

Digital Camera: the camera was used in capturing geological feature and important field work events.

Rotary Drilling Rig: used for drilling a borehole (Plate VIII). Geological down-hole logging was carried out at the drilled point to validate the result of the geophysical investigation carried out in the area



Plate VIII: Rotary Drilling Rig

viii. Software made use of to help and facilitates the research data organization and explanations include:

a. Microsoft office package: The software was employed for type setting, processing of data and statistical analysis, management of project, report presentation by power point and figure or picture editing.

b. Golden Surfer Software: used for data management of the geographic information system. Precisely utilized for digitizing and construction of maps.

c. ArchGIS 10.1: Used for evaluating spatial image.

d. Rockworks 15: Used for several geological and hydrogeological data interpretations.

e. Winresist: applied in the outlining data of 1D resistivity. Producing and re-iteration of resistivity curve.

f. RES2DWIN and Diprowin: Used for explaining data of 2D resistivity. Similarly used in generating resistivity pseudo sections of the subsurface.

3.2 Methods of Data Acquisition

The sets of data acquired for this research work included data from geological field mapping, hydrogeological investigation and geophysical subsurface investigations.

3.2.1 Preliminary desk study/ Reconnaissance survey

Existing works that were published on the hydrogeology and regional geology of the area of study were carefully studied.

The topography sheet of the region on the scale of 1:50,000 was sourced for from the Office of the Surveyor General of the Federation of Nigeria (OSGF) and reproduced as base map on the scale of 1:12,500. The area regional geological map was received from the office of the Nigerian Geological Survey Agency (Geological Survey of Nigeria, 1994). Available proximate related borehole log and technical reports were collected from the Benue State Rural Water Supply and Sanitation Agency (BSRWSSA) and the Lower

Benue River Basin Development Authority (LBRBDA). All the available materials were carefully studied.

Preliminary assessment of the research area and terrain familiarization was carried out. The potential routes for the traverse were identified. Findings from the desk study were cross checked during the reconnaissance to identify areas where adjustments could be made.

3.2.2 Fieldwork

The fieldwork was conducted in three major phases inside the area of study: geological mapping, hydrogeological mapping and hydrogeophysical investigation. Hydrogeological problems require some basic geological information prior to use of geophysical techniques to mitigate the problem. The field works were aimed at compiling data with aim of determining the lithofacies characterization and groundwater potential of the area.

3.2.2.1 Geological mapping

In any hydrogeological investigation, a distinct comprehension of the geology of the area is paramount in comprehending the hydraulic factors of the aquifer system (John and Richard, 2004).

A field map on the scale of 1:25,000 was developed from a topographic map on the scale 1:50,000 of Otukpo Sheet 270 SW and used for the mapping exercise. The network of traverse routes and accessibility of the study area were also examined from the

topographical map. Traverse method of geological mapping was employed; stream channels, road cuts and natural valleys were visited in search for outcrops.

Lithological samples from hand dug wells and geological log of a drilled borehole were taken to establish the lithology underlying the area of study.

3.2.2.2 Hydrogeophysical investigation

The geophysical resistivity methods are bases of the reaction of the earth to the stream of electrical current. The near subsurface resistivity, a material invariable, is a function of the degree of the current, the documented difference in potential, and the electrode array geometry.

3.2.3 Geophysical data acquisition

The geophysical data acquisition was carried out by a lightweight, custom-built resistivity multi-electrode data acquisition imaging system with rapid automatic data acquisition. A multi-electrode system developed by ABEM (Sweden, 2010) was used for data acquisition in this study. The system consists of a standard earth resistivity meter (ABEM Terrameter SAS 4000), four reams electrode cables (two current and two potentials), four steel electrodes with various connectors and metal hammers (Plate VIII). The electrode control module amplifies the AC transmitter current of 0.25 to 30 Hz up to a maximum of 100mA and 400V peak to peak. The change in voltage is measured at the receiver electrodes (MN).

The system is run with a 12 volt lead battery. The equipment facilitates high mobility and rapid data acquisition.

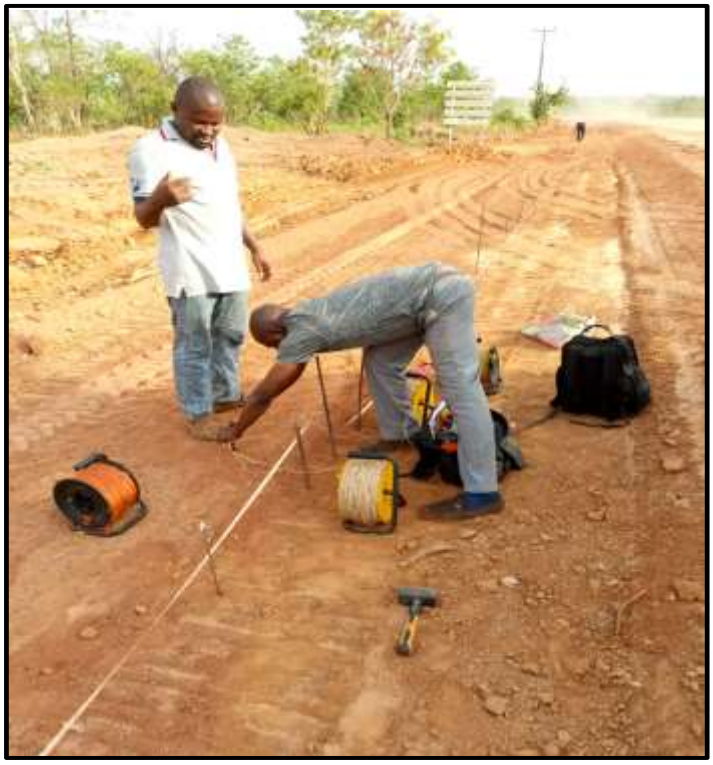

Plate IX: Hydrogeophysical exploration at location 10

To successfully carry out the geophysical measurement, a series of important geological and traditional elements were considered; these elements include but not limited to the target nature, target depth of burial, interval of measurement points and the data calibration.

***Nature of the target*:** The targeted geophysical signature in this research is groundwater which is believed to be an anomaly which differs from the background subsurface geology.

***Depth of burial of target*:** The depth to groundwater occurrence as the feature of interest in this area of study is unknown. The 1-Dimentional vertical electrical sounding is a method

of geophysics that is capable of achieving a greater penetration depth. The 2-dimensional resistivity imaging has the capacity of investigating shallow depths with high resolution.

***Measurement station interval*:** Due to lack of adequate information on the geology, as well as the depth of burial and geometry of the anomaly, the 2D data were acquired randomly along 100 m and 200 m long profiles.

***Collection of the field data*:** Measurement were performed by employing the ABEM *SAS 4000* Terrameter, a digital sign enhancing device incorporated with a microprocessor. It is characterised by high-impedance, precision and accuracy across an extensive series of situations. The global positioning system of type Garmin was used to determine sounding locations, while the coordinates in latitude and longitude are transformed into UTM and decimals using the geological software Rockware2013.

3.2.4 Induced polarisation (IP)

The measurements of IP were done in the field with the use of the four-electrode procedure. IP is the chargeability (capacitance effect) exhibited by electrically conductive materials. Induced polarisation uses capacitive actions or ground charge retention upon current introduction to subsurface in locating chargeable zones within host rocks (Börner, *et al.*, 1996; Kemna, *et al.*, 2004). Measurement of induced polarisation can be conducted in frequency domain or time domain. The time domain measurement was adopted for this research work (Figure 3.1).

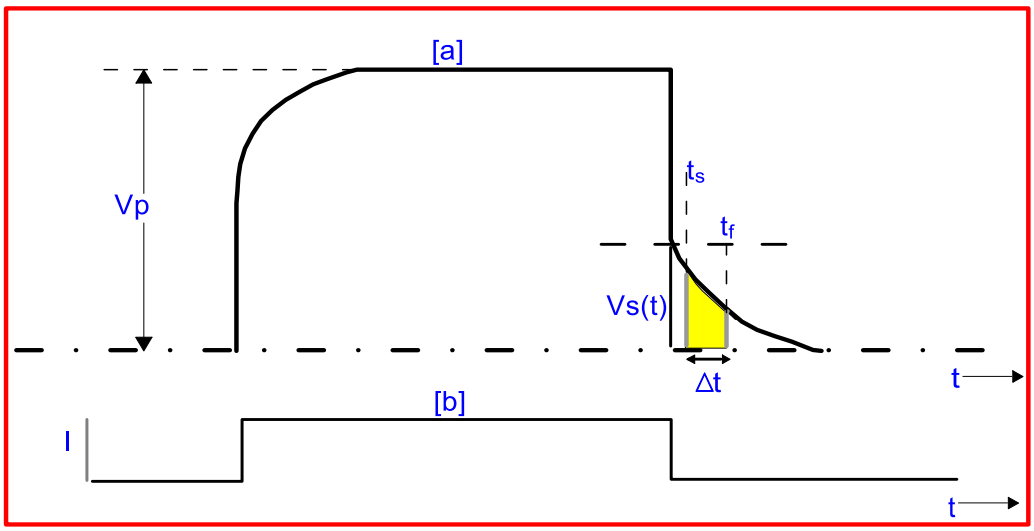

Figure 3.1: [a] Time domain signal of IP acquired showing parameters measured [b] Current waveform: Square-wave is produced at low frequency (~ 1Hz) and polarity is continually switched (After Bleil, 1953)

In the time domain IP measurement, current was transmitted symmetrically (the negative and positive polarities were of equivalent length) into the subsurface along a pair of current electrodes while difference in potentials was measured through another pair of potential electrodes to determine the resistivity. A broad cycle consisted of one positive section of length T (called current on) and one negative section of similar length T (current off). The transient potential waning on the land was measured in one or numerous interludes of time windows after the current was turned off (Figure 3.2). The time was fit to the order as follows: 1, 1.5, 2, 2.5, 3 ... sec in paces of 0.5 sec.

The voltage was incorporated across a series of intervals of time and the SAS 4000 measured up to ten such interval of time. The complete time of integration was restricted to 8 sec. The first interval begins after the early time delay Δt_d. The length of the time intervals difference was stated by the equation.

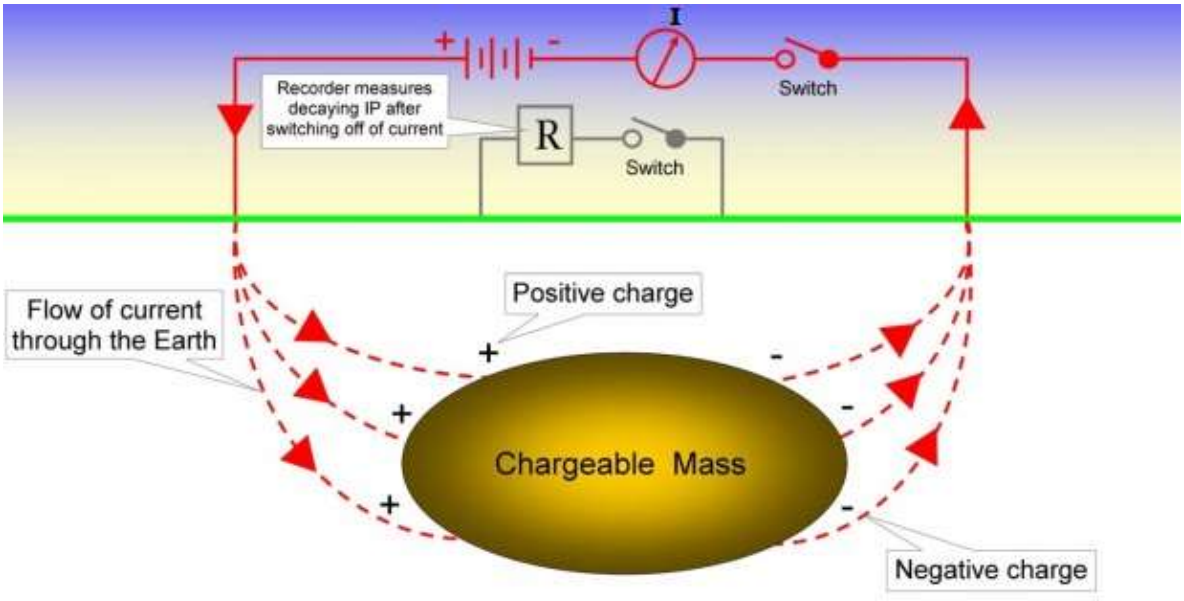

Figure 3.2: Schematic illustration of IP method (After Bleil, 1953)

$\Delta t_d = n \cdot f^{i-1} \Delta t_0$

Where

- Δt_0 is the essential interval of time (20 msec in places with 50 Hz key frequency of power, accordingly 16.67 msec in areas with 60 Hz power frequency)
- *n* is a factor of multiplication (default = 1)
- *f = 1 or 2* (default *f = 2*) is an incremental function
- *i* is the time window indices (1, 2, ... , 10)

The factor used to compute the time domain IP is the normalized chargeability (*M*) which is referred as the relation of the transmitted current secondary potential over the primary potential (Magnusson *et al*, 2010; Sumner, 2012). The chargeability is computed in the unit meters per second (*msec).*

The mathematical expression for the normalized chargeability (*M)* in induced polarisation is given by:

$$M = \frac{\int_{t_s}^{t_f} V_s\, dt}{V_p} \frac{1}{\Delta t} \quad (msec)$$

Where V_S is the residual voltage

t_s and $t_f$times after current shut off,

V_P is the measured voltage before the turning off the current.

3.2.5 Resistivity

The utility of a particular geophysical technique in hydrogeological survey is dependent on factors such as the geological setting and the subsurface structural configuration. Basically there are two resistivity survey procedures irrespective of the electrode expanse employed. The first one is known as Horizontal Electrical Profiling (HEP) while the second is Vertical Electric Sounding (VES). The HEP was employed for resistivity variation with lateral extent while VES was used to study variation in resistivity of the subsurface lithology with depth.

The common field configurations used in this research included Schlumberger configuration for the 1D Vertical Electrical Sounding (VES) and the Wenner-Alpha

configuration for the 2D Subsurface Electrical Imaging. The two arrays are based on the four electrodes principle. Using these geophysical methods, information about the subsurface lithology over the area was collected in a cost-effective and non-invasive manner.

A stable subsurface electrical field was generated by driving direct current across two unpolarized current electrodes fixed at the earth surface and measured the potential (voltage) differences between the other two electrodes placed in the middle of the current electrodes (Lowrie, 2007). The reason for the electrical surveys is to establish the spreading of subsurface lithological resistivity by conducting measurements on the ground surface. The ground resistivity is linked to different geological factors for example permeability, porosity and degree of water saturation in a geological material.

The Schlumberger configuration was used to perform the conventional vertical electrical sounding (VES) at twenty (20) different locations within the study area with a peak current electrodes sepration (AB) ranging from 1000 m to 1200 m. Quantitative and qualitative analysis of the acquired data were performed. Geoelectric curves were generated using the traditional partial curve matching comprising the principal and secondary curves to acquire the different layers at various depths. The computer iteration technique (Winresist software) was used to produce the final model curves. The 1-D VES is principally directed at identifying the disparities in subsurface settings, in the thickness aspect, strata depths and the extent of the subsurface geomaterials saturation. It is carried out based on the belief on horizontal strata layering. This indicates that the subsurface lithological resistivity varies only with depth difference and not in horizontal trend.

2-D electrical imaging (tomography) survey involving the Wenner Alpha resistivity method was also used for shallow subsurface investigation. The 2-D resistivity subsurface tomography discloses both vertical and horizontal evidence alongside the direction of traverse. It determined the sequence of geology and shapes of the subsurface lithology. As a result of the disposition of the area of study the traverse length (L) was restricted to an incessant recurrent break of 100 m at four locations and 200 m at two locations. Twenty one (21) electrodes were used for 100 m spread while a total of 42 electrodes were used for the 200 m spread in the 2-D survey.

3.2.5.1 The four electrode principle (VES)

The theory of electrical resistivity is normally on the basis of the famous Ohm's law. Four electrodes were collinearly organized; A and B serves as current electrodes on the outside whereas M and N serve as potential electrodes in-between A and B electrodes.

Measurements were generally effected on the land by directing current into the surface of the ground via the set of current electrodes (A and B). The ensuing change in voltage (V) was measured between a further set of potential electrodes (C and D) (Figure 3.3). The resistance (R) as a petrophysical parameter was developed from the voltage and current (V and I correspondingly) values with the aid of Ohm's law (R= V/I).

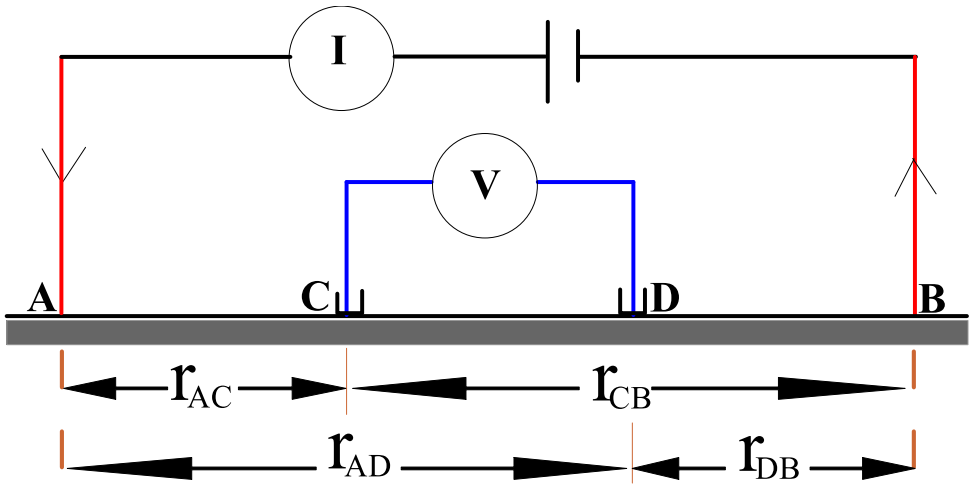

Figure 3.3: Common configuration of four-electrode for measuring resistivity consisting of a pair of current electrodes (A, B) and a pair of potential electrodes (C, D) (Loke, 1999)

The current electrodes 'A' functioned as source whereas 'B' functioned as sink **(**Figure 3.3). At the potential electrode detection 'C', the source 'A' imply $+pI/(2\pi\ r_{AC})$, whereas the potential caused by the sink electrode B imply $-pI/(2\pi\ r_{CB})$ (Lowrie, 2007). The potential (U) which was merged at electrode 'C' is presented as

$$UC = \frac{\rho I}{2\pi}\left(\frac{1}{r_{AC}} - \frac{1}{r_{CB}}\right) \qquad \text{equation 1}$$

Similarly the subsequent potential difference at 'D' is presented as

$$UD = \frac{\rho I}{2\pi}\left(\frac{1}{r_{AD}} - \frac{1}{r_{DB}}\right) \qquad \text{equation 2}$$

Consequently the distinction in measured potential by a digital voltmeter (V) attached between C and D is presented as

$$V = \frac{\rho I}{2\pi}\left\{\left(\frac{1}{r_{AC}} - \frac{1}{r_{CB}}\right) - \left(\frac{1}{r_{AD}} - \frac{1}{r_{DB}}\right)\right\} \qquad \text{equation 3}$$

All measurement of parameterswere carried out on the surface of the ground except the resistivity (ρ). The value of resistivity calculated does not represent the correct subsurface resistivity, rather an apparent value of resistivity (ρ_a), which gave the same voltage and current values for the same electrode arrangement

$$\rho_a = \mathrm{K}\frac{V}{I} \qquad \text{equation 4}$$

K is known as geometric factor (unit: meter) and was computed from the spacing of electrode by

$$K = \frac{1}{2\pi}\left\{\left(\frac{1}{r_{AC}} - \frac{1}{r_{CB}}\right) - \left(\frac{1}{r_{AD}} - \frac{1}{r_{DB}}\right)\right\}^{-1} \qquad \text{equation 5}$$

The apparent resistivity (ρ_a) for the four electrode configuration calculated is as;

$$\rho_a = 2\pi\frac{V}{I}\left\{\left(\frac{1}{r_{AC}} - \frac{1}{r_{CB}}\right) - \left(\frac{1}{r_{AD}} - \frac{1}{r_{DB}}\right)\right\}^{-1} \qquad \text{equation 6}$$

Two out of the four methods of electrodes were employed for the investigation; Wenner and Schlumberger. The four electrodes in both of the arrangements are collinear however they are dissimilar in their spread and geometry. In Wenner array the sets of potential and current electrodes divide a generic mid-point and the spacing of inter electrodes are equivalent, therefore r_{AC}=r_{DB}=a, and r_{CB}=r_{AD}=2a (Figure 3.4).

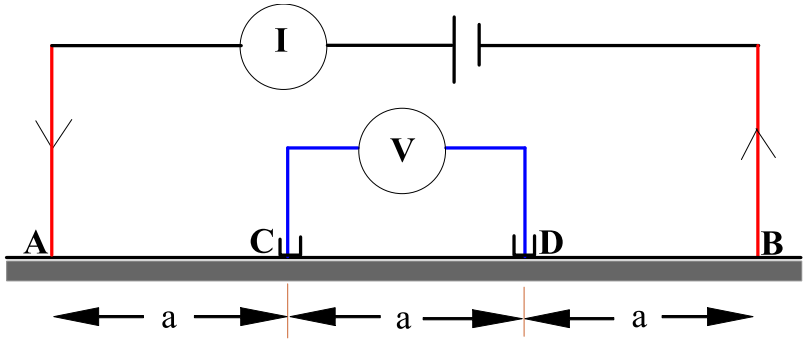

Figure 3.4: Wenner Array of Electrical Resistivity Method (Loke,1999)

Substituting the above electrode values into eq. (6) gives

$$\rho_a = 2\pi \frac{V}{I}\left\{\left(\frac{1}{a}-\frac{1}{2a}\right)-\left(\frac{1}{2a}-\frac{1}{a}\right)\right\}^{-1} \qquad \text{equation 7}$$

$$\rho_a = 2\pi a \frac{V}{I} \qquad \text{equation 8}$$

In the Schlumberger array (Figure 3.5), the duo of potential and current electrodes uses a joint mid-point but the spacing of inter electrode are not equivalent.

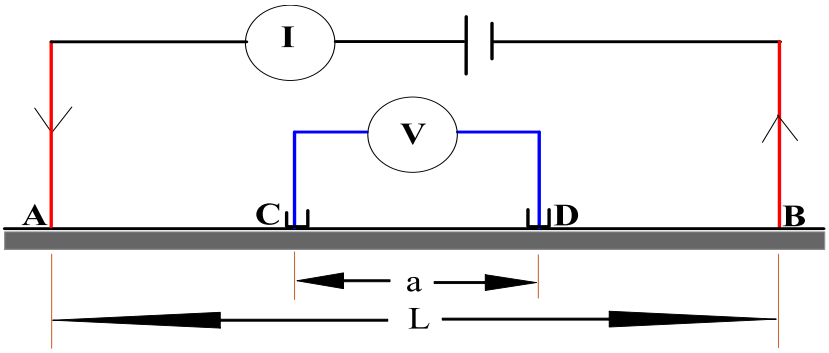

Figure 3.5: Schlumberger Configuration of Electrical Resistivity Method (Loke, 1999)

Considering the partitions amid the two electrodes; potential and current to be *L* and *a*, correspondingly, then r_{AC}=r_{DB}=(*L*– *a*)/2 and r_{CB}=r_{AD}= (*L*+*a*)/2. Replacing these quantities into equation 6 produces:

$$\rho_a = 2\pi \frac{V}{I}\left\{\left(\frac{2}{L-a}-\frac{2}{L+a}\right)-\left(\frac{2}{L+a}-\frac{2}{L-a}\right)\right\}^{-1} \quad \text{equation 9}$$

$$\rho_a = \frac{\pi V}{4I}\left(\frac{L^2-a^2}{a}\right) \quad \text{equation 10}$$

3.2.5.2 Schlumberger array instrumentation and measurement

Schlumberger soundings provide sufficient penetration to examine the underlying subsurface lithology with relations to groundwater occurrence. The direct current (DC) from a 12 volt battery was used for the resistivity measurements. Four electrodes were collinearly positioned with the current electrodes A and B on the exterior and the potential electrodes M and N on the interior.The successive electrode spacing was approximately equally spaced on a logarithmic scale. Schlumberger sounding was carried out under the constraint that MN is small compared to AB/2. It was ensured that MN did not exceed 20% AB/2. In the course of the measurement, AB/2 was expanded while MN positions were retained. To change the depth range under investigation in order to attain greater depth the expanse AB was gradually expanded outward proportionally in logarithmic scale, having MN permanent. This process yields a rapidly increasing potential difference across MN,

this is accompanied by a potential drop across MN which ultimately exceeded the measuring capabilities of the instrument. At this point, increase in MN was necessitated, a new value for MN was established, typically two to three times larger than the preceding value, and the survey was continued. At any AB/2, reading was taken at numerous MN/2 so as to show the existence of lateral inhomogeneity. The last one or two AB/2 values were duplicated with the new MN value.

3.2.5.3 Two dimensional (2-D) electrical subsurface imaging

They are different electrodes arrangement as well as geometric factors for different arrays (Figure 3.6). The signal strength of an array is inversely proportional to the factor of geometry used in the computation of the value of apparent resistivity for the array (Loke, 1999). The Wenner-Alpha array was used for this research work. For the Wenner array, $\mathbf{2\pi a}$ is the factor of geometry, which is lesser than the factor of geometry for other arrays. In the midst of the familiar arrays, the Wenner array has the sturdiest signal strength.

An inspection hydrogeological survey was performed in the study area which was subsequently followed by suitable preparation for feasibility to perform two dimensional (2D) resistivity surveys. The 2D multi-electrode resistivity subsurface investigation is executed to enhance groundwater exploration.

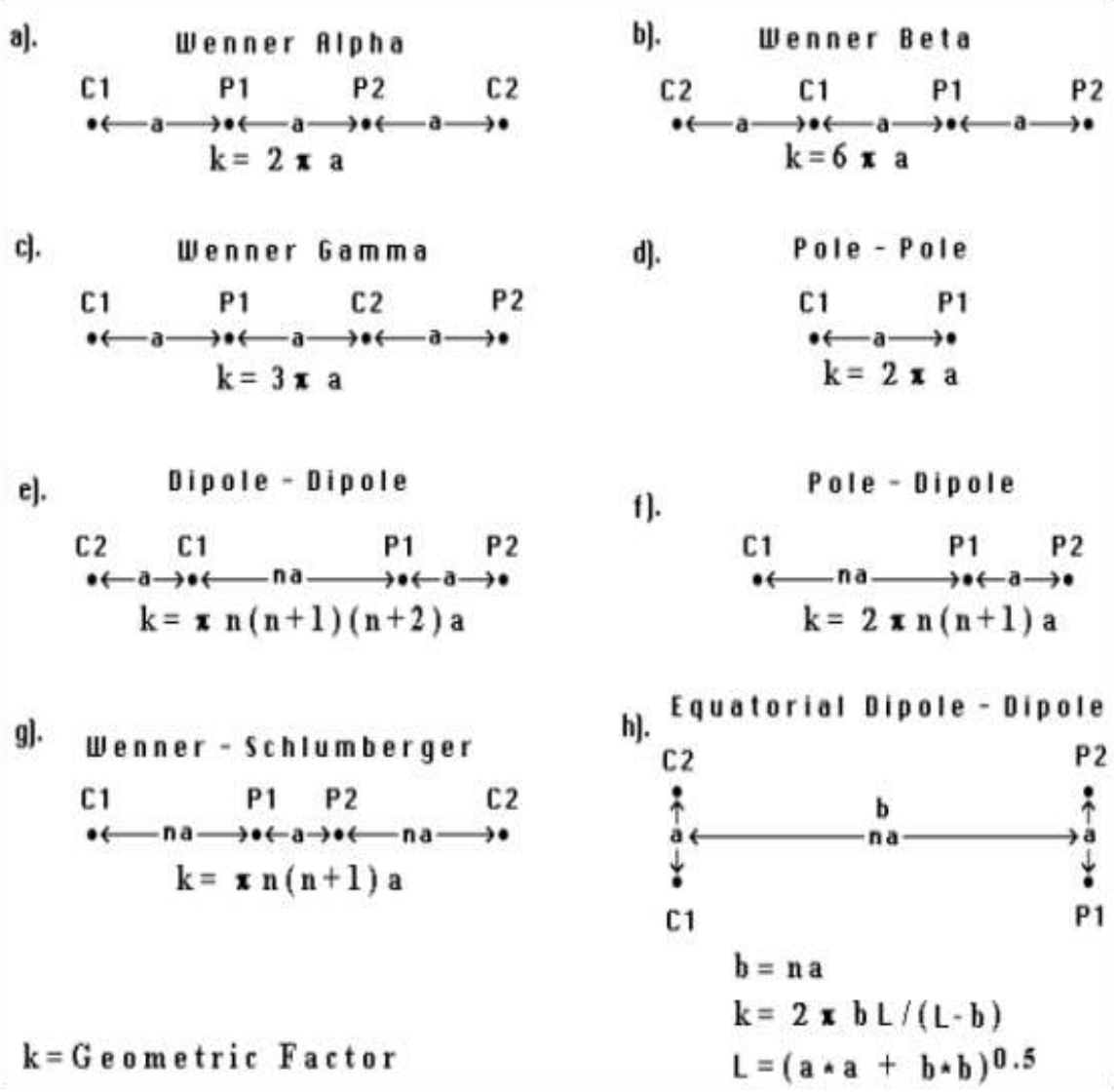

Figure 3.6: Regular configurations used in resistivity surveys and their geometric factors (Loke, 1999)

The Wenner-Alpha arrangement by Loke (1999) was used for the 2D investigation (Figure 3.7). The Wenner-Alpha is appropriate for lesser spacing of electrode and reliable horizontal and vertical depths information was selected for carrying out the near subsurface study (Loke, 1999). The Wenner Alpha had meaningfully greater strength indicator to

observe diligently the high resolution data of 2D resistivity and similarly it is less altered by the isolated electrode.

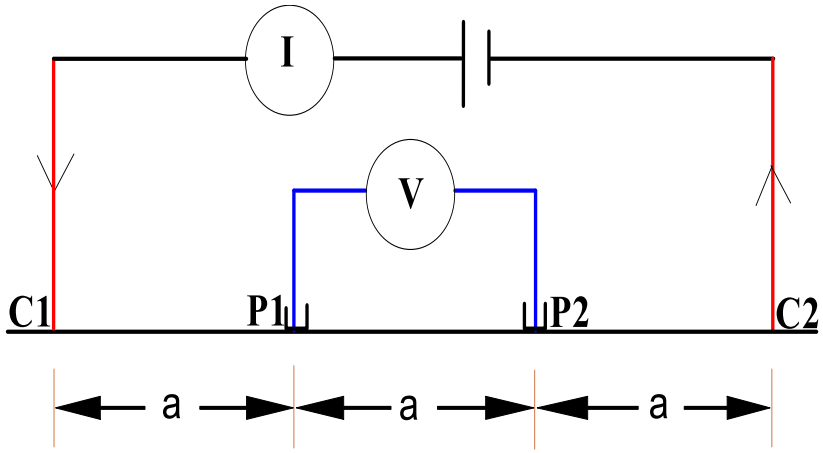

Figure 3.7: Wenner Alpha Configurations for 2D Subsurface Electrical Imaging (After Loke, 1999)

The selection of the Wenner-Alpha array was preferred for its strong strength of signal. The traverse length (L) of the electrical cable spread was restricted to an uninterrupted recurrent break of 100m to 200m in selected locations across the study area. This was due to the obtainability of extended length of undeviating space and interference posed by tarred and concrete roads, buildings, drainages and buried underlying cables.

For the initial series of measurement for the 100m transverse the spacing in the middle of nearby electrodes (a) at 1a was put at 5m. For the initial measurement, electrodes numerals 1, 2, 3 and 4 represent C1, P1, P2 and C2 in that order (Figure 3.8). For the following measurement, numbers of electrodes 2, 3, 4, and 5 represented C1, P1, P2 and C2 in that order. This arrangement was sustained till electrodes numbers 18, 19, 20 and 21 represent C1, P1, P2 and C2 in turn. Eighteen mid-points were evaluated at the event of the investigation at the termination of each 100m sequence.

The subsequent progression of measurement with 2a was done. The contiguous space between electrodes was raised from 5m to 10m, but yet sustaining the corresponding horizontal electrode change of 5m. Electrodes 1, 3, 5 and 7 were then utilized as C1, P1, P2 and C2 correspondingly for the initial groups of measurement. The 2, 4, 6, and 8 electrodes were for the following groups of measurement. This progression was replicated along the line of profiling till 15, 17, 19 and 21 electrodes are measured in the sequence of 2a.

The entire measurement technique was replicated for 3a, 4a, 5a, 6a etcetera. Beginning at the first series of measurement 1a, a total number of 18 mid-points was achieved, and the mid-point decreases by three in successively sequences measured. For a profile of 100m, at 2a, mid-points =15, at 3a=12, 4a =9, 5a=6 and 6a=3 (Figure 3.8). The amount of measurement declines with rise in spacing of electrode, resulting to the work out of the entire examine depth.

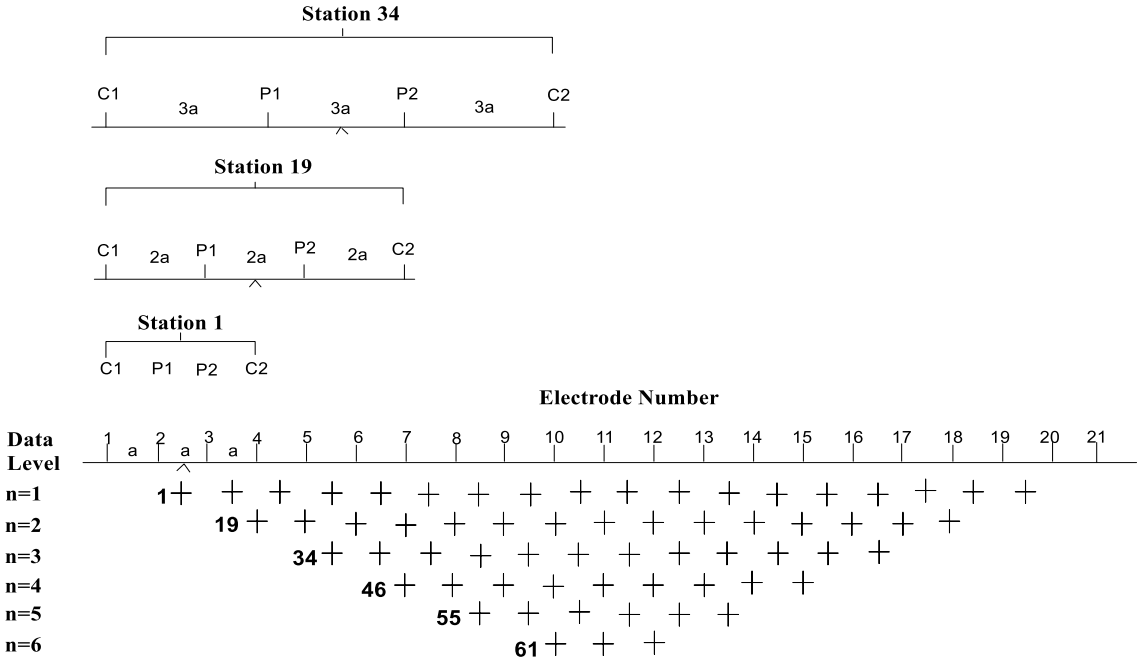

Figure 3.8: Sequence of 2D Wenner Alpha resistivity measurement used to build a pseudosection (Loke, 1999)

The same sequence of measurement was carried out for the 200 meter transverse. At 200m the spaces between neighbouring electrodes (a) was set at 10m. a total of eighteen mid-points were similarly measured at the completion of every 200m sequence study. The figures acquired were quantitatively explained by transposition with the aid of the RES2DINV software.

3.3 Data Treatment

3.3.1 1-D VES preliminary data treatment

Quantitative and qualitative sequences of interpretation were adopted for the field data treatment. This was carried out in order to convert the field records into relations of geology of the subsurface, so that appropriate maps can be drawn for many relevant geophysical factors. As data were taken, they were plotted on a manual double log graph. Measurement errors during data collection in the field were checked. Any value collected that was noticed to be obviously out of step was subjected to repeatability check or mutuality check. In the repeatability check the process of data collection was carefully repeated while the mutuality check was prepared by switching the electrode pairs applied for measurement of voltage with the electrode pair used for injection of current (Orellana and Mooney, 1966). The data were further iterated to enhance better resolution using the Winresist computer programme developed by Van der Velpen and Sporry, (1992).

Quantitative interpretation of Vertical Electrical Sounding (VES) data involves analytical, empirical or semi empirical. Quantitative interpretation carries the detail of the thickness and depth range of the various geological lithologies having different resistivity values.

Qualitative interpretation gives detail evidence in relation to the geological structure and the modifications in the geological section at the subsurface.

Qualitative interpretation is dependent on the quantitative interpretations. The interpretation is enhanced by the preparation of iso-resistivity maps of various layers thickness to determine the subsurface lithological information and their structures.

3.6.2.1 Curve types

There are basically two forms of curve in relation to VES data; Ascending and Descending curve types (Orellana and Mooney, 1966; Rijkswaterstaat, 1969). The ascending curve types are recognized where the land has a structure of two-layer, mostly where the crystalline basement (highly resistive) underlying topsoil or weathered layer. The descending curve types are recognized wherever a top stratum is covering a dense clay or aquifer of saline water. Visual inspection can tell how many layers are present in a VES curve. Each kink or curvature change shows the presence of a new layer. Furthermore there are four major kinds of resistivity curves for basic sections of geo-electric. These curve types include A, K, H and Q types (Figure 3.9).

'A' curve types are obtained in basement rock environment or sedimentary environment with conductive topsoil. The resistivity of the layers increases continuously ($\rho_1 < \rho_2 < \rho_3$/Low-Low-High). 'K' curve types sounding have highest summit inhabited by low value of resistivity. The first layer resistivity is less than that of the second layer whereas the second layer resistivity is greater than the third layer ($\rho_1 < \rho_2 > \rho_3$/Low- High-Low). 'K' type curves stem from distinct geological environments. 'H'-type curves are sounding

curves with central minimum ($\rho_1>\rho_2<\rho_3$/High-Low-High). The formations with the 'H' curves contains dehydrated top soil of great resistivity as the first layer, saturated water layer of least resistivity as second layer and third layer with elevated resistivity. 'Q' curve types are sounding curves with continuously decreasing resistivity ($\rho_1>\rho_2>\rho_3$/High-Low-Low). The 'Q'-type curves are commonly obtained in sedimentary environment mostly in coastal region.

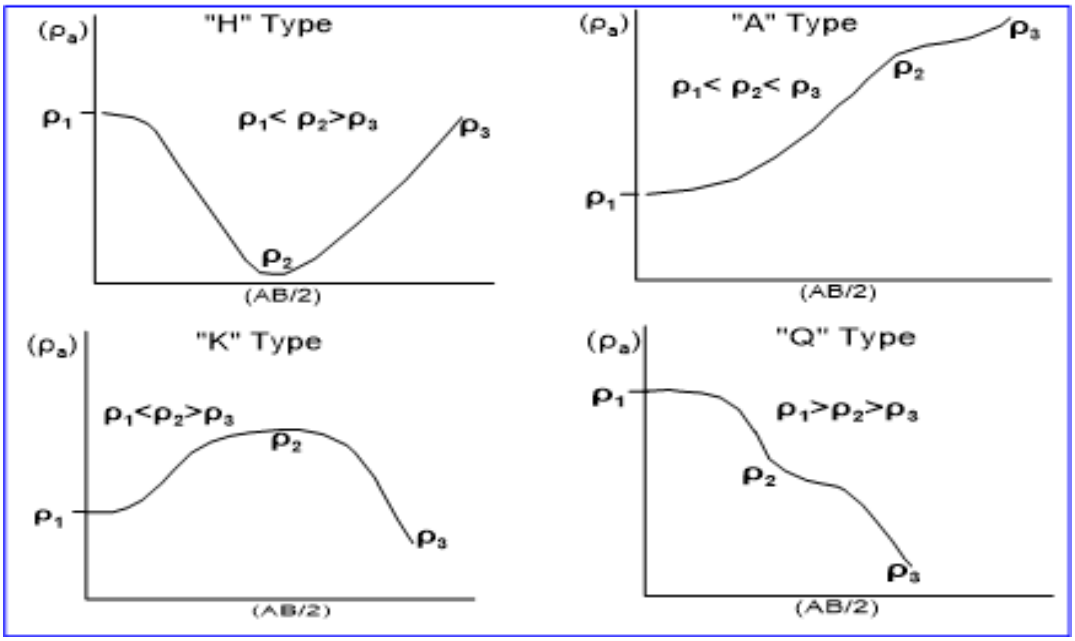

Figure 3.9: Types of Apparent Resistivity Curve (Orellana and Mooney, 1966)

A pattern of the different curve types can exist in a mixed geological environment with more than three layers.

3.6.3 2-D data treatment

The measured two-dimensional (2-D) resistivity data were processed with the RES2DINV version 3.54 inversion program designed by Geotomo software 1995-2005. About 35000

maximum numbers of data points can be processed at a single time while 16000 maximum numbers of electrodes can be processed by the software. An inspiron 15R, core i7 Dell computer system was utilised for treating the data. The data inversion is an iterative process aimed at finding a parameter model to give synthetic measurements that are similar to the actual field measurement.

3.4 Data Presentation

The methodology adopted for data presentation comprises of three steps:

i. Pseudosection plotting of the apparent resistivity measured

ii. Estimated apparent resistivity pseudosection plotting

iii. Inversion and plotting of the resistivity sections in ohm.m

The obtained 2-D resistivity field data were initially treated and filtered by removing every raucous or harmful data points in the obtained dataset. Subject to the evenness of the resistivity data, inhibiting and enmesh strictures were allotted to the singular dataset and realistic subsurface resistivity models were achieved. The interpreted field data were given in the mode of resistivity pseudo sections with thick specimen of measurements of apparent resistivity at superficial depth (Loke, 1997) with massive attention together in vertical and lateral variations. The treated and purified data was reversed utilising least squares inverse method with evenness inhibited (Sasaki, 1992; Loke, 1997) and with a regular Gauss-Newton optimization procedure employing the RES2DINV.EXE programme.

This process of data treatment showed to be effectual in removing effects of electrode geometry such that the last models of inverted resistivity offer an estimated appearance of the true hydrogeology and geology of the subsurface (Kumar *et al.*, 2014).

The value of the inverted resistivity product was linked to the feature of the obtained field resistivity data. This was revealed in expressions of Root Mean Square (RMS) error on the reversed resistivity prototypes. This was achieved by computing the residuals between the resistivity measured and the computed value of the subsurface apparent resistivity (Sudha *et al.*, 2009).

The inverted 2-D resistivity sections represented an estimation of the subsurface lithological resistivity which was lastly elucidated in relations to hydrogeology and geology in the hydrogeophysical setting.

3.5 Ambiguity in Electrical Resistivity

The electrical resistivity method is not without some ambiguities. These ambiguities were resolved by understanding the geology of the area and by minimizing presumption and assumption in the field. Some of the causes of the ambiguities include near surface inhomogeneity, topographic effect, equivalence, conductive overburden, anisotropy, natural noise, dipping beds and vertical contacts.

3.5.1 Near surface inhomogeneity

This is the distortion of field readings from the actual earth resistivity which may be due to effects of buried pipelines, road, ditches and buried cables. This error was minimized by choosing suitable areas for the sounding.

3.5.2 Topography

Topographic effects can increase or lower the values dependent on whether the anomaly is situated in a hilly or valley terrain. This was surmounted by choosing relatively flat terrain and by including the topographical effects in the 2-D modelling.

3.5.3 Equivalence

The theory of equivalence articulates that a sounding curve measured is essentially associated with lots of substantially equivalent prototypes that may vary substantially thereby creating ambiguity in the interpretation of data (Reinhard, 2006). For instance, a tinny layer inserted between two layers with considerably greater resistivity will create lots of the current to stream through it. If the resistivity and width of the tinny layer are improved by identical fraction, the quantity of current streaming across it will stay unaffected. Therefore the two circumstances will be equivalent electrically. This condition was controlled by using appropriate existing geological material of the area of study.

3.5.4 Conductive overburden

This is a situation at which the resistivity of the proximate surface lithologic structure is greatly lower than the lithology underlying it. This set off lots of the current to concentrate in the overburden and might not touch the bottom rock and resolution comes to be almost poor or not possible. To surmount this challenge, measurement was completed with two transverses using several electrode spacing.

3.5.5 Anisotropy

In actuality, geological formations are mostly not isotropic, particularly in shale and clay lithologies. In clay lithology, for example, the resistivity is similar in all directions along a layer but differs if the direction is at right angles to the stratification. It can be revealed that if resistivity is measured in the field with a configuration oriented parallel to the bedding planes the measured resistivity is greater than the longitudinal resistivity by a ratio (Keller and Frischknecht, 1966).

3.5.6 Natural noise

Telluric current, rainstorms and other natural electromagnetic occurrence can make the earth to acquire induced currents, therefore influencing measurements of resistivity. The equipment used possessed a system which just accepted data inside a suggested amplitude extent.

3.6 Hydrogeological Mapping

Hydrogeological investigations carried out included water level measurements in wells of situated at the upper section of the subsurface layer (well inventory), the borehole log from the drilled hole and spring sites were also visited. 200 water wells were randomly investigated in the study area. Water levels measurements were conducted manually in wells terminated in the upper section of the subsurface litological layer (less than 25 m deep). The distance of between two adjacent wells was considered. The basic procedure of water level measurement was strictly adhered to. The latitude, longitude and elevation (co-ordinates) of every sampling location and the static water level in hand-dug wells were

acquired with the help of Global Positioning System (GPS) and water level dipper (Dip-Meter) respectively. The 30 m long dip-meter is graduated in meter and fractions of a meter. Two major measurements were taken on lowering the dip-meter inside the well; the depth to water level which was recorded from an established reference elevation. The second is the total depth of well which was measured from the ground surface to the bottom of the well.

Access to the wells was gained by taking permission from relevant well owners in the area. The well cap was removed before measurements were taken. The water level dipper device was lowered down the well to obtain readings. The water level dipper comprises a twin-core cable length, calibrated in centimetres and metres, would on to a cylinder and with a probe fastened to the bottom. Once the static-water level is encountered, an electrical circuit is completed; an audible buzzer was activated to indicate the water level. Most of the water level measurements were taken early in the morning before the wells were put into use (discharged) to maintain stabilized water levels in the wells. In cases where the wells were already been used, the wells were allowed to recover (recharge) before measurements were taken. Notes were also taken wherever the water table is believed to intersect the ground surface (springs).

The data obtained were used to create the groundwater configuration map and the digital static groundwater elevation contour map of the unconfined aquifer of the area using geologically related software.

3.6.1 Hydraulic head/Groundwater flow direction

Elements that effect movement of groundwater consist of: hydraulic head, hydraulic gradient and velocity according to Darcy's law. Further components comprise topography, geology and aquifer kind and properties (Todds, 1980). The well inventories taken from the study area were used to calculate the hydraulic head for each of the measured wells. Groundwater flow direction map was created from the calculated hydraulic head data acquired from measurement of wells. The hydraulic head (H) is the determination of the mechanical energy that makes groundwater to move from higher head to lower head. Hydraulic head can be obtained in two ways:

(a.) The totality of elevation head and pressure head

(b.) The variance between depth to table-water and land elevation.

In constructing the map of groundwater flow, the geographical coordinate of every one of the wells was acquired with the aid of the global positioning system (GPS). The elevations of water table were ascertained at different well sites within the study area by deducting depth to water level in the wells from the measurement of well elevation (Plate X). The golden surfer software tool was used to draw the groundwater flow direction map of the area, inputting the coordinate's the longitude as Y, latitude as X and the variant in water tables as Z data points.



Plate X: Measuring water level in well (Well Inventory)

3.6.2 Borehole drilling and logging

The borehole drilling was carried out by a mud rotary drilling rig employing the reverse rotary drilling method. The drilling rig comprises of drilling rods (5 m length), drilling bit, mud pump, drilling accessories and a compressor. A sedimentation pit (mud pit) was constructed to enhance the circulation of the drilling fluid and the collection of drilled cuttings (Plate XI). A water tanker supplied water for the drilling fluid. The drilling fluid was made up of only clean water without any additive due to the geology of the area. The quality of the drilling fluid was maintained to assure the collection of a good representative sample of the formation materials. The drilling mast was plumbed and properly positioned to the VES point. The plumpness of the mast was carried out in order not to allow the hole to vary in vertical alignment. Water as drilling fluid was distributed through the drill pipe and move backward the bore hole to get rid of the drill cuttings. Hydrostatic pressure of the

flowing fluid and a cake of mud that built up on the borehole wall by the shale lithology during the drilling process caused the walls of the borehole stable without collapsing.

Borehole logging was undertaken to be sure of the subsurface lithology in the area. The borehole lithotological cuttings were taken at the sedimentation well and washed exhaustively with fresh water and air-dried prior to being kept in the sample box. The logged samples were arranged in sequence and the strata log was recorded from visual inspection and classifications. The selection was performed at 5 m interval of penetration, excluding where there existed a rapid change in lithologic formation. A serial and comprehensive explanation of samples stored in the sample box was used to ascertain the subsurface geology of the study area.



Plate XI: Drilling in progress

CHAPTER FOUR

4.0 RESULTS PRESENTATION AND DISCUSSION

The outcome of geological and hydrogeological investigations as well as hydrogeophysical investigation are presented and discussed in this chapter while field data, graphs of 1-D and 2-D geophysical survey are shown in the appendices.

4.1 Geology of the Area

The principal geological setting of any area plays an important role in influencing the storage and flow of groundwater resources in such area. The topography of Otukpo is relatively undulating with surface elevations fluctuating between 124 m and 208 m above the median sea level. The geology of Otukpo and its environs generally falls within the Cretaceous sedimentary formation of the Southern Benue Trough. Otukpo and its environs is part of the linear stretch of the sedimentary elongated rift like basin of the Benue Trough. Lithologic samples from shallow hand excavated wells and a drilled borehole log were collected to ascertain the actual subsurface lithological condition of the area.

The lithologic unit of Otukpo shallow subsurface interval (between 0-3m) is constituted by silty/sand and lateritised mudstones. There exist intercalations of silty-sand with clayey-sand to the shallow depth of around 20 m. Underneath this interval is a zone of buff clay and dark shale. The dark shale constitutes the Awgu Formation (Figure 4.1).

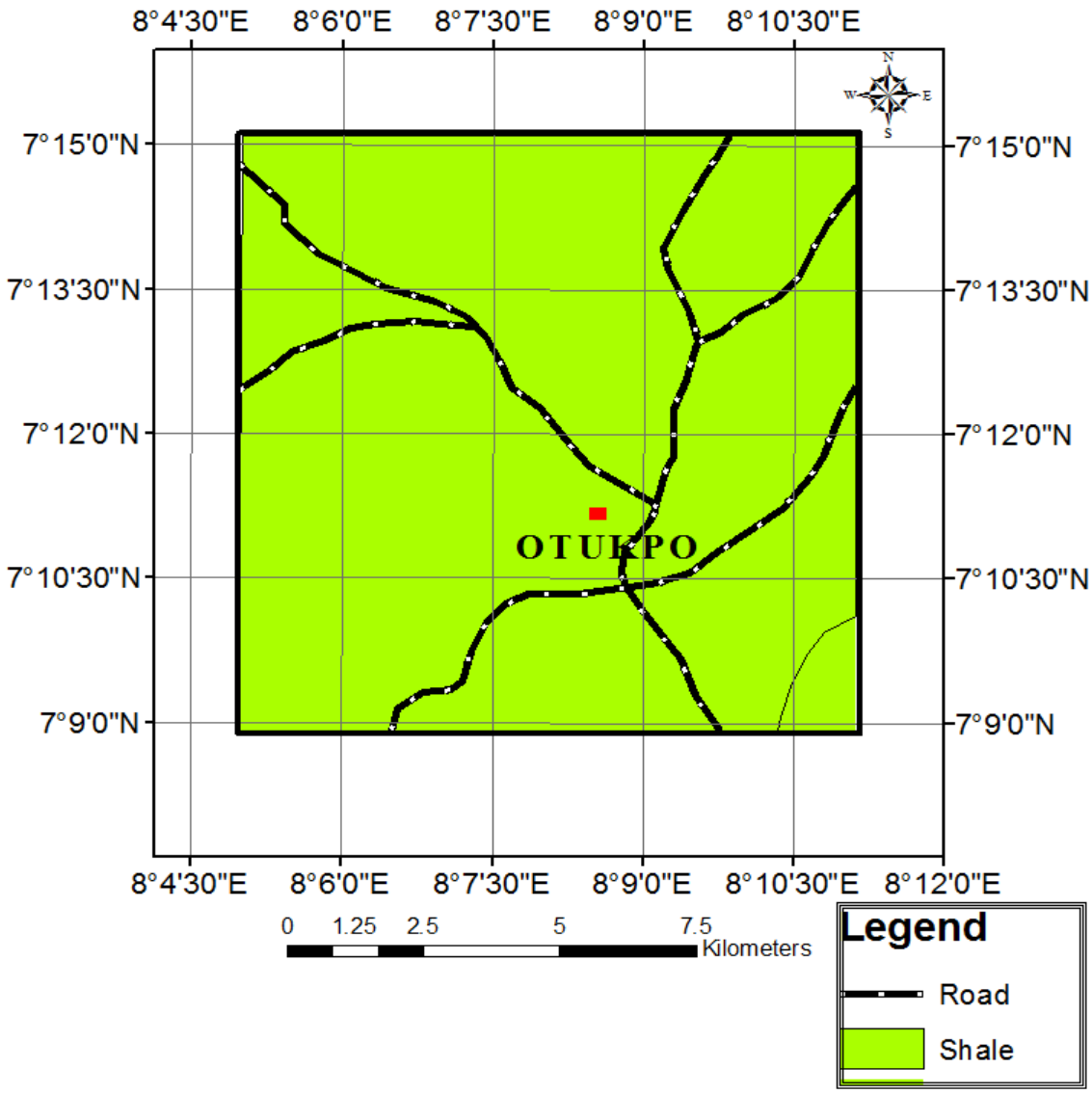

Figure 4.1: Geology of Otukpo and Environs

4.2 Hydrogeology

The surface elevation of Otukpo and its environs ranges from 124 m to 208 m above the mean sea level. The southern portion of the study area with an average well depth of 11 m shows a relatively deeper depth of wells compared to other locations in the area. Shallow well depths of 5 m average were documented on the south-western part of the study area (Figure 4.2). The minimum total depth of well in the area is 2.3 m while the area has a maximum well depth of 14.2 m as measured in the field measurement (Appendix A)

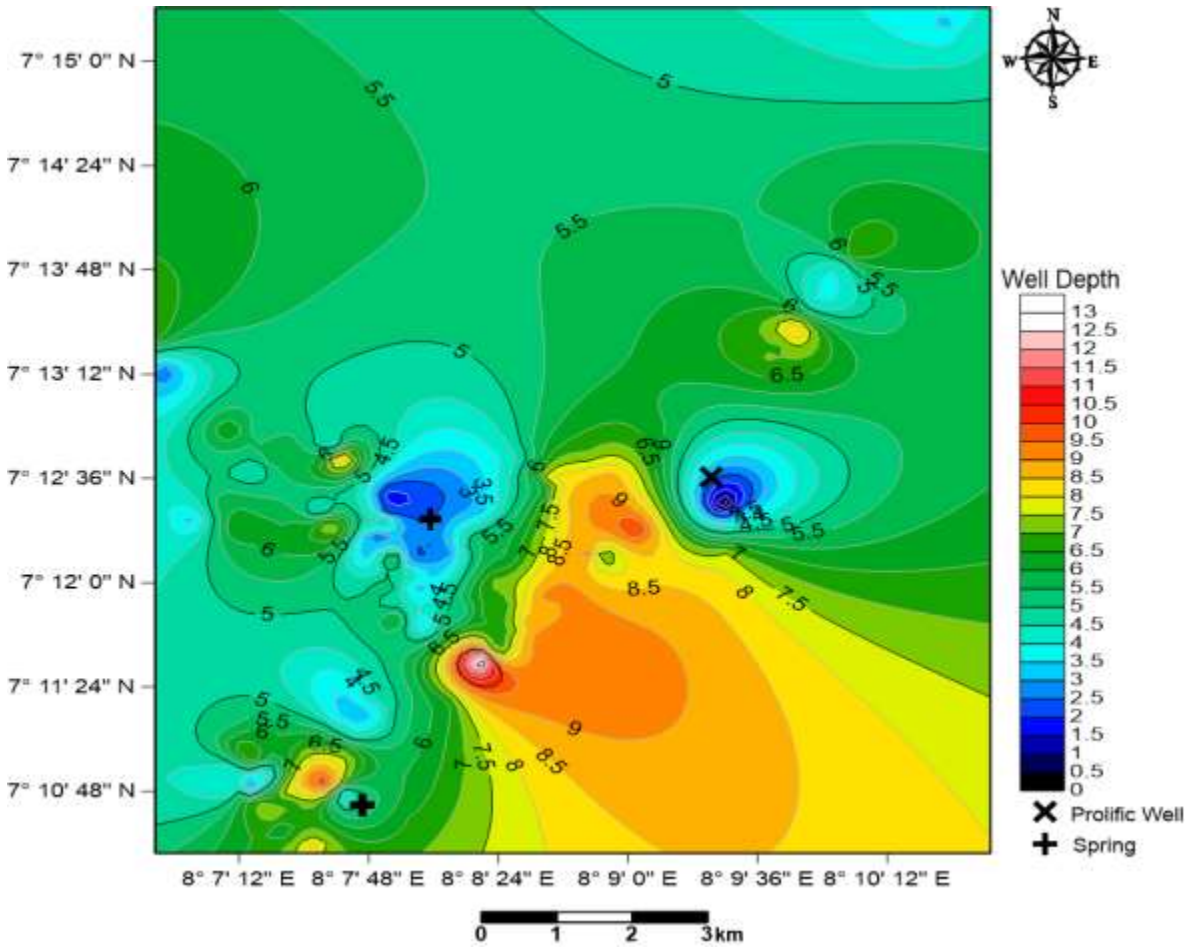

Figure 4.2: Well Depth in Otukpo and Environs

There exists a trend of variation in water levels in the individual wells. Static water level in the wells ranges from 1.8 m to 13.0 m (Figure 4.3). Wells completed close to the surface in the northern district of the study gave similar water levels whereas wells completed in the southern region showed higher relative heads. The elevation of the wells above sea level ranges from 117 m to 196 m (Table A). Groundwater level in the shallow wells situated in the upper subsurface layer of the study area rises at the rapidly of the wet season and dropped rapidly at the peak of the dry season.

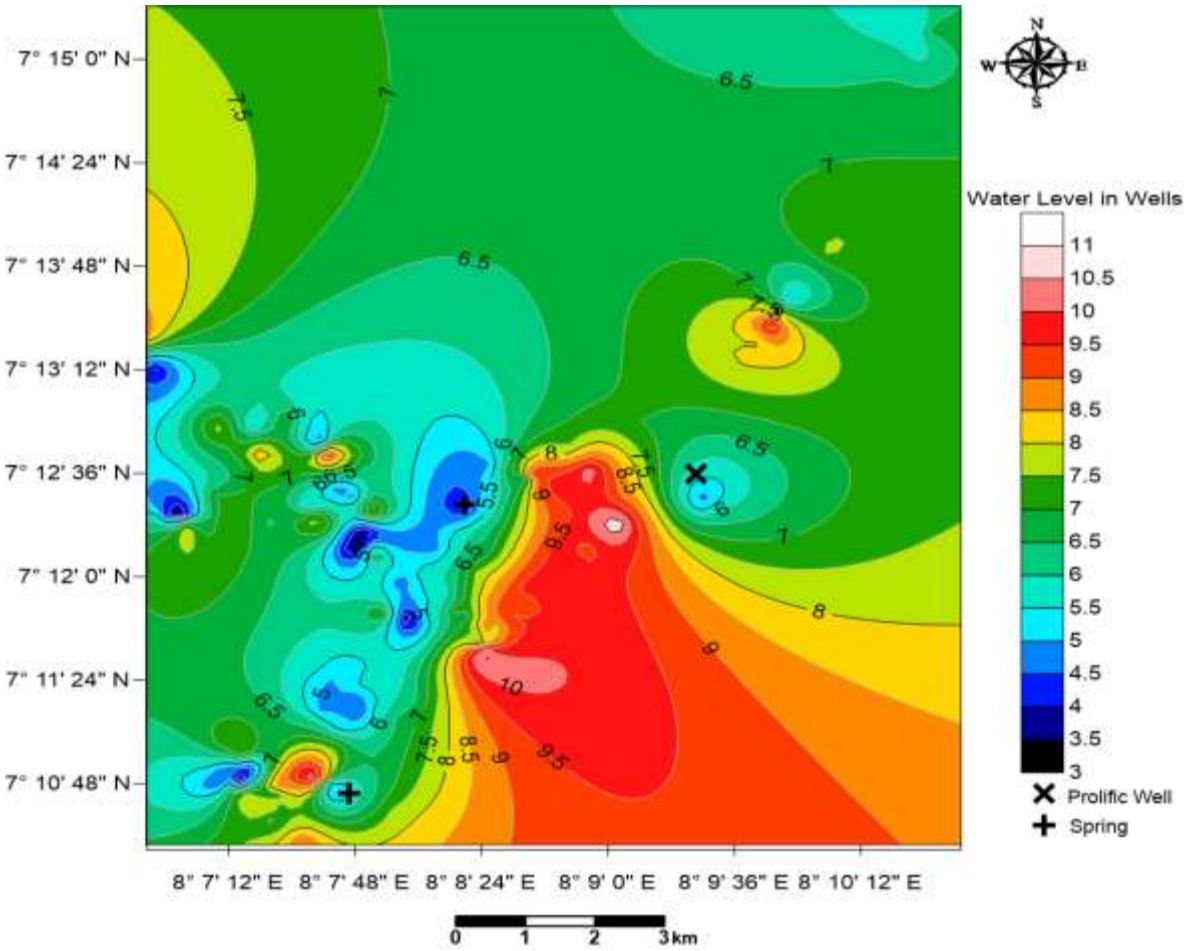

Figure 4.3: Groundwater level in hand-dug wells in Otukpo and its Environs

Groundwater flows in the direction of decreasing hydraulic head or from high potential energy to low energy potential. The contours epitomize the hydraulic head (Isohypses) and the arrow indicates the inferred groundwater flow direction (Figure 4.4). The total head values in the southern section of the area are higher than the head values in the northern section. The water-table map shows an approximate northward groundwater flow as the dominant direction of groundwater flow (Figure 4.4) within the shallow subsurface layer of Otukpo and its environs. At the southern section of the mapped area with high hydraulic head, potential energy increases with depth making the area to possess the character of a groundwater discharge area. With lower head values, the potential energy at the northern section decreases with depth, establishing the section as a groundwater discharge area relative to the shallow unconfined subsurface layer. The water level data collected designate that the shallow unconfined subsurface layer is being recharged by rainfall events. All wells finalised in the shallow subsurface layer show an immediate response to rainy season actions**.**

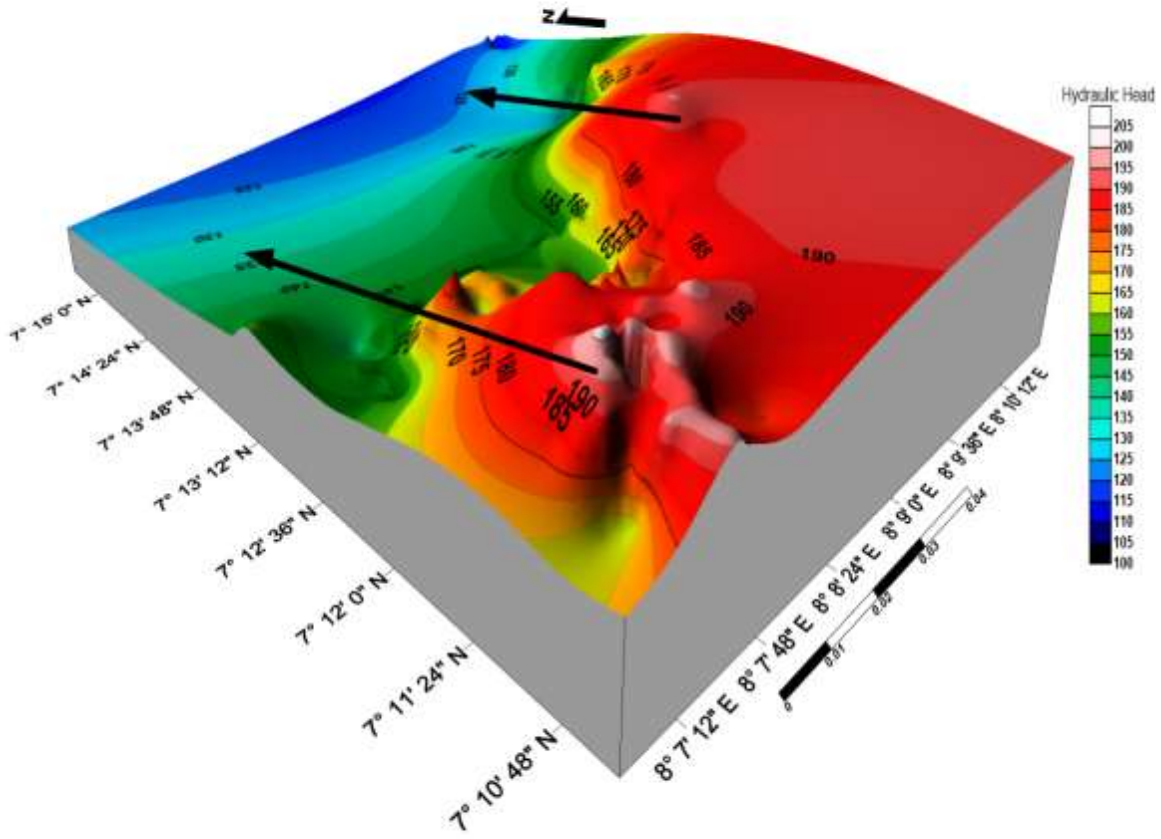

Figure 4.4: Groundwater Flow Direction of Otukpo and its Environs

4.2.1 Shallow groundwater abstraction

Groundwater abstraction structures in Otukpo and its environs are limited to shallow hand dug wells. The hand-dug wells penetrate the shallow unconfined near surface layer. The near surface layer is overlain with a very resistive lateritic layer that is conspicuously observed in most parts of the area.

Most of the wells are unlined with a few of the wells lined with concrete rings or bricks with mortar. The wells experience seasonal recharge with much groundwater all through the rainy season and low groundwater recharge during the dry season. Thin sandy

intercalation between the clayey and shaly formation is responsible for the low hydraulic conductivity that may have stimulated the poor groundwater recharge of the layer.

Two water springs were observed in the area of study where the water-table is understood to have intersected the land surface. These include the Okokolo spring which is located at longitude 7°12′26.4″ and latitude 8°08′19.8″ and the Ukplo spring located at longitude 7°10′34.0″ and latitude 8°08′13.4″. The Okokolo spring has its active sources (eyelets) at Okokolo area (Plate XII and Plate XIII). The drainage area of the stream is moderately small. The stream maintains a flow downstream in the northeast direction. The springs discharge from a sandy-silt unit which is overlain by lateritic cover and underlain by shale sequence.



Plate XII: Section of Okokolo Spring at its source



Plate XIII: The downstream side of Okokolo Springs

At longitude 7°12′49.9″ and latitude 8°09′06.6″ located around Upu road, there exists a hand dug well with a maximum depth of five meters (5m). The well supplies water to about five (5) water tankers per day with 11,000 litres capacity. The well intercepted a shallow confining groundwater discharge area, which makes it productive as a result of the confining pressure from the bottom of the layer by shale and at the top by unfractured lateritic formation.

4.3 Hydrogeophysics

The results of the induced polarization (IP), geoelectrical resistivity investigation, comprising VES and 2D resistivity subsurface tomography (Wenner Alpha array) are presented in Table 4.1 (Appendix B, C and D respectively). The first six (6) points of the VES were re-investigated using the time domain IP method. Five (5) profile lines (AA, BB, CC, DD and EE) were established for the VES, employing the Schlumberger array (Figure 4.5).

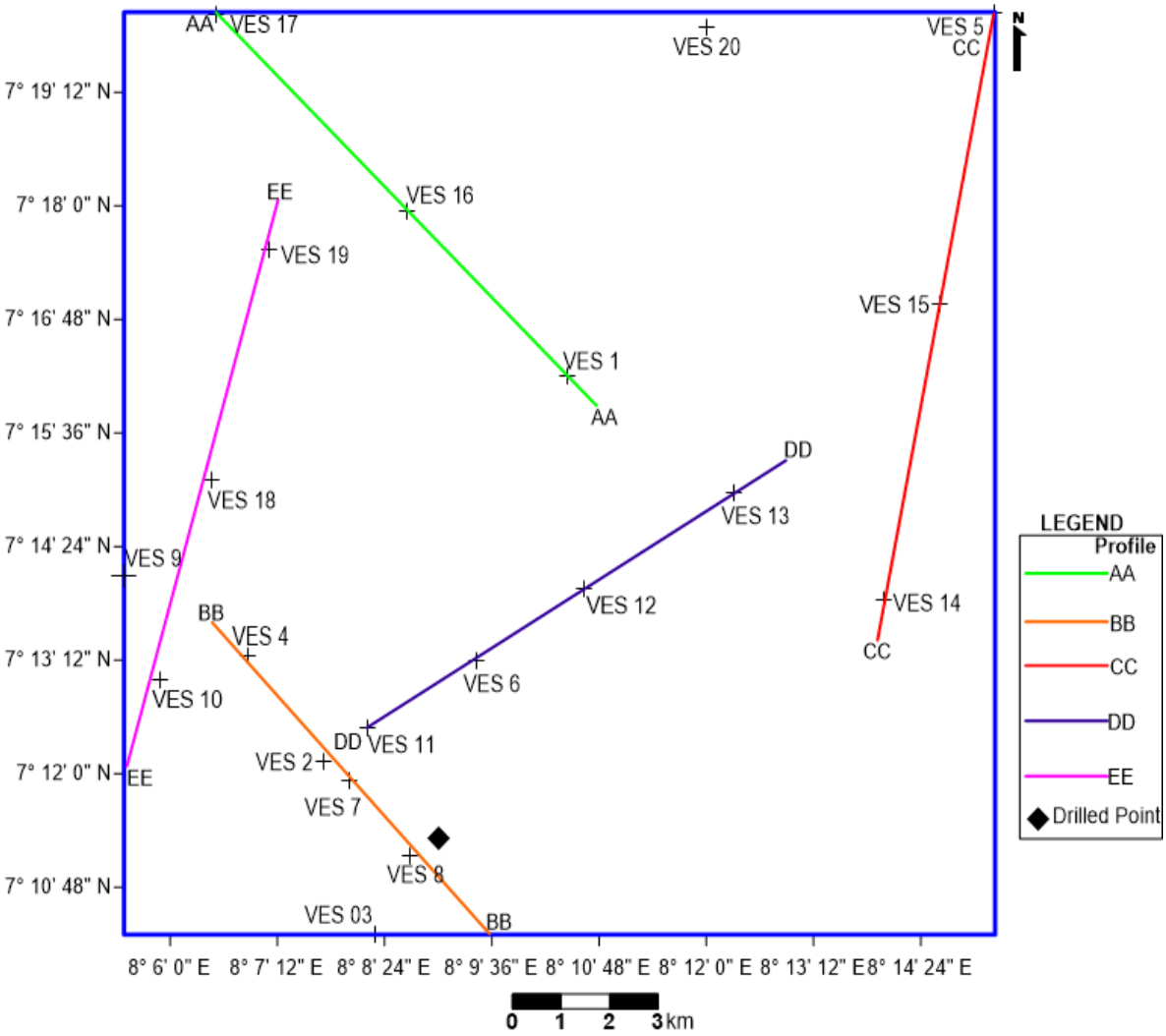

Figure 4.5: Location of VES points and geoelectrical survey profile lines

4.3.1 Induced polarization (IP)

The chargeability figures obtained in the field (Table 4.1) were plotted on a graph against the values of electrode separation. The chargeability pattern shown in the plots reflects the alteration of the underlying subsurface lithologies within the study area.

Table 4.1 IP Chargeability (msec) Data for Otukpo and its Environs

AB/2	IP OTK 01	IP OTK 02	IP OTK 03	IP OTK 04	IP OTK 05	IP OTK 06
1	1.61	1.117	2.86	1.16	0.93	0.89
2	2.7	1.73	3.81	1.43	1.32	1.16
3	3.11	1.79	4.42	2.05	1.28	1.36
4	3.69	1.98	4.04	-0.6	2.73	1.57
4	3.83	1.79	4.38	0.29	2.15	1.62
6	4.12	2	-13.1	-0.39	2.17	1.99
8	4.65	2.21	44.3	172	2.71	2.31
10	4.87	2.79	68.9	75.6	2.97	2.95
12	0.83	4.49	26.6	34.6	3.21	2.71
15	-5.31	4.78	82.37	8.86	3.66	5.44
20	-91.1	20	25	6.32	3.96	9.02
20	-17.3	8.36	22	6.32	3.81	4.69
25	31.3	3.66	100	-5.69	4.18	4.88
30	25	4.47	22.1	-7.08	4.95	5.38
35	8.15	-4.14	25.2	-9.65	3.98	11.6
40	74	-17.4	2.5	-42.4	10.1	11.6
50	-130	-11.3	-205	-116	15.9	9.23
60	-100	36.4	-108	-50	-2.63	3.65
80	-84.5	-43	-451	-121	-21.7	-51.2
80	-34.1	-5.74	-419	-115	-7.21	-22.8
100	-246	-40.9	-320	-136	-11	-10
125	-258	-49.7	-481	-191	-9.5	-30.6
150	-272	-50	-306	-143	-10.79	-145
150	-252	-38	-552	-70	-34.8	-96
200	-270	-117	-289	-42.9	-36.9	-12.7
250	-272	-12.3	-280	-50.9	-318	-87.7
300	-273	18.6	-278	-47.9	-23.99	-157
350	-430	16.2	-262	-40	-634	-264
400	-89	-121	-205	13	-243	-112
400	-90	-133	-291	11	-187	-98.5
500	54	10	10.2	54	301	51.05
600	94	15.2	44.5	98	400	66.9
600	105	56.3	52.3	100		

The IP OTK 01 plot (Figure 4.6) shows consistent low chargeability values of 0.83 msec to 4.87 msec at the shallow subsurface depth, varying from 1 m to 12 m. There is a consistent increase in the negative chargeability values from -246 at 100 m depth to -430 msec at 350 m depth. The IP plot shows appreciable chargeability increase of 54 msec at 500 m to 105 msec at 600 m depth.

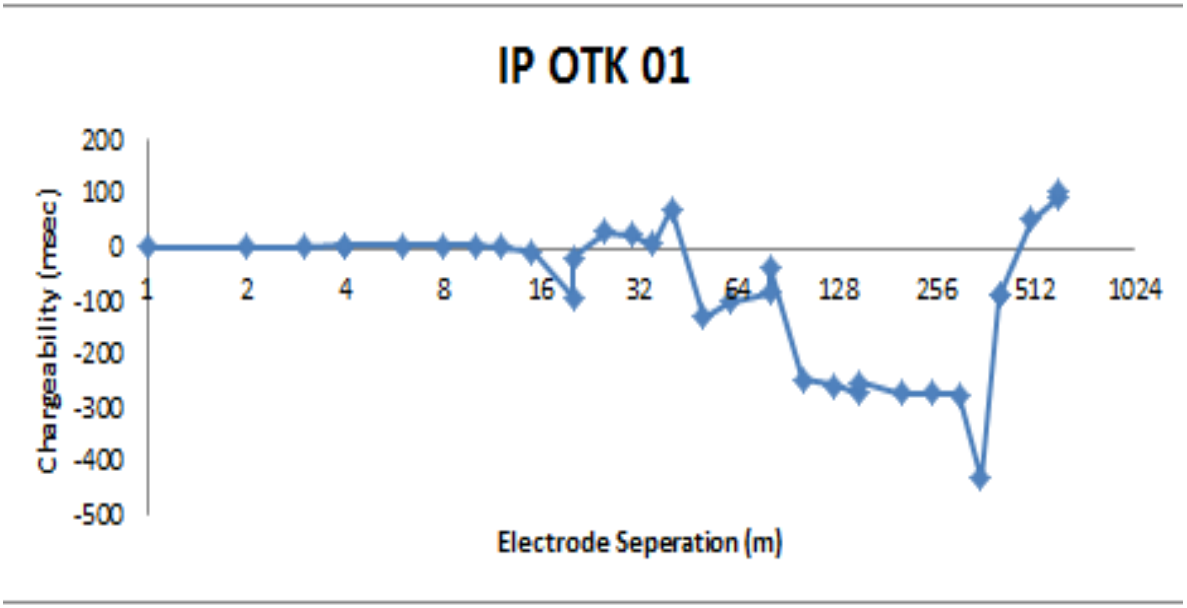

Figure 4.6: OTK 01 Chargeability Curve

The shallow subsurface of section 2 sounding shows fairly low chargeability values of 1.12 msec to 4.47 msec at the depth range of 1m to 30 m indicating a sharp increase of 20.0 msec at 20 m depth. The IP curve shows a sharp decline or decrease in chargeability to -4.14 msec value at 35 m depth. The corresponding negative chargeability peaks at station 3 sounding at 400 m depth of the electrode separation. At 500 m and 600 m the values increase to 10.0 msec to 56.3 msec respectively (Figure 4.7).

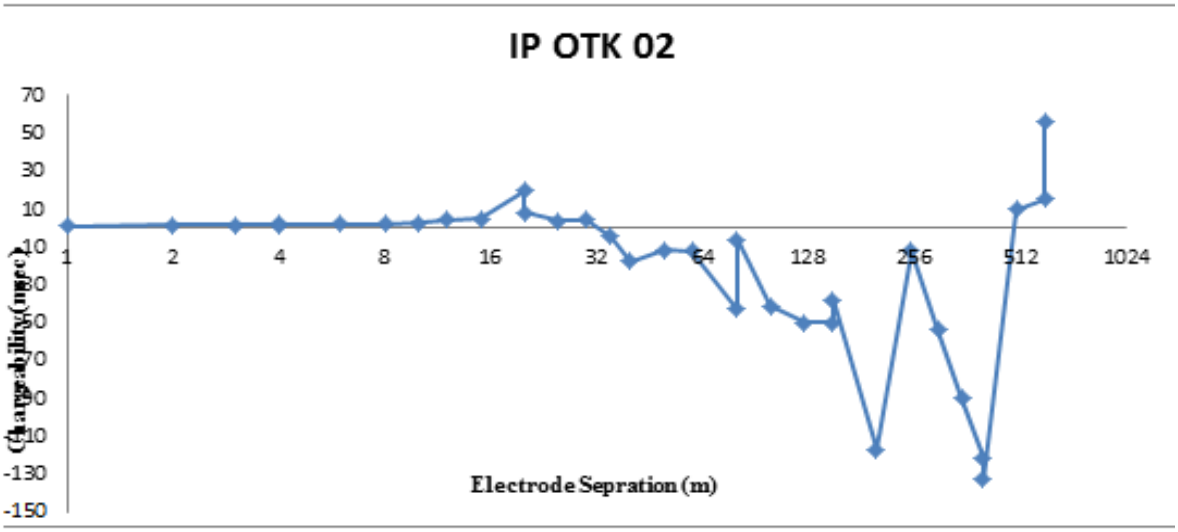

Figure 4.7: OTK 02 Chargeability Curve

The shallow subsurface of section 3 sounding shows fairly low chargeability value of 2.9 msec to 82 msec at theapproximate depth range of 1 m to 20 m. The IP curve shows a sharp negative chargeability value at 50 m depth. The corresponding negative chargeability peaks at station 3 sounding within the depth range of 50 m to 400 m electrode separation. At 500 m and 600 m AB/2 the values increase to between 10.2 msec and 52.3 msec respectively (Figure 4.8).

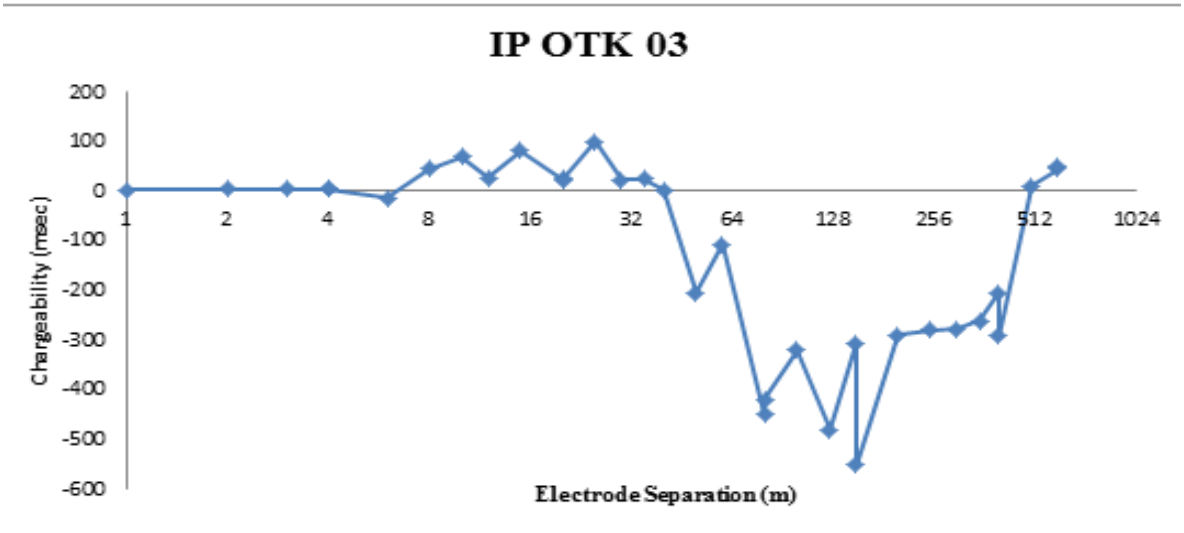

Figure 4.8: OTK 03 Chargeability Curve

At Station 4, chargeability increase was noticed at shallow depth between 01 m and 06 m after which the curve showed a peak increase of 75.6 msec in chargeability at 8 m depth which gradually dropped to 6.3 msec at 20 m depth. There was a sudden drop to negative chargeability values range of less than -10 msec to -191msec at the depth of 32 m to 300 m, with an abrupt positive increase of 11 msec and 100 msec at the depth range of 400 m to 600 m respectively (Figure 4.9).

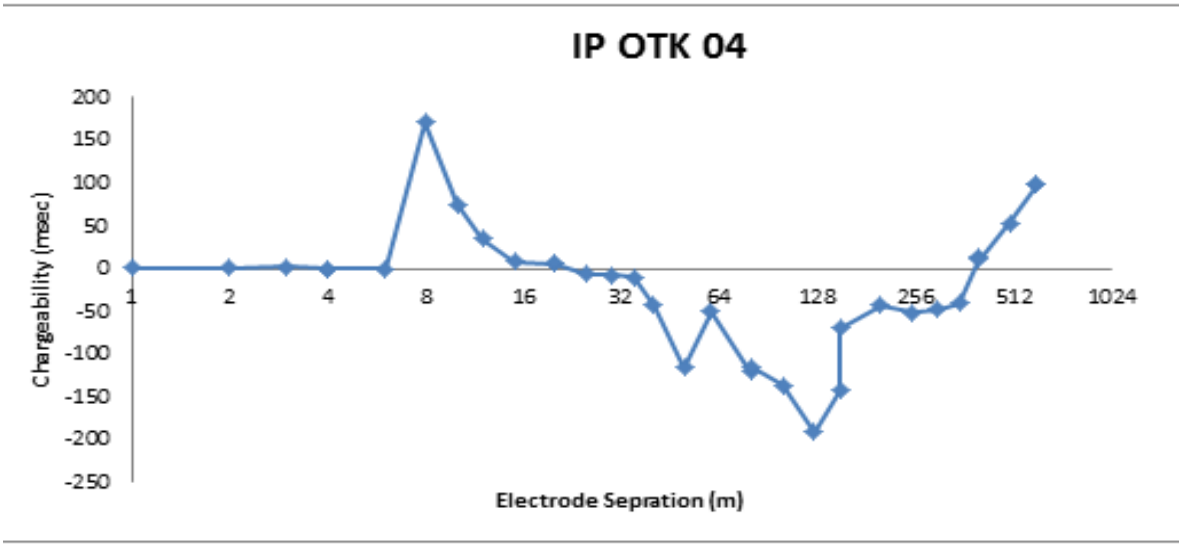

Figure 4.9: OTK 04 Chargeability Curve

Station 5 is indicative of consistently low chargeability ranging from 0.93 msec to 15.9 msec at the depth range of 1 m to 50 m respectively (Figure 4.10). Negative chargeability value of -2.63 msec was observed at 60 m depth, the peak negative chargeability of -634 msec was shown at 350 m depth. At 500 m and 600 m positive fairly high chargeability of 301 msec and 400 msec were indicated.

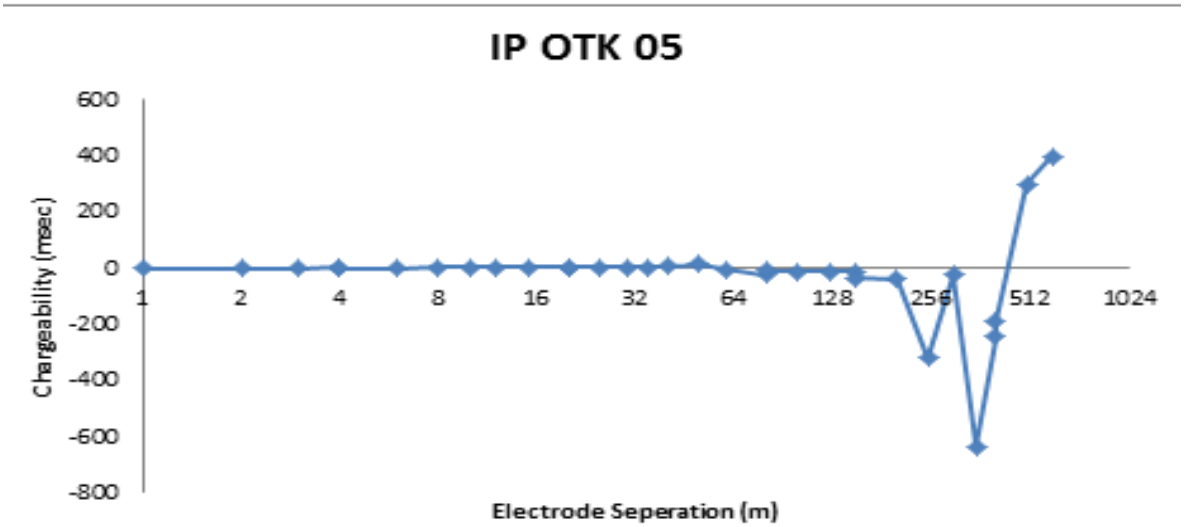

Figure 4.10: OTK 05 Chargeability Curve

The chargeability as indicated in Plot 6 (Figure 4.11), gave a low value of 0.89 msec at 1m depth and 3.65 msec at 60 m depth. Negative chargeability increase was observed at 80 m to 400 m depths with chargeability values ranging from -10msec to -262 msec. 500 m to 600 m at the sounded point showed a fairly positive increase in chargeability of 51.05 msec and 66.9 msec respectively (Figure 4.11).

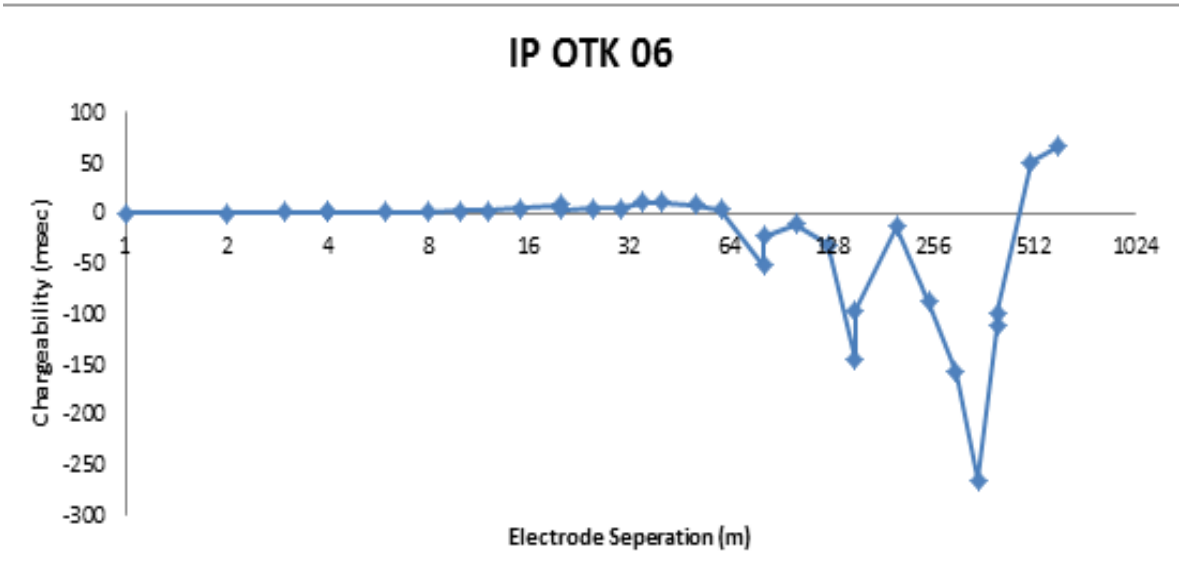

Figure 4.11: OTK 06 Chargeability Curve

4.3.1.1 Summary of IP survey

From the interpretation on the chargeability signatures, compositional heterogeneity of Otukpo and environs subsurface became evident when all measurements of chargeability depicted three to four layers. The first layer is modelled with consistent fairly moderate IP effect observed in near subsurface at (AB/2) depth between 01 m - 20 m. These volumes with low to moderate chargeability are interpreted to consist of lithological matrix of loess sand, silty-sand and moist sandy-clay soils.

The IP effects of the near subsurface is noticed at the depth below 25 m electrode separation, the models also predict considerable low (negative) chargeability at varying depth for all the surveyed points. It is most likely that paradoxical behaviour of the subsurface showing strong negative chargeability responses in this study may be attributed to the effect of highly conductive zone made up of wet clay/shale concentrations within the studied sedimentary formation. This is supported by the findings of Dahlin and Loke (2015), which revealed that negative chargeability can rise as a result of the dissemination of chargeable zones in the subsurface. If the chargeable subsurface zones are predominantly located in zones of negative sensitivity, and there exist low to no chargeability in the positive sensitivity, volumes in the studied subsurface will result in negative apparent IP (chargeability). The negative chargeability value of the subsurface clay/shale lithology is also supported by the findings of Brandes and Acworth (2003), which states that alternate soft clay possesses pH gradients that are large which form under an applied electrical field. Relaxations of these pH gradients at the samples exterior will create a potential in the opposite sign (negative) to the applied potential, and so produce negative chargeability values.

An appreciable increase in positive chargeability value was observed at proximate sounded electrode separation of 500 m and 600 m in all the plots, indicating clay/shale free sediments composed of saturated sandstone. The deviation from the negative chargeability values to positive chargeability values at greater depth in the sounded points indicate the occurrence of fresh water in the sandstone environment.

4.3.2 1-D Vertical electrical sounding

Detailed description of the VES curves showing the different geoelectric layers including their respective resistivity, thickness, depths and curve types are presented in Table 4.2. The VES is limited to the vertical dissemination of electrical resistivity within the earth in the study area. Representative VES curves from the research area are displayed in Figures 4.12, 4.13, 4.14 and 4.15 showing different geoelectric curve types encountered. Iso–parametric maps are also shown in Figures 4.16 to 4.21. The table in Appendix B indicates the VES data. The plot of VES data of all the sounded points are presented in Appendix C.

The iterated model converges within 3 to 5 iterations demonstrating that the data quality is decent and reliable which is also appreciated from the RMS value which ranged from 5.7 to 18.5 for the individual model results. Five subsurface geoelectric units were delineated beneath the VES sections. There existed a resistivity overlapping values between highly conductive geomaterials of clay, shale and silty-sand.

Table 4.2: Summary of the geoelectric parameters including their respective resistivity, thickness, depths and curve types

	APPARENT RESISTIVITY ℓ (Ωm) / THICKNESS T (m) / DEPTH d (m)									
LAYER	VES. OTK 01	VES. OTK 02	VES. OTK 03	VES. OTK 04	VES. OTK 05	VES. 0TK 06	VES. OTK 07	VES. OTK 08	VES. OTK 09	VES. OTK10
Layer 1 ℓ1/T1/d1	500/1.2/1.2	151/1.1/1.1	911/1.6/1.6	103/2.0/2.0	380/2.6/2.6	204/0.7/0.7	134/0.9/0.9	154/0.7/0.7	230/1.0/1.0	779/1.0/1.0
Layer 2 ℓ2/T2/d2	710/4.8/6.0	249/7.5/8.6	641/0.6/2.3	17/10.3/12.3	29/24.6/27.2	833/5.4/7.1	416/6.2/7.2	1055/4.5/5.3	274/6.0/7.1	1462/2.3/3.3
Layer 3 ℓ3/T3/d3	9/94.0/100.0	5/1119.7/127.7	11/8.0/10.2	4/80.3/92.5	2/101/128.3	6/30.2/37.3	5/91.7/98.9	19/26.3/31.6	4/110.0/125.0	49/18/21.3
Layer 4 ℓ4/T4/d4	28/370.0/470.0	12/272.4/333.1	3/335.0/350.0	49/343.8/436.4	10/267.3/395.5	4/250.0/300.0	119/344.8/443.7	6/310.0/350.0	12/225.0/350.0	7/275/300
Layer 5 ℓ5/∞	29/∞	25/∞	34/∞	24/∞	28/∞	113/∞	50/∞	194/∞	52/∞	127/∞
Curve Type	QHK	KH	QH	QH	QHK	KQH	KH	KQH	QH	QH
LAYER	VES. OTK11	VES. OTK12	VES. OTK13	VES. OTK14	VES. OTK15	VES.OTK16	VES.OTK17	VES.OTK18	VES.OTK19	VES.OTK20
Layer1 ℓ1/T1/d1	196/1.2/1.2	250/1.2/1.2	851/0.9/0.9	2289/0.7/0.7	7347/1.3/1.3	107/0.8/0.8	1986/1.3/1.3	1352/3.2/3.2	911/1.0/1.0	107/1.7/1.7
Layer 2 ℓ2/T2/d2	287/6.7/7.8	30/6.7/7.9	254/9.4/10.3	233/3.7/4.3	63/5.5/6.7	238/3.7/4.5	102/2.8/4.1	137/8.5/11.7	98/9.0/10	70/1.7/3.4
Layer 3 ℓ3/T3/d3	7/22.6/30.4	7/30.5/38.4	5/144.2/154.5	8/25.7/38.1	7/16.0/22.7	7/18.1/22.6	9/19.8/23.8	10/48.1/59.8	8/190/200	32/16.8/20.2
Layer 4 ℓ4/T4/d4	10/365.0/400.0	5/310/350	10/250/400.0	3/370/400	3/395.0/420.0	3/350.0/370.0	3/475/500	4/315/355.0	68/200/400	6/365.0/400.0
Layer 5 ℓ5/∞	73/∞	89/∞	40/∞	84/∞	61/∞	49/∞	70/∞	92/∞	127/∞	92/∞
Curve Type	QH	QH	QH	QH	QH	KH	QH	QH	QH	QH

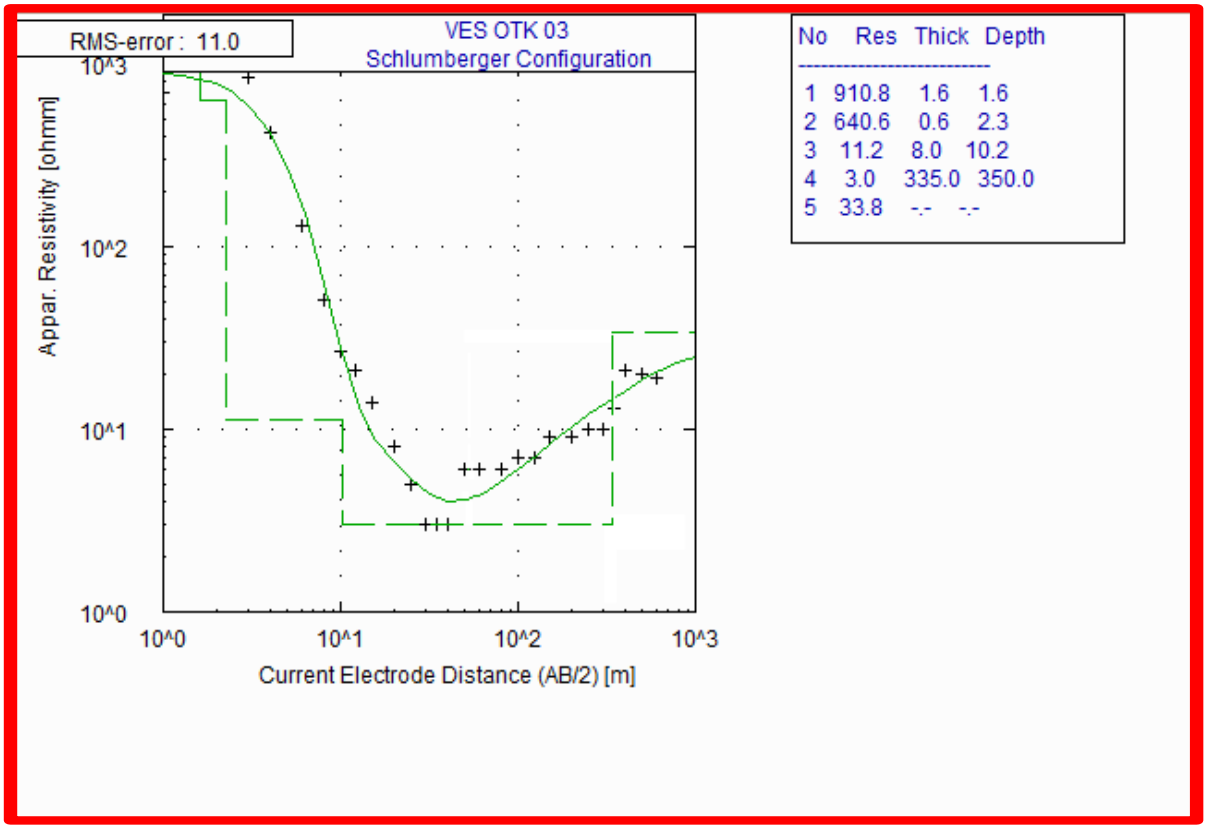

Figure 4.12: QH Curve Type

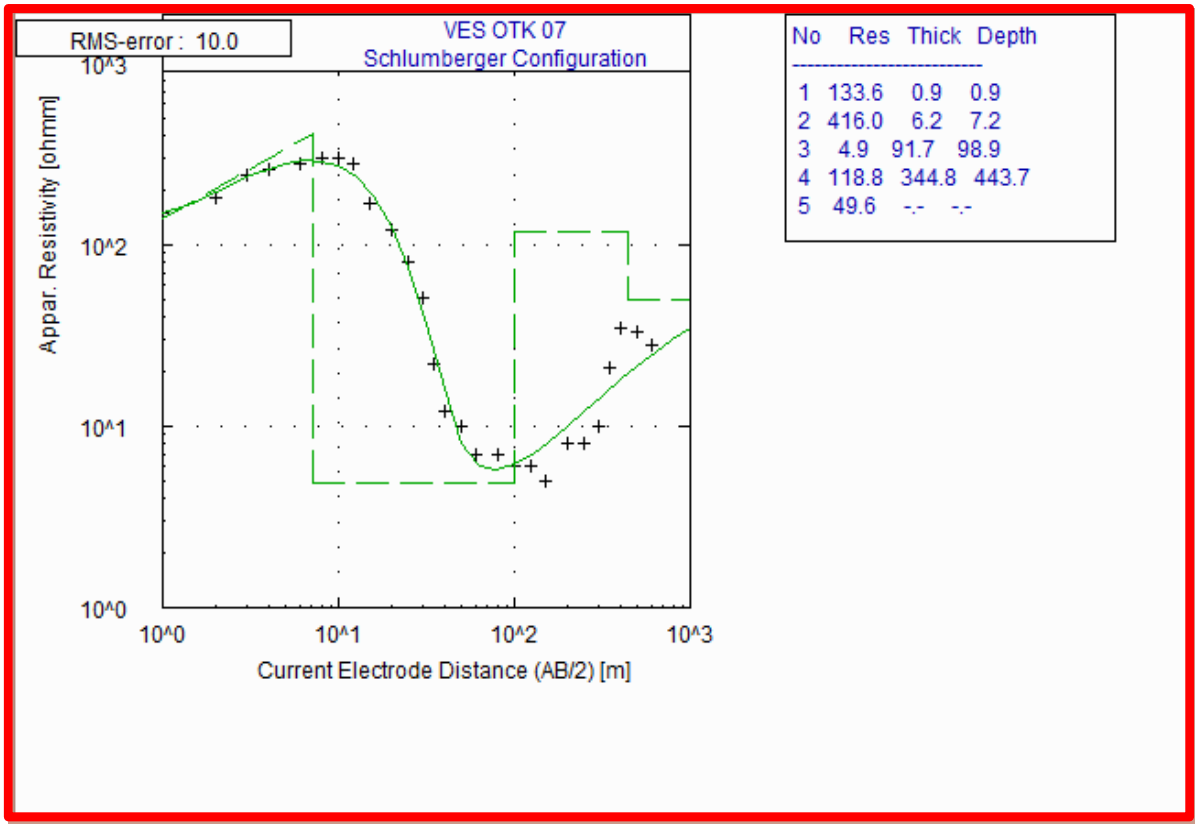

Figure 4.13: KH Curve Type

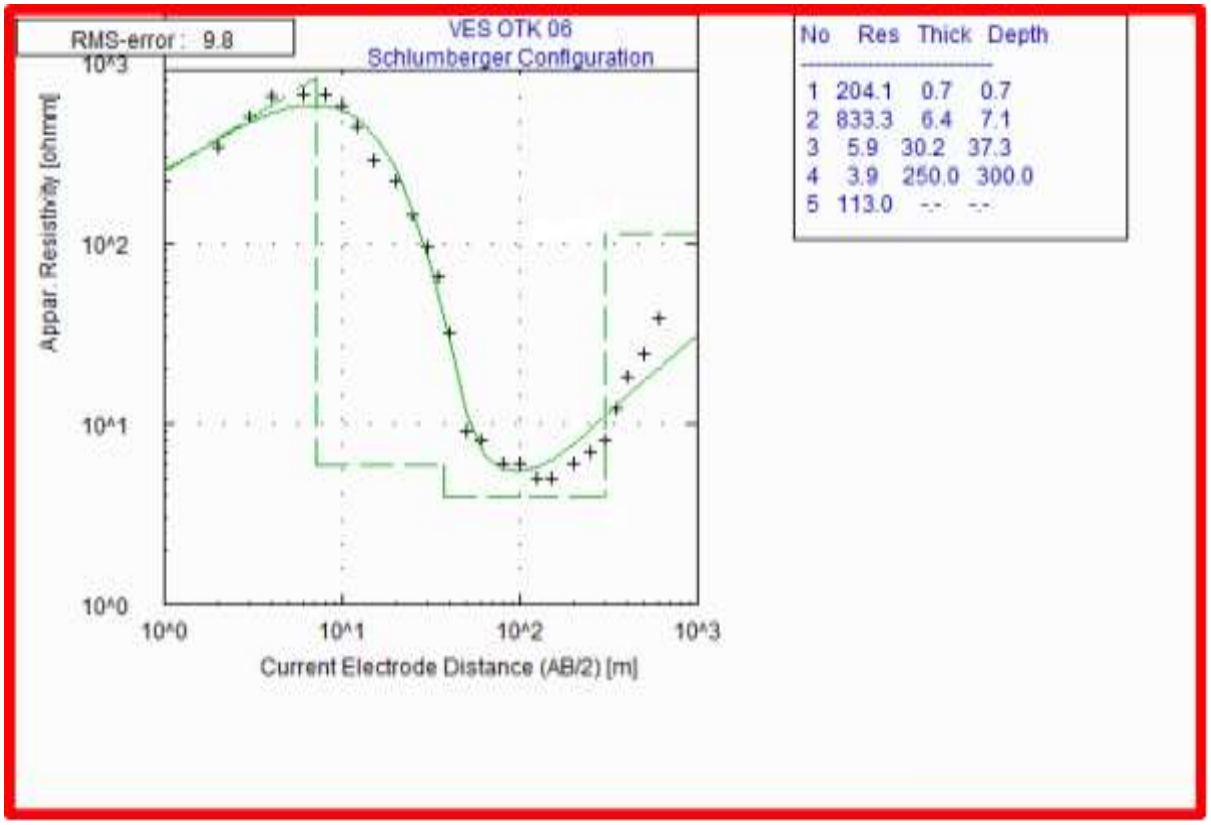

Figure 4.14: KQH Curve Type

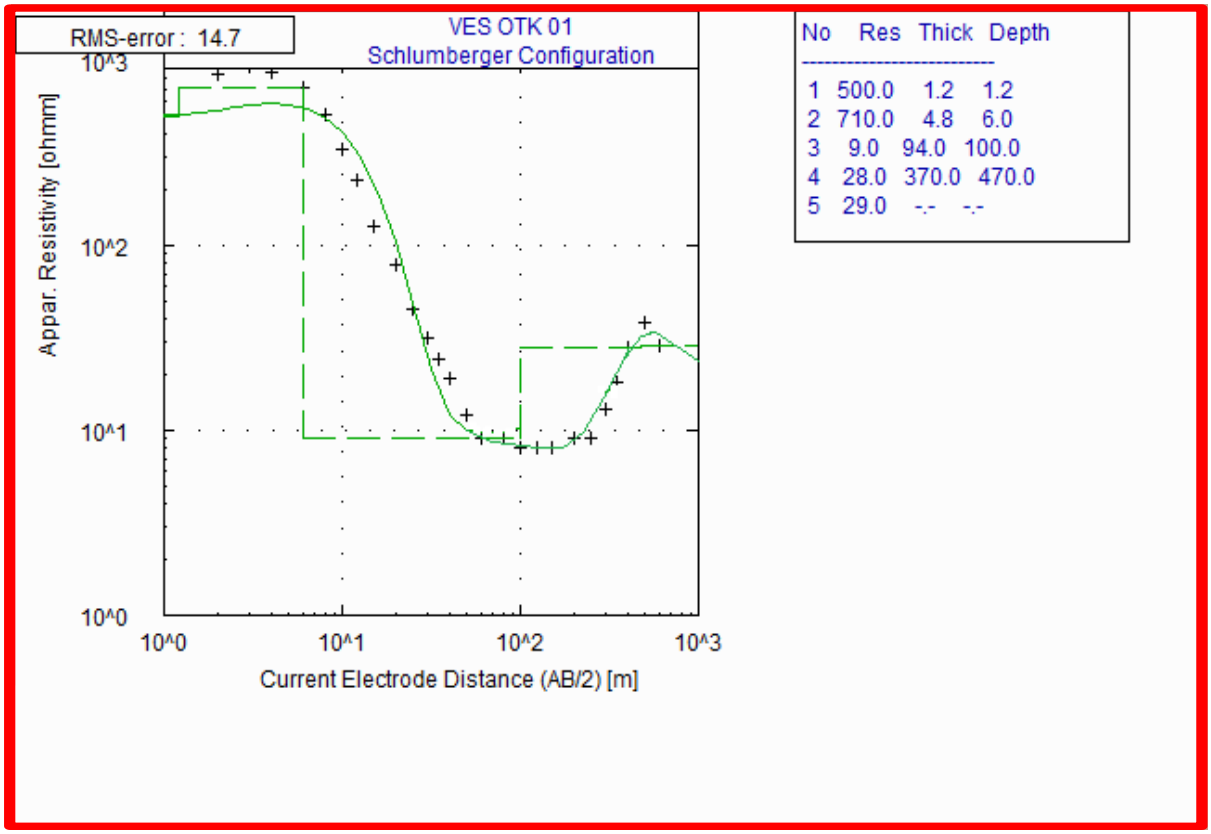

Figure 4.15: QHK Curve Type

Information from the VES reveals that there exists a near surface layer of moderate to high resistivity of 103.0 Ωm to 2298.0 Ωm and from 0.6 m to 3.7 m average depth range with an apparent thickness ranged of 0.6 m to 3.7 m. Alternate layers of geomaterial composed of silty-sand and lateritic soil constitute the upper layers of the investigated areas at different points of the VES.

The second geoelectric layer is made up of lose sand and silty-sandy soils with resistivity range of 17.0 Ωm to over 1462.0 Ωm. The second layer is containing geomaterials of alternating sand and silt with laterite in some places. This layer has a relative depth value range of 3.3 m to 27.2 m and a thickness range of 1.7 m to 24.6 m.

The clayey and clayey-shale layer which represents the third geoelectric layer shows resistivity that ranged in values from 2.0 Ωm to 49.0 Ωm with a thickness range varying from 5.2 m to 190.0 m. Clay has high conductivity than sandstone which may be attributed to the occurrence of iron cluster on the surface of clay.

The forth layer is associated with extremely low resistivity in most of the VES points with moderate resistivity at depth in some of the VES points. The apparent resistivity of the predominantly shale layer drops to less than 4 Ωm and the relative increase in resistivity of 194 Ωm in a few metres depth is attributed to the matrix of shale and sandstone. The layers thickness ranged from 68.3 m to 344.8 m with a mean depth range of 300.0 m to 500.0 m.

The fifth geoelectric layer which is composed of sandstone showed moderate to high resistivity compared to the overlying shale layer. The resistivity of the layers ranged in value from 24 Ωm to 194 Ωm, extending to a fairly infinite depth. The curves show a substantial change in the resistivity data values between the overlying shale layer and the underlying sandstone layer.The depth to this sandstone layer varies negligibly across the studied area.

The minimum and maximum resistivities obtained in the study area ranged from 2.0 Ωm 2298 Ωm, representing lateritic soil and shaly-clay respectively. This shows the lithological variability of the subsurface of the study area. Information revealed by the geoelectric layers showed that the shale layer of low resistivity is differentiated from the sandstone in a few hundred meters depth with increase in resistivity values. It is observed that the shale effect in the subsurface is quite apparent.

The VES results (Appendices B and C) revealed that all the curve types possess five (5) distinctive layers, where ℓ_1, ℓ_2, ℓ_3, ℓ_4 and ℓ_5 are the resistivity of the first layer, second, third, fourth and fifth layers respectively. In the morphological analysis of the field curves, the resulting geoelectrical sections were of the curve types QH, KH, KQH and QHK. The QH curve has 65% dominance in the area with the KH having 15%, KQH 10% and the QHK type also having 10%.

4.3.2.1 Summary of VES investigation

Taking into account the morphology of the VES field curves and the variation in the resistivity values, the following curve types are evident in Otukpo and its environs:

QH = $\ell_1 > \ell_2 > \ell_3 \geq \ell_4 < \ell_5$	65%
KH = $\ell_1 < \ell_2 > \ell_3 > \ell_4 < \ell_5$	15%
KQH = $\ell_1 < \ell_2 > \ell_3 \geq \ell_4 < \ell_5$	10%
QHK = $\ell_1 > \ell_2 < \ell_3 > \ell_4 > \ell_5$	10%

The portions of the curves that show frequently low electrical resistivity are those where electrical conductivity is dominant with clay/shale as the major lithology. Those portions of the curves with electrical resistivity appreciating at depth relative to the lower resistivity of

shale at the overlying layer is related to saturated, porous and permeable formation where sandstone is dominant. All the VES model curve types produced from the iterated geoelectric data are typical models of a sedimentary formation.

4.3.3 Correlation of resistivity and IP sections

A careful analysis of the resistivity and chargeability in the 1D result shows that the observed low resistivity values did not reflect distinct and relatively high chargeability values. Clay is expected to produce high chargeability anomaly due to cation exchange capacity and greater conductance surface and minerals that help in the particle charging procedure but in this case negative chargeability values were recorded. The low-resistivity and negative chargeability layers corresponded to pure clay/shale layers while low-resistivity and medium to high chargeability layers depicted saturated sandstone layer.

The Otukpo and its environs subsurface description designated that the top part of the near subsurface is composed of laterite and silty-sand at variable locations. The apparent resistivity of these top layers range varied from 103.0 Ωm to 1462.0 Ωm, while that of normalized chargeability ranged from 0.83 msec to 75.6 msec. The middle of the aquifer system consist of a layer with clay/shale content, and the resistivity value ranges from 2.0 Ωm to 49.0 Ωm, whereas the normalized chargeability is between the range of -2.63 msec to -634 msec. The bottom of investigated subsurface consisted of a layer with resistivity value rangeof24 Ωm to 194 Ωm, however the normalized chargeability is between the range of10 msec and 400 msec. The presence of saturated sandstone deposits at the bottom layer might be responsible for the approximate increase in the apparent resistivity and an abrupt change from negative to positive normalize chargeability.

The results of normalized chargeability displayed a clear trend of decreasing (negative) IP values in layers with high clay/shale content, and lower positive values in coarse material of sandstone, the major lithological content at the bottom (Table 4.3). Resistivity values at the top layer is associated with lateritic soil and silty-sand; at the middle layers it is attributed to clay/shale while at the bottom layer it is attributed to saturated sandstone.

Table 4.3: Apparent resistivity and chargeability data of Otukpo and its environs

Distance	7°16.192′N 8°10.451′E OTK 01		7°12.131′N 8°07.714′E OTK 02		ASA OTK 03		7°13.241′N 8°06.871′E OTK 04		7°20.04′N 8°15.22′E OTK 05		7°13.189′N 8°09.433′E OTK 06	
AB/2	ℓa	IP	ℓa	IP	ℓa	IP	ℓa	IP	ℓa	IP	ℓa	IP
1	500	1.61	139	1.117	700	2.86	99	1.16	230	0.93	220	0.89
2	849	2.7	175	1.73	950	3.81	88	1.43	355	1.32	338	1.16
3	920	3.11	202	1.79	846	4.42	74	2.05	511	1.28	499	1.36
4	861	3.69	209	1.98	419	4.04	57	-0.6	646	2.73	647	1.57
4	860	3.83	209	1.79	419	4.38	57	0.29	646	2.15	647	1.62
6	710	4.12	216	2	129	-13.1	43	-0.39	724	2.17	671	1.99
8	515	4.65	227	2.21	51	44.3	22	172	733	2.71	660	2.31
10	334	4.87	234	2.79	27	68.9	18	75.6	707	2.97	578	2.95
12	226	0.83	218	4.49	21	26.6	17	34.6	690	3.21	438	2.71
15	127	-5.31	169	4.78	14	82.37	14	8.86	661	3.66	289	5.44
20	79	-91.1	100	20	8	25	11	6.32	524	3.96	219	9.02
20	79	-17.3	100	8.36	8	22	11	6.32	524	3.81	219	4.69
25	45	31.3	62	3.66	5	100	9	-5.69	378	4.18	145	4.88
30	34	25	37	4.47	3	22.1	8	-7.08	272	4.95	95	5.38
35	26	8.15	22	-4.14	3	25.2	7	-9.65	158	3.98	65	11.6
40	20	74	14	-17.4	3	2.5	6	-42.4	140	10.1	32	11.6
50	13	-130	9	-11.3	6	-205	5	-116	73	15.9	9	9.23
60	10	-100	8	36.4	6	-108	5	-50	42	-2.63	8	3.65
80	10	-84.5	6	-43	6	-451	4	-121	18	-21.7	6	-51.2
80	10	-34.1	6	-5.74	6	-419	4	-115	18	-7.21	7	-22.8
100	11	-246	5	-40.9	7	-320	4	-136	10	-11	6	-10
125	11	-258	5	-49.7	7	-481	5	-191	6	-9.5	5	-30.6
150	12	-272	4	-50	9	-306	5	-143	3	-10.79	5	-145
150	13	-252	5	-38	9	-552	5	-70	3	-34.8	5	-96
200	14	-270	6	-117	9	-289	7	-42.9	3	-36.9	6	-12.7
250	15	-272	7	-12.3	10	-280	8	-50.9	3	-318	7	-87.7
300	28	-273	9	18.6	10	-278	12	-47.9	5	-23.99	8	-157
350	32	-430	15	16.2	13	-262	13	-40	6	-634	12	-264
400	50	-89	21	-121	21	-205	15	13	22	-243	18	-112
400	52	-90	21	-133	21	-291	15	11	22	-187	18	-98.5
500	95	54	30	10	34	10.2	13	54	32	301	24	51.05
600	161	94	42	15.2	82	44.5	11	98	45	400	38	66.9
600	167	105		56.3	82	52.3		100			38	

4.3.4 Isoresistivity interpretations

The apparent resistivity distribution of the subsurface lithology at 25 m depth (Figure 4.16) shows that the resistivity at the northern section is uniformly distributed. The lowest resistive

zone is situatedat the eastern segment of the area of study. Areas with more conductive zones are decent signal of porous lithological unit. The resistivity at the eastern section might be attributed to the effect of pure clay or shale lithology. The resistivity showed an elevated increase range of 55 Ωm to 145 Ωm at the southern portion of the area. This is indicative of silty-sand and sandy-clay lithologies which make up the shallow subsurface groundwater bearing layer producing seasonal groundwater to wells.

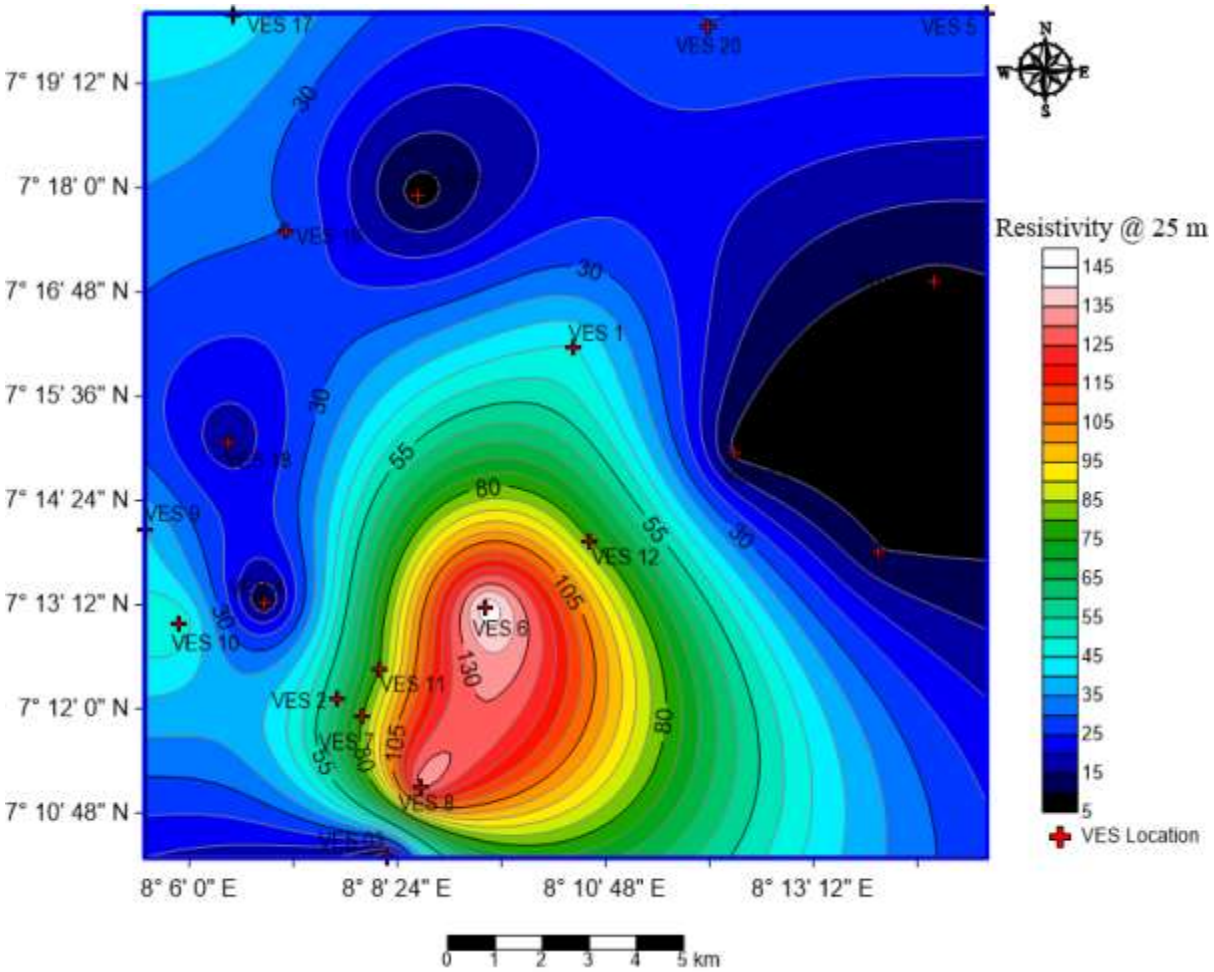

Figure 4.16: Isoresistivity at 25 m depth in Otukpo and its Environs

At 100 m depth the values of resistivity less than 15 Ωm as revealed on the map indicates that the depth at 100 m is composed of shale. The variation in the resistivity may be attributed to pure shale and shale matrix with clay. The lowest apparent resistivity (about 3 Ωm) in the

area is indicated around the eastern section, suggesting that pure shale is underlying the area at 100 m depth (Figure 4.17).

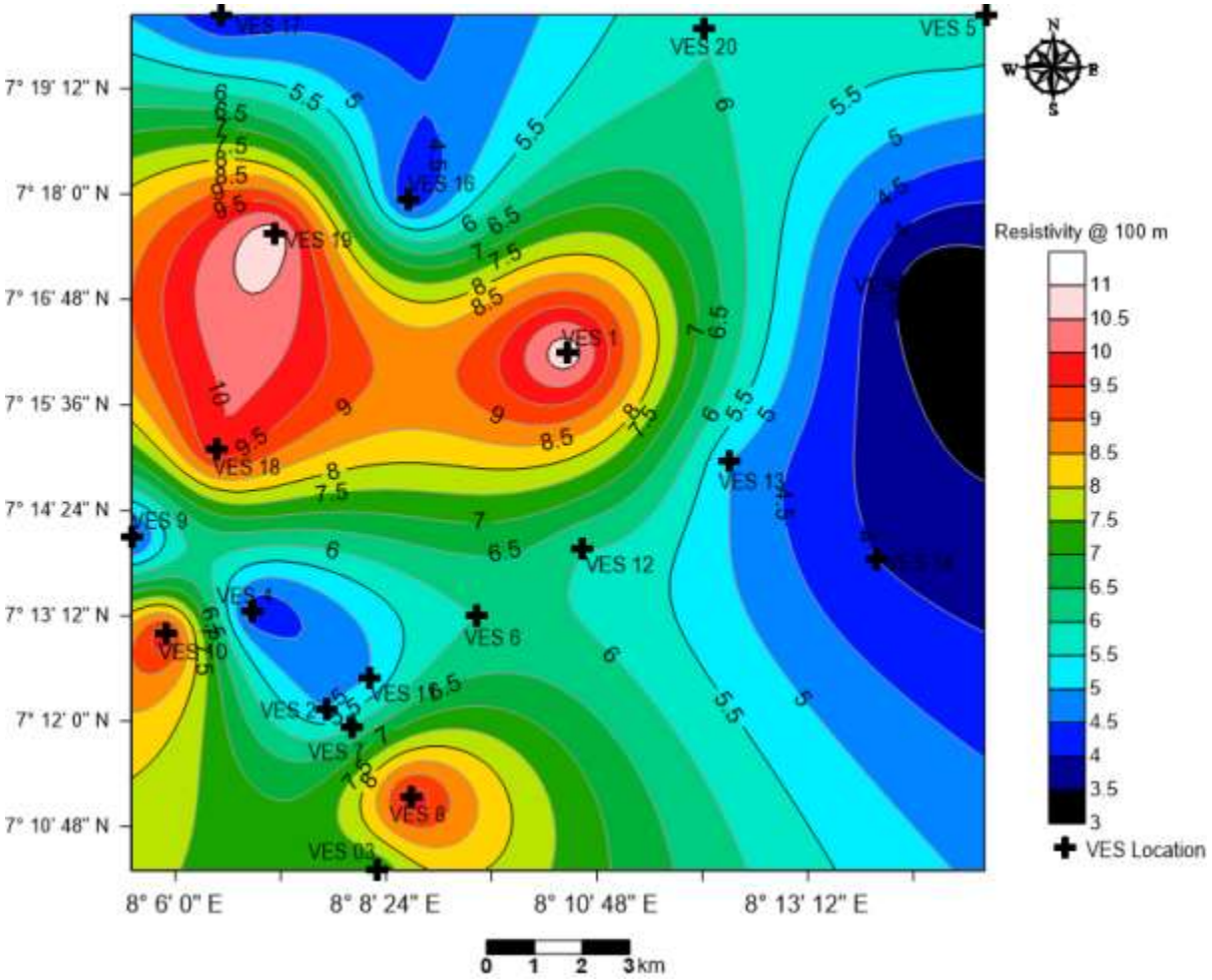

Figure 4.17: Isoresistivity at 100m depth in Otukpo and its Environs

The non-uniqueness of the apparent resistivity at 200 m depth within the study area suggests a slight variation in the lithological properties underlying the subsurface at this depth (Figure 4.18). The areas with low resistivity range of 2 Ωm to 7 Ωm are indicative of saturated shale while the western part of the area with variable apparent resistivity is attributed to the occurrence of relatively unsaturated shale.

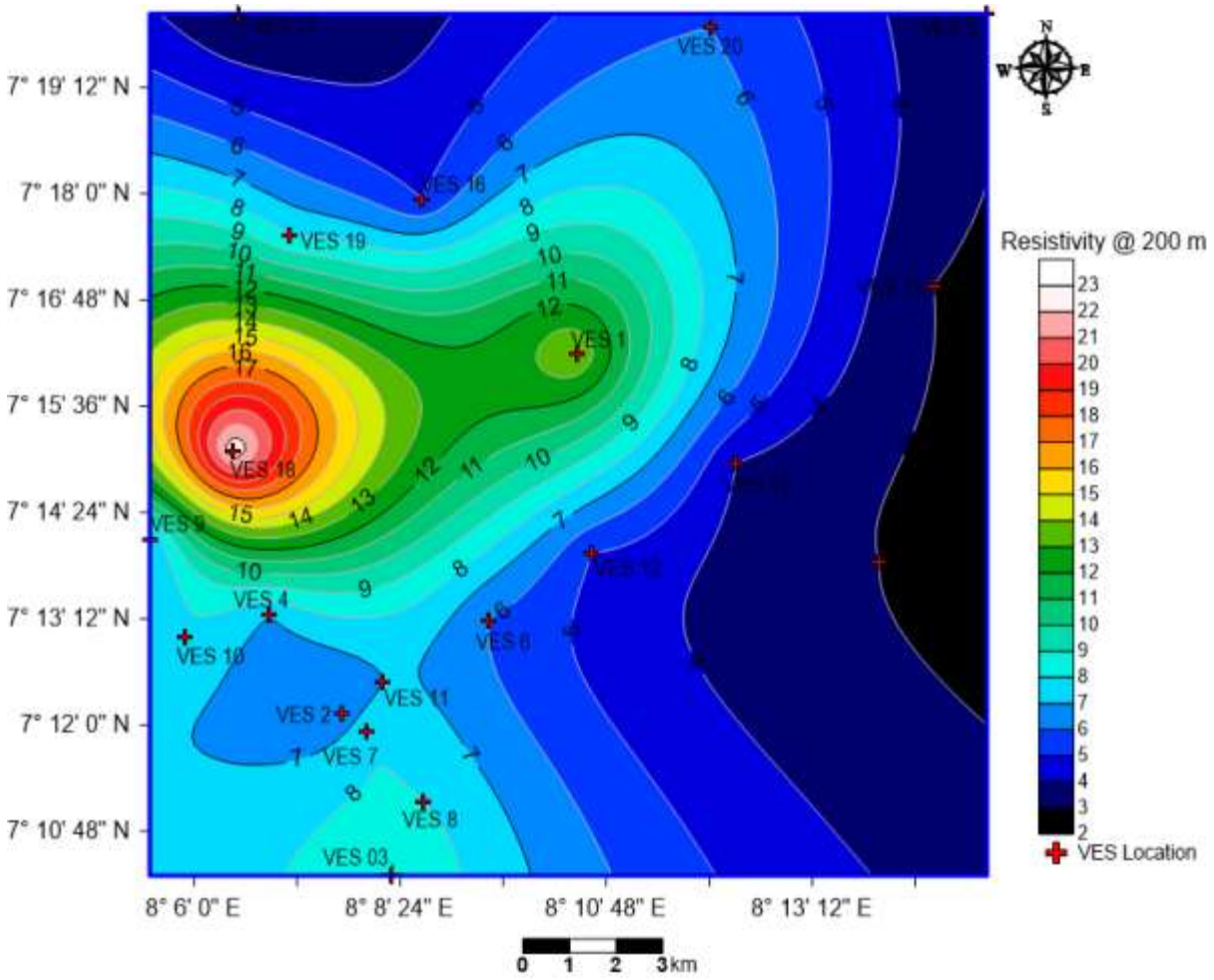

Figure 4.18: Isoresistivity at 200 m in Otukpo and its Environs

The Isoresistivity map at 400m depth in theinvestigated area is indicative of the presence of shale dominating the south-eastern section of the area of study. The north-western portion of the study area is indicative of silt-stone/sandstone intercalation with resistivity values range of 45 Ωm to 75 Ωm. The potential for groundwater is visible at 400 m depth on the north-western segment of the area of study (Figure 4.19).

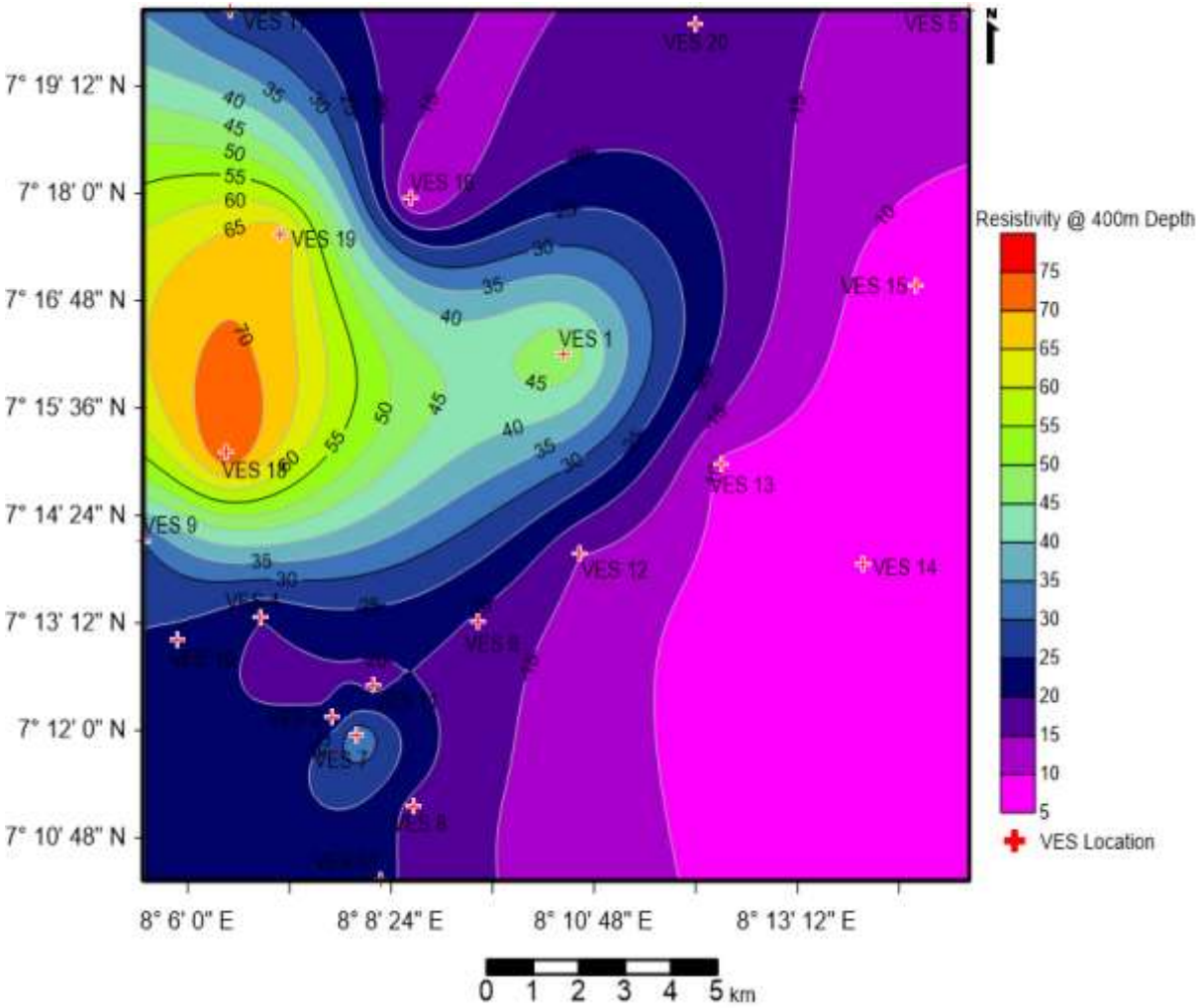

Figure 4.19: Isoresistivity map at 400 m depth in Otukpo and its Environs

Elevated resistivity of up to a 100 Ωm on the north-western segment of the area of study indicates that the sandstone underlying the shale is more pronounced in the north-western portion. The south-eastern portion is composed of saturated siltstone/sandstone formations owing to the apparent resistivity signature range of 10 Ωm to 45 Ωm (Figure 4.20).

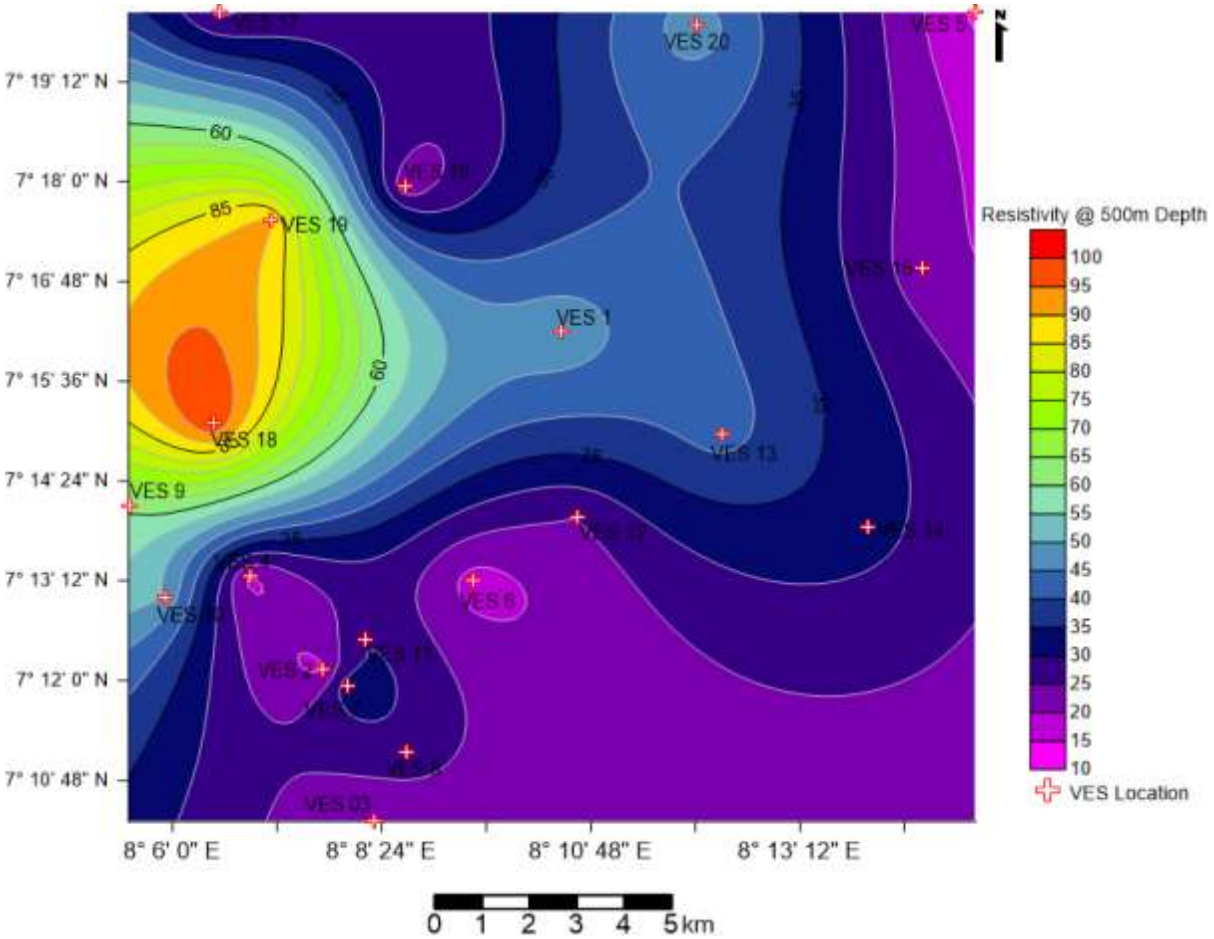

Figure 4.20: Isoresistivity at 500 m depth in Otukpo and its Environs

The isoresistivity plot of the five layer model curves specify that the resistivity value is lower at the south-eastern portion of the area compared to the northwestern part of the area (Figure 4.21). From the isoresistivty map the area with higher resistivity values (northwest) indicated presence of moderately conducting materials while areas with lower resistivity values (northeast and southeast) have highly conductive geomaterials. This indicates that groundwater potential in these area is high. The more saturated the stanstone the better is the groundwater storage and this implies that the northeast and southeast sectors hold greater potential for groundwater storage. Northeast and southeast portions correspond to groundwater recharge zone while the northwest portion are areas of groundwater discharge.

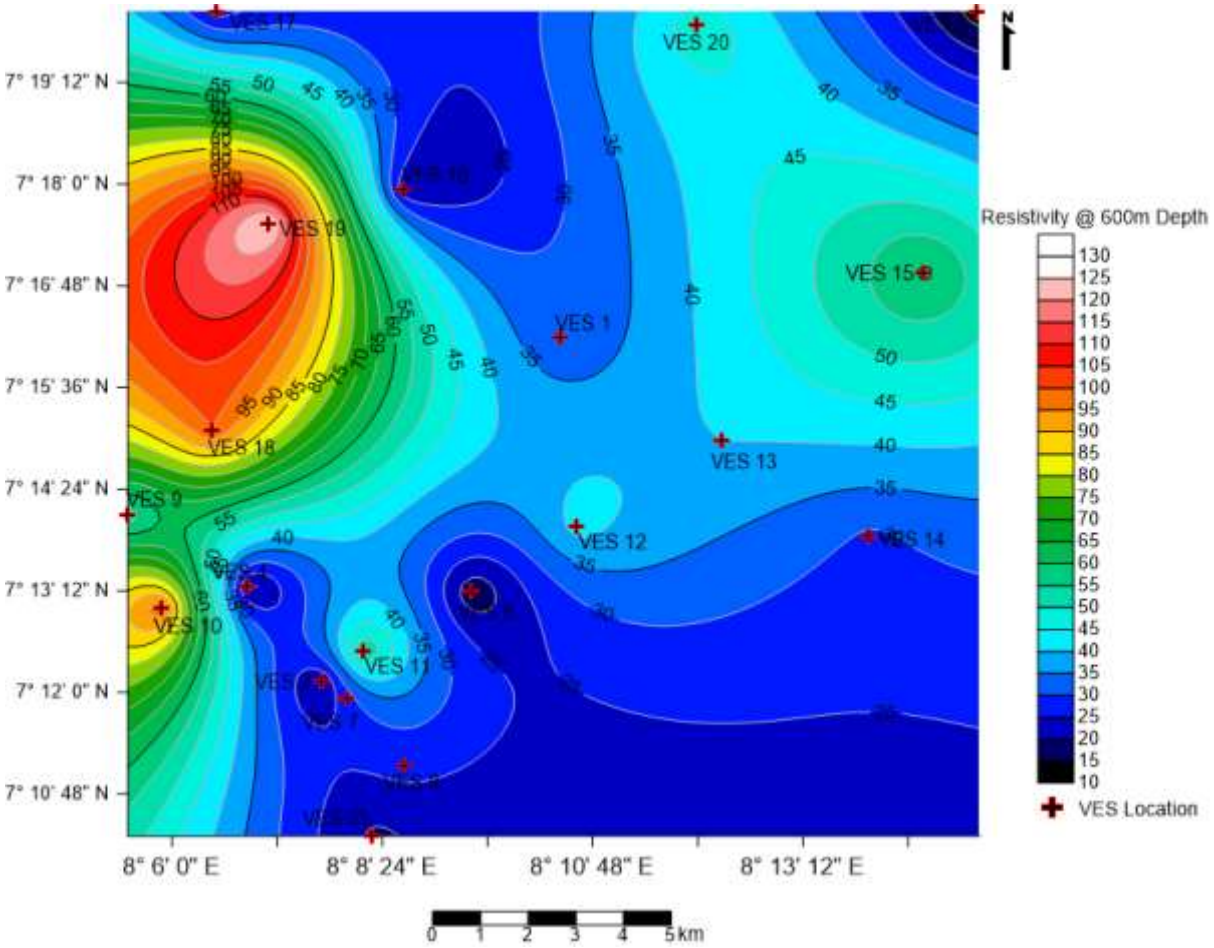

Figure 4.21: Isoresistivity at 600 m depth in Otukpo and its Environs

4.3.5 2-D Geoelectric subsurface tomography

The 2-D geoelectric profile sections show a qualitative 2-D variation of resistivity contained in the subsurface (vertical and lateral variations). This reveals the lateral and vertical facies changes inferred from the apparent resistivity. The results of the 2-D electrical resistivity tomographyare shown as measured apparent resistivity pseudosection, calculated apparent resistivity pseudosection and inverse model resistivity sections. The measured and calculated resistivity pseudosectionsalong with the section of the inverted resistivity sectionsfor traverses 01 to 06 are presented in Figures 4.21 to 4.27. Appendix D shows the measured 2-D resistivity field data. The inverted geoelectric sections create replicas for the subsurface resistivity using an iterative smoothness constrained least square inversion programme.

Three to four subsurface geoelectric units were delineated beneath these sections. These include the resistive top soil, the silty-sandy soil, sandy-clay, clayey soil and shaley formation.

At OTK profile 01 (Figure 4.22), the ground was tested with a 100 m-measuring profile line, to the depth of about 16m. From 0 m – 35 m and 40 m to 50 m on the profile, the transverse is underlain by lateritic top soil to the depth of 8 m. The profile is indicative of a good prospect for shallow groundwater at 55 m to 65 m on the profile where the profile is shown to be underlain by silty-sand. The profile is underlain by clayey materials of low resistivity values at the depth range of 13 m to 15 m.

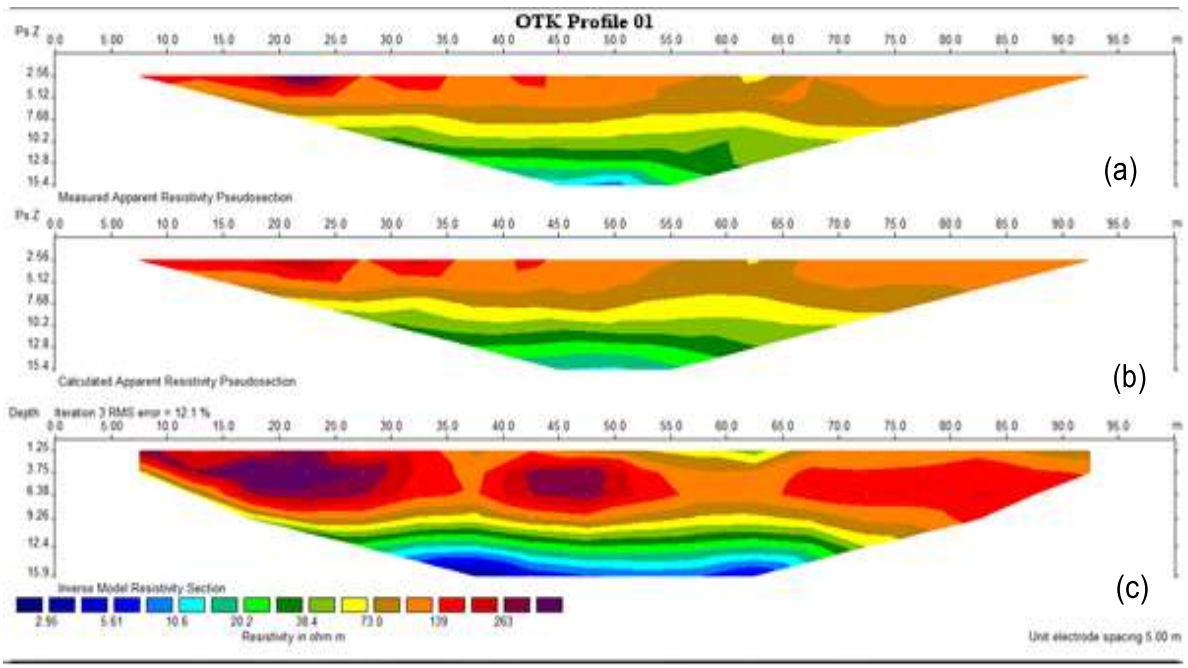

Figure 4.22: (a) Measured resistivity pseudosection (b) Calculated resistivity pseudosection (c) Inverse model resistivity sections at profile OTK 01.

At OTK profile 02 (Figure 4.23), at the profile range of 0 m to 100 m there exist a continuity of the lateritic/clayey layer from the near surface to the depth average range of 6 m to 8 m. From the range of about 9 m to 12 m depth on the profile, the subsurface is underlain by lenses of sandy-silt, sandy-clay and clay materials. At depth ranging from 14 m to 15 m the profile is underlain by shale which showed a resistivity range of less than 4 Ωm to 10 Ωm. At

0m to 15m, 30m to 40m, 51m to 54m on the profile, shallow wells can be drilled to an approximate depth of about 12m.

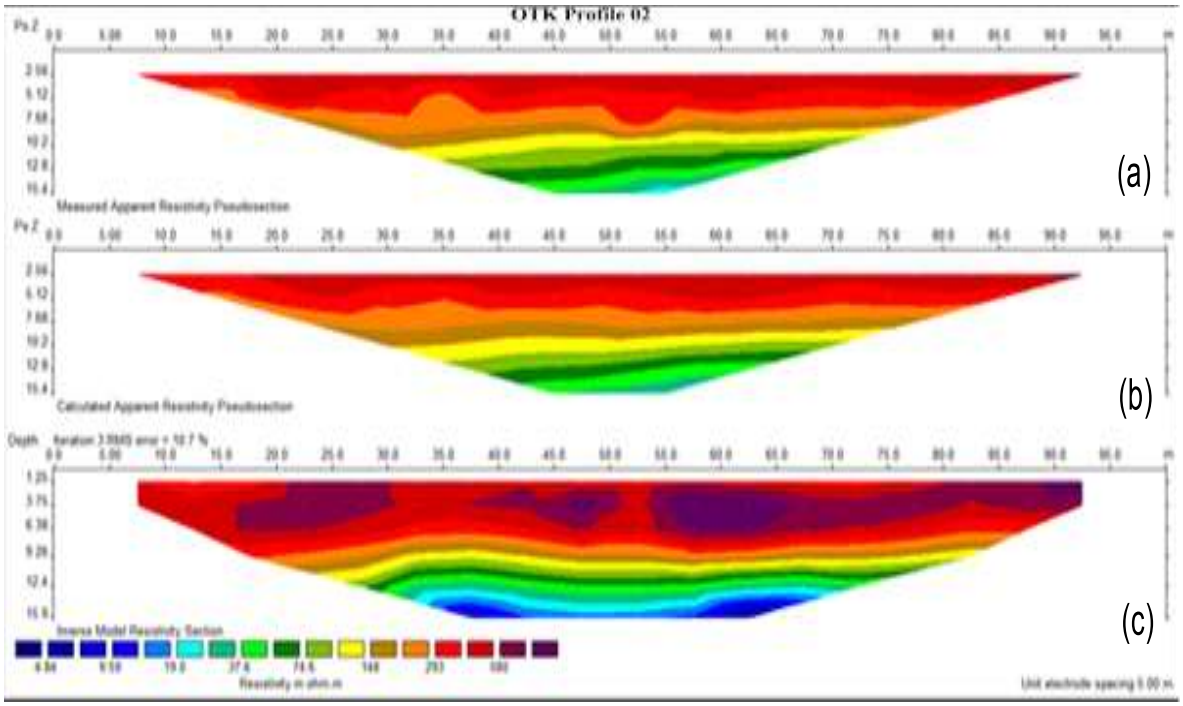

Figure 4.23: (a) Measured resistivity pseudosection (b) Calculated resistivity pseudosection (c) Inverse model resistivity sections atprofile OTK 02.

From 0m to 15 m and 35 m to 45 m, the OTK profile 03 (Figure 4.24) indicated possible prospects for groundwater from shallow wells. There is a significant decrease in the resistivity of the subsurface material from 775 Ωm to <5 Ωm at an average depth range of 12m to about 16m. Such a contrast of resistivity data indicated a change in lithology. On this profile the low resistivity showed represented shale formation.

On the OTK profile 04 line (Figure 4.25) the overlying layers are at shallow range of 3m to 15m depth on the profile distance of 50 m to 60 m are underlain by shale. It is characterised by sandysilt and clay startingfrom the near surface to the depth average of 16m along the profile length of 0 m to 45 m. From 80m to 85m on the profile line it is also underlain by silty-sand. At 85m to 95m, the subsurface seems to be underlain by lateritic-clay on or after the near surface to the approximate depth 6 m.

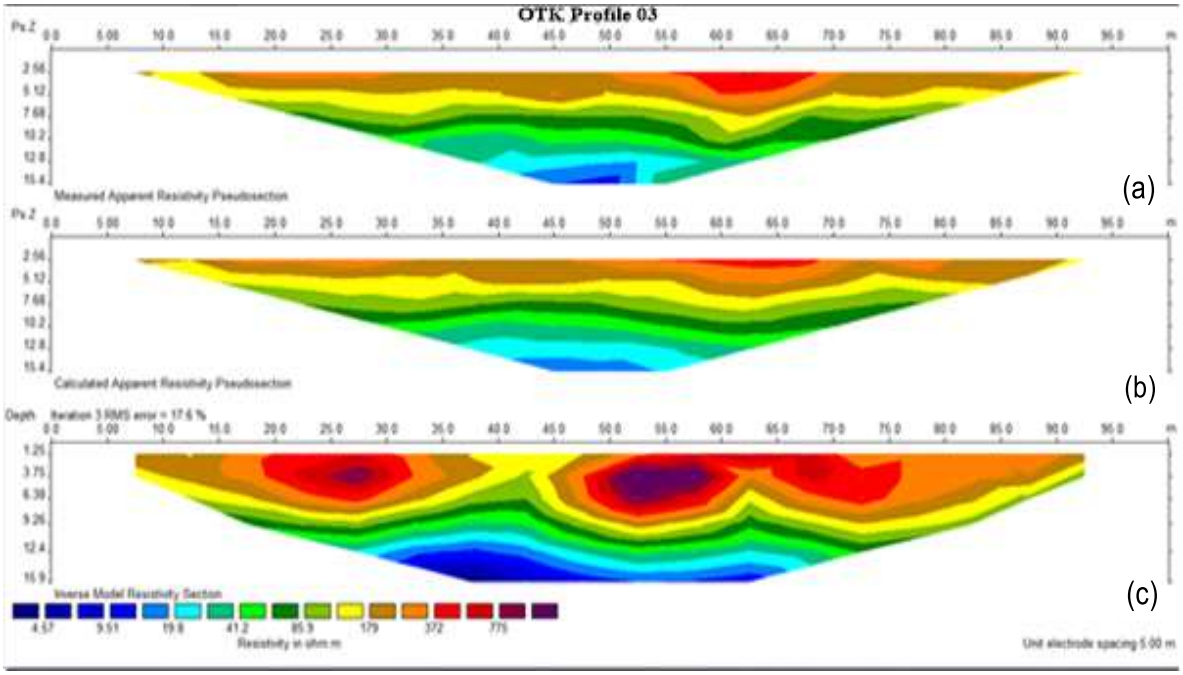

Figure 4.24: (a) Measured resistivity pseudosection (b) Calculated resistivity pseudosection (c) Inverse model resistivity sections at profile OTK 03.

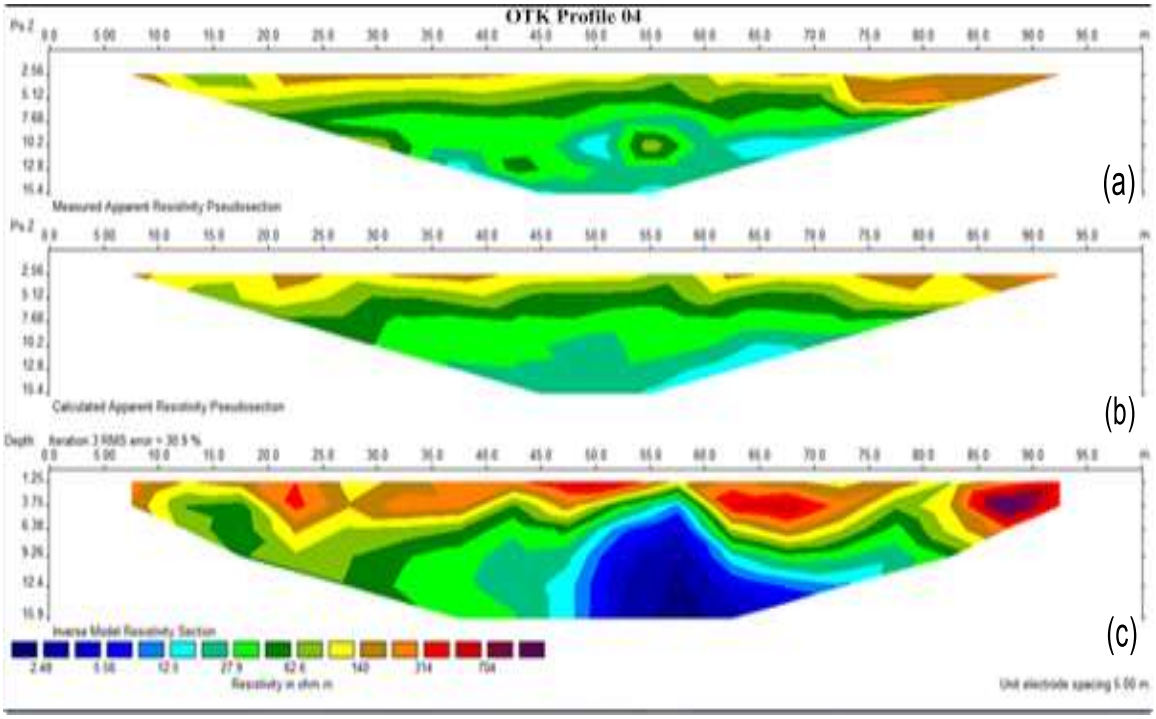

Figure 4.25: (a) Measured resistivity pseudosection (b) Calculated resistivity pseudosection (c) Inverse model resistivity sections at profile OTK 04.

The inter electrode spacing on the OTK profile 05 (Figure 4.26) was limited to 10 m while the profile length was extended to 200 m on the surface. The surface of the whole measuring

profile is composed of lateritic-clay to the depth average range of 2.5 m to 8 m. The lateritic-clay layer is underlain by silty-sand. Shale exists on the profile at the length of 90 m to 120 m from the depth average range of 10m to 31.9m with resistivity range of 1 Ωm to <2 Ωm. Shallow wells can be sited to the depth range of 18m to 20m at the profile length 70m to 85m and 120 m to 190m.

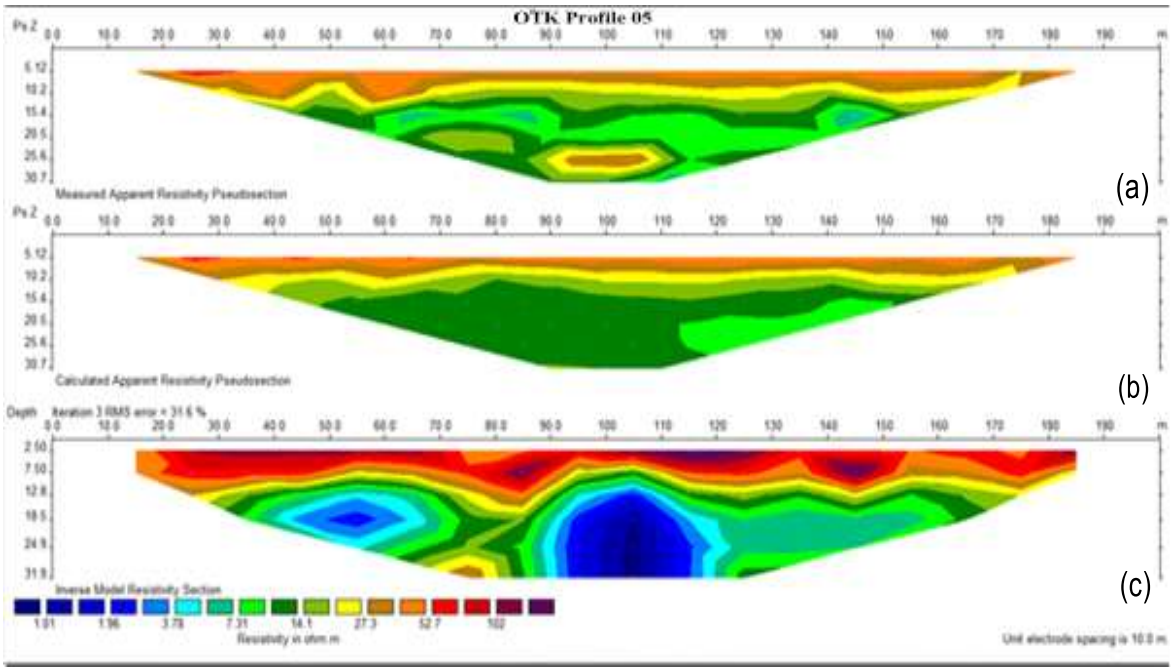

Figure 4.26: (a) Measured resistivity pseudosection (b) Calculated resistivity pseudosection (c) Inverse model resistivity sections for profile OTK 05.

OTK profile 06 (Figure 4.27) shows a subsurface intercalation of lithologies. The profile surface length of 20 m to 90 m and 130 m to 190 m the profile is underlain with lateritic-clay to the depth range of 2.5 m to 12 m with resistivity ranging from 504 Ωm to 1254 Ωm. at 100 m to 130 m on the profile, it is underlain with sandy-clay and a tin lens of silty-sand to the depth average range of 7 m to 30 m. There is a moderate resistivity reading of 32.7 Ωm to 81.4 Ωm indicative of the intercalation of silt, sand and clay. This is suggestive of a good prospect for shallow well. The resistivity range of 2.13 Ωm to 5.29 Ωm (blue area) characterise the profile at the surface distance of 50 m to 90 m with an average depth range of 20 m to 31.9 m on the profile.

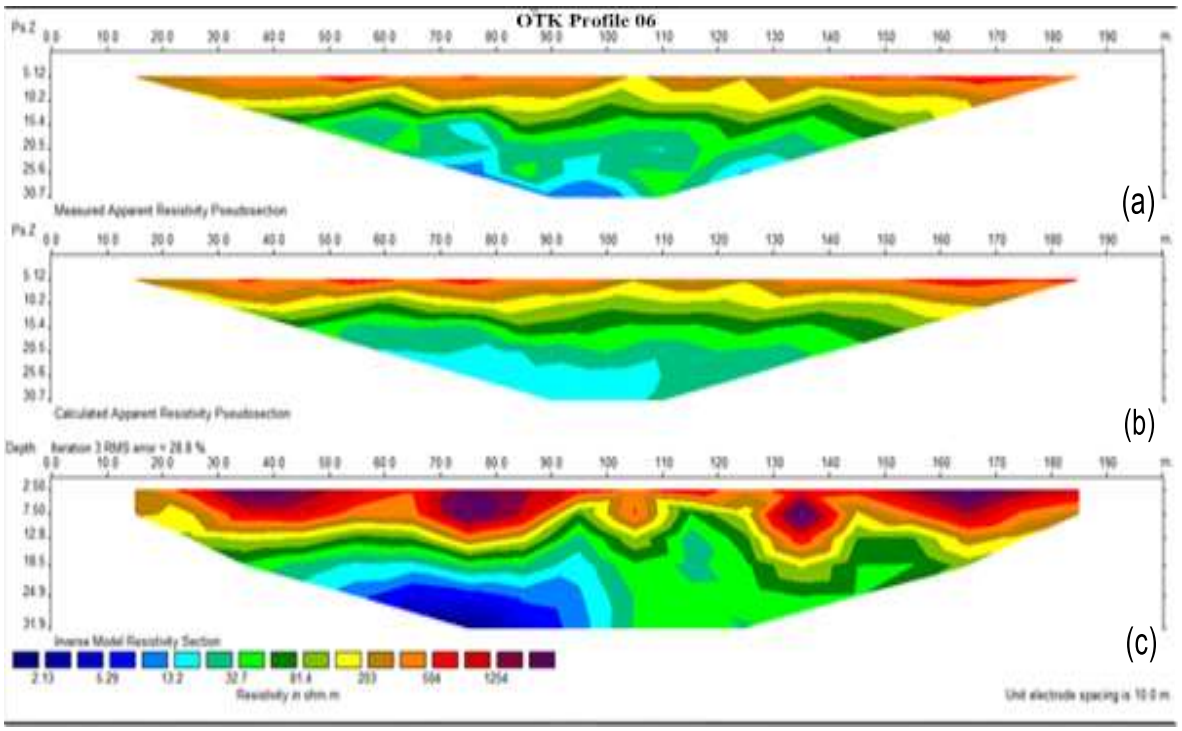

Figure 4.27: (a) Measured resistivity pseudosection (b) Calculated resistivity pseudosection (c) Inverse model resistivity sections for profile OTK 06.

4.3.5.1 Discussion of 2-D subsurface tomography

In summary, the inverse resistivity model sections revealed a strong inclination of high resistivity at the topmost layers with apparent resistivity values range of 102 Ωm up to 1254 Ωm extending from the depth range of 1 m to 7.5 m. This is attributed to the occurrence of a product of intense chemical weathering and leaching of soluble materials (lateritic soil) underlying the near subsurface (brown, red and pink zones). The second layer shows a resistivity value range of 7.3 Ωm to 85.9 Ωm with atypical depth range of 12.8m to 18.5m (yellow and green zones). The middle layer is composed of sand, sandy-clay, silty-sand and silty-clay. The middle layer is the water bearing layer for seasonal groundwater abstraction because it is made up of weathered lithological materials possessing moderate to low porosity. At the bottom layer of the 2D sections, the resistivity values are low with an average range of 1.01 Ωm to 10.6 Ωm indicative of clay to clayey-shale (blue zones).

On profile 4 (GRA) the clay content is seen to overlap at the depth of 6.38 m at the surface profile length of 55 m to 60 m while on profile 5 (Sabon Gari), the clayey soil is found at the depth of 7.5m at the surface profile length of 40m to 60m and 90m to 100m respectively. The computed apparent resistivity pseudo-section validates the measured field data despite the negligible instrumental errors. Hence the model reflects the actual subsurface conditions of the study area near subsurface. In all the 2-D transverses, the resistivity decreased with depth, attaining as little as 1 Ωm within a depth of less than 20 meters, confirming the dominance of shaley formation in the study area, which if not well interpreted can be mistaken for a saturated aquiferous zone.

4.4 Direct Subsurface Exploitation (Drilling)

The drilled borehole validated the result obtained from the geophysical investigation conducted within the area of study (Table 4.4). It confirmed the low resistivity values are from saturated shale in the area.

Lithologic samples from drilled borehole as well as hand-dug water wells indicated that the high resistive unit expressed by the near subsurface from the resistivity reading is predominantly composed of dry literitic top soil. The observed silt and sand lenses together with weathered lateritic soil depicted lateral facies changes and near-surface heterogeneities that normally characterised the Otukpo and its environs subsurface (Figure 4.28). The clay/shale formation account for the low resistivity values witnessed for this relatively thick unit. The absence of caving while drilling the borehole without the use of chemicals (drilling fluids) to stabilize the borehole wall indicated the degree and extent of clayey-shale in the area. The drilling has established the dominance of clay/shale formation which is in agreement with the stratigraphy of the area.

Table 4.4: IP and VES data for drilled borehole point

Coordinate	**7°11′24.0″N 8°07′33.3″E** Borehole Point	
AB/2	ℓa	IP
1	850	1.12
2	511	1.31
3	320	1.27
4	230	2.81
4	230	2.81
6	131	3.14
8	102	2.81
10	96	2.96
12	85	4.21
15	72	12.64
20	14	4.01
20	13	3.85
25	9	3.24
30	8	4.87
35	8	4.01
40	5	11.1
50	5	7.9
60	4	-14.6
80	3	-120.7
80	3	-17.2
100	3	-111.8
125	3	-25.1
150	2	-60.9

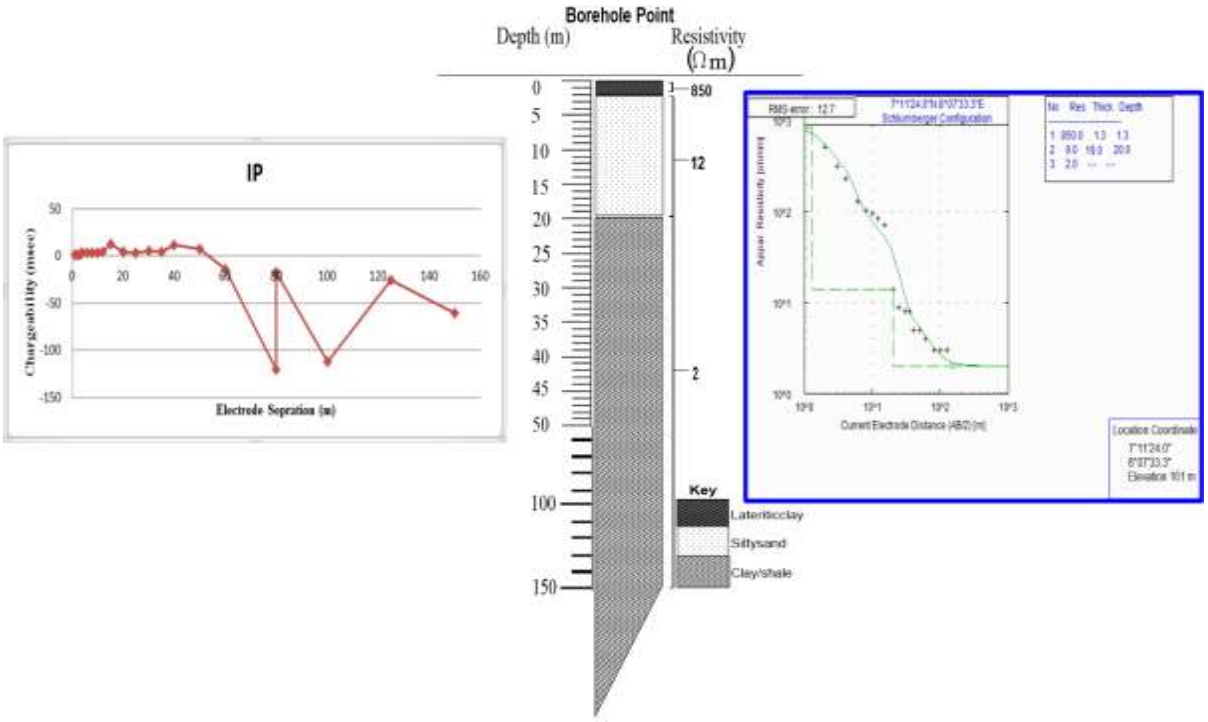

Figure 4.28: IP , VES Curves and Geoelectrical Log for Borehole Point

4.4.1 Lithologic logging

A closer look at the strata-log from the drilled borehole (Figure 4.28) shows that Otukpo subsurface geology is shale dominated, in confirmation of the geophysical investigation result. The lithological log showed a clear and realistic lithostratigraphic profile of the formation that makes up the near subsurface lithology of Otukpo and its environs. The sample box (Plate XIV) further confirmed the existence of an extensive unsaturated shale formation in the area.



Plate XIV: Sample Log box section

Laterite

Laterite is an indurated magenta incrusted soil horizon or a concretionary soil horizon that has an elevated content of sesquioxides of iron (Fe_3) and or aluminum (SiO_2 / $Al_2O_3^{-2}$) which are formed when favourable conditions for laterization are present for an appropriate length of time. The lateritic soil is characterized by red to brown colours which are often the results of chemical weathering. Lateritic soil appears as the topmost lithological unit underlying the thin loose sandy top soils marking erosional surface in the area.

Observation from the unlined hand dug wells showed that lateritic profile in Otukpo region varied from place to place because of the complexity in the interrelationships of the controlling soil forming factors which include rainfall and topography. There exists a great difference in the depth and thickness of the lateritic soil in the area at lateral distance of a few meters apart.

Clay

Clays are termed as argillaceous alteration products of geological materials due to hydrothermal action. Clays are formed as a product of the weathering of alumino-silicates due to the effects of parent rock, climate, vegetation, topography and time. The characteristic movement of groundwater through the zone of alteration leads to the formation of the clay.

The lateritic soil in the area is underlain by clayey soil. The clay soil in the study area is exogenous in origin (sedimentary/weathering). The clay possesses a reasonable level of porosity and a very low level of permeability.

As the clay profile proceeds downward, there is an intercalation of clay and silt (an overlap in both particle size and other physical properties). The silts appears as fine grained formation which particles are larger than clay and are void of clay minerals.

Shale

Shale is a laminated, indurated, lithified mud rock. It is a rock with sedimentary signature that composes mostly of silt and clay-size particles. The main constituent of the shale encountered in the study area is clay believed to be fashioned as a product of weathering of argillaceous clastic sediments. The shale encountered in the area is dark gray-black in colour (Figure 4.29). The groundwater supply potential of shale is strictly limited by it generally very low transmissivity.

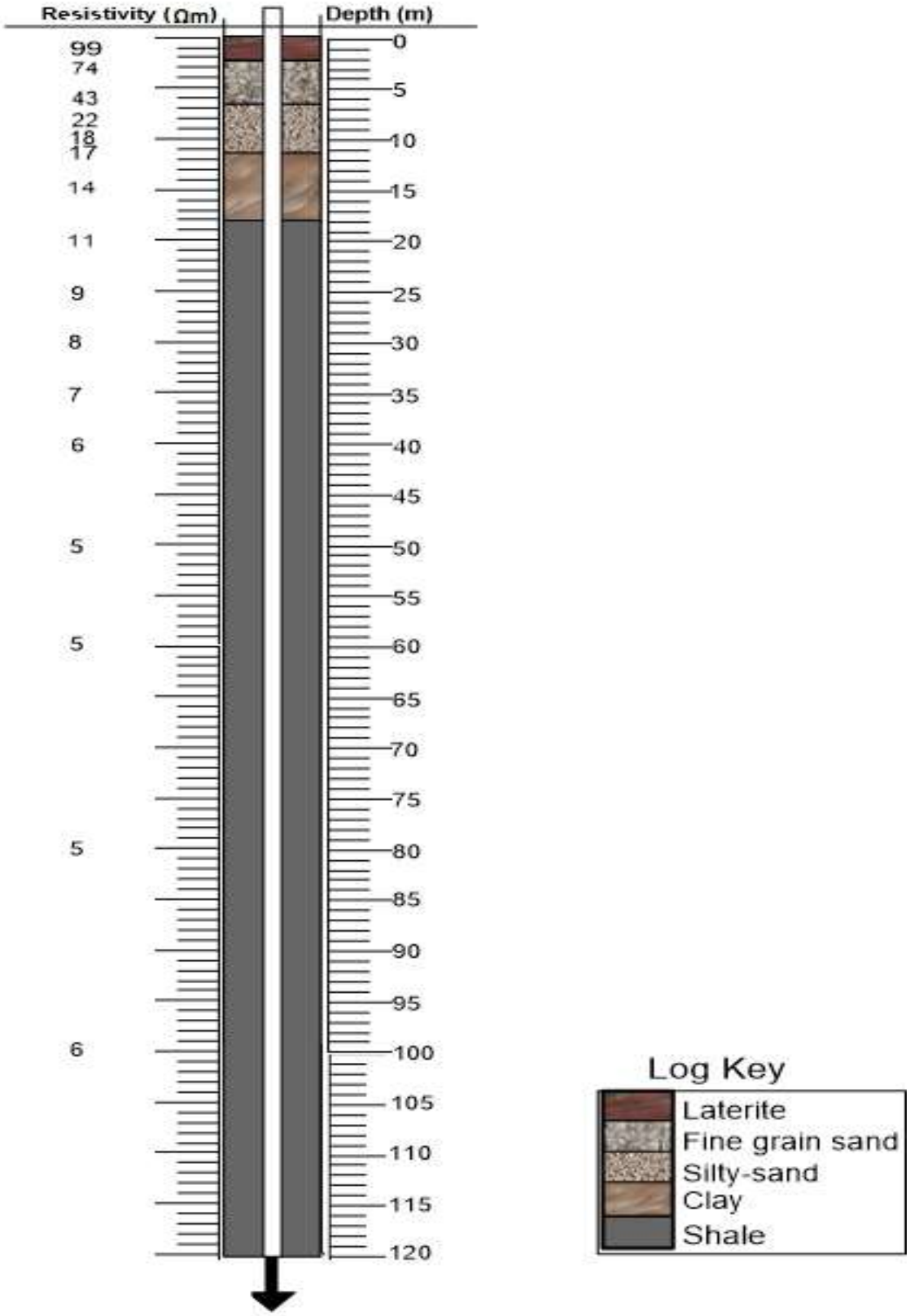

Figure 4.29: Simplified borehole lithologic log

4.5 Groundwater Potential

The shallow unconfined groundwater potential/availability map of Otukpo and its environs displays relatively low, medium and high groundwater potential areas (Figure 4.30). The southern section of the area indicated a shallow groundwater potential while the north-eastern and part of the north-western section indicated low to moderate groundwater potential.

The shallow seasonal water bearing layer typically comprise of alternating permeable layers of (silty-sand and silty-clay) and less (permeable layers of clay and shale), replicating the intricate nature of Otukpo and its environs subsurface. The yield of groundwater in wells penetrating upper seasonal groundwater layer is highly variable in time and space. The groundwater potential of the shallow subsurface could be much less comprehensive but can quiet store groundwater in volumes that could be important mechanism of seasonal water sources for domestic household use.

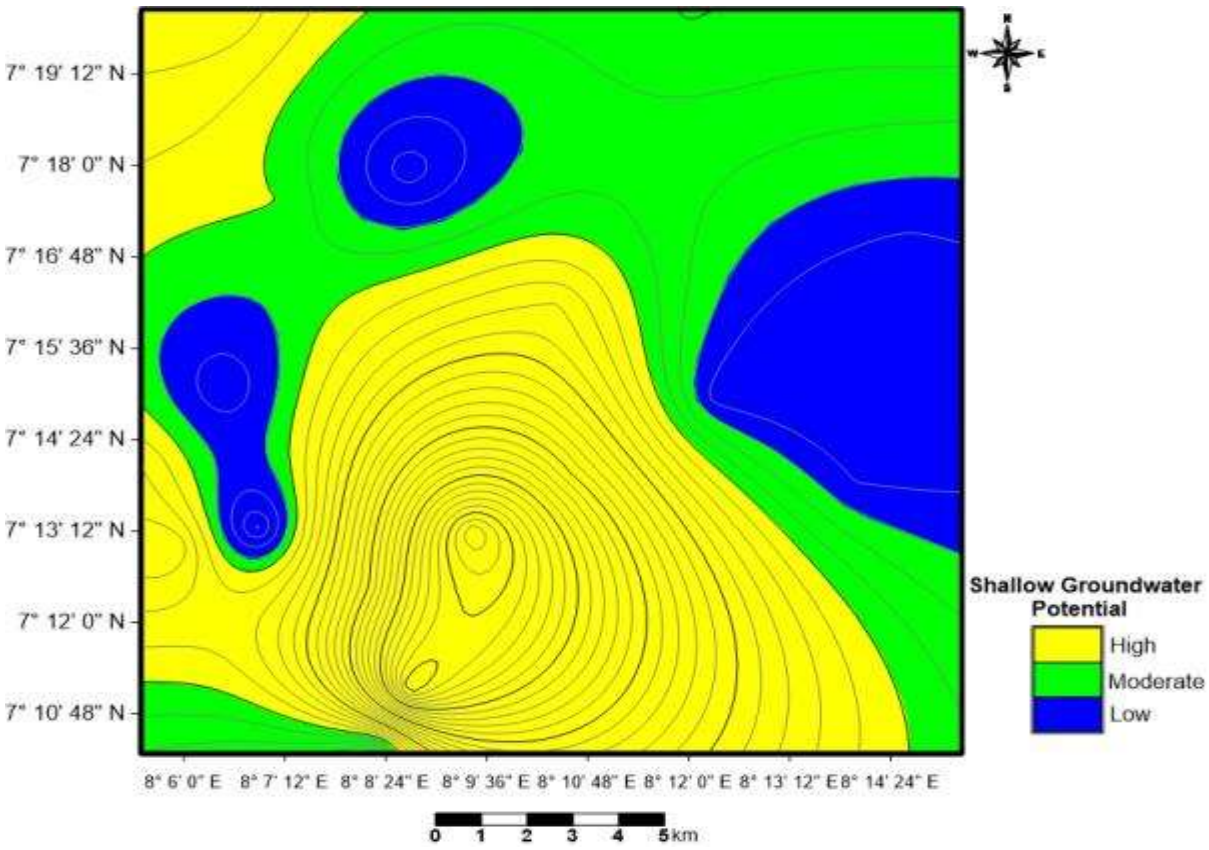

Figure 4.30: Areas shallow groundwater potential in Otukpo and its environs (1m -25m)

The deep sub-surface confined aquifer in Otukpo and its environs has been classified into low, moderate and high zones of groundwater potential (Figure 4.31). Otukpo and its environs groundwater potential map revealed that the productive potential groundwater bearing zones, designated as high zones occur at the south-eastern, and subordinately in the north-western as well as part of the north-eastern sections of the area. The moderate groundwater potential zones are located majorly at the north-eastern to central sections as well as part of the north-west section and south-western part of the studied area. The western section of the mapped area is demarcated as low potential groundwater zone which is the groundwater recharge zones.

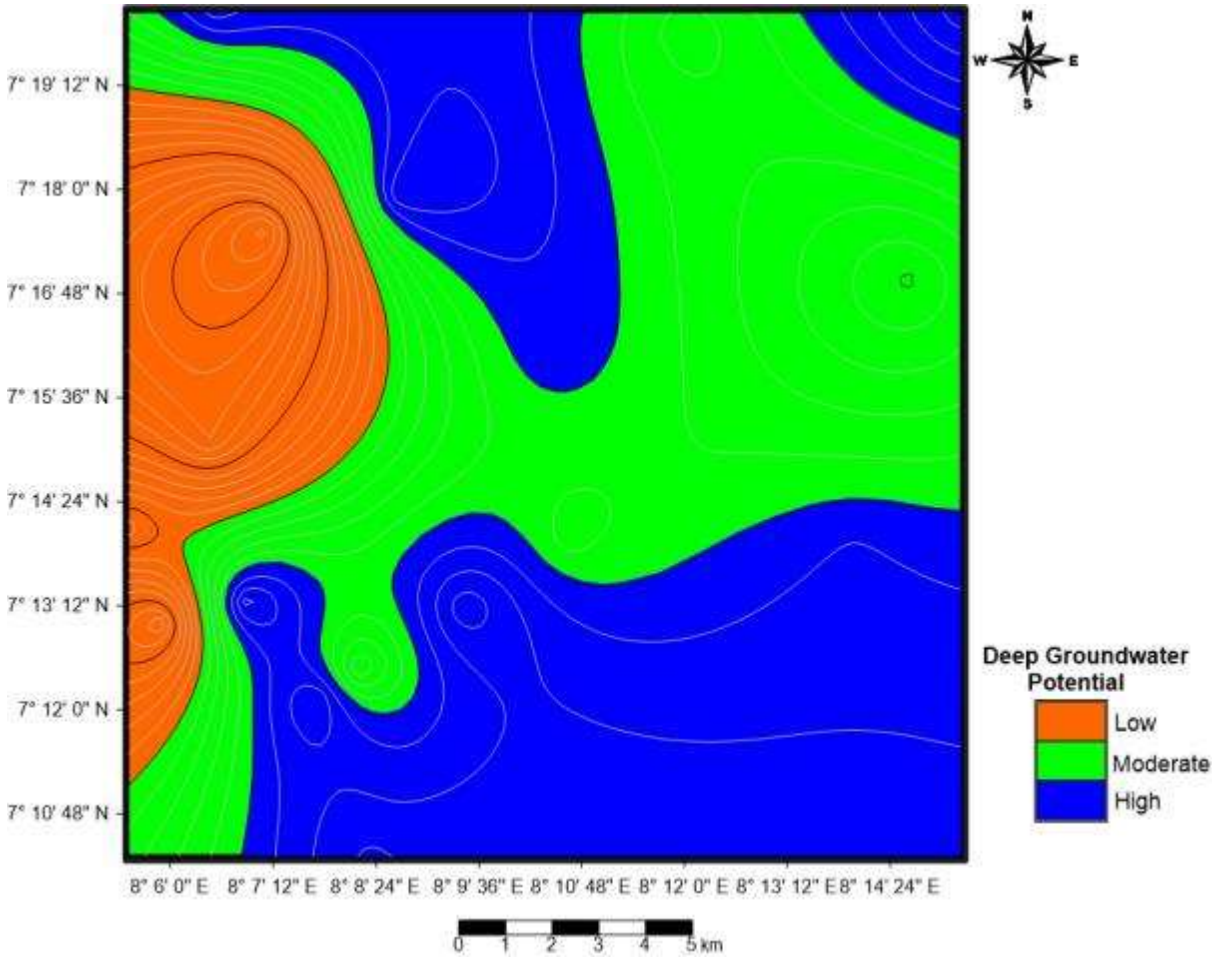

Figure 4.31: Deep groundwater potential zones (500 – 600 m) in Otukpo and its Environs

CHAPTER FIVE

5.0 CONCLUSION AND RECOMMENDATIONS

5.1 Conclusion

The lithological inhomogeneities of Otukpo and its environs subsurface have been unravelled through geological mapping, hydrogeological evaluation and geophysical investigations. Otukpo area is part of the sedimentary formation of the Lower Benue Trough and it is underlain by the Awgu shale which is dark grey to black. The surface altitude of the study area ranges from 124m to 208m above the datum sea level. The minimum total depth of wells in the area is 2.3 m while the area has a maximum well depth of 14.2 m as recorded from the field measurement. Static water level in the wells ranged from 1.8m to 14.0m. Groundwater flow in the area is in the direction of maximum change in hydraulic head which ranges from 113.0 to 201.9. The groundwater flow is in the northward direction.

The electrical method of IP and resistivity were used for the subsurface investigation. The time domain IP approach was utilized. The chargeability data obtained were plotted against the values of the electrode separation (AB/2) to reflect existing alteration of the underlying subsurface lithology. The chargeability models curves, shows considerable low (negative) chargeability at varying depth for all the investigated points. The paradoxical behaviour of the subsurface showing strong negative chargeability responses are attributed to the effect of highly conductive zone made up of pure clay/shale concentrations. An appreciable increase in positive chargeability value was observed at proximate sounded electrode separation of 500 m and 600 m in all the plots, indicating clay/shale intercalation with sandstone. The VES revealed that all the curve types possess five (5) distinctive layers, where ℓ_1, ℓ_2, ℓ_3, ℓ_4 and ℓ_5 are the resistivity of the first layer, second layer, third layer, fourth and fifth layer respectively. The first layer, second layer, third layer, fourth and fifth layer have resistivity

ranges of 103Ωm to 138Ωm, 17Ωm to 1462Ωm, 2Ωm to 49Ωm, 4Ωm to 143Ωm and 24Ωm to 194Ωm respectively. Four curve types of various combinations were derived from the VES plots; these included the QH, KH, KQH and QHK with 65%, 15%, 10% and 10% respectively.

The apparent resistivity and normalized chargeability in the 1-D outcomes show that the low-resistivity as well as the negative chargeability layers corresponds to the aquitard variability of the subsurface. The normalized chargeability demonstrate a clear fashion of decreasing (negative) IP values in the subsurface layers with elevated clay/shale content, and low positive values where coarse sandstone is the foremost lithological content at the bottom. Resistivity values at the top layer are associated with lateritic soil and silty-sand; at the middle layers it is attributed to clay/shale while at the bottom layer it is attributed to saturated sandstone at deep subsurface depth range of 500m to 600m. The Otukpo and environs shale extends laterally over several kilometres with very low electrical resistivity. The shale underlying the study area has been suggested as possible causes for a number of low electrical resistivity anomalies found in the subsurface. Groundwater is expected to be found in the Agbani sandstone formation which is directly underlying the Awgu shale Formation. The Agbani sandstone Formation is expected to constitute the principal aquifer zone in Otukpo and its environs.

Isoresistivity map of the five layers model curves indicates that the resistivity value is lower at the south-eastern section of the area compared to the northwestern section of the area. The northeast and southeast sectors of the area hold greater potential for groundwater storage.

2-D subsurface investigation revealed that the top layer, second layer and third layer are characterised by resistivity values ranges of 102 Ωm up to 1254 Ωm, 7.3 Ωm to 85.9 Ωm and

1.01 Ωm to 10.6 Ωm respectively. In all the traverses the resistivity decreases with depth, extending to as low as 1 Ωm within the depth of less than 20 meters.

Coherency was established between the pre-drilling geophysical investigation, drilling operations and down-hole geological logging. Lithologic log from the drilled borehole and hand-dug water wells indicate that the elevated resistive unit is predominantly composed of unsaturated lateritic top soil. The observed silt and sand lenses overlying the lateritic soil depicts rapid lateral facies changes and near-surface heterogeneities that commonly characterised the study area. The clay/shale formations account for the low resistivity values observed for this relatively thick unit. The shale encountered in the area is dark grey to black.

Two groundwater potential areas were demarcated; the shallow and deep groundwater potential zones. The shallow subsurface seasonal water bearing layer have more limited lateral extent and depth (less than 25 m), while the deep-seated aquifers of restricted size and magnitude occur in confined states at an approximate depth of 500 m to 600 m. Even with the beneficial effects of the intercalation of silt and sand with clay and shale, the volume of water retained in this shallow subsurface layer are generally limited, well yields are very low. Groundwater is mostly used for providing seasonal water supplies for domestic use from the shallow wells.

This research has successfully integrated geological, hydrogeological and hydrogeophysical investigations for groundwater systems in Otukpo and its environs. Stratigraphically, Otukpo and its environs are underlain by shaley carbonaceous mudstones with thin shaley limestone and sandstone belonging to the Awgu Formation. The confined aquifer of Otukpo and its environs is part of the consolidated sedimentary intergranular/fractured rock and it is considered as moderately productive.

Groundwater system of Otukpo is composed of two aquifer types; the shallow unconfined aquifer and the deep confined aquifer. Discharge occurs locally to streams and springs from the shallow aquifer. The springs replenish the streams. The shallow seasonal groundwater bearing layers are recharged by rain events as it journeys through overlying laterite and weathered lithological materials and discharges to springs and shallow water hand-dug wells domiciled in the area of study. Valuable aquifers of great groundwater potential occur in confined state deeply seated at about 500 m to 600 m beneath the surface and are capable of supporting substantial borehole yields. The aquifer is confined at the top by thick layer of impermeable clay/shale layer. The Otukpo area is within the Agbani sandstone formation directly underlying the Awgu shale Formation within the Awgu Group. This aquifer is recharged by a transboundary Benue Trough aquifer shared by Cameroon and Nigeria. The confined aquifer system of the study area falls within the consolidated sedimentary hydrogeological environments of Africa. This work has successfully indicated potential groundwater bearing zones in Otukpo and its environs.

5.2 Recommendations

The interpretation of the subsurface conditions of the study area, based on the integrated geoscientific methods, should be verified through deep well drilling by relevant authorities in order to alleviate the need for potable water by the inhabitant of Otukpo and its environs.

References

Adelana, S. M., Olasehinde, P. I., Bale, R. B, Vrbka, P., Goni, I. B. & Edet, A. E. (2008). An Overview of the Geology and Hydrogeology of Nigeria. In: (Adelana, S.M and MacDonald, A. M.). Applied Groundwater Studies in Africa.IAH (International Association of Hydrogeologist) Selected Papers on Hydrogeology, 13, 518, CRC Press/Balkema, London.

Africa Groundwater Atlas, (2011). Overview of Groundwater in Africa. British Geological Survey. Retrieved from www.earthwise.bgs.ac.uk

African Climate Policy Centre (ACPC), (2013). Management of Groundwater in Africa: Implications for Meeting MDGs, Livelihood Goals and Adaptation to Climate Change. ClimDev-Africa, Policy Brief 5. Retrieved from www.Ise.ac.uk

Allen, R. F. & John, A. C. (1979). Groundwater. Department of Earth Sciences, University of British Columbia, VANCOUVER, British Columbia.

Amadi, A. N. (2007). Aquifer Characterization and Groundwater Vulnerability around Owerri, Southeast Nigeria. Unpublished M. Tech. Thesis, Federal University of Technology, Minna.

Amadi, A. N. & Olasehinde, P. I. (2009). Assessment of Groundwater Potential of parts of Owerri, Southeastern Nigeria. *Journal of Science, Education and Technology*, 1(2), 177-184.

Amadi, A. N., Ameh, M. I., Idris-Nda, A., Okoye, N. O. & Ejiofor, C. I. (2013).Geological and Geophysical Investigation of Groundwater in Parts of Paiko, Sheet 185, North-Central Nigeria. *International Journal of Engineering Research and Development* 6 (1), 01-08.

Amadi, A. N., Olasehinde, P. I., Obaje, N. G., Unuevho, C.I., Yunusa, M.B., Keke, U. & Ameh, I. M. (2017). Investigating the Quality of Groundwater from Hand-dug Wells in Lapai, Niger State, North-central Nigeria using Physico-chemical and Bacteriological Parameters.*Minna Journal of Geoscience*, 1(1), 77 – 92.

Andy A. B., Rosli, S., Edy, T. M., Mark, J., Azwin, I. N., Norsalkini, M. A. T. & Nordiana, M. M. (2012). Electrical Resistivity and Induced Polarization Data Correlation with Conductivity for Iron Ore Exploration. *Electronic Journal of Geotechnical Engineering*, 17, 3223-3337.

Benkhelil, J. (1986). Structure and Geodynamic Evolution of the Intracontinental Benue Trough (Nigeria). *Elf Nig. Ltd., Nigeria. Bull Centres Rech. Explor. Prod. Elf-Aquitaine* (BCREDP), 12, 29-128.

Binley, A. & Kemna, A. (2005). DC Resistivity and Induced Polarization Methods. In Hydrogeophysics, 129-156.Springer, Dordrecht.

Bleil, D. F. (1953). Induced Polarisation: A Method of Geophysical Prospecting. *Geophysics*, 18(3), 636 – 661. Retrieved from geosiamservices.com.

Börner, F. D., Schopper, J. R. & Weller, A. (1996). Evaluation of transport and storage properties in the soil and groundwater zone from induced polarization measurements: *Geophysical Prospecting*, 44, 583–601, doi: 10 .1111/gpr.1996.44.issue-4.

Braga, A. C., MlaguttiF^{o}, W., Dourado, J. C. & Chang, H. K. (1999). Correlation of Electrical Resistivity and Induced Polarization Data with Geotechnical Survey Standard Penetration Test Measurements. *Journal of Environmental & Engineering Geophysics*, 4(2), 123-130. doi: 10.4133/JEEG4.2.123

Brandes, I. (2005). The negative chargeability of clays. A thesis submitted in fulfilment of the requirements for the degree of Doctor of Philosophy. School of Civil and Environmental Engineering, the University of NSW.

Brandes, I. & Acworth, R. I. (2003). Intrinsic Negative Chargeability of Soft Clays. *ASEG Extended Abstracts*, 2, 1-4. Retrieved from https://www.tandfonline.com/loi/texg19.doi: 10.1071/ASEG2003ab017

Chilton, J. & Seiler, K. P. (2006). Groundwater Occurrence and Hydrogeological Environments. World Health Organization. Protecting Groundwater for Health: Managing the Quality of Drinking-water Sources.IWA Publishing, London, UK.

Cratechley, C. R. & Jones, J. P. (1965). An Interpretation of the Geology and Gravity Anomalies of the Benue valley, Nigeria. Overseas Geological Survey, *Geophysics paper*, 1, 26.

Dahlin, T. & Loke, M. H. (2015). Negative apparent chargeability in time domain induced polarisation data. *Journal of applied geophysics*, 123, 322-332.

Daniels, F. & Alberty, R. A. (1966). *Physical Chemistry*. John Wiley and Sons, Inc.

Darcy, H. (1856). The public fountains of the city of Dijon. *Dalmont, Paris*, 647.

David, K. T. & Larry, W. M. (2005). *Groundwater Hydrology*. Third Edition. John Wily & Sons, Inc.

Davis, S. N. (1969). *Porosity and permeability of natural materials.* Flow Through Porous Media, ed. R. J.M. De Wiest. Academic Press, New York, 54-89.

Dawei, H. (2010). *Concise Hydrology*. Dawei Han & Ventus Publishing ApS. Bookboon.com

Dwain, K. B. (2015). Historical and Conceptual Synopsis of Hydrogeophysics. Applied Geophysics Consultancy, Vicksburg, Mississippi, US. Retrieved from www.researchgate.net/publication/308897925.

Fetter, C. W. (2007) *Applied Hydrogeology*: Second edition, Oshkosh, University of Wisconsin.

Ford, D. C. & Williams, P. W. (1989). *Karst geomorphology and hydrology* (Vol. 601). London: Unwin Hyman.

Freeze, R. A. & Cherry, J. A. (1979).*Groundwater, Prentice Hall*, Englewood Cliffs, New Jersey.

Geological Survey of Nigeria, (1994).Geologic map of Nigeria. Geological survey Department, Ministry of Petroleum and Mineral Resources: Abuja Nigeria. Wright, J.B, (1981). Review and the origin and evolution of the Benue Trough in Nigeria. *Earth Evolution Sciences*, 1.

Gonzales, A., Dahlin, T., Barmen, G. & Rosberg, J. E. (2016). Electrical Resistivity Tomography and Induced Polarization for Mapping the Subsurface of Alluvial Fans: A Case Study in Punata (Bolivia). *Geosciences*, 6(4), 51.

Groundwater Atlas, (2019). Transboundary Aquifers. British Geological Survey. Retrieved from earthwise.bgs.ac.uk. 23/08/19

Idris-Nda, A., Abubakar, S. I., Waziri, S. H., Dadi, M. I. & Jimada, A. M. (2015). Groundwater development in a mixed geological terrain: a case study of Niger State, central Nigeria. *WIT Transactions on Ecology and the Environment*, 196, 77-87. Retrieved from www.witpress.com

JICA, (2014). The project for review and update of Nigeria national water resources master plan. Vol.2. Japan International Cooperation Agency: Yachiyo Engineering Co., Ltd.: CTI Engineering International Co. Ltd.: Sanyu Consultants Inc.

John, W. B. & Richard, J. L. (2004). *Basic Geological Mapping (Forth Edition)*. John Wiley & Sons Ltd. The Atrium, Southern Gate, Chichester, West Sussex PO19 8SQ, England.

Keller, G. V. & Frischknecht, F. C. (1966). *Electrical methods in geophysical prospecting*. Pergamon Press Inc., Oxford.

Kemna, A., Binley, A. & Slater L. (2004). Crosshole IP imaging for engineering and environmental applications: *Geophysics*, 69, 97–107, doi: 10.1190/1.1649379.

Kevin, M. H. (2005). *Hydrogeology: principles and practice*. Oxford, UK, Blackwell Publishing Company.

Kogbe, C. A. (1981). Major Transgressive episodes in the Benue valley of Nigeria on Earth. *Evol. Sci*., 2, 133 – 134.

Kumar, D., Rao, V. A. & Sarma, V. S. (2014).Hydrogeological and geophysical study for deeper groundwater resource in quartzitic hard rock ridge region from 2D resistivity data. *Journal of Earth Sysem Science*. 123(3), 531–543

Lattman, L. H. & Parizek, R. R. (1964). Relationship between Fracture traces and occurrence of groundwater in carbonate rocks. *Journal of Hydrology*, 2(2), 73-91.

Loke, M. H. (1997). Res2DINV software user's manual. *University Sains Malaysia, Penang*.

Loke, M. H. (1999). Electrical imaging survey for environmental and engineering studies. *A practical guide to*, 2. Retrieved from http://www.abem.se/files/res/2dnotes.pdf.

Lower Benue River Basin Development Authority (2014). Water Resources Development in the Benue River Basin; Current Status, Opportunities and Challenges: Status Report Presented at Stakeholders Workshop on Flood Risk Reduction and Sustainable Water Resources and Management in the River Basin.

Lowrie, W. & Fichtner, A. (2019). *Fundamentals of Geophysics*. New York, Cambridge University Press.

Lowrie, W., (2007). Fundamentals of Geophysics. New York, Cambridge University Press.

MacDonald, A. M. & Davies, J. (1998). The Hydrogeology of the Oju/Obi Area, Eastern Nigeria: Ochingini area data report. *British Geological Survey Technical report* WC/98/51R.

MacDonald, A. M., Bonsor, H. C., Dochartaigh, B. ´E. ´O. & Taylor, R. G. (2012). Quantitative maps of groundwater resources in Africa. *Environmental Research Letters*, 7(2) Retrieved from (http://iopscience.iop.org/1748-9326/7/2/024009).

MacDonald, A. M., Davies, J. & Calow, R. C. (2008). "African hydrogeology and rural water supply", in Adelana SMA, MacDonald AM (ed.) *Applied Groundwater Studies in Africa*. International Association of Hydrogeologists, 137-158. CRC Press.

Magnusson, M. K., Fernlund, J. M. & Dahlin, T. (2010). Geoelectrical imaging in the interpretation of geological conditions affecting quarry operations. *Bulletine of Engineering Geology and the Environment*, 69(3), 465–486.

Marescot, L. (1995). Electrical Surveying. Part-I: Resistivity method; Lecture A. *WS*0506.

Mbiimbe, E. Y., Goni, I. B., Umar, I. & Mboringong, M. M. (2016).Groundwater Investigation Using Vertical Electrical Sounding (VES) within and around Billiri, North Eastern Nigeria. *Water resource journal of the Nigerian Association of Hydrogeologists,* 26 (1&2), 1-14.

Mijiyawa, M. U., Aji, M. M., Yusuf, S. N. & Goni, I. B. (2013).Hydrogeological and Geophysical Investigation for Locating Optimal Drilling Point(s) for Daura Town, North-eastern Nigeria. *Water resource journal of the Nigerian association of Hydrogeologists*, 23 (1&2), 20-34.

Morris, B. L., Lawrence, A. R., Chilton, P. J., Adams, B., Calow, R. & Klinck, B. A. (2003). *Groundwater and its Susceptibility to Degradation: A global assessment of the problem and options for management* (Vol. 3). United Nations Environmental Programme.

National Population Commission.(2006). The Nigeria population census 2006. Accessed on, 21 (1), 2018.

Nwabineli, E. O., Awalla, C. O. C., Ogedi, H. I. & Nwokoye, O. (2012). Aquifer Characteristic of the Lafia Sub-Basin of the Middle Benue River Basin, Nasarawa State, Nigeria. *The International Journal of Engineering and Science*, 1(2), 155-157.

Nwachukwu, S. O. (1972). The Tectonic Evolution of the Southern Portion of the Benue Trough. *Nigeria Geol. Mag*, 109, 411 – 419.

Nwajide, C. S. (1986). A Systematic Lithostratigraphy of the Makurdi Sandstones Benue Trough. Nigeria, *Journal of Mining and Geology*, 22, 9-23.

Nwajide, C. S. (2013). *Geology of Nigeria's Sedimentary Basins*.CSS Bookshops Limited, Lagos, Nigeria.

Nwankwoala, H. O. (2015). Hydrogeology and Groundwater Resources of Nigeria. *New York Science Journal*, 8(1), 89-100.

Obaje, N. G. (2009). *Geology and Mineral Resources of Nigeria*, 120.Springer, Verlag.

Offodile, M. E. (1976). A Hydrogeochemical interpretation of the Middle Benue and Abakiliki brine fields. *Journal of Min Geol. Nigeria*. 13 (2), 73-86.

Offodile, M. E. (1991). *An Approach to Groundwater Study and Development in Nigeria*. Mecon Geology and Eng. Services Ltd. Jos, Nigeria, 194-204

Offodile, M. E. (2002). *Groundwater Study and Development in Nigeria*.2nd Edition. Mecon Geology and Eng. Services Ltd. Jos, Nigeria.

Ogah, V. E. & Jatau, B. S. (2014). Airborne Magnetic Study of Otukpo Area. International Research *Journal of Pure and Applied Physics*, 2 (3), 15-24.

Olasehinde, P. I. (1999). An Integrated Geological and Geophysical Exploration Techniques for Groundwater in the Basement Complex of West Central Part of Nigeria. *Journal of Nigerian Association of Hydrogeologist (Water Resources)*, 10 (1), 46-49.

Omali, A. O. (2014). Hydrogeophysical Investigation for Groundwater in Lokoja Metropolis, Kogi State, Central Nigeria. *Journal of Geography and Geology*, 6 (1), 81-95.

Orellana, E. & Mooney A. M. (1966).Master curve and table for Vertical Electrical Sounding Over Layered Structures. *Interciencia*, Escuela, Spain.

Reinhard, K. (2006). *Groundwater Geophysics*. Springer-Verlag Berlin Heidelberg Press London, 92.

Reyment, R. A. (1964). Review of Nigeria Cretaceous Cenozoic Stratigraphy. *Journal of Mining and Geology*, 1, 61-80.

Reyment, R. A. (1965). *Aspect of the Geology of Nigeria*, Ibadan University press, 145-147.

Rijkswaterstaat. (1969). Standard Graph for Resistivity Prospecting. *European Association of Exploration Geophysics*, Hague, the Netherlands.

Sandberg, S. K., Slater, L. D., & Versteeg, R. (2002).An Integrated Geophysical Investigation of the Hydrogeology of an Anisotropic Unconfined Aquifer. *Journal of Hydrology*, 267 (3-4), 227-243.

Sasaki, Y. (1992). Resolution of Resistivity Tomography Inferred from Numerical Simulation 1. *Geophysical Prospecting*, 40(4), 453-463.

Selemo, A. O. I. (2011). Using electrical logs to delineate fresh water zones: A case study from Onne-Eleme, Port-Harcourt, Southern Nigeria. Natural and Applied Sceince Journal. 12 (1), 101-109.

Slater, L. D. & Glaser, D. R. (2003). Controls on induced polarization in sandy unconsolidated sediments and application to aquifer characterization. *Geophysics*, 68, (5), 1547–1558.

Slater, L. D., Ntarlagiannis, D., Day-Lewis, F. D., Mwakanyamale, K.., Versteeg, R. J., Ward, A., Strickland, C., Johnson, C. D. & Lane Jr., J.W. (2010). Use of electrical

imaging and distributed temperature sensing methods to characterize surface water-groundwater exchange regulating uranium transport at the Hanford 300 Area, Washington: *Water Resources Research*, 46 (10).

Slater, L. & Lesmes, D. (2002). IP interpretation in environmental investigations, *Geophysics*, 67 (1), 77–88, doi: 10.1190/1.1451353.

Sudha, K, Israil, M., Mittal, S. & Rai, J. (2009).Soil characterization using electrical resistivity tomography and geotechnical investigations. *Journal of Applied Geophysics*, 67(1), 74–79.

Sumner, J. S. (2012). *Principles of Induced Polarization for Geophysical Exploration*; Elsevier: Amsterdam, The Netherlands, 5.

Sweden, A. I. A. (2010). Instruction Manual Terrameter SAS 4000/SAS 1000.

Taiwo, A. M., Olojumi, O. O., Bamgbose, O. & Arowolo, T. A. (2012). Surface water quality monitoring in Nigeria: Situation Analysis and Feature Management Strategy. *Water quality management and assessment*, 13,301-320.

Tijani, M., Crane, E., Upton, K. & Ó Dochartaigh, B. E. (2010). Africa Groundwater Atlas: Hydrogeology of Nigeria. *British Geological Survey*. Retrieved from earthwise.bgs.ac.uk/index.php/Hydrogeology of Nigeria.

Todd D. K. (1980). *Groundwater Hydrology*. JohnWiley and Son Inc. New York, 410 - 413.

UNESCO. (1999). World Water Resources at the Beginning of the 21st Century, CD version, UNESCO, Paris.

Unuevho, C., Onuoha, K. M., Ogunbanjo, M. I. & Amadi, A. N. (2016). Hydrogeological and geoelectrical prospecting of groundwater within part of Northern Bosso, Minna, North-Central Nigeria. *Water resource journal of the Nigerian Association of Hydrogeologists*, 26 (1&2), 110-121

Van der Velpen & Sporry, R. J. (1992). Resist- A Computer Program to Process Resistivity Sounding Data on PC- Compatibles. *Computer and Geosciences*, 19, 691-703.

Wait, J. R. (1982). *Geo-electromagnetism.* Academic Press, SanDiego,CA.)

WaterAid, (2016). Curbing water borne diseases in Nigeria: *WaterFront Magazine*, 18(1), 26-27

Willem, G. M. (2000). Environmental Isotopes in the Hydrological Cycle; Principles and Applications. International Atomic Energy Agency and United Nations Educational, Scientific and Cultural Organization. *Water Resources Programme*.

World Health Organisation, (2010). Access to safe drinking water improving; sanitation needs greater efforts. http://www.who.int/medicentre/news/releases/2010/water

World Health Organization, (2006). Protecting Groundwater for Health: Managing the Quality of Drinking-water Sources. Edited by O. Schmoll, G. Howard, J. Chilton and I. Chorus. ISBN: 1843390795. Published by IWA Publishing, London, UK.

World Resources Institute (2018). New Initiative Calls for Urgent Action on Water and Security. Washington. DC. Retrieved from https://www.wri.org/publication/mapping-public-water.

Wright, J. B. (1981). Review of the Origin and Evolution of the Benue Trough in Nigeria. *Earth Evolution Science*, 2, 98-103.

Zektser, I. S. & Everett, L. G. (2004). Groundwater Resources of the World and their use. IHP – VI Series on Groundwater, 6, 346.

Zohdy, A. A. R., Eaton, G. P. & Mabey, D. R. (1974). *Application of Surface Geophysics to Groundwater Investigation*. U. S. G. S. Techniques of Water-Resource Investigation, Book 2.

APPENDIX A

Hydrogeological Well Inventory Data

Table A. Well Inventory

S/N	Co-ordinates		Altitude	SWL	Well	Hydraulic
	N(º)	E(º)	(m)asl	(m)	Depth	Head
W1	7º11′48.5″	8º08′17.3″	204	6.5	8.0	197.5
W2	7º11′47.4″	8º08′18.8″	175	6.2	6.4	168.8
W3	7º11′50.1″	8º08′20.6″	170	7.0	7.5	163
W4	7º11′51.7″	8º08′24.6″	178	6.3	8.4	171.7
W5	7º11′59.1″	8º08′20.6″	176	6.9	7.2	169.1
W6	7º12′01.4″	8º08′22.5″	165	7.0	7.6	158
W7	7º12′08.6″	8º08′24.3″	164	6.0	6.7	158
W8	7º12′07.9″	8º08′26.7″	160	6.0	7.0	154
W9	7º12′15.9″	8º08′22.9″	158	5.5	6.2	152.5
W10	7º12′14.4″	8º08′15.9″	162	5.4	5.7	156.6
W11	7º12′10.3″	8º08′10.6″	162	2.8	4.7	159.2
W12	7º12′08.4″	8º07′59.3″	174	2.4	5.2	171.6
W13	7º12′02.1″	8º08′01.1″	178	4.6	5.2	173.4
W14	7º12′01.6″	8º08′07.2″	165	3.5	5.8	161.5
W15	7º11′55.7″	8º08′08.8″	175	4.5	5.7	170.5
W16	7º11′49.8″	8º08′14.7″	171	5.2	6.4	165.8
W17	7º11′48.0″	8º08′15.5″	169	5.5	6.6	163.5
W18	7º11′50.0″	8º08′08.2″	177	5.0	5.5	172
W19	7º11′46.7″	8º08′07.7″	187	4.8	5.4	182.2
W20	7º11′45.3″	8º08′03.2″	180	3.0	3.1	177
W21	7º11′58.8″	8º08′00.9″	182	3.0	4.6	179
W22	7º11′10.3″	8º07′10.6″	184	5.5	7.0	178.5
W23	7º11′56.2″	8º07′53.1″	190	5.9	6.0	184.1
W24	7º11′54.8″	8º07′53.0″	192	4.4	5.5	187.6
W25	7º11′47.3″	8º07′56.2″	195	6.2	7.2	188.8
W26	7º11′49.3″	8º08′00.2″	187	4.3	4.8	182.7
W27	7º12′20.7″	8º08′20.5″	161	4.6	4.9	156.4
W28	7º12′23.4″	8º08′19.3″	158	3.2	4.0	154.8
W29	7º11′10.1″	8º07′44.8″	189	3.6	4.7	185.4
W30	7º11′09.5″	8º07′40.5″	200	4.7	6.0	195.3
W31	7º11′12.6″	8º07′38.4″	190	3.7	4.8	186.3
W32	7º11′11.3″	8º07′36.2″	193	4.9	5.8	188.1
W33	7º11′09.8″	8º07′31.6″	198	5.6	6.4	192.4
W34	7º11′06.3″	8º07′29.5″	206	6.4	6.7	199.6
W35	7º11′05.0″	8º07′25.7″	202	6.2	6.9	195.8
W36	7º11′01.7″	8º07′24.1″	196	6.2	6.5	189.8
W37	7º10′59.8″	8º07′22.1″	196	5.7	6.8	190.3
W38	7º10′57.4″	8º07′19.3″	193	5.7	6.4	187.3
W39	7º10′57.6″	8º07′16.1″	194	6.8	7.3	187.2
W40	7º11′02.7″	8º07′11.3″	192	6.8	7.4	185.2
W41	7º10′56.8″	8º07′08.5″	176	4.2	6.0	171.8
W42	7º10′55.1″	8º07′19.3″	173	3.1	4.3	169.9
W43	7º10′53.4″	8º07′10.0″	171	4.2	4.7	166.8
W44	7º10′51.0″	8º07′08.4″	166	4.9	5.4	161.1
W45	7º10′48.8″	8º07′08.4″	165	3.5	3.9	161.5
W46	7º10′48.0″	8º07′12.3″	166	5.2	6.1	160.8
W47	7º10′48.4″	8º07′15.2″	174	1.8	2.3	172.2
W48	7º10′46.4″	8º07′15.8″	171	6.8	7.5	164.2
W49	7º10′44.7″	8º07′22.5″	204	6.7	7.0	197.3
W50	7º10′47.2″	8º07′25.2″	198	8.3	9.2	189.7

Table A. Well Inventory

S/N	Co-ordinates		Altitude	SWL	Well	Hydraulic
	N(º)	E(º)	(m)asl	(m)	Depth	Head
W51	7º10′45.8″	8º07′25.8″	203	6.5	7.2	196.5
W52	7°10′40.3″	8°07′22.0″	196	7.6	8.3	188.4
W53	7º10′35.1″	8º07′24.1″	199	5.9	6.7	193.1
W54	7º10′27.7″	8º07′33.3″	207	8.7	9.2	198.3
W55	7º10′26.6″	8º07′34.3″	199	7.5	8.9	191.5
W56	7º10′38.8″	8º07′58.9″	181	6.5	7.6	174.5
W57	7º10′44.6″	8º07′44.1″	182	4.7	5.0	177.3
W58	7º10′46.4″	8º07′40.8″	197	3.2	4.5	193.8
W59	7º10′49.8″	8º07′37.1″	205	9.9	10.3	195.1
W60	7º10′51.8″	8º07′33.5″	199	9.9	10.1	189.1
W61	7º11′00.4″	8º07′41.2″	204	7.4	7.6	196.6
W62	7º11′02.3″	8º07′43.2″	204	6.8	7.0	197.2
W63	7º11′06.0″	8º07′43.2″	198	4.8	5.8	193.2
W64	7º11′08.7″	8º07′41.1″	200	4.6	5.5	195.4
W65	7º11′11.3″	8º07′44.3″	192	3.5	5.2	188.5
W66	7º11′14.4″	8º07′43.7″	199	3.3	4.7	195.7
W67	7º11′13.7″	8º07′49.9″	195	3.5	4.5	191.5
W68	7º11′17.4″	8º07′49.6″	197	3.7	4.8	193.3
W69	7º11′20.5″	8º07′48.8″	200	4.7	5.0	195.3
W70	7º11′23.4″	8º07′45.1″	187	3.7	5.6	183.3
W71	7º11′23.7″	8º07′41.5″	188	3.6	4.8	184.4
W72	7º11′24.8″	8º07′37.9″	194	3.5	5.3	190.5
W73	7º11′27.4″	8º07′39.6″	190	3.8	5.4	186.2
W74	7º11′25.9″	8º07′45.6″	195	4.2	4.9	190.8
W75	7º11′22.8″	8º07′50.8″	188	4.7	5.7	183.3
W76	7º11′22.4″	8º07′53.4″	195	4.8	5.7	190.2
W77	7º11′22.5″	8º07′59.4″	198	5.5	5.8	192.5
W78	7º11′19.0″	8º08′09.7″	196	6.3	7.1	189.7
W79	7º11′15.3″	8º08′08.7″	208	6.1	7.1	201.9
W80	7º11′15.2″	8º08′04.4″	197	6.0	6.4	191
W81	7º11′11.7″	8º08′00.2″	194	5.6	6.6	188.4
W82	7º11′14.0″	8º07′52.6″	192	4.7	5.4	187.3
W83	7º11′52.8″	8º08′42.4″	197	9.3	9.6	187.7
W84	7º11′52.2″	8º08′41.3″	188	9.3	9.7	178.7
W85	7º11′52.7″	8º08′39.6″	186	8.7	9.7	177.3
W86	7º11′53.4″	8º08′38.4″	183	9.5	10.2	173.5
W87	7º11′52.4″	8º08′38.3″	191	8.1	9.2	182.9
W88	7º11′52.6″	8º08′36.9″	196	8.9	9.2	187.1
W89	7º11′50.0″	8º08′36.3″	187	8.6	9.3	178.4
W90	7º11′47.3″	8º08′31.7″	185	8.7	9.7	176.3
W91	7º11′43.3″	8º08′28.4″	169	7.3	8.4	161.7
W92	7º11′42.1″	8º08′25.7″	178	6.8	9.4	171.2
W93	7º11′50.8″	8º08′17.6″	171	5.6	6.4	165.4
W94	7º11′53.3″	8º08′15.8″	183	6.2	6.5	176.8
W95	7º11′52.7″	8º08′14.9″	173	5.3	6.5	167.7
W96	7º11′53.6″	8º08′13.7″	170	5.5	5.6	164.5
W97	7º11′37.3″	8º08′23.3″	185	6.6	7.2	178.4
W98	7º11′39.7″	8º08′26.8″	188	7.3	8.1	180.7
W99	7º11′39.1″	8º08′28.6″	186	8.0	8.3	178
W100	7º11′39.6″	8º08′33.1″	191	9.1	9.3	181.9

Table A. Well Inventory

S/N	Co-ordinates		Altitude	SWL	Well	Hydraulic
	N(º)	E(º)	(m)asl	(m)	Depth	Head
W101	7º12′17.8″	8º07′40.8″	157	7.0	7.2	150
W102	7º12′16.0″	8º07′39.9″	165	6.6	6.9	158.4
W103	7º12′21.0″	8º07′36.3″	190	7.4	7.8	182.6
W104	7º12′22.6″	8º07′35.8″	189	6.2	6.7	182.8
W105	7º12′23.3″	8º07′35.1″	182	4.0	5.4	178
W106	7º12′20.6″	8º07′30.2″	183	6.0	6.9	177
W107	7º12′21.4″	8º07′28.5″	177	6.1	7.0	170.9
W108	7º12′19.1″	8º07′24.7″	169	6.0	6.3	163
W109	7º12′19.6″	8º07′21.7″	177	6.1	6.7	170.9
W110	7º12′17.7″	8º07′13.7″	167	6.1	7.4	160.9
W111	7º12′18.3″	8º07′10.8″	159	6.6	7.5	152.4
W112	7º12′16.7″	8º07′06.1″	155	5.4	6.6	149.6
W113	7º12′18.3″	8º06′59.8″	159	4.0	8.0	155
W114	7º12′20.8″	8º06′52.6″	157	4.2	5.7	152.8
W115	7º12′21.5″	8º06′54.8″	155	3.7	3.9	151.3
W116	7º12′20.6″	8º06′59.3″	155	3.0	3.5	152
W117	7º12′28.1″	8º07′07.6″	153	6.0	7.1	147
W118	7º12′34.2″	8º07′09.6″	158	5.1	6.1	152.9
W119	7º12′39.2″	8º07′16.6″	147	4.3	7.0	142.7
W120	7º12′43.0″	8º07′21.0″	152	5.9	8.6	146.1
W121	7º12′47.2″	8º07′21.3″	156	6.0	7.2	150
W122	7º12′51.8″	8º07′19.0″	142	4.9	5.5	137.1
W123	7º12′56.3″	8º07′26.1″	149	5.5	6.2	143.5
W124	7º12′55.8″	8º07′28.6″	151	5.5	7.7	145.5
W125	7º12′56.9″	8º07′31.5″	153	4.8	5.8	148.2
W126	7º12′49.2″	8º07′37.0″	152	4.8	5.0	147.2
W127	7º12′46.3″	8º07′38.0″	158	3.5	3.9	154.5
W128	7º12′43.4″	8º07′39.7″	152	9.5	10.3	142.5
W129	7º12′31.6″	8º07′42.1″	170	4.7	4.8	165.3
W130	7º12′28.3″	8º07′48.0″	169	4.0	4.7	165
W131	7º12′31.1″	8º07′51.9″	169	1.9	6.2	167.1
W132	7º12′28.4″	8º07′57.8″	164	1.9	6.2	162.1
W133	7º12′23.7″	8º07′53.2″	170	2.2	7.9	167.8
W134	7º12′20.3″	8º07′52.5″	172	6.4	7.2	165.6
W135	7º12′18.4″	8º07′51.8″	174	2.8	4.0	171.2
W136	7º12′15.4″	8º07′50.6″	172	2.4	3.5	169.6
W137	7º12′15.0″	8º07′46.9″	174	3.0	4.0	171
W138	7º12′09.3″	8º07′47.0″	174	3.0	3.4	171
W139	7º12′09.3″	8º07′49.1″	169	3.9	4.0	165.1
W140	7º12′10.9″	8º07′52.3″	173	4.2	5.1	168.8
W141	7º12′11.9″	8º07′56.3″	164	3.6	4.6	160.4
W142	7º12′08.9″	8º07′55.9″	175	6.0	6.1	169
W143	7º12′08.2″	8º07′54.1″	173	6.1	7.0	166.9
W144	7º12′05.2″	8º07′50.3″	178	4.1	5.1	173.9
W145	7º12′26.7″	8º09′26.5″	196	0.0	4.6	196
W146	7º12′23.5″	8º09′31.2″	198	3.5	6.0	194.5
W147	7º13′23.2″	8º06′49.0″	149	6.3	8.7	142.7
W148	7º13′24.0″	8º06′48.6″	152	6.9	8.7	145.1
W149	7º13′13.4″	8º06′51.0″	159	2.4	3.8	156.6
W150	7º12′52.4″	8º07′09.1″	151	6.6	7.8	144.4

Table A. Well Inventory

S/N	Co-ordinates		Altitude	SWL	Well	Hydraulic
	N(º)	E(º)	(m)asl	(m)	Depth	Head
W151	7º12′09.9″	8º09′27.3″	195	7.6	7.6	187.4
W152	7º12′18.5″	8º09′02.5″	196	10.3	11.0	185.7
W153	7º12′27.6″	8º09′02.5″	190	8.5	9.1	181.5
W154	7º12′53.4″	8º09′08.1″	183	6.2	7.0	176.8
W155	7º13′00.0″	8º09′10.4″	175	5.9	7.1	169.1
W156	7º13′17.4″	8º09′39.4″	170	7.1	8.2	162.9
W157	7º13′36.2″	8º09′51.7″	153	4	5.4	149
W158	7º15′18.7″	8º10′30.1″	118	3.7	5.9	114.3
W159	7º15′12.1″	8º10′29.7″	130	3.3	5.7	126.7
W160	7º15′11.4″	8º10′40.8″	126	4.4	6.7	121.6
W161	7º15′11.0″	8º10′31.9″	117	4.0	6.7	113
W162	7º15′02.2″	8º10′26.9″	125	4.2	5.5	120.8
W163	7º15′00.7″	8º10′24.7″	130	4.4	6.4	125.6
W164	7º13′53.2″	8º10′02.8″	151	7.0	7.6	144
W165	7º13′49.2″	8º09′59.1″	124	4.0	6.7	120
W166	7º13′36.0″	8º09′59.4″	169	4.2	6.2	164.8
W167	7º13′27.6″	8º09′46.6″	165	9.0	10.1	156
W168	7º13′22.3″	8º09′42.3″	159	6.8	7.8	152.2
W169	7º12′43.8″	8º08′48.8″	165	7.1	7.6	157.9
W170	7º12′35.9″	8º08′58.8″	176	8.4	9.5	167.6
W171	7º12′37.4″	8º08′55.3″	173	8.7	10.3	164.3
W172	7º12′23.2″	8º08′48.7″	178	9.0	9.4	169
W173	7º12′30.1″	8º08′42.5″	165	8.3	9.4	156.7
W174	7º12′30.3″	8º08′41.3″	172	8.6	9.5	163.4
W175	7º12′32.4″	8º08′38.9″	167	6.2	8.3	160.8
W176	7º12′35.5″	8º08′37.7″	160	8.0	9.5	152
W177	7º12′34.6″	8º08′38.0″	163	7.9	8.2	155.1
W178	7º12′34.5″	8º08′36.7″	153	6.0	6.1	147
W179	7º12′37.5″	8º08′34.7″	140	6.5	7.3	133.5
W180	7º12′43.9″	8º08′33.0″	155	5.1	6.5	149.9
W181	7º12′47.3″	8º08′33.1″	150	5.5	6.3	144.5
W182	7º12′41.3″	8º08′27.5″	154	4.2	5.5	149.8
W183	7º12′39.4″	8º08′26.4″	154	4.3	4.9	149.7
W184	7º12′35.6″	8º08′32.4″	164	5.7	7.2	158.3
W185	7º12′09.3″	8º08′53.1″	187	6.7	9.1	180.3
W186	7º12′09.9″	8º08′49.3″	191	9.2	9.9	181.8
W187	7º12′08.7″	8º08′49.4″	188	8.6	10	179.4
W188	7º12′43.9″	8º08′33.0″	189	9.4	10.2	179.6
W189	7º12′43.9″	8º08′33.0″	183	8.7	9.3	174.3
W190	7º12′43.9″	8º08′33.0″	183	10	10.7	173
W191	7º11′33.3″	8º08′19.3″	186	14.0	14.2	172
W192	7º11′34.5″	8º08′24.2″	184	7.7	8.2	176.3

abs = above sea level SWL= Static Water Level

APPENDIX B

Vertical Electrical Sounding (VES) Data

Table B 1A. VES 01 to 06 Data

			VES01	VES02	VES03	VES04	VES05	VES06
Latitude (N°)		⟶	7°16′11.6″	7°12′07.9″	7°10′18.1″	7°13′14.5″	7°20′02.4″	7°13′11.3″
Longitude (E°)		⟶	8°10′27.1″	8°07′43.0″	8°08′17.9″	8°06′52.2″	8°15′13.3″	8°09′25.9″
AB/2	**MN/2**	**K**	**ℓ_a**	**ℓ_a**	**ℓ_a**	**ℓ_a**	**ℓ_a**	**ℓ_a**
1	0.3	5	500	139	700	99	230	220
2	0.3	20	849	175	950	88	355	338
3	0.3	47	920	202	846	74	511	499
4	0.3		861	209	419	57	646	647
4	1	24	860	209	419	57	646	647
6	1	55	710	216	129	43	724	671
8	1	99	515	227	51	22	733	660
10	1	156	334	234	27	18	707	578
12	1	225	226	218	21	17	690	438
15	1	352	127	169	14	14	661	289
20	1	627	79	100	8	11	524	219
20	5	118	79	100	8	11	524	219
25	5	189	45	62	5	9	378	145
30	5	275	32	37	3	8	272	95
35	5	377	24	22	3	7	158	65
40	5	495	19	14	3	6	140	32
50	5	778	11	9	6	5	73	9
60	5	1124	9	8	6	5	42	8
80	5	2004	9	6	6	4	18	6
80	10	990	10	6	6	4	18	7
100	10	1556	8	5	7	4	10	6
125	10	2440	8	5	7	5	6	5
150	10	3520	8	4	9	5	3	5
150	20	1737	10	5	9	5	3	5
200	20	3112	9	6	9	7	3	6
250	20	4880	9	7	10	8	3	7
300	20	7040	13	9	10	12	5	8
350	20	9594	18	15	13	13	6	12
400	20	12541	28	21	21	15	22	18
400	50	4950	30	21	21	15	22	18
500	50	7779	38	30	34	13	32	24
600	50		29	42	82	11	45	38
600	80		167		82			38

AB=Current Electrode MN=Potential Electrode K=Constant ℓa=Apparent Resistivity

Table B 2A. VES 07 to 13 Data

			VES07	VES08	VES09	VES10	VES11	VES12	VES13
Latitude (N°) →			7°11′55.7″	7°11′07.4″	7°14′05.6″	7°12′59.8″	7°12′28.8″	7°13′56.9″	7°14′57.9″
Longitude (E°) →			8°08′00.2″	8°08′40.6″	8°05′29.8″	8°05′53.5″	8°08′12.1″	8°10′37.9″	8°12′18.4″
AB/2	**MN/2**	**K**	**ℓ_a**	**ℓ_a**	**ℓ_a**	**ℓ_a**	**ℓ_a**	**ℓ_a**	**ℓ_a**
1	0.3	5	150	180	250	700	200	250	640
2	0.3	20	180	300	250	950	230	108	490
3	0.3	47	240	440	200	1150	199	89	360
4	0.3		260	548	198	1000	189	67	300
4	1	24	260	548	198	1000	189	67	265
6	1	55	282	620	200	800	210	53	250
8	1	99	300	612	209	610	221	32	239
10	1	156	300	550	220	324	240	20	200
12	1	225	280	500	198	220	209	19	190
15	1	352	171	270	115	122	180	16	171
20	1	627	121	214	80	80	120	13	120
20	5	118	121	214	82	80	120	13	121
25	5	189	80	135	40	50	80	11	79
30	5	275	51	100	9	32	29	10	48
35	5	377	22	70	8	32	20	9	20
40	5	495	12	29	8	25	12	9	14
50	5	778	10	15	6	15	6	7	8
60	5	1124	7	15	6	14	6	7	7
80	5	2004	7	12	5	11	5	6	7
80	10	990	7	12	5	11	5	6	6
100	10	1556	6	10	4	10	5	6	5
125	10	2440	6	10	4	9	5	6	5
150	10	3520	5	8	6	9	6	7	5
150	20	1737	5	8	6	9	6	6	6
200	20	3112	8	8	7	8	7	5	4
250	20	4880	8	6	7	8	7	7	4
300	20	7040	10	12	8	8	10	8	5
350	20	9594	21	15	12	10	13	12	7
400	20	12541	35	18	30	24	19	15	9
400	50	4950	35	19	30	24	19	15	10
500	50	7779	51	28	61	50	30	25	42
600	50		80	65	102	99	55	42	120
600	80		80		102	99	55		118

AB=Current Electrode MN=Potential Electrode K=Constant ℓa=Apparent Resistivity

Table B 3A. VES 14 to 20 Data

UNPLOTTED			VES 14	VES 15	VES 16	VES 17	VES 18	VES 19	VES20
Latitude (N°) ⟶			7°13′50.2″	7°16′57.7″	7°17′56.5″	7°20′01.8″	7°15′05.7″	7°17′32.1″	7°19′53.1″
Longitude (E°) ⟶			8°13′58.8″	8°14′36.7″	8°08′39.1″	8°06′31″	8°06′27.9″	8°07′06.8″	8°12′00.4″
AB/2	**MN/2**	**K**	**ρ_a**	**ρ_a**	**ρ_a**	**ρ_a**	**ρ_a**	**ρ_a**	**ρ_a**
1	0.3	5	1015	1500	100	1050	800	911	100
2	0.3	20	502	2750	180	750	1200	400	99
3	0.3	47	320	3000	220	600	1250	314	100
4	0.3		250	1800	153	448	1180	211	92
4	1	24	250	100					
6	1	55	184	100	120	125	869	150	60
8	1	99	98	75	100	60	520	119	38
10	1	156	75	55	100	25	329	98	37
12	1	225	43	41	95	21	200	19	37
15	1	352	19	21	80	10	125	18	36
20	1	627	9	10	20	8	81	16	34
20	5	118	9			8			
25	5	189	8	10	9	7	44	16	30
30	5	275	7	8	8	9	34	15	26
35	5	377	7	6	7	7	28	15	22
40	5	495	6	5	7	6	11	14	17
50	5	778	6	4	5	6	10	14	13
60	5	1124	5	4	4	5	10	13	10
80	5	2004	5	3	4	5	9	12	7
80	10	990	5	3	5	4	9	12	6
100	10	1556	4	3	4	4	9	11	
125	10	2440	3	3	4	4	9	10	6
150	10	3520	3	3	4	4	7	9	5
150	20	1737	3	3	3	3	7	9	6
200	20	3112	3	3	5	3	6	8	6
250	20	4880	4	4	5	8	6	12	6
300	20	7040	5	4	5	20	5	18	7
350	20	9594	5	5	6	32	6	26	10
400	20	12541	10	6	10	78	10	68	16
400	50	4950	10	6	12	75	12	68	18
500	50	7779	32	22	22	75	38	91	48
600	50		81	58	49	70	92	127	90
600	80		84	61	49	70	105	127	92

AB=Current Electrode MN=Potential Electrode K=Constant ρ_a=Apparent Resistivity

APPENDIX C

Vertical Electrical Sounding (VES) Model Curves and Geoelectric Sections

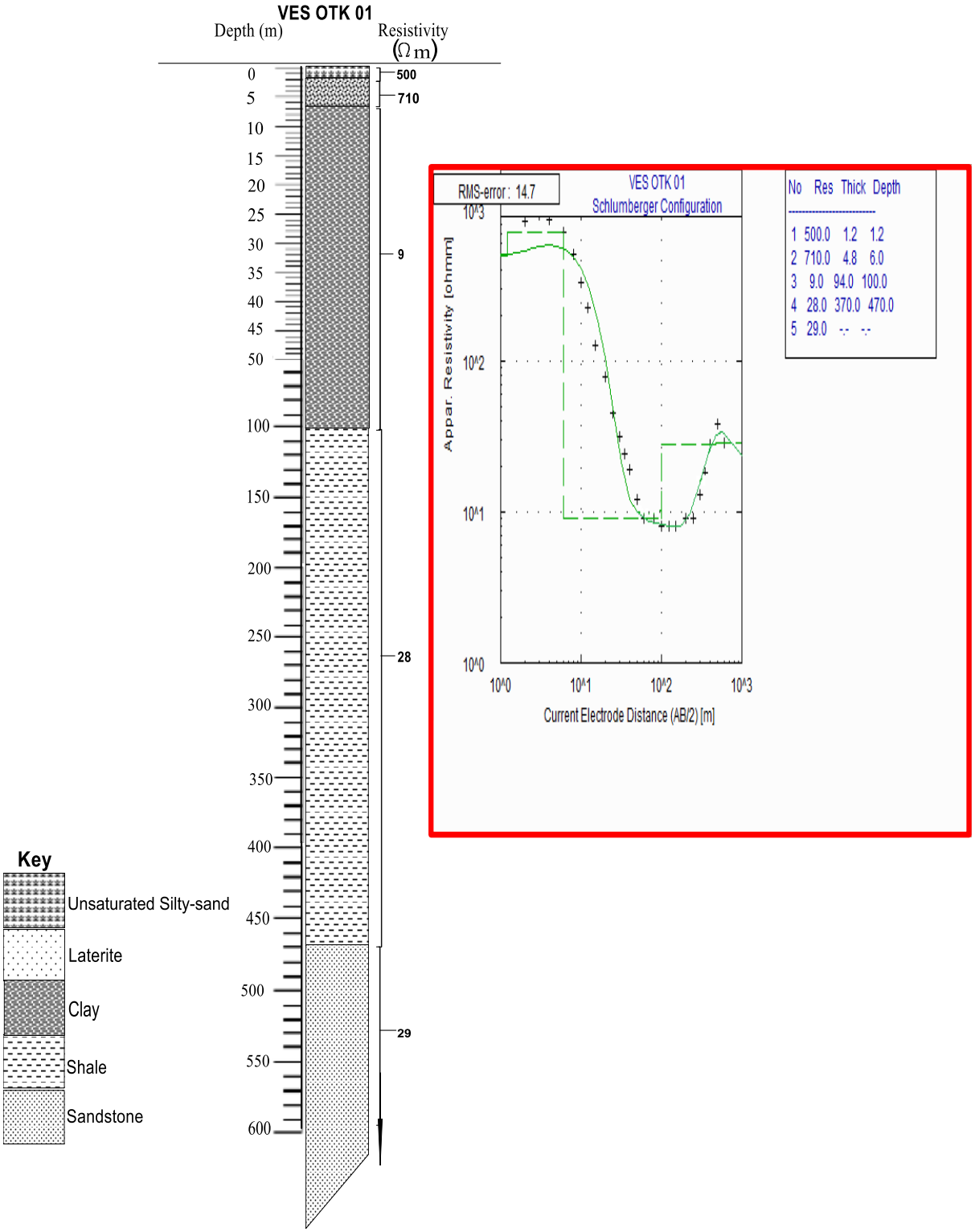

Figure C1.QH Sounding Model Curve Type and Geoelectric Section VES OTK 01

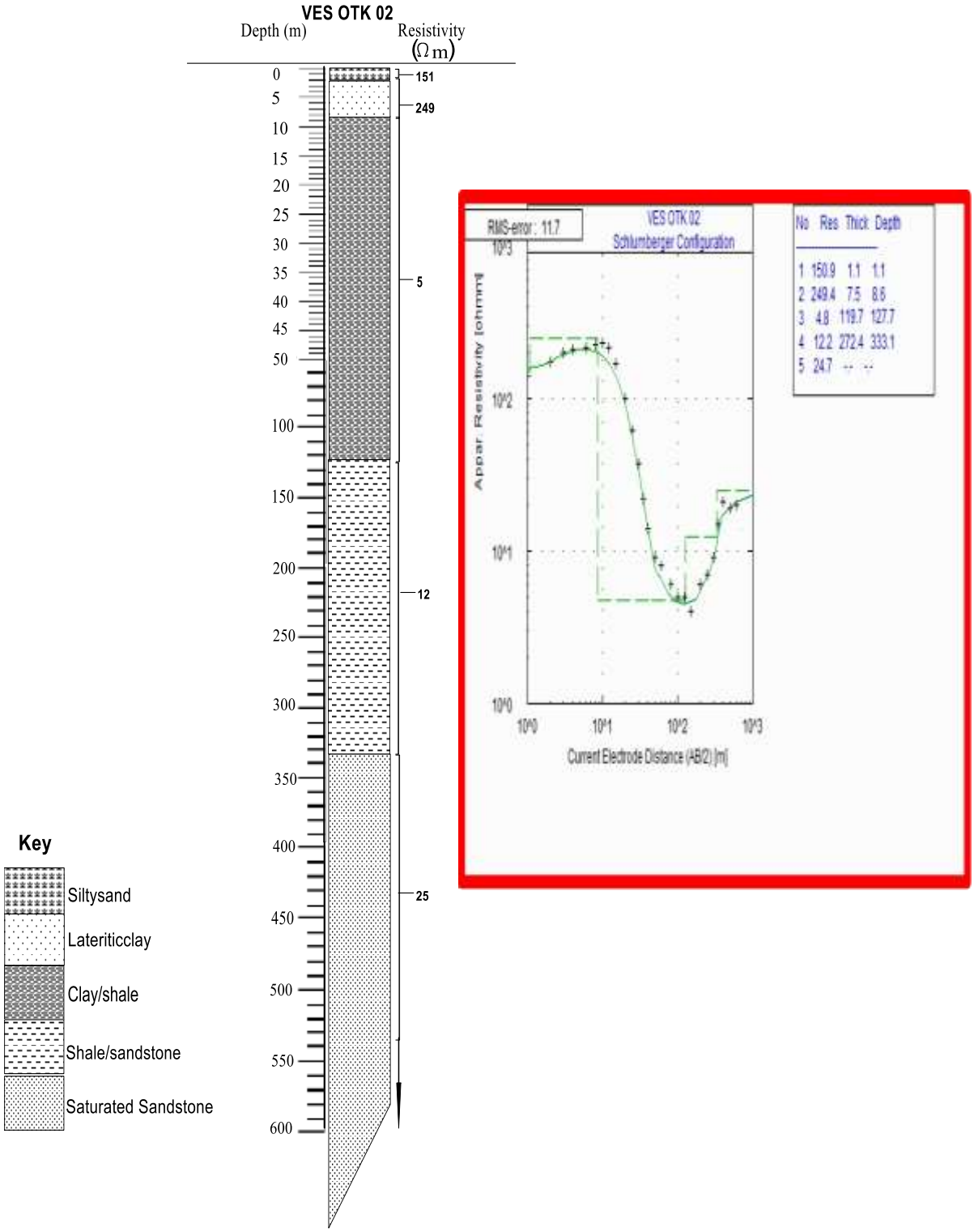

Figure C2.KH Sounding Model Curve Type and Geoelectric Section, VES OTK 02

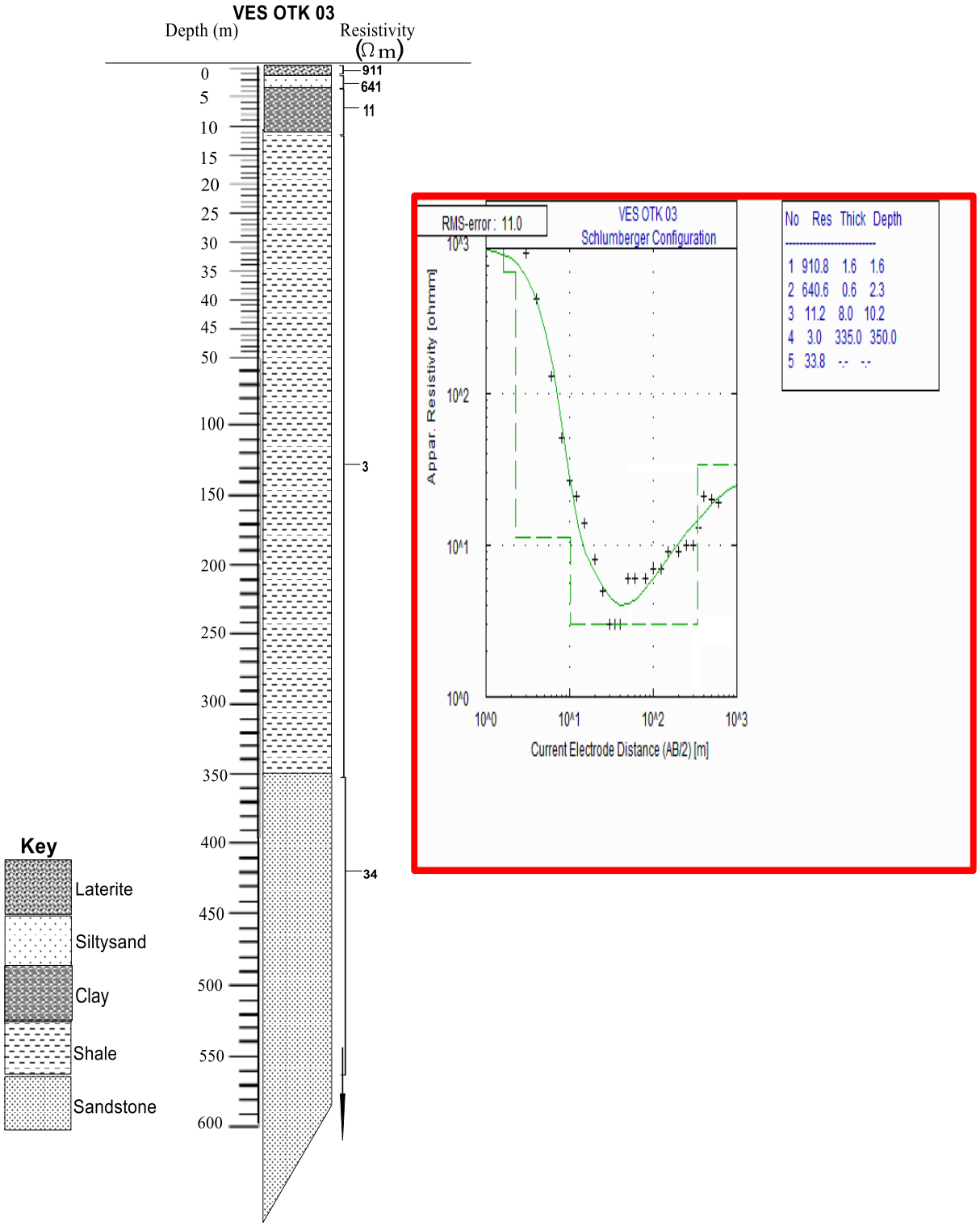

Figure C3.QH Sounding Model Curve Type and Geoelectric Section, VES OTK 03

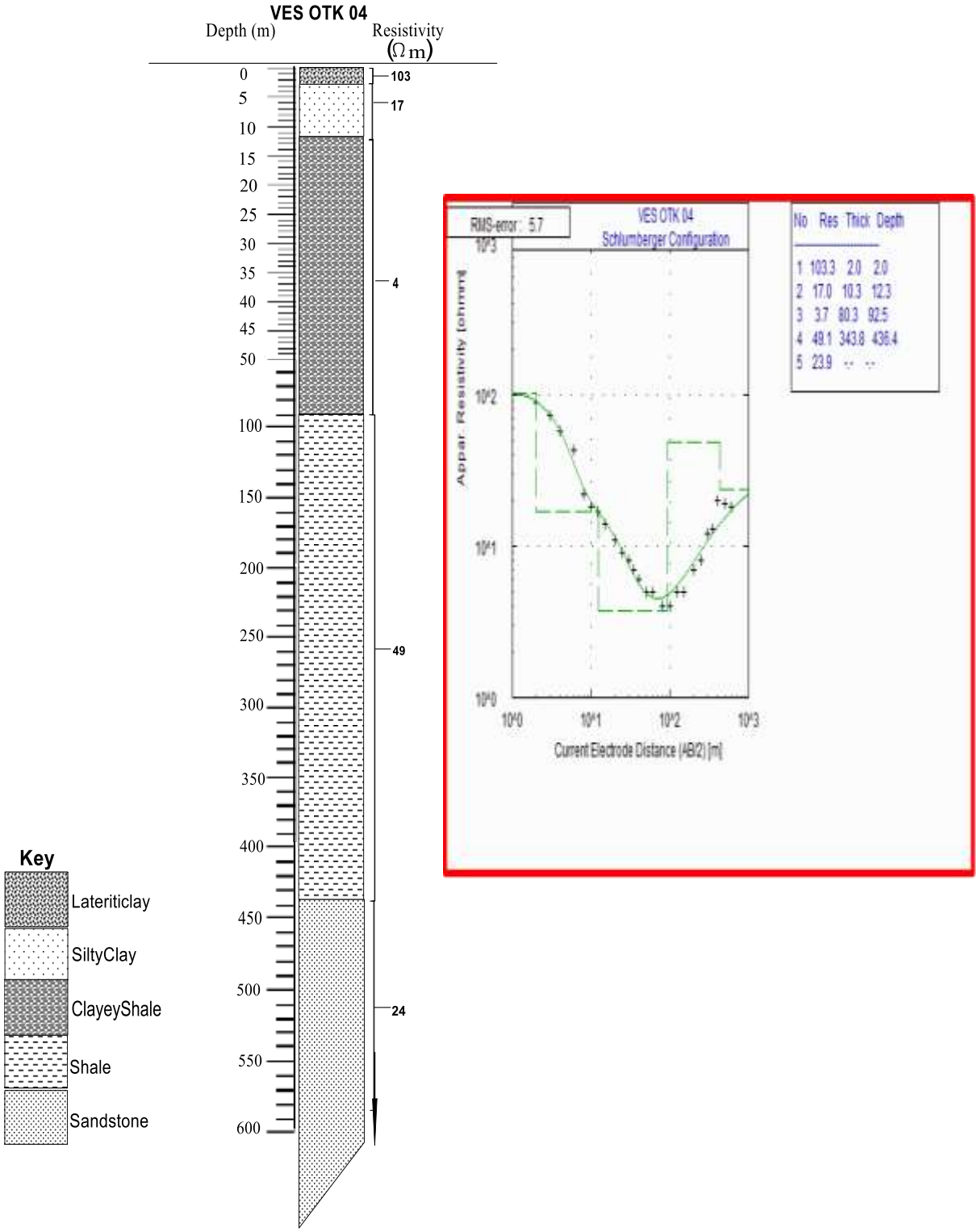

Figure C4.QH Sounding Model Curve Type and Geoelectric Section, VES OTK 04

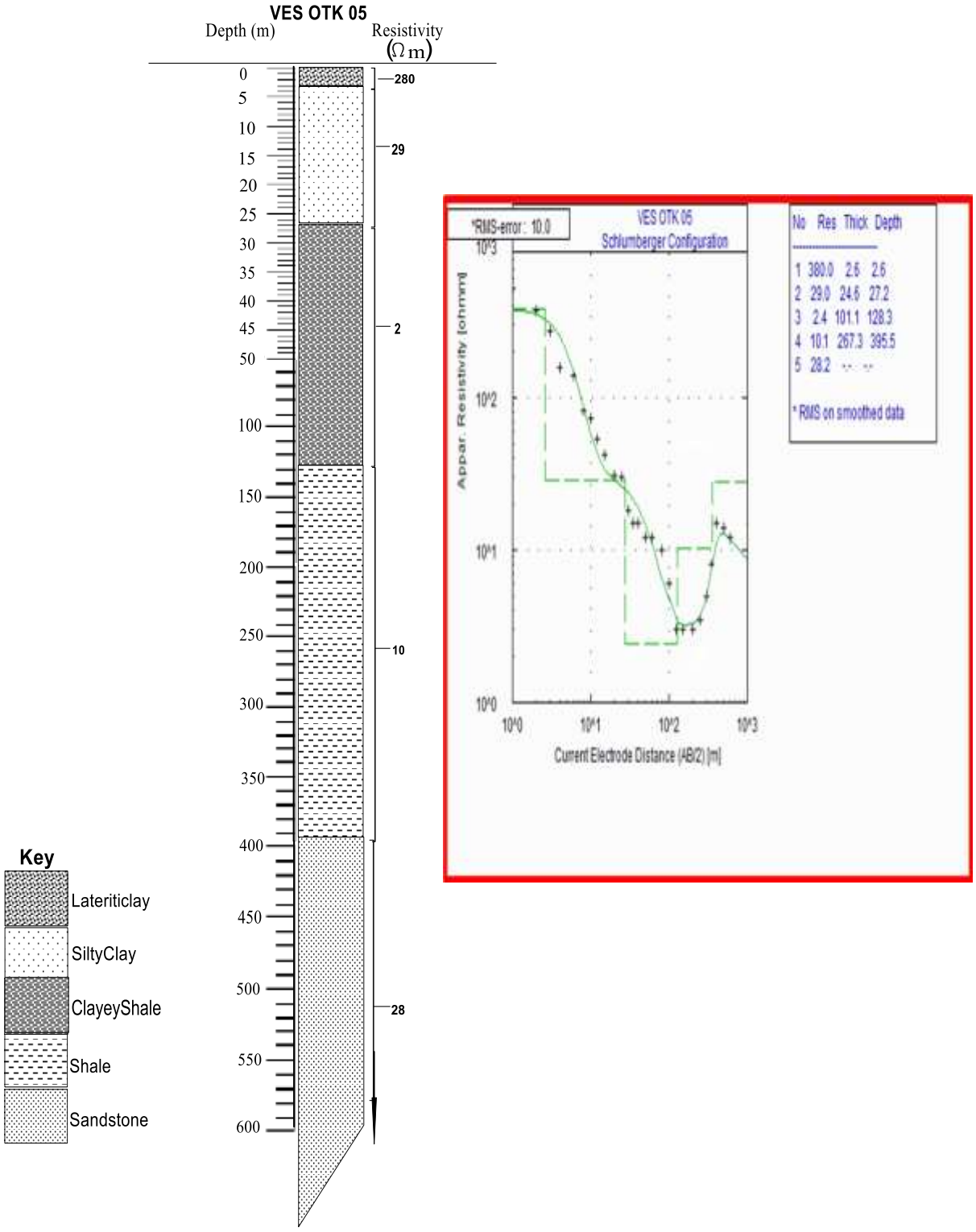

Figure C5.QHK Sounding Model Curve Type and Geoelectric Section, VES OTK 05

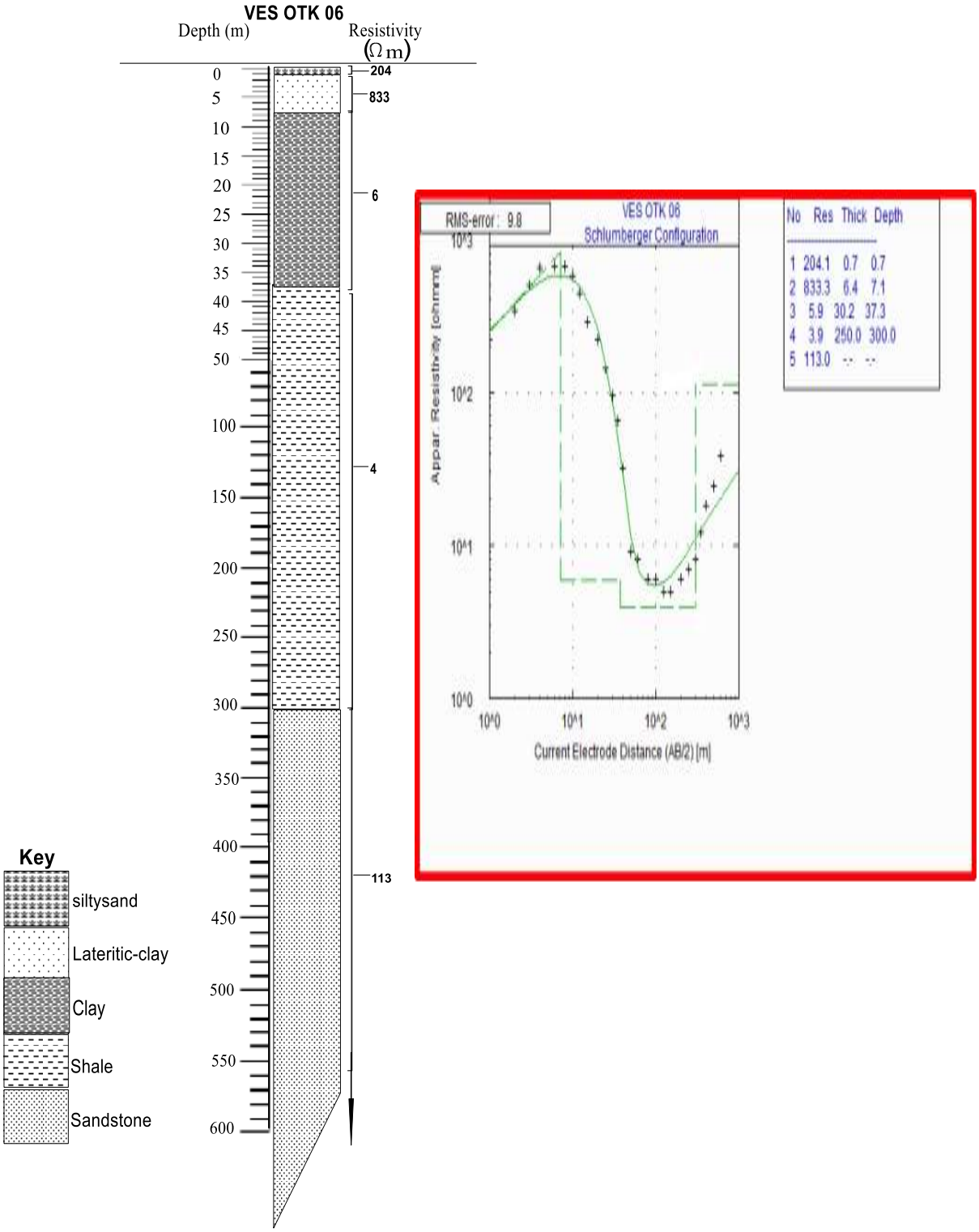

Figure C6.KQH Sounding Model Curve Type and Geoelectric Section, VES OTK 06

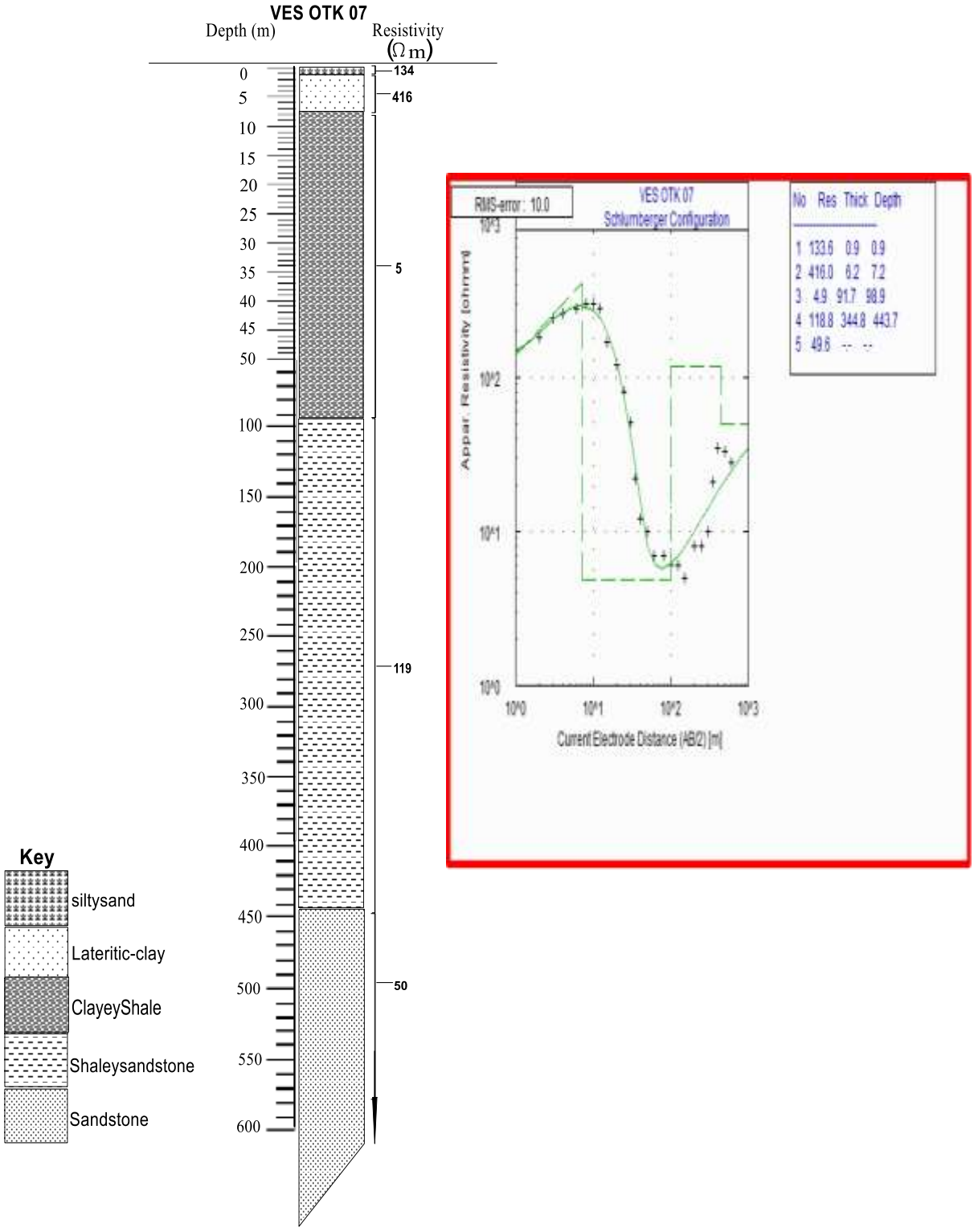

Figure C7.KH Sounding Model Curve Type and Geoelectric Section, VES OTK 07

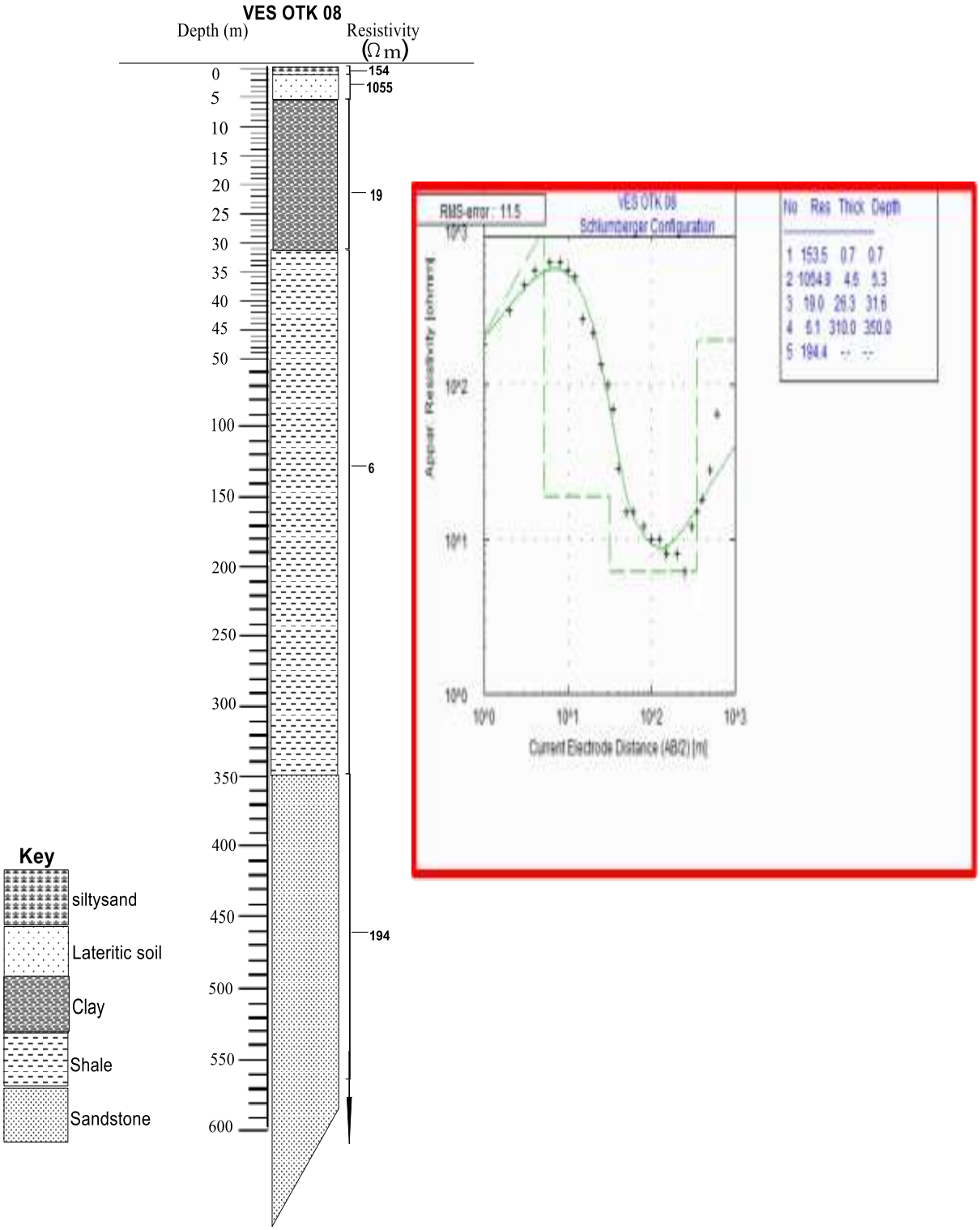

Figure C8.KQH Sounding Model Curve Type and Geoelectric Section, VES OTK 08

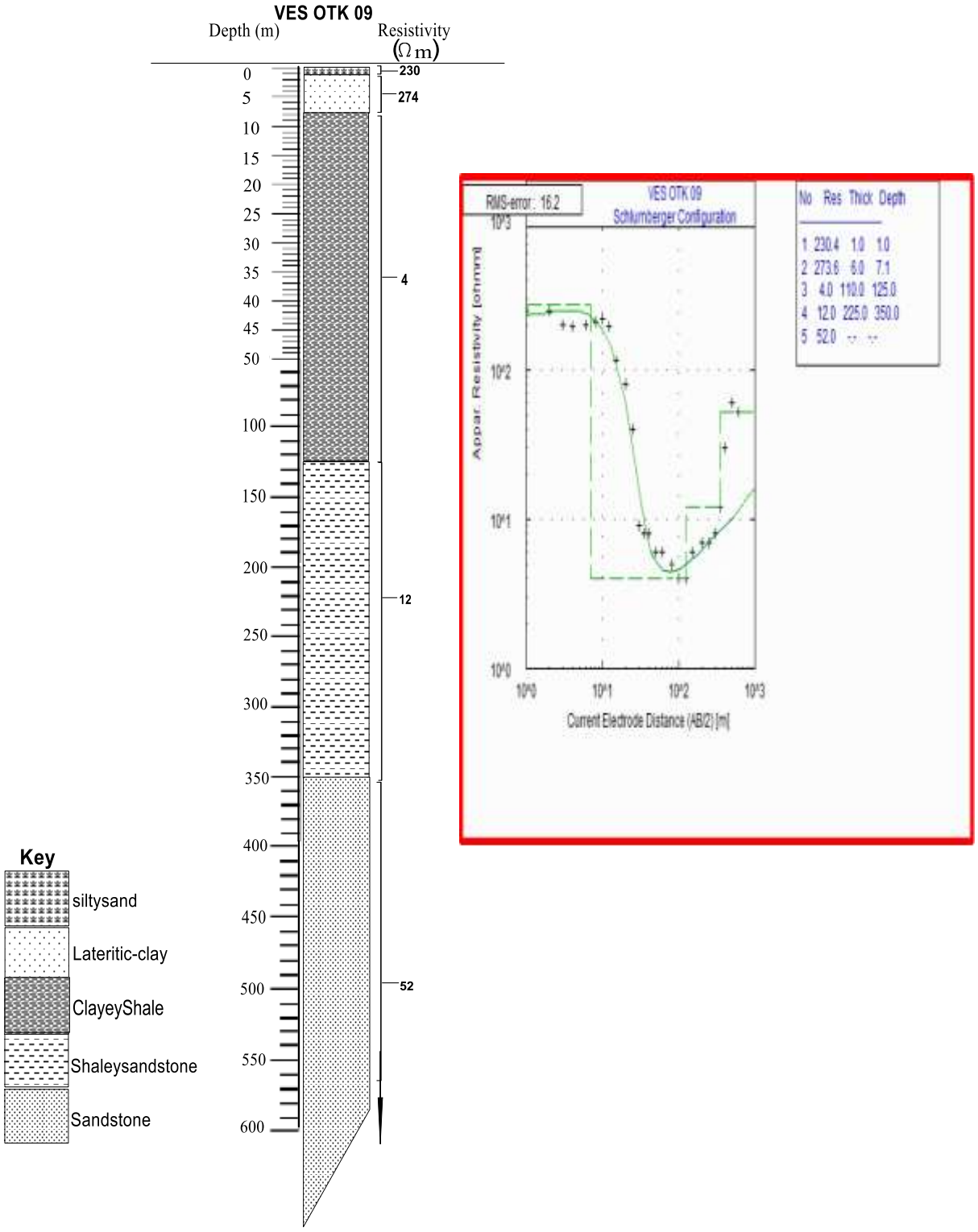

Figure C9.QH Sounding Model Curve Type and Geoelectric Section, VES OTK 09

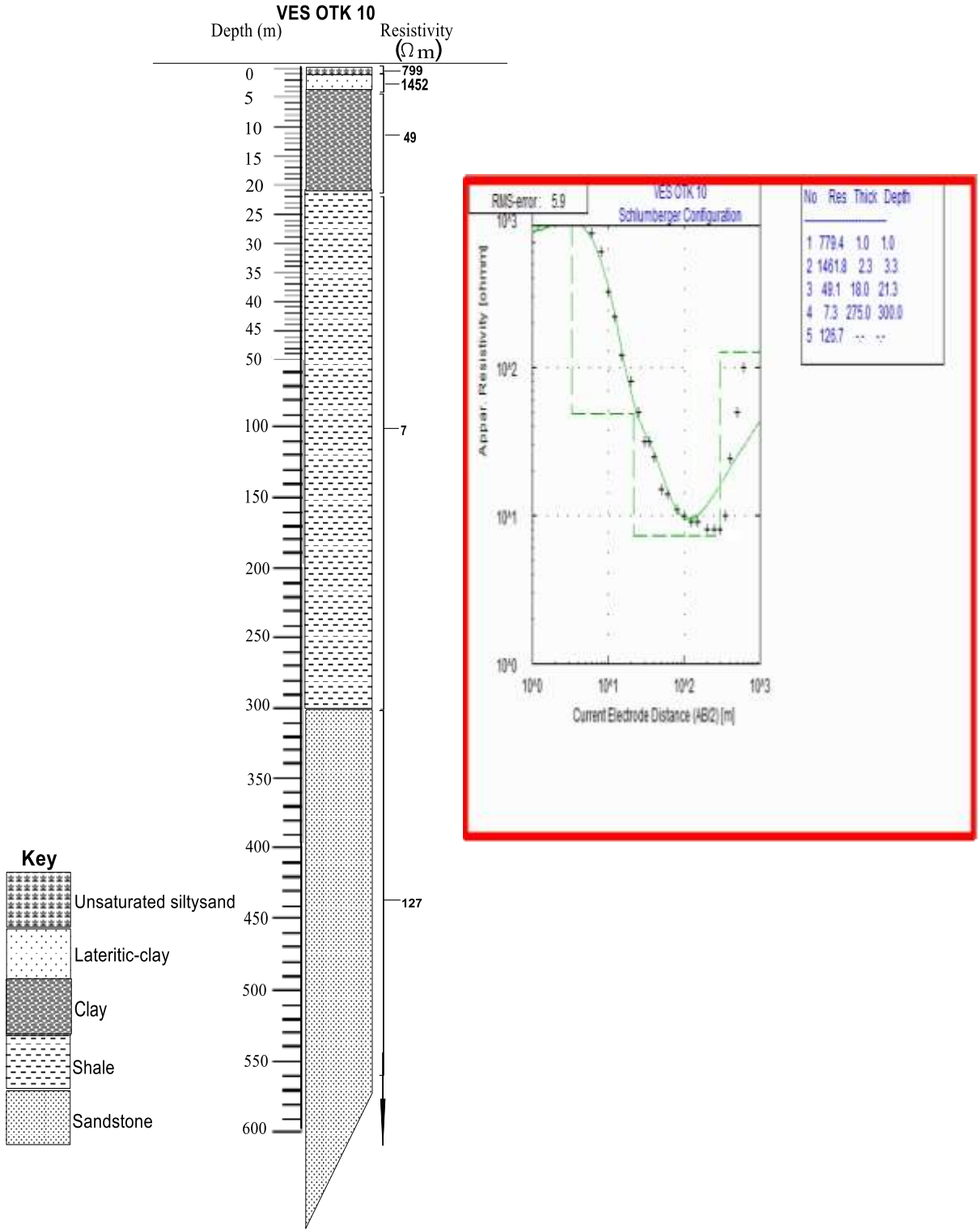

Figure C10.QH Sounding Model Curve Type and Geoelectric Section, VES OTK 10

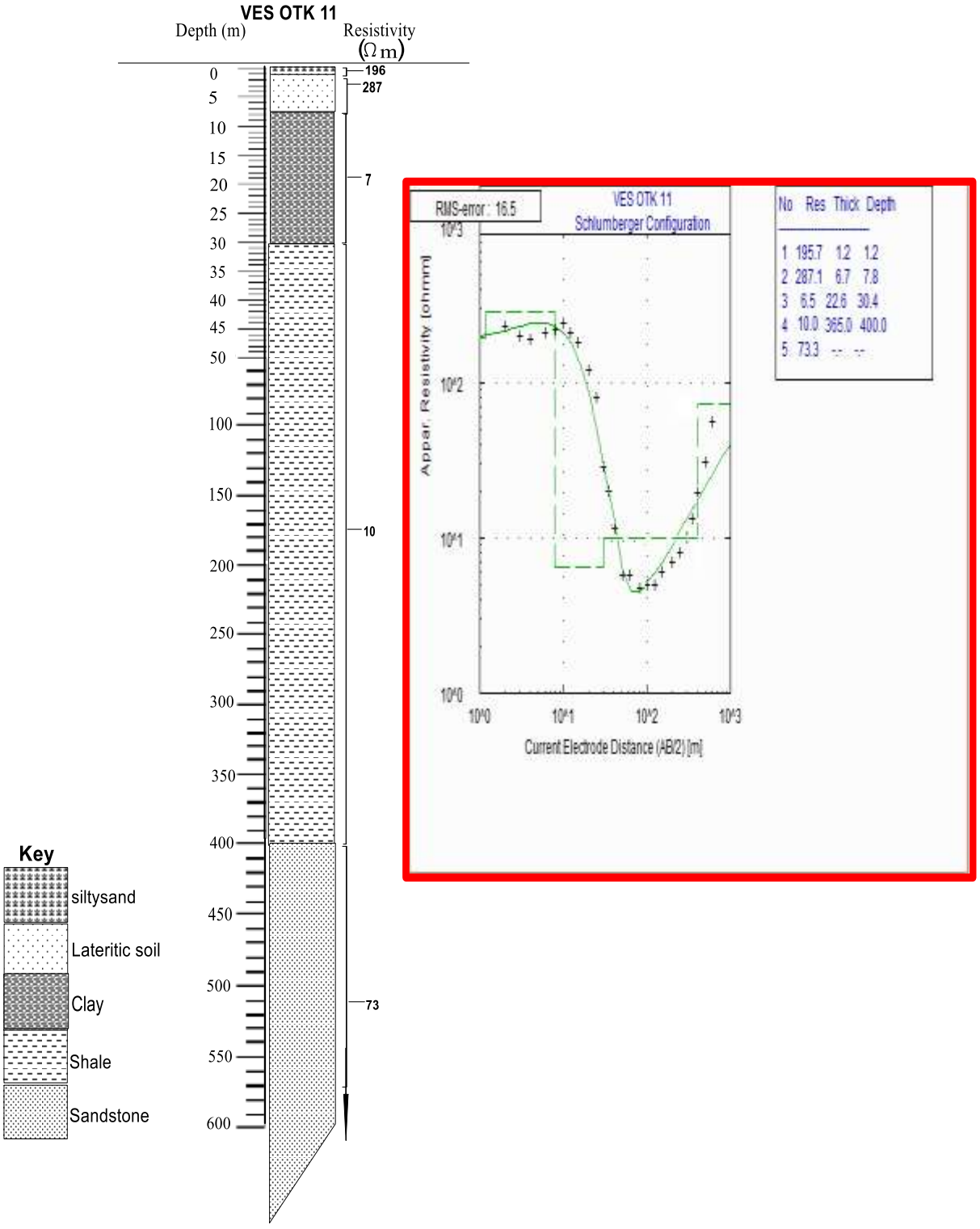

Figure C11.QH Sounding Model Curve Type and Geoelectric Section, VES OTK 11

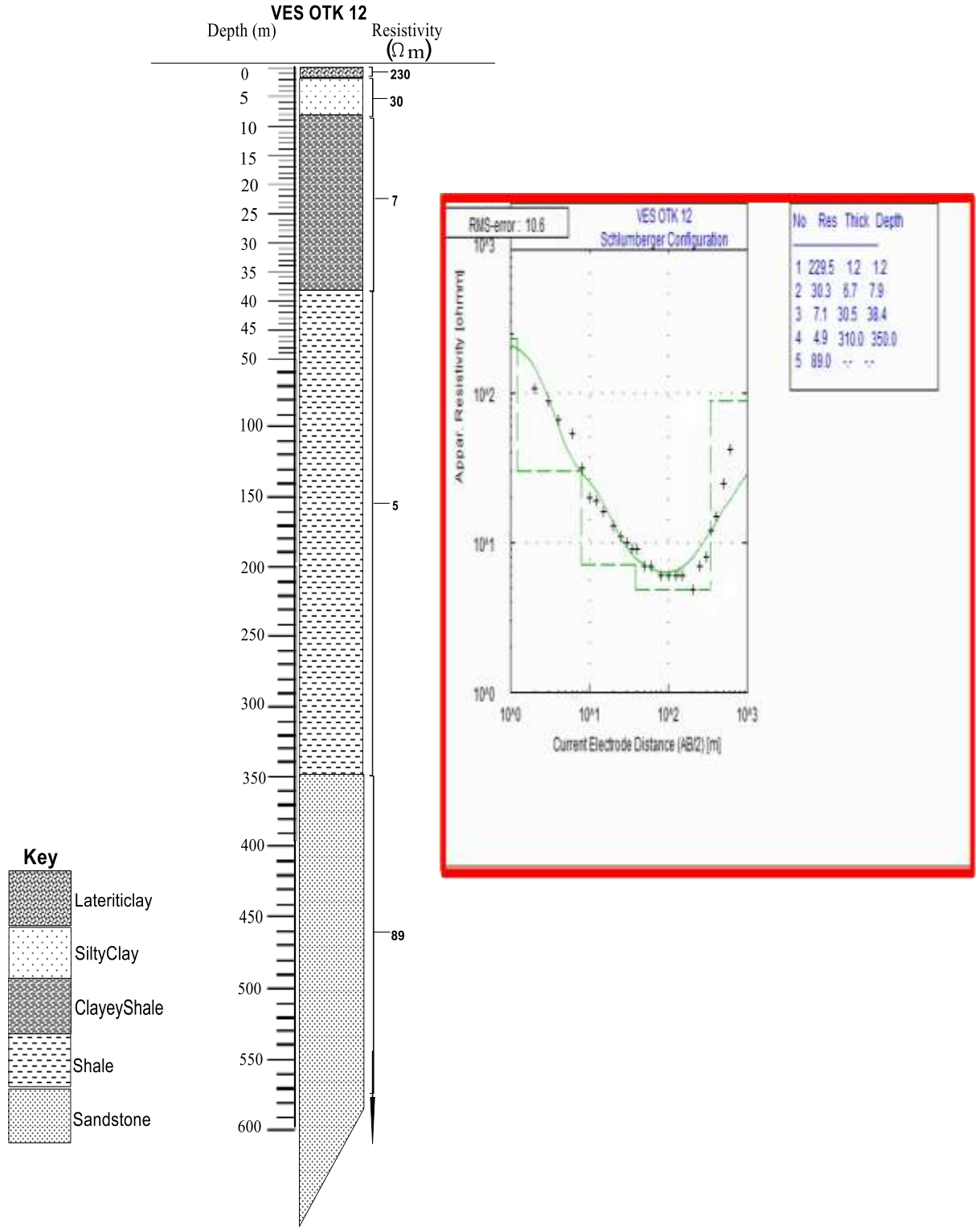

Figure C12.QH Sounding Model Curve Type and Geoelectric Section, VES OTK 12

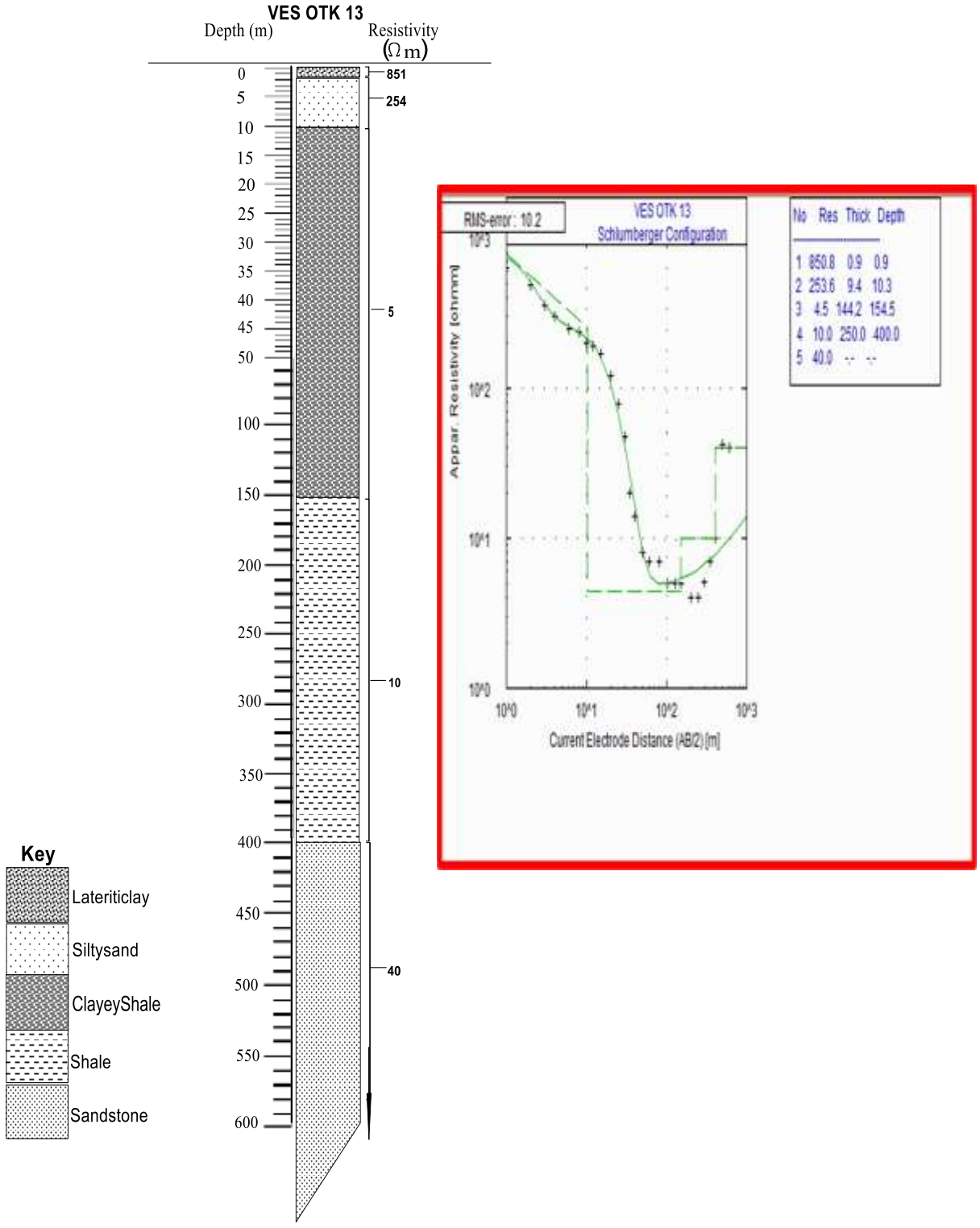

Figure C13.QH Sounding Model Curve Type and Geoelectric Section, VES OTK 13

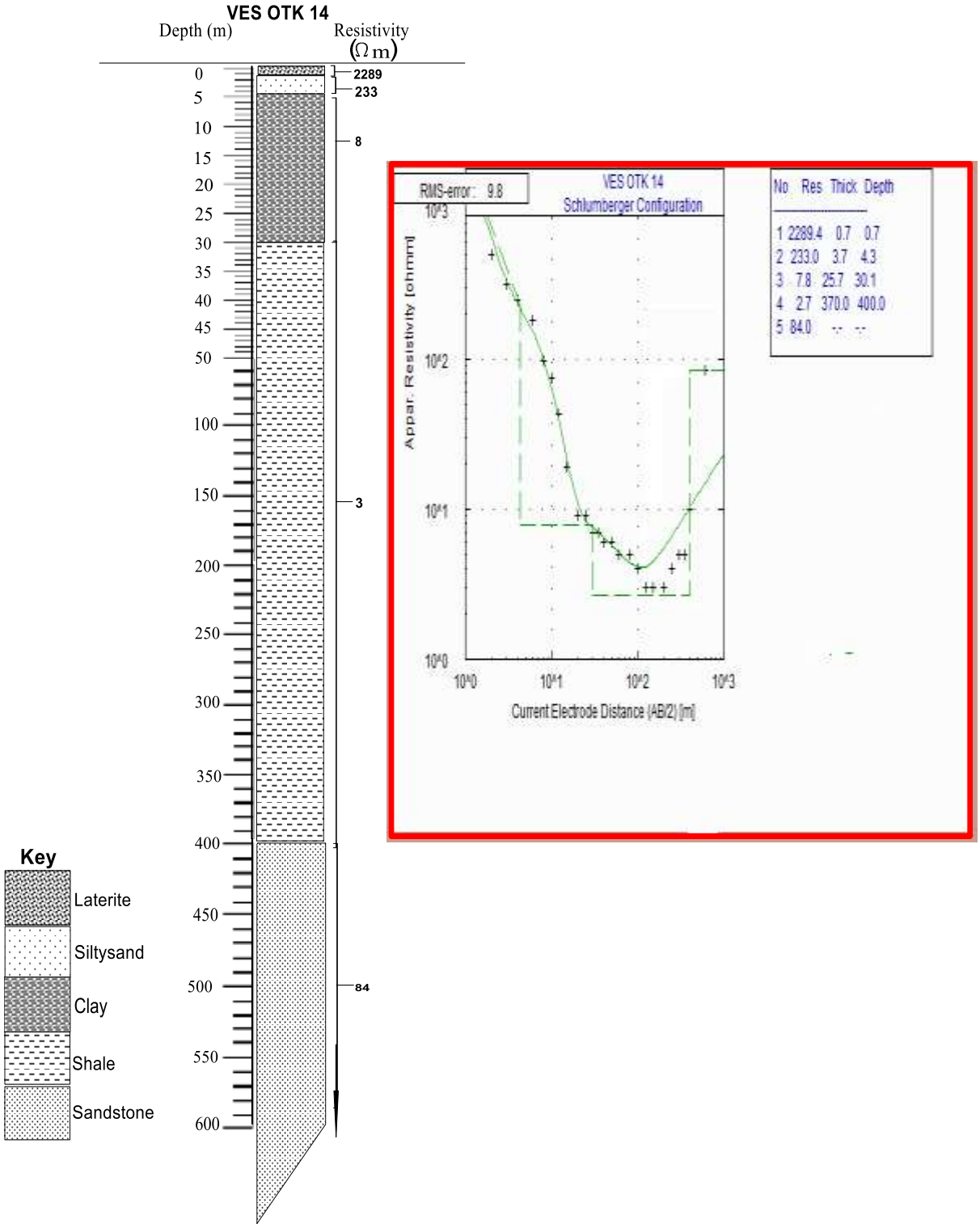

Figure C14.QH Sounding Model Curve Type and Geoelectric Section, VES OTK 14

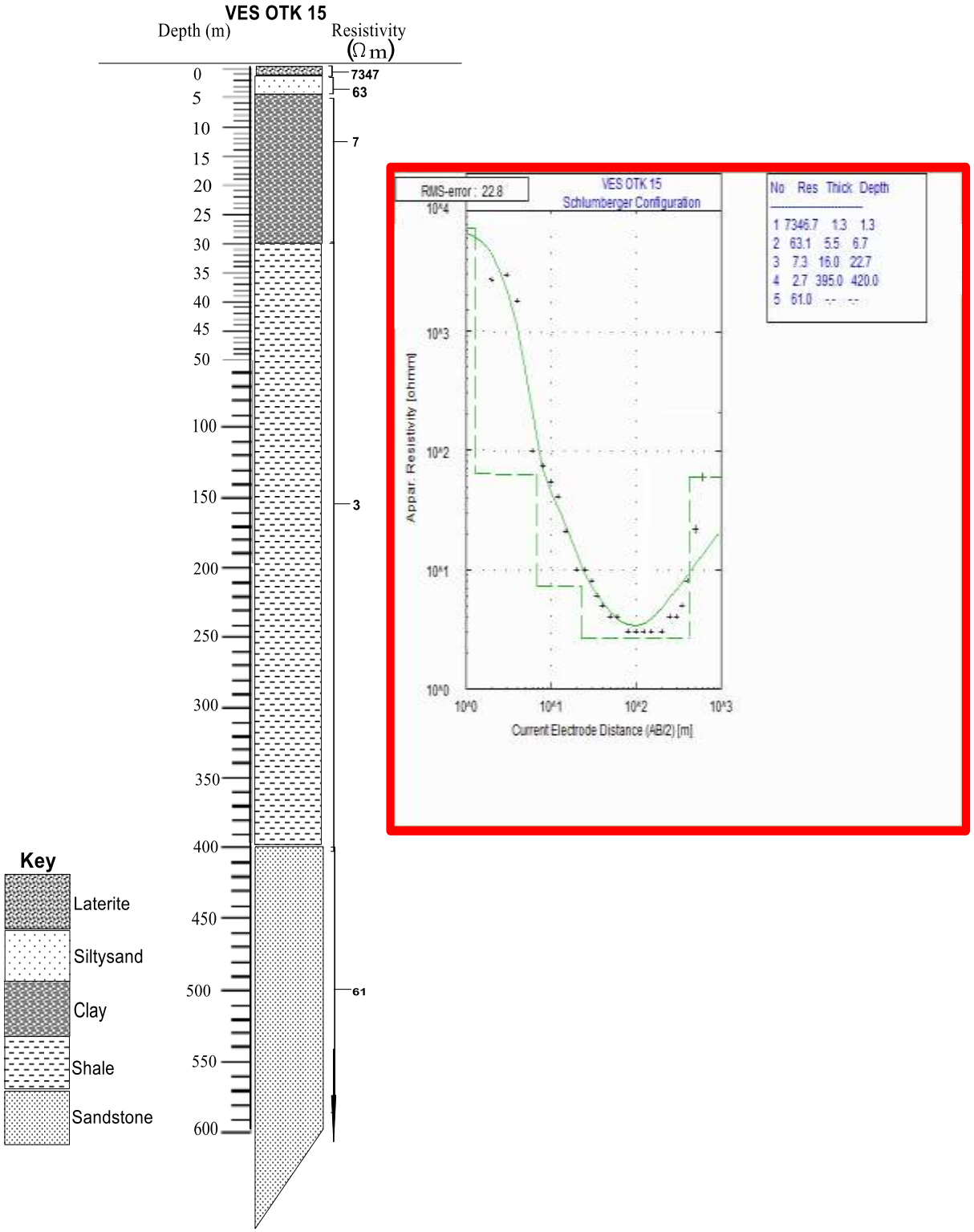

Figure C15.QH Sounding Model Curve Type and Geoelectric Section, VES OTK 15

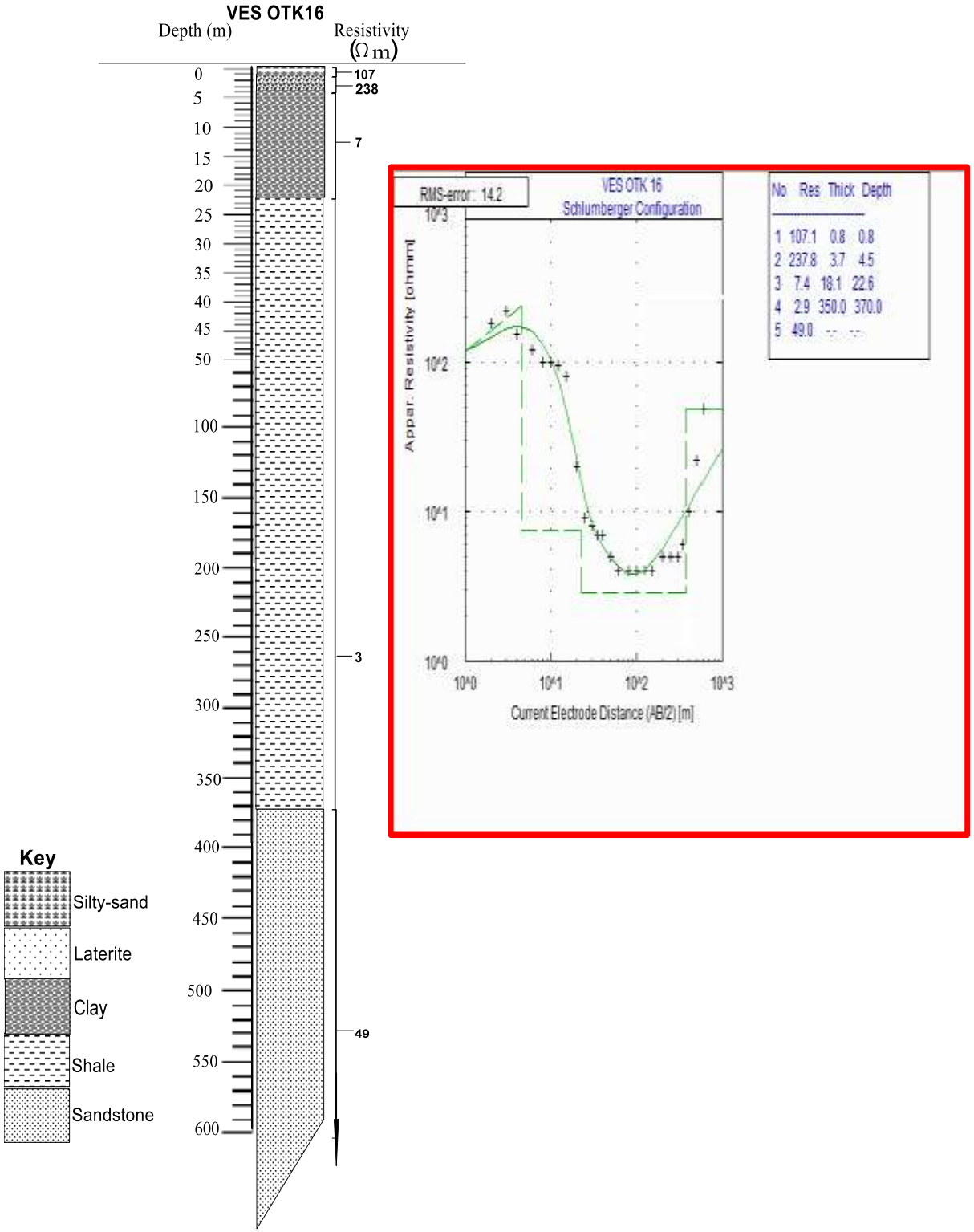

Figure C16.KH Sounding Model Curve Type and Geoelectric Section, VES OTK 16

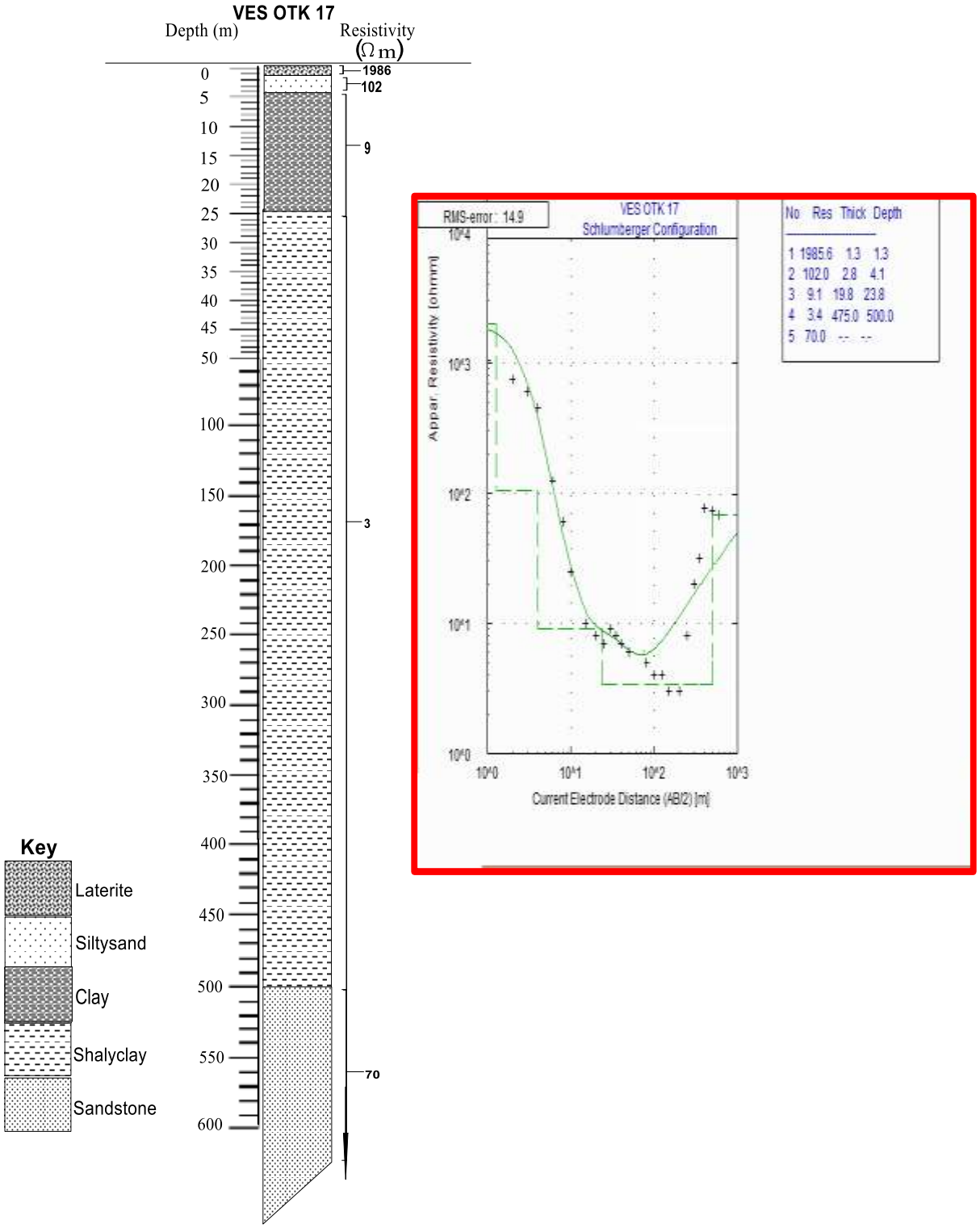

Figure C17.QH Sounding Model Curve Type and Geoelectric Section, VES OTK 17

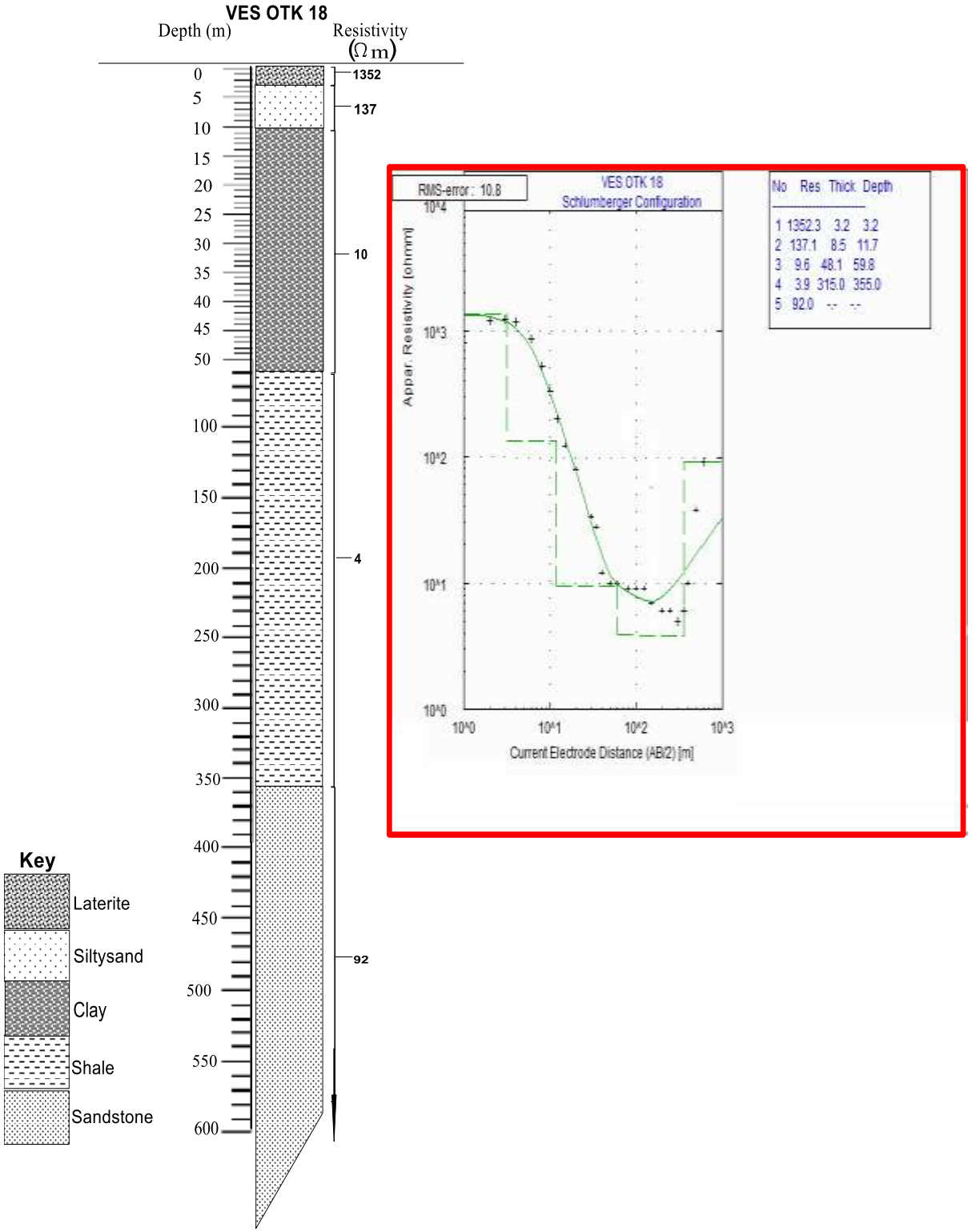

Figure C18.QH Sounding Model Curve Type and Geoelectric Section, VES OTK 18

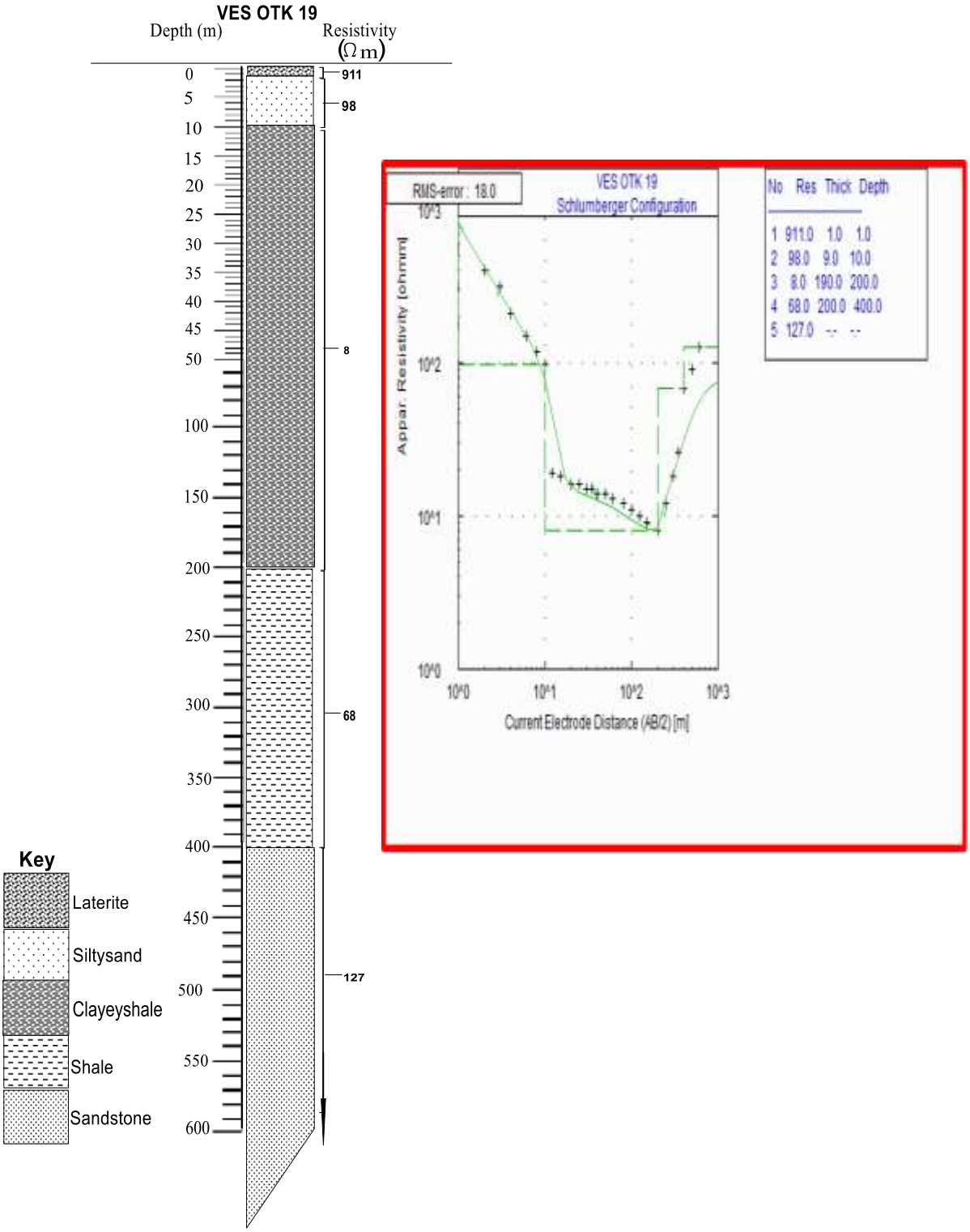

Figure C19.QH Sounding Model Curve Type and Geoelectric Section, VES OTK 19

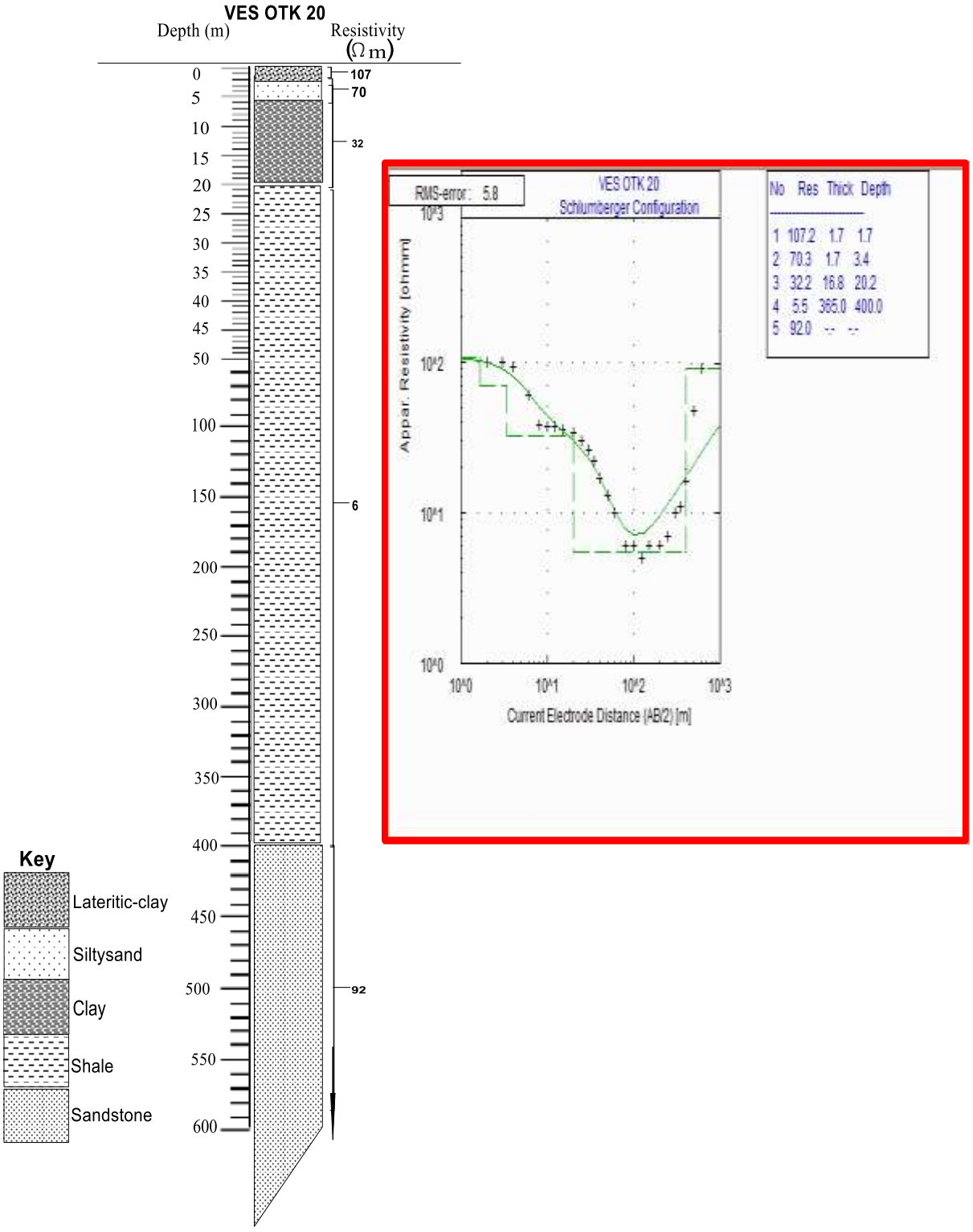

Figure C20.QH Sounding Model Curve Type and Geoelectric Section, VES OTK 20

APPENDIX D

2D Subsurface Tomography Field Data

Table D1. 2D OTK Profile 01 Data

a = 5			a = 10			a = 15			a = 20			a = 25			a = 30		
MP	ES	Ωm	MP	ES	Ωm	MP	ES	Ωm	MP	ES	Ωm	MP	ES	Ωm	MP	ES	Ωm
7.5	5	173	15	10	93	22.5	15	65	30	20	34	37.5	25	22	45	30	12
12.5	5	147	20	10	124	27.5	15	64	35	20	46	42.5	25	23	50	30	9
17.5	5	195	25	10	121	32.5	15	61	40	20	48	47.5	25	26	55	30	20
22.5	5	454	30	10	121	37.5	15	79	45	20	47	52.5	25	26			
27.5	5	134	35	10	122	42.5	15	80	50	20	47	57.5	25	33			
32.5	5	174	40	10	111	47.5	15	78	55	20	45	62.5	25	42			
37.5	5	110	45	10	121	52.5	15	67	60	20	38						
42.5	5	159	50	10	118	57.5	15	66	65	20	45						
47.5	5	98	55	10	95	62.5	15	62	70	20	51						
52.5	5	107	60	10	92	67.5	15	82									
57.5	5	101	65	10	106	72.5	15	85									
62.5	5	65	70	10	92	77.5	15	86									
67.5	5	101	75	10	110												
72.5	5	111	80	10	107												
77.5	5	112	85	10	107												
82.5	5	120															
87.5	5	111															
92.5	5	112															

MP=Midpoint ES (a)=Electrode Spacing Ωm=Resistivity

Table D2. 2D OTK Profile 02 Data

a = 5			a = 10			a = 15			a = 20			a = 25			a = 30		
MP	ES	Ωm	MP	ES	Ωm	MP	ES	Ωm	MP	ES	Ωm	MP	ES	Ωm	MP	ES	Ωm
7.5	5	403	15	10	228	22.5	15	180	30	20	165	37.5	25	76	45	30	37
12.5	5	410	20	10	451	27.5	15	233	35	20	147	42.5	25	72	50	30	32
17.5	5	445	25	10	403	32.5	15	264	40	20	124	47.5	25	69	55	30	21
22.5	5	468	30	10	385	37.5	15	236	45	20	107	52.5	25	52			
27.5	5	438	35	10	251	42.5	15	216	50	20	106	57.5	25	52			
32.5	5	484	40	10	422	47.5	15	202	55	20	96	62.5	25	36			
37.5	5	488	45	10	361	52.5	15	343	60	20	93						
42.5	5	524	50	10	341	57.5	15	199	65	20	91						
47.5	5	484	55	10	372	62.5	15	218	70	20	78						
52.5	5	587	60	10	453	67.5	15	198									
57.5	5	493	65	10	387	72.5	15	193									
62.5	5	488	70	10	363	77.5	15	160									
67.5	5	470	75	10	374												
72.5	5	476	80	10	415												
77.5	5	486	85	10	360												
82.5	5	565															
87.5	5	518															
92.5	5	641															

MP=Midpoint ES (a)=Electrode Spacing Ωm=Resistivity

Table D3. 2D OTK Profile 03 Data

a = 5			a = 10			a = 15			a = 20			a = 25			a = 30		
MP	ES	Ωm	MP	ES	Ωm	MP	ES	Ωm	MP	ES	Ωm	MP	ES	Ωm	MP	ES	Ωm
7.5	5	187	15	10	139	22.5	15	74	30	20	51	37.5	25	30	45	30	14
12.5	5	164	20	10	154	27.5	15	104	35	20	38	42.5	25	25	50	30	11
17.5	5	299	25	10	155	32.5	15	117	40	20	32	47.5	25	22	55	30	38
22.5	5	310	30	10	179	37.5	15	77	45	20	47	52.5	25	20			
27.5	5	301	35	10	168	42.5	15	77	50	20	45	57.5	25	27			
32.5	5	240	40	10	175	47.5	15	82	55	20	55	62.5	25	37			
37.5	5	210	45	10	264	52.5	15	83	60	20	104						
42.5	5	207	50	10	171	57.5	15	109	65	20	64						
47.5	5	216	55	10	203	62.5	15	178	70	20	61						
52.5	5	333	60	10	372	67.5	15	84									
57.5	5	411	65	10	339	72.5	15	92									
62.5	5	573	70	10	176	77.5	15	81									
67.5	5	427	75	10	194												
72.5	5	211	80	10	147												
77.5	5	261	85	10	163												
82.5	5	251															
87.5	5	286															
92.5	5	155															